Investigation of an enhancer-based regulation of LILRB1 gene and the differential functions of LILRB1 variants in natural killer cells

by

Kang Yu

A thesis submitted in partial fulfillment of the requirements for the degree of

Doctor of Philosophy

in

Immunology

Department of Medical Microbiology and Immunology
University of Alberta

Abstract:

Human cytomegalovirus (HCMV) causes severe disease in immunocompromised people such as transplant patients. NK cells are crucial in controlling HCMV whereas HCMV developed multiple strategies to evade NK cell surveillance. HCMV encodes a human MHC-I homolog called UL18 to target an inhibitory receptor called leukocyte immunoglobulin-like receptor B1 (LILRB1) expressed on NK cells. LILRB1 is also broadly expressed on other immune cells and associated with viral infection, autoimmune diseases, and cancer. LILRB1 expression exhibits dramatic heterogeneity among different types of immune cells and LILRB1 gene transcription in lymphoid and myeloid cells arises from the distal promoter and the proximal promoter, respectively. LILRB1 is expressed on subsets of human NK cells and the frequency of LILRB1-positive NK cells differs among people. I verified in this thesis that NK clones have either single or double allelic expression. Notably, the frequency of LILRB1-positive NK cells has been shown to increase in the context of HCMV infection. Our group demonstrated that LILRB1 polymorphisms are associated with the frequency of LILBR1+ NK cells, and there are “high” and “low” haplotypes involving the SNPs in the regulatory regions that are correlated with relatively high and low frequency of LILRB1-positive NK cells, respectively. Intriguingly, our group found that the kidney transplant patients homozygous for the SNPs linked with the “low” haplotype were more susceptible to HCMV infection. This thesis aimed to explore the mechanism contributing to the LILRB1 heterogeneity on NK cells

and investigate how LILRB1 polymorphisms influence the NK cell response controlling HCMV in transplant patients.

To understand by what mechanism polymorphisms may influence the LILRB1 expression in NK cells, our group previously compared the distal promoter activity from the two haplotypes using a luciferase reporter assay in an NK cell line but did not detect any difference. We further found one CpG site in the distal promoter of the "high" haplotype had a higher methylation rate compared with the "low" haplotype. In this thesis, I characterized a 3.2 kb enhancer in the intron 1 of the LILRB1 gene in NK cells. This polymorphic region possesses multiple YY1 sites and the promoter/enhancer complexes can be isolated using the YY1 antibody in a ChIP-loop assay. CRISPR-mediated deletion of this region reduced LILRB1 expression in an NK cell line. Together, these results suggest that the intronic enhancer positively regulates LILRB1 transcription in NK cells through the scaffold function of YY1.

There are four non-synonymous SNPs in the region coding the ligand-binding domains of LILRB1 and two of which are strongly linked with the expression-correlated SNPs. The second part of my thesis investigated whether those SNPs influence the function of LILRB1 on NK cells. I found the two naturally occurring LILRB1 variants expressed in a model NK cell line showed functional differences with target cells expressing UL18 and classical MHC-I, but not with HLA-G. The altered functional recognition was recapitulated in a binding assay with the purified binding domains of LILRB1. Interestingly, the stronger binder is linked with the "low" haplotype and worse control of HCMV in transplant patients. Each of the four substitutions

contributes to the binding tested and one SNP controls the addition of an N-linked glycan which is also important to ligand binding. These findings indicate that specific LILRB1 alleles correlated with poor control of HCMV are restricted by limiting surface expression on NK cells.

Additionally, I observed that UL18 transduction of a B cell line could induce cell aggregation. This phenotype was not influenced by the functional blocking of LILRB1. CRISPR-mediated knockout of the LILRB1 gene indicated that LILRB1 is important in the formation while dispensable for maintaining the phenotype. I further revealed that this phenotype was dependent on LFA-1. However, neither the LFA-1 expression nor the LFA-1 activating status was notably changed by the UL18 transduction. Nevertheless, these results uncovered a novel function of UL18 in cell adhesion that is potentially involved in HCMV pathogenesis.

Collectively, this thesis extends our knowledge of LILRB1 transcriptional regulation and LILRB1 heterogeneity in NK cells. It also explains how the genetic variation of the LILRB1 gene influence the differential responses of NK cells to HCMV, ultimately may inform developing LILRB1 as a marker to predict the outcome of HCMV in the transplant patients.

Acknowledgments

First, I would like to thank my supervisor Dr. Debby Burshtyn for her conscientious support on my research and my life in Canada. She always trained me to have scientific logic in doing research which I found very helpful to resolve the problems I met in the experiments. She also usually helps improve my writing skills in English. We discussed the experiment results and shared thoughts almost every week. All of these and more make a very wonderful experience for me as an international student.

I also want to thank my committee members, Dr. Jim Smiley and Dr. Rob Ingham, for the continuous support on my project. Their suggestions often open a window for me to think about my research.

As well, I appreciate the support and communications on my research from the past or current Burshtyn lab members. Particular thanks to the flow core members, Dorothy, Aja, and Sabina, for the training and help on my flow cytometry experiments. Also, I am very thankful for all the shared research equipment from the MMI and the help from the people in Dr. Lynne Postovit's lab in the Department of Oncology. I want to thank Dr.Arun Kommadath from Dr. Paul Stothard's group for helping me with the analysis of the RNA-Seq data. I also want to thank my friends that I made in MMI and other departments at the University of Alberta for all their generous supports on my research and my life. Special thanks to the MMI office staff, Anne Giles, Debbie Doudiet, Tabitha Vasquez, and Melissa Northmore to help me with the graduate student affairs. Also, I would like to thank the china scholarship council for financial support in my first four years of my study.

Last but not least, I want to thank my wife and my parents. I am very grateful for their understanding and consideration for me every day. Every time I feel lonely or stressed, they are always there as my strongest backing.

Table of Contents

List of Tables:

List of Figures:

Abbreviations

3C	chromosome conformation capture
ADCC	antibody-dependent cellular cytotoxicity
ATAC-Seq	transposase-accessible chromatin using sequencing
ATG	anti-thymocyte globulin
BAC	bacterial artificial chromosome
C/EBP	Ccaat enhancer-binding protein
CBP	CREB-binding protein
ChIP	chromatin immunoprecipitation
CPM	counts per million
CREB	cAMP response element-binding protein
CTV	CellTrace Violet
DC	dendritic cells
DC	dendritic cell
DE	differential expression
DHS	DNase I hypersensitivity sites
EGFR	epidermal growth factor receptor
ERV	endogenous retrovirus
FC	fold change
FcγR	Fc receptor gamma chain
FDR	false discovery rate
FRET	fluorescence resonance energy transfer
HA	hemagglutinins
HCMV	human cytomegalovirus
HiC-Seq	high throughput 3C by sequencing
HIV-1	human immunodeficiency virus type 1
HPC	hematopoietic progenitor cell
HTA	homotypic adhesion
ICAM	intercellular adhesion molecules
IE	immediate-early gene
IFN	interferon
Ig	immunoglobulin
ITAM	immunoreceptor tyrosine-based activation motif
ITIM	immunoreceptor tyrosine-based inhibitory motif
ITSM	immunoreceptor tyrosine-based switch motif
KIR	killer-cell immunoglobulin-like receptor
LD	linkage disequilibrium
LFA-1	lymphocyte function-associated antigen 1
LILR	leukocyte immunoglobulin-like receptor

LINE	long interspersed nuclear element
LRC	leukocyte receptor complex
LTR	long terminal repeat
MHC	major histocompatibility complex
MLL5	mixed-lineage leukemia-5
Mt-tRNA	mitochondrial transfer RNA
NCR	natural cytotoxicity receptor
NK	natural killer
NKC	NK gene complex
PAM	protospacer adjacent motif
PC	pyruvate carboxylase
PDGFRα	platelet-derived growth factor receptor-α
Nrp2	neuropilin2
PIR	paired Ig-activating receptor
RA	rheumatoid arthritis
SH2	Src-homology 2
SINE	short interspersed nuclear element
SLE	systemic lupus erythematosus
SNP	single-nucleotide polymorphism
SOT	solid organ transplant
STCS	Swiss Transplant Cohort Study
TRAIL	TNF-related apoptosis-inducing ligand
UL	unique long
US	unique short
UTR	untranslated region
YY1	Yin Yang 1
β_2m	β_2 microglobulin

CHAPTER 1

Introduction

1.1 General overview

Human cytomegalovirus (HCMV) is a very common virus that can cause severe illness in high-risk patients e.g. immunocompromised transplant patients. Natural killer (NK) cells are important innate immune cells in controlling HCMV infection. Activation of NK cells is regulated by the integrated signals of the surface activating and inhibitory receptors when NK cells contact target cells. Upon co-evolution with humans, HCMV developed strategies to evade the NK cell response such as targeting NK cell receptors to obstruct NK cell activation [1]. Meanwhile, the interplay between the virus and the human immune system also drives the selection of alleles of genes encoding NK receptors [2]. Thus, differences in the genetic background among transplant patients matter in response to HCMV infection and the development of HCMV disease. Finding biological markers is beneficial for identifying patients more susceptible to HCMV and making personalized precision medicine available for targeted treatment and prophylaxis. Through screening the single nucleotide polymorphisms (SNPs) in the gene encoding leukocyte immunoglobulin-like receptor B1 (LILRB1), our group found several SNPs associated with the ability to control HCMV infection in transplant patients. Moreover, our group also demonstrated those SNPs are associated with LILRB1 expression on NK cells [3]. Following those findings, in this thesis, I explored the potential mechanism of the heterogeneous LILRB1 expression patterns in NK cells. In addition, I also investigated how the polymorphisms influence the receptor binding and NK cell function and the resultant information may explain the different responses to HCMV infection in transplant patients. To provide background for the research presented in this thesis, I will give a review on aspects of HCMV and NK cells, the NK cell receptors with a focus on the LILRB1 receptor, the interplay of HCMV with NK cells particularly through the LILRB1/UL18 axis, regulation of LILRB1 gene expression, LILRB1 gene polymorphisms and the clinical relevance.

1.2 HCMV

HCMV is an enveloped double-stranded DNA virus that belongs to betaherpesvirinae which is a subfamily of herpes virus. It is extremely widespread throughout the world, but often asymptomatic. A sound immune system can generally suppress viral infections; however, similar to all the other herpesviruses, HCMV is able to establish latent lifelong infection in their hosts and enter latency. Reactivation of HCMV can occur from the latent phase, and HCMV is able to spread through peripheral blood to many organs [4-7]. HCMV can be transmitted through saliva, sexual contact, placental transfer, breastfeeding, blood transfusion, and solid-organ or bone marrow transplantation [8].

In immunocompromised patients, particularly in solid organs or bone marrow transplant recipients, HCMV causes severe disease and even significantly increases mortality [9-11] because the use of immunosuppressive drugs tends to allow viral reactivation [8, 12]. The virus can be controlled in transplant patients with antivirals but infection remains a serious complication that often leads to graft loss when immunosuppression is lowered. HCMV has also been recognized as the leading cause of infection-related congenital abnormalities of neonates through vertically transmitted infections [13].

1.2.1 HCMV infection, replication, and treatment

The primary targets of HCMV infection include epithelial cells, endothelial cells, and fibroblasts. Peripheral leukocytes are also susceptible to viral infection and presumably responsible for viral spread and reactivation in multiple tissues. In addition, HCMV can also infect some specialized parenchymal cells including smooth muscle cells in the gastrointestinal tract, hepatocytes, and neuronal cells in the retina and brain [5, 12, 14]. Platelet-derived growth factor receptor alpha (PDGFRα) and Neuropilin-2 (Nrp2) have been identified as the host receptor for viral entry and cell tropism of HCMV. Specifically, PDGFRα is required for the viral infection of fibroblasts through interacting with the gH/gL/gO trimer complex of HCMV

while Nrp2 is the central receptor for the infection of epithelial, endothelial, and myeloid cells targeting by the gH/gL/pUL128/pUL130/pUL131A pentamer. The glycoproteins gB expressed on the viral envelope is known to be essential for membrane fusion [15, 16]. Following the membrane fusion, proteins on viral tegument are released to activate the lytic infectious cycle. The viral genome is transferred to the cell nucleus and initiates the expression of immediate early genes (IEs) [17]. In a highly regulated sequential pattern, viral DNA replication occurs with the help of early gene expression, and the viral structural proteins are in turn expressed from the late genes [18, 19]. After assembly of the viral capsid, the capsid egresses from the nucleus and is coated with tegument protein in the cytoplasm. Tegumented capsid can acquire the envelope through budding into cytoplasmic vesicles [20]. For HCMV latent infection, early myeloid lineages, particularly the CD34+ progenitors and the derived monocytes, are regarded as the primary sites [21]. Compared with the lytic infection, the viral genome persists in the infected cells during the latency but expresses latency-associated transcripts and proteins that do not support the production of infectious virions, and the major IE promoter associates with transcription-repressive histone modifications and protein [21].

Currently, the favored traditional antiviral drug for HCMV is ganciclovir which targets and inhibits the DNA polymerase UL54 encoded by HCMV [22]. There have been several other antivirals targeting UL54 such as cidofovir and foscarnet but the resistance mutations of HCMV to ganciclovir also cause cross-resistance to these drugs, and foscarnet is known to cause nephrotoxicity [22]. A recently approved antiviral drug for HCMV called letermovir targets the UL56 from the herpesvirus-highly-specific terminase complex which is involved in the capsid assembly of HCMV shows much stronger inhibition on HCMV replication but also has concerns for drug resistance and limited application on particular transplant patients [23].

1.2.2 The immune response to HCMV

NK cells are important innate immune cells to control and clear CMV infection in mice [8]. Studies in humans showed that individuals deficient in NK cells are more susceptible to HCMV infection and more prone to developing severe HCMV diseases [24, 25]. Moreover, a study also revealed that NK cells were able to control CMV in a human without T cells [26]. Evidence suggests that, besides the ability to secret interferon (IFN)-γ, NK cells also play a role in inducing IFN-β from HCMV-infected cells to inhibit viral transmission in fibroblasts, endothelial and epithelial cells [27, 28]. For humoral immunity against HCMV, early studies revealed that the HCMV glycoprotein gB can induce the generation of neutralizing antibodies to reduce the disease severity and improve the survival in transplant patients [29, 30]. More recent studies reported that the isolation of antibodies targeting epitopes from the pentameric gH/gL/pUL128/pUL130/pUL131A complex or single proteins has a potent neutralizing effect on infection of endothelial and epithelia relative to fibroblasts [31-34]. Thus, these envelope proteins are potential targets for HCMV vaccines. However, so far, there is no licensed vaccine against HCMV, but there are recombinant subunit vaccines including pp65 and gB under clinical trials showed some promising benefits in transplant patients and protections in young people [35, 36].

T cells are also important effectors to control HCMV infection [8], and transplant patients lacking virus-specific $CD4^+$ and $CD8^+$ T cells are at higher risk to develop HCMV disease [37]. Adoptive transfer of HCMV-specific T cells has been a therapeutic strategy for HCMV disease in bone marrow transplant patients [38-41]. However, through millions of years of co-evolution with humans, HCMV developed many immune evasion mechanisms to subvert both of the innate and adaptive immune responses.

1.2.3 Immune evasion by HCMV

The genome of HCMV is very large for a virus at around 240 kb [42]. The genome contains unique long (UL) and unique short (US) regions respectively flanked by a terminal (TRL and TRS) and internal (IRL and IRS) inverted repeats region [43]. HCMV utilizes a large part of US and UL regions for encoding genes to modulate human immune responses.

HCMV has strategies to hinder apoptosis of the infected cells in order to establish a persistent infection. IE1 and IE2 protein up-regulate the expression of anti-apoptotic protein Bcl-2 [44, 45], and HCMV also encodes a Bcl-2 homolog. UL36 and UL37 play a role in the anti-apoptotic effect by preventing caspase activation or blocking mitochondria permeabilization [46, 47]. In addition, HCMV encodes genes whose products are homologs of cytokines and cytokine receptors through molecular mimicry [48] to globally dampen the anti-viral immunity.

HCMV employs several ways to evade NK cell responses. I will introduce the details about NK cell activation and NK cell receptors below. UL83, a main tegument protein of HCMV, is able to prevent NK cell activation by binding an NK cell activating receptor NKp30 [49]. HCMV can also down-regulate surface expression of virtually all the ligands for the NK activating receptor NKG2D through several viral products including UL16 [50, 51], UL142 [52, 53], micro-RNA UL122 [54], US9 [55], US18 and US20 [56]. As many other viruses do, HCMV encodes lots of viral proteins to down-regulate the surface expression of major histocompatibility complex (MHC) class I and class II molecules on infected cells. The down-regulation of MHC molecules prevents the antigen presentation for T cell activation [57] and also obstructs T-cell dependent activation of B cells. Down-regulation of MHC-I on target cells makes the infected cells susceptible to NK cell recognition. HCMV encodes UL40 to selectively promote the surface expression of HLA-E, a ligand for CD94/NKG2A inhibitory receptor, to evade NK cell surveillance [58, 59]. Importantly, HCMV encodes a human MHC-I homolog called UL18 which binds an NK cell inhibitory receptor LILRB1 and suppresses NK lysis [60, 61] and is a major focus of this thesis. In the following part of Chapter 1, I will introduce the biology of NK cells and the leukocyte Ig-like receptors (LILRs) particularly the LILRB1.

1.3 NK cells

NK cells are large granular lymphocytes playing important roles in resistance against cancer and infectious diseases. NK cells were discovered in the early 1970s when researchers noticed that lymphoid cells from healthy individuals could also react with allogeneic tumor cells [62, 63]. They found this natural cytotoxicity for tumor cells was derived from a subpopulation of lymphoid cells initially characterized in mouse and named N-cells [64, 65]. About 2% to 18% of the human peripheral blood lymphocytes are NK cells and they also widely reside in lymphoid and non-lymphoid tissues [66]. With fast and spontaneous cytotoxicity and cytokine-producing functions, NK cells were classified as innate immune cells for many years. Without expressing clonotypic antigen-specific receptor of B cells and T cells [67, 68], NK cells form different NK cell repertoires by expressing subsets of the diverse inhibitory and activating receptors in development, education, activation [69, 70].

However, NK cells also possess features of adaptive immune responses. It has been shown that the resting NK cells from humans or mice exhibit relatively low effector activities before the "priming" process [71, 72]. Studies on mice revealed the "memory-like" features in subsets of NK cells including self-renewing and robust secondary response specific to certain haptens, mouse CMV, and tumors [73-76]. Pre-activating murine NK cells with combining IL-12, IL-15, and IL-18 could also induce memory-like properties [77], which was similarly observed for human NK cells [78]. In humans, expansion of NK cells expressing the NKG2C receptor with enhanced functional responses in acute infection and reactivation of HCMV supports an adaptive feature [76, 79, 80], and those NKG2C+ NK cells exhibit enhanced capacity for IFNγ production [81]. In addition, it has been reported that subsets of human NK cells deficient for FcRγ but with increased CD57 and NKG2C expression showed antibody-dependent memory features in the context of HCMV infection [82-84].

1.3.1 Functions of NK cells

NK cells have the name “natural killer” because they can recognize and kill certain viral-infected cells and tumor cells through cytotoxic activity. The cytotoxic response from NK cells requires direct contact with the target cells and formation of an interface called the “lytic synapse” that involves various receptor-ligand interactions. The intracellular granules containing lytic molecules such as perforin and granzymes are then transported to the lytic synapse by the cytoskeletal machinery. Perforin is able to permeabilize the plasma membrane of the target cells which allows granzymes and other cytotoxic molecules to enter and induce cell apoptosis [85]. Due to the coating on the target cells by specific antibodies, NK cells can recognize the cells through a low-affinity Fc receptor CD16 to generate the lytic synapse and then kill the target cell. This process is referred to as antibody-dependent cellular cytotoxicity (ADCC). Aside from perforin and granulysin-dependent cytotoxicity, NK cells can also mediate apoptosis by FAS ligand, membrane-bound or secreted TNF-α and secreted TNF-related apoptosis-inducing ligand (TRAIL) [86].

Another effector response of NK cells is the secretion of cytokines and chemokines. Besides the secretion of TNF-α mentioned above, NK cells are known as strong producers of IFN-γ which is a pleiotropic cytokine that not only directly interferes viral entry and replication but also plays immune-regulatory roles such as being a stimulator of macrophages and a modulator for the differentiation and maturation of T cells and B cells [87]. NK cells can produce chemokines to induce chemotaxis of other immune cells and to some extent play an immune-regulatory role [88]. Different subsets of human NK cells, for example, marked by distinct expression of the intensity of CD56 and CD16, showed different functional properties and preference for mediating cytotoxicity and cytokine secretion in response to stimulation [66].

In addition to the effector functions in innate immunity, NK cells are believed to work as a type of specialized lymphocytes to bridge innate and adaptive immunity. This involves the crosstalk of NK cells with dendritic cells (DCs), T, and B cells. For example, IFN-γ and TNF-α produced by NK cells can induce maturation of DCs, and the IL-12, IL-15, IL-18 secreted by

DCs can, in turn, activate and proliferate NK cells [89-91]. The killing of target cells by NK cells can promote the cross-presentation of antigen by DCs to activate the antigen-specific adaptive immune response. Apart from producing IFN-γ to enhance the priming and polarized differentiation of T cells and B cells [92-95], NK cells also express CD40L and OX40L to provide co-stimulatory signals to T and B cells through direct contact [96, 97]. NK cells also play a role in maintaining the homeostasis of both innate and adaptive immune cells [98-103].

1.3.2 Regulation of NK cell activation by NK cell receptors

Instead of using antigen-specific receptors by T and B cells, mature NK cells express an array of germline-encoded activating and inhibitory receptors to differentiate healthy and non-healthy cells. The "missing self" recognition ensures mature NK cells can be quickly activated and efficiently respond to target cells losing self MHC-I molecules on the surface while, importantly, maintaining tolerance to normal cells. Two main types of receptor families are expressed on NK cells in humans to recognize MHC-I molecules: the C-type lectin superfamily receptors encoded in a region called "NK gene complex (NKC)" on chromosome 12 and the immunoglobulin (Ig) superfamily receptors encoded in a region called "leukocyte receptor complex (LRC)" on chromosome 19 [104, 105]. Mice also have an NKC region on chromosome 6 with encoded receptors such as Ly49s, NKG2/CD94, and NKR-P1s. There is no homolog for Ly49 receptors in human but there are one NKR-P1 and the NKG2/CD94 genes encoded in the human NKC region. Human LRC encodes two main groups of receptors: the KIRs and the LILRs while mice only have paired Ig-activating receptors (PIRs) to bind MHC-I encoded in the LRC on chromosome 7 [104].

Major determinants for being inhibitory or activating NK cell receptors are the tyrosine-based motifs on the cytoplasmic domain or the associated adaptor proteins. Take KIRs as an example, the inhibitory KIRs bear ITIMs in their long cytoplasmic tails [106, 107]. Tyrosine phosphorylation of ITIMs is able to recruit two Src-homology 2 domain

(SH2)-containing protein tyrosine phosphatases SHP-1 and SHP-2 [108-110]. Due to the short cytoplasmic tail and a charged residue in the transmembrane domain, the activating KIRs transduce signals by associating with membrane adaptor protein DAP12 which contains immunoreceptor tyrosine-based activation motif (ITAMs) in their cytoplasmic domain [111, 112]. Following tyrosine phosphorylation, the ITAMs can recruit tyrosine kinases Syk and ZAP-70 and then activate downstream pathways that trigger NK cell effector functions and proliferation [113, 114]. In turn, following phosphorylation of ITIMs, inhibitory receptors recruit the protein tyrosine phosphatases to dephosphorylate proximal protein substrates phosphorylated by the tyrosine kinases recruited by activating receptors and thus dampen the transmission of activating signals to NK cells [115]. Consequently, NK cell activation is dynamically regulated through balancing the activating and inhibitory signals transmitted from the surface receptors [105, 116] (Figure 1.1).

Besides the receptors recognizing MHC-I as ligands, there are also receptors interacting with non-MHC-I molecules to regulate NK cell functions. Human natural cytotoxicity receptors (NCR) family including NKp46, NKp44, and NKp30 are activating receptors and there their ligands include stress-induced cell surface protein B7-H6, tumor ligand mixed-lineage leukemia-5 protein (MLL5), viral hemagglutinins (HA) and tegument pp65 [117]. The activating receptor NKG2D from the NKG2/CD94 family can recognize some structural homologs of MHC-I such as MICA, MICB, ULBP1–3, and RAE-1β which are highly expressed in tumors and stressed cells but not in normal cells. Inhibitory receptors LAIR-124 and KLRG1were reported using collagen and E-cadherin, respectively as their natural ligands [117]. The dynamic and fine-tuning interactions between the activating and inhibitory receptors of NK cells ensure the efficiency in the immune surveillance while maintaining the tolerance to healthy cells.

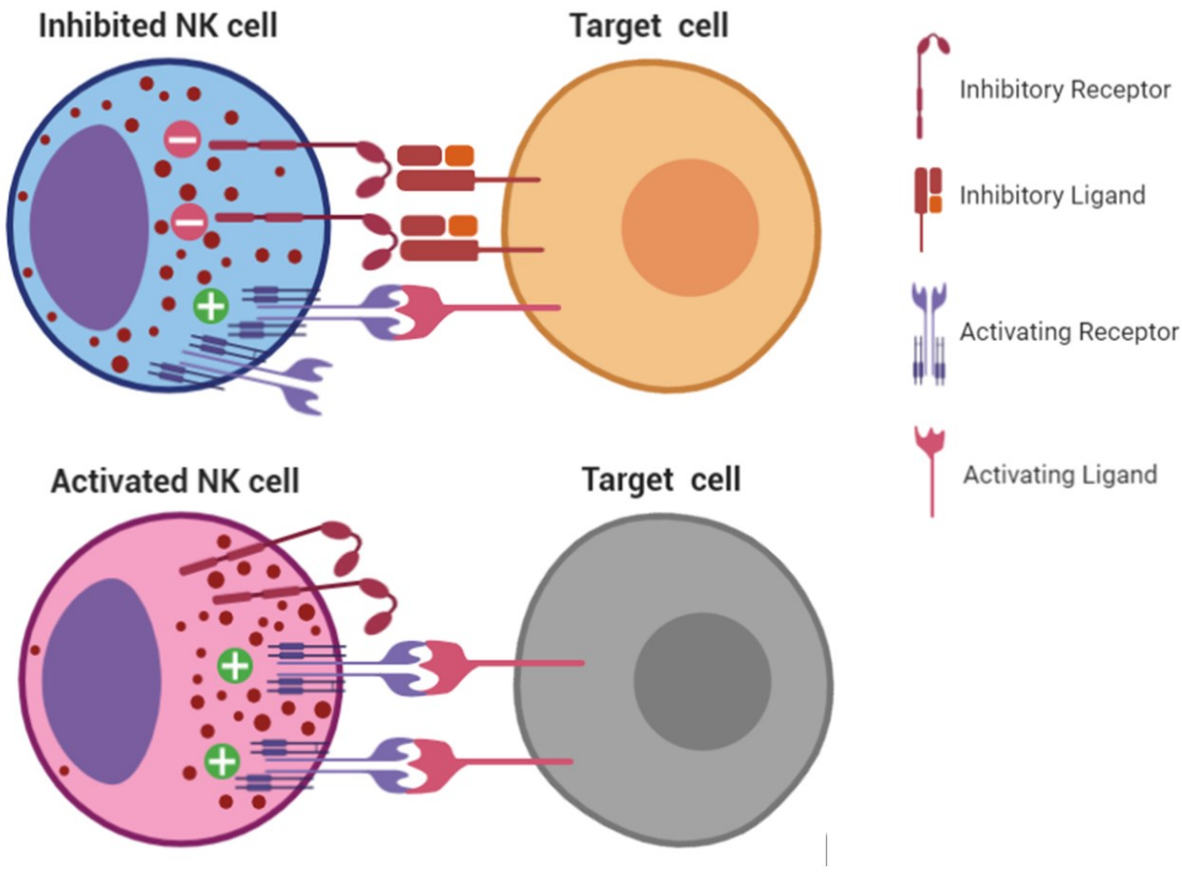

Figure 1.1 Regulation of NK cell activation by NK receptors.
NK cell is not activated and does not respond to the target cell when the inhibitory signal is dominant. If the activating signal is stronger than the inhibitory signal due to loss of inhibitory ligand and/or up-regulation of activating ligand on the target cells, NK cell is activated and kill the target cell.

1.3.3 NK cell development

One of the chapters in my thesis is related to the transcriptional regulation of LILRB1 gene in NK cells. To appreciate how and when NK cells acquire their functions and repertoire of receptors, I will review relevant aspects of human NK cell development.

Similar to B cells and myeloid lineage cells, it has been well-characterized that NK cells can develop and mature in the bone marrow. $CD56^{high}$ NK cells have also been reported to develop from $CD34^{+}$ hematopoietic precursor cells (HPCs) in the lymph node [118]. Several studies also found NK cells develop in the thymus, liver, and possibly intestine [119-121]. In the very beginning, a subset of multipotent hematopoietic stem cells (HSCs) differentiate into lymphoid-primed multipotential progenitors (LMPPs) expressing CD45RA. NK cells develop from the $CD34^{+}$ $CD45RA^{+}$ common lymphoid progenitors (CLPs) which transited from the LMPP and are capable to develop into other lymphoid lineages [122, 123]. NK cell development can be defined by three main stages in a linear model: lineage commitment, NK receptor repertoire selection, and functional maturation (Figure 1.2). NK lineage commitment happens downstream of CLPs with expressing CD122 and gives rise to $CD45RA^{+}\alpha4\beta7^{high}CD7^{+/-}CD10^{-}$ NK precursors (NKP) [124, 125]. The immature NK cells (iNK) without cytotoxic and cytokine-production capabilities defined by the expression of NKR-P1(CD161) can then acquire the expression of CD56, CD16, activating and inhibitory receptors through incubation with stromal cells and cytokines such as IL-15 or Flt3-L *in vitro*, which may mimic the NK receptor repertoire selection process *in vivo* [126-129]. The further maturation of NK cells is also dependent on the signals from stromal cells, which allow them to express multiple activating and inhibitory receptors and the markers indicative of maturation including CD94/NKG2, KIR and CD57 [130, 131]. It is still controversial for the transition from the $CD56^{bright}$ phenotype to $CD56^{dim}$ [131] and it has been suggested that the $CD56^{dim}$ NK cells can be directly differentiated from iNK cells [132].

Some cytokines are known to drive the development of NK cells. The combinations of cytokines among c-kit ligand, flt3 ligand, IL-2, IL-3, IL-7, IL-12, IL-15, and IL-21 have been

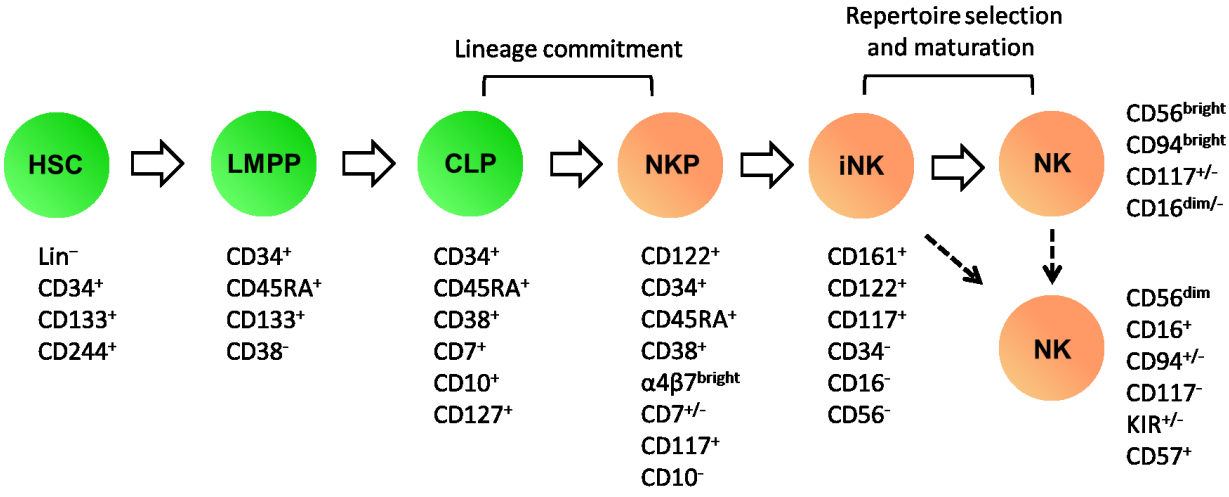

Figure 1.2 Linear model of human NK cell development (Adapted from [122, 123, 130]). Human NK cells can develop and mature in the bone marrow and secondary lymphoid organs. Green and orange circles indicate the developmental stages before and after the NK lineage commitment, respectively. The molecular markers for each stage are listed below or on the right side. Lin^- means lineage negative. The dashed lines indicated the possible transitions that happened during NK maturation.

shown to generate NK cells from CD34+ HPCs *in vitro* while IL-15 was reportedly the most important factor [133]. A two-step traditional model for early NK cell development suggests there is a transition of $CD34^+$ HPCs which are non-responsive to IL-15 to IL-15-responsive NK developmental intermediates and then transition to mature NK cells. Those steps require stimulations from several factors such as IL-3, IL-7, c-kit ligand, and flt3 ligand [130]. A study in a mouse model reported that mice deficient for IL-15 or the IL-15 receptor components still had normal numbers of NK precursors. This study indicates the role of IL-15 is acting to maintain the viability and facilitate the proliferation of developing NK cells instead of a differentiation factor at an early-stage [134]. Nonetheless, some groups revealed that humans or mice lacking IL-15 or IL-15 receptor components were deficient in NK cells to a much greater extent compared to those lacking IL-2 or IL-7 signals [133].

A number of transcriptional factors and pathways were identified that drive changes in gene expression during different stages of NK cell development. Id2, which was an inhibitory protein of basic helix–loop–helix transcription factors, was reported to block the differentiation of T, B, and pDCs from $CD34^+$ HPCs. Id2 is also a critical factor for NK cell early development as Id2−/− mice were are in NK precursors [122, 135]. Notch signaling is known to trigger the commitment of both T cell and NK cells from $CD34^+$ HPCs [136, 137]. Ets-1, PU.1, Ikaros are also regarded to play important roles in early NK cell development [68]. Acquisition of full cytotoxicity and cytokine secretion functions and developing into mature NK cells also need certain specific transcription factors such as Gata-3, T-bet, eomesodermin, NF-κB, CEBPγ, MITF, IRF-1 and IRF-2 [68, 129, 138]. However, except Id2, the transcription factors mentioned above are not only specifically implicated in the development of NK cells but also other lymphoid lineages [68]. Not surprisingly, another candidate transcription factor that tends to specifically drive NK cell development is E4BP4 which regulates the expression level of Gata-3 and Id2 [139]. More evidence was reported that E4BP4-deficient mice lack mature NK cells but maintain the normal number of T and B cells [140, 141]. Notably, E4BP4 was proposed to

function downstream of the IL-15 signaling pathway, highlighting the importance of IL-15 in NK cell development [139].

1.3.4 NK cell education

"Missing self" recognition, a critical part of NK cell surveillance, means that NK cells can differentiate "self" and "non-self" by detecting the level of autologous MHC-I molecules expressed on target cells (e.g. tumor cells) using their inhibitory receptor such as Ly49 in mouse or KIR in humans [84]. NK cells need to be trained to properly interact with the MHC-I molecules before acquiring the full functions during the development in bone marrow, which is known as the "NK education" process [142]. The work on NK education followed the discovery of the hybrid resistance in mice in the 1960s to 1970s that researchers observed that the parental bone marrow transplants were rejected by some unknown bone marrow-derived cells of the F1 hybrid mice in a thymus-independent manner [143-145]. NK cells were then successively found to be implicated in this MHC-I-mismatch-induced rejection [146-148]. Soon afterward, it was thought that every NK cell expresses at least one inhibitory receptor for self MHC-I [149, 150], and the interaction between inhibitory receptors on NK cells and MHC-I molecules was necessary to develop functional NK cells [151-155]. However, researchers observed that there were numbers of NK cells with mature characteristics in humans and mice without expressing any inhibitory receptors that can bind autologous MHC-I molecules [152, 155, 156]. Distinct from T cell selection in the thymus, NK cells do not undergo a process of clonal deletion in humans and mice because normal individuals still have hyporesponsive but not autoreactive NK cells [152, 153, 155, 157-161]. Interestingly, studies showed that mature NK cells with or without normal responsiveness can be re-educated to change their responsiveness and functionality through engrafting into a different MHC class I environment [162, 163]. Furthermore, a more recent study reported that hyporesponsive human NK cells can acquire KIR

expression and became functional only through cytokine stimulation suggesting the responsiveness can also be changed in the periphery [164].

Several models were proposed to depict how NK cells selectively become anergic or responsive through the education process and all those models highlighted the necessity of the signaling from inhibitory receptors upon binding to MHC-I molecules [142]. Direct evidence is that the mutations of immunoreceptor tyrosine-based inhibitory motif (ITIM) in the inhibitory receptors made NK cells tend to be hyporesponsive in the presence of the cognate MHC-I ligands [152]. KIR and Ly49 receptor families are both polygenic and polymorphic, expressed in a partially stochastic and heterogeneous fashion on NK cells, and interact with polymorphic MHC-I ligands, and all of which make NK cells a highly heterogeneous population [165]. Conceivably, given the complexity of those inhibitory receptors and MHC-I molecules, NK cells may gain different responsiveness in the education process due to the different ligand-receptor interacting strength [154, 165, 166] and form unique subsets with distinct inhibitory receptor repertoires through unidentified mechanisms [142, 167]. Besides the NK education process through Ly49 or KIR with self-classical MHC-I molecules, some other inhibitory receptors including CD94-NKG2A, 2B4, NKR-P1B, and more are also shown to involve in NK education through recognizing non-classical MHC-I or non-MHC-I molecules [168]. Furthermore, a "confining model" which was derived from a recent discovery of the receptors compartmentalization on the NK plasma membrane explains how NK cells acquire efficient responsiveness from the education process [168]. This model highlights the role of adhesion molecules in coordinating both inhibitory and activating receptors in the education-induced well-confined compartmentalization [168]. Given that both LILRB1 and KIR are inhibitory receptors and bind MHC-I and share similarities in many aspects which will be introduced below, it is still unknown whether LILRB1 plays a role in NK cell education.

1.4 LILRs family

The human LILR family proteins are encoded within the LRC spanning around 1 million base pairs (bp) of chromosome 19q13.4 neighboring to the highly related KIR loci [169, 170], and consists of five inhibitory (B1, B2, B3, B4, B5) and four activating (A1, A2, A4, A5, A6) transmembrane receptors, one soluble receptor (A5), and two pseudogenes (P1, P2) [171]. Those 11 genes are distributed in two clusters, centromeric and telomeric cluster, based on the relative position on the chromosome. The two clusters are separated by around 200 kb and the genes in these two clusters are organized in opposite transcription orientations [172] (Figure 1.3). This family was discovered much later than KIRs in the late 1990s [173], and are homologous to the paired immunoglobulin-like receptors (PIRs) and gp49 receptor from mice [174]. Similar to KIRs, all members of LILRs possess at least two extracellular C-2 type Ig domains. The activating and inhibitory receptors are also defined by the tyrosine-based motifs on the cytoplasmic tail and whether the transmembrane domain is able to associate with signaling adaptor proteins as introduced above [174]. Different from KIRs, the adaptor protein that forms a complex with activating receptors in the LILR family is the Fc receptor gamma chain (FcγR) [175]. Many genes from the KIRs and LILRs are highly polymorphic and exhibit extensive allelic variabilities and copy-number variations. Although LILRs are relatively conserved in gene organization compared with KIRs, both families have rapidly evolved to result in substantial interspecies differences which makes it difficult in the study of their functions and regulation in animal models [174, 176-178].

LILR receptors are widely expressed on myelomonocytic cells and partially expressed on lymphoid lineages, osteoclasts, endothelial cells, placental cells, and vascular smooth muscle cells [179]. Each family member displays a unique expression pattern on immune cells and can be constitutively expressed or induced under particular conditions [180]. Although MHC-I molecules are considered as the main ligands for LILRs e.g. LILRB1, B2, B5, A1, and A3, a large diversity of ligands have been reported to bind LILR family receptors in recent years. Those different types of ligands range from host immune-modulatory proteins, endogenous

proteins found in the central nervous system to intact bacteria and virus [181] (Figure 1.3). The wide expression and broad spectrum of ligands mean that LILRs are involved in many biological processes including innate/adaptive immune responses to cancer and infections, immune tolerance, inflammation, hematopoietic differentiation, and neurogenesis. Reciprocally, the genetic diversity of LILR genes has been linked to disease susceptibility, and the multifunctional regulatory role of LILR receptors make them potential modulators in some immune-related pathologies and targets for immunotherapies [171, 178-180, 182-184]. As the focus of my thesis is LILRB1 and NK cells, the following part of this chapter is a detailed review of the LILRB1 literature.

1.5 LILRB1 (CD85j/LIR-1/ILT2/MIR7)

LILRB1 was first cloned and reported as an inhibitory receptor for the cytotoxic response of NK and T cells through binding with MHC-I molecules by Colonna and colleagues in 1997 [185, 186]. Later in the same year, another group independently discovered the LILRB1 receptor and found it was able to bind MHC-I and HCMV-encoded MHC-I homolog UL18 [60]. Both groups revealed the broad expression of LILRB1 on immune cells and that myelomonocytic cells and B cells had predominant LILRB1 expression while subsets of NK and T cells expressed LILRB1 [60, 186]. With increasing numbers of studies highlighting its immune-regulatory role, this multifunctional receptor LILRB1 is currently regarded as a target of pathogen immune evasion, a potential regulator for immune cell differentiation and a potential therapeutic target in cancer [187].

1.5.1 LILRB1 functions in NK cells and other immune cells

LILRB1 contains 4 extracellular Ig-like domains (i.e. D1-D4 from the N- to C-terminus), a stem region, a transmembrane domain, a cytoplasmic tail with 4 tyrosine-based motifs where the distal two can directly recruit SHP-1 phosphatase [188]. LILRB1 is the only LILR receptor

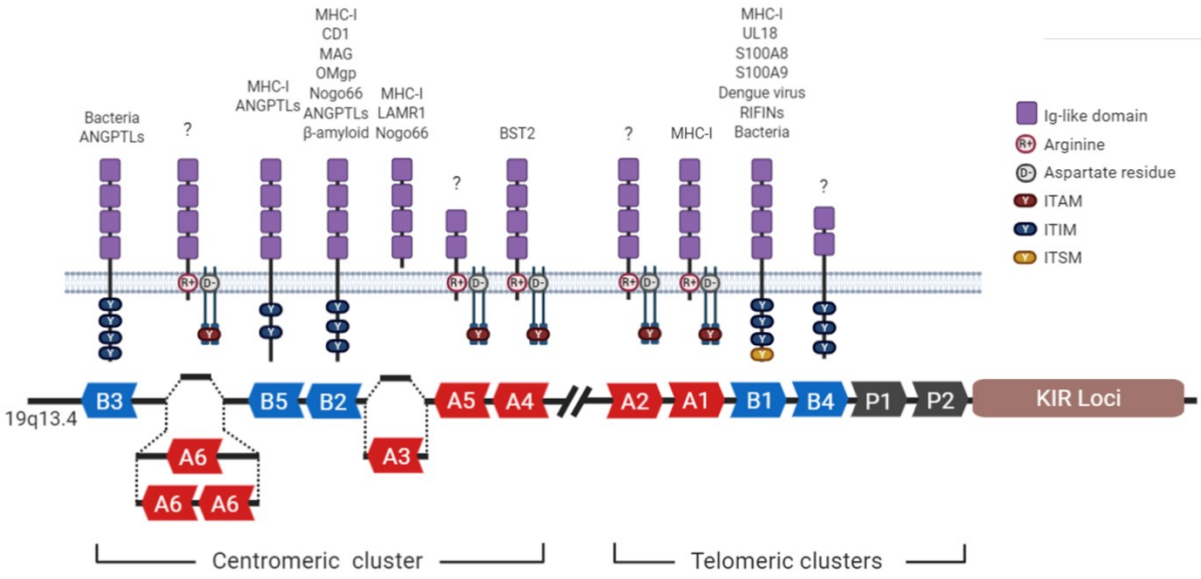

Figure 1.3 Genomic organizations of LILR family genes and schematic LILR receptors. LILR genes are located next to KIR loci in the LRC region mapped on chromosome 19q13.4. LILR genes are organized to form two clusters based on the relative position to centromere or telomere where the genes inside of each cluster have the same transcription direction as depicted by the arrowheads. The copy number variation of LILRA3 and LILRA6 is depicted. The genes encoding activating, inhibitory receptors, and pseudogenes are filled with red, blue, and grey, respectively. Corresponding translated proteins of each gene are shown above with currently known natural ligands listed. Structures of LILR receptors can be differentiated by the number of extracellular Ig-like domains, a transmembrane domain and associated FcγR, and tyrosine-based motifs on the cytoplasmic tail. ANGPTLs, angiopoietin-like proteins; MAG, myelin-associated glycoprotein; OMgp, oligodendrocyte myelin glycoprotein; LAMR1, 37/67 kDa laminin receptor; BST2, bone marrow stromal cell antigen 2; RIFINs, repetitive interspersed families of polypeptides.

expressed in NK cells [104]. However, the mice ortholog of LILRB1, PIR-B, is expressed in B cells and myeloid cells but not NK cells [189]. It has been shown that NK cytotoxicity and cytokine production can be inhibited by broad alleles of MHC-I molecules and UL18 by engagement of LILRB1. Many studies support that the expression of LILRB1 on NK cells negatively controls HCMV dissemination and cancer [186, 190-196]. Furthermore, engagement of LILRB1 with HLA-G which is a non-classical MHC-I molecule and highly expressed on trophoblast cells was reported to inhibit NK cell cytotoxicity, which suggests a protective role of LILRB1 in fetal tolerance [197]. Moreover, a recent study found that the LILRB1 expressed on a unique subset of $CD49a^{+}Eomes^{+}$ decidual NK cells can interact with HLA-G and enhance growth-promoting factors secretion in early pregnancy [198], which highlighted the contribution of LILRB1 to fetal development.

Similarly, most studies demonstrated that the LILRB1 expressed on T cells is inhibitory to antigen recognition, CD3/TCR-mediated activation, cytotoxic response, cytokine production, and proliferation through engagement with MHC-I or UL18 [186, 199-203]. However, one study reported that $CD8^{+}$ T cells lysed HCMV-infected fibroblasts *in vitro* dependent on the LILRB1-UL18 axis in a non-MHC-restricted fashion [204]. Another study discovered a new ligand S100A9 for LILRB1 and its ligation with LILRB1 enhances the ability of NK cells to control the replication of human immunodeficiency virus type 1(HIV-1) in $CD4^{+}$ T cells *in vitro* [205]. Similar to the one focused on $CD49a^{+}Eomes^{+}$ decidual NK cells, these studies proposed an activating role of LILRB1 on $CD8^{+}$T cells and NK cells. About ten years ago, a study reported the interaction of LILRB1 with HLA-G in human decidual macrophages and NK cells played an activating role in cytokine secretion. They found the last tyrosine-based motif on the LILRB1 cytoplasmic tail was an immunoreceptor tyrosine-based switch motif (ITSM) [206]. ITSM transduces signals in a context-dependent manner and can selectively recruit SHP-2, SHIP phosphatase, SAP, EAT-2 adaptor proteins, the Src family kinase Fyn or the p85 subunit of phosphatidylinositol-3 kinase, dependent on the type of receptors and the type of immune cells to transduce an activating or inhibitory signal [207, 208]. Intriguingly, a study on T cell revealed

that HLA-G and LILRB1 interaction inhibited cell proliferation dependent on the activation of SHP-2 but not SHP-1[200], presumably involves the ITSM of LILRB1. Thus, the presence of the ITSM on the cytoplasmic tail may make LILRB1 selectively exhibit activating or inhibitory functions in different scenarios. LILRB1 was also shown to inhibit early B cell activation and subsequent production of antibody and cytokines [186, 209]. In an earlier study, LILRB1 was also demonstrated to inhibit Fc receptor-mediated activation of monocytes [210]. LILRB1 was recently reported to be expressed on over half of the tumor-associated macrophages and *in vitro* and *in vivo* disruption of LILRB1 or its ligand MHC-I enhanced phagocytosis of tumor cells by macrophages under the condition of blocking SIRPα-CD47 axis, which makes LILRB1 a potential target of cancer immunotherapy [211]. Studies on dendritic cells (DCs) revealed that LILRB1 plays roles in modulating the phenotype profile and survival during the differentiation from monocyte precursors, inhibiting early activation, cytokine secretion and stimulatory effect on T cell proliferation [186, 212, 213].

1.5.2 Ligands of LILRB1

The most well-studied ligands for LILRB1 are MHC-I molecules associated with β2m including HLA-A, B, C, E, F, G, and HCMV-encoded MHC-I homolog UL18. The D1-D2 domains of LILRB1 have been co-crystallized with HLA-A2, HLA-G, HLA-F, and UL18, respectively, and recently, the co-crystallization of the 4 Ig domains of LILRB1with HLA-G was resolved [214-218] (Figure 1.4A). These studies revealed a similar interacting pattern between LILRB1 and the homologous ligands in which the D1 and D2 domains of LILRB1 directly contact the α3 and β2m domains in a highly conserved docking orientation (Figure 1.4B). It is worth mentioning that the co-crystallization of HLA-G1 with all the four Ig-like domains of LILRB1 showed that D3 and D4 domains worked as a scaffold rather than directly interacting with the ligand [215]. Given that α3 is relatively non-polymorphic compared with the peptide-binding domains α1 and α2 from the MHC-I heavy chain, and that β2m is highly

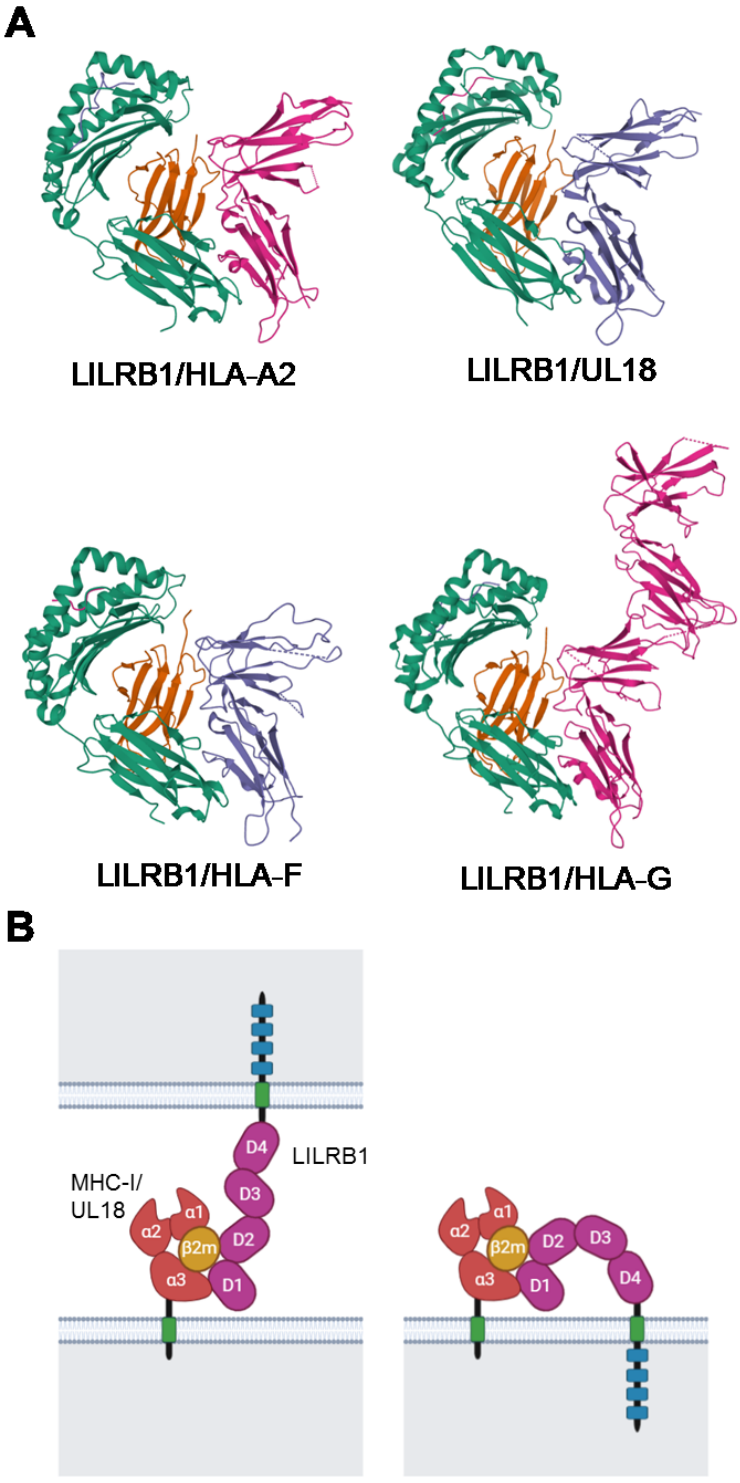

Figure 1.4 Co-crystallization and schematic interaction of LILRB1 with MHC-I/UL18. (A) Co-crystallization of LILRB1 with HLA-A2 (PDB: 4NO0), UL18 (PDB: 3D2U), HLA-F (PDB: 5KNM), HLA-G (PDB: 6AEE), respectively. (B) *Trans*-interaction (left) and proposed *cis*-interaction (right) between LILRB1 and MHC-I/UL18.

conserved among species [219], it is not surprising that LILRB1 is capable to bind a broad range of MHC-I molecules and UL18 in a similar molecular fashion. Consistently, most of the residues that form contact with LILRB1 are conserved among different classical and non-classical MHC-I molecules [220]. Nevertheless, the binding affinities of those homologous ligands with LILRB1 are significantly different. UL18 was reported to have the highest binding affinity with LILRB1 with an equilibrium dissociation constant (K_D) at the nanomolar level while the binding affinities of MHC-I molecules are various but all ranges from 15 to 100 μM [221]. HLA-G was subsequently shown to have 3 to 4 fold higher binding affinity than classical MHC-I molecules [222]. A recent study determined that the peptide-bound β2m-HLA-F has a 2 μM binding affinity with LILRB1 which makes HLA-F the strongest ligand among human MHC-I molecules for LILRB1 but still not that close to UL18 [217]. Compared with MHC-I/LILRB1, UL18/LILRB1 complex has more contacting residues, a larger buried surface area, and more H-bonds and van der Waals contacts in between, which are consistent with the much higher affinity of UL18 binding with LILRB1 [215]. It has been speculated that the heavily coated N-linked glycans on UL18 might be another potential reason for its high affinity [221], and this is supported by an early study that reported the importance of the correct glycosylation of UL18 in its inhibitory effect on NK lysis [61]. However, UL18 produced from insect cells with shortened N-glycans showed only slightly decreased binding affinity to LILRB1 compared with that produced from mammalian cells [221]. More experimental evidence is needed to explain the role of N-glycans on UL18 in the interaction with LILRB1. In addition, spontaneous mutations in α1 and α3 domains of UL18 among HCMV strains impact the binding affinity with LILRB1 [223]. The possible reason for the impact of the mutations in the α1 domain is that those mutations are close to and may directly interact with the hinge region between the D2 and D3 domains of LILRB1 as indicated by structural modeling [223].

Besides *trans*-interaction, LILRB1 also interacts with MHC-I molecules in *cis* on the surface of the same cell (Figure 1.4B). The first report of a *cis*-interaction was for the mouse homolog of LILRB1, PIR-B which was shown to constitutively *cis*-interact with MHC-I on

mouse mast cells using fluorescence resonance energy transfer (FRET), and this *cis*-interaction may transduce inhibitory signals and control mast cell activation [224]. The same group subsequently provided evidence for the *cis*-interaction of LILRB1 with classical MHC-I molecules using the same method on human osteoclasts. Importantly, LILRB1 was found constitutively tyrosine-phosphorylated and associated with SHP-1 which may down-regulate osteoclast differentiation [225]. Our group previously demonstrated that the *cis*-interaction of LILRB1 with MHC-I molecules influences the accessibility of specific LILRB1 antibodies and the binding of ligands in *trans* [226]. In addition, the *cis*-interaction of LILRB1 with MHC-I presumably has a similar contact interface as for the *trans*-interaction since the *cis*-interaction can be disrupted using an MHC-I antibody which blocks the functional *trans*-recognition of MHC-I by LILRB1 [226]. This hypothesis was supported by another study that proposed a model of *cis*-interaction between LILRB1 and HLA-G [215].

From the initial discovery of MHC-I and UL18 as the ligands of LILRB1, the spectrum of LILRB1 ligands was extended to some degree. As mentioned above, S100A8 and S100A9 which are expressed by phagocytic myeloid cells were found as novel ligands for LILRB1 and could potentiate NK cell-mediated control of HIV-1 infection of $CD4^+$ T cells [205]. However, as non-MHC-I molecules, the mechanism by which S100A8 and S100A9 interact with LILRB1 was not further investigated in the study. Besides the ligands expressed on the cell surface, LILRB1 is able to directly interact with the intact dengue virus, malaria, and bacteria, although the molecules that LILRB1 directly contacts were not fully understood [227-229]. The plasticity of LILRB1 to interact with ligands with various conformations makes it reasonable to be exploited by different types of pathogens to induce inhibitory signals in immune recognition.

1.5.3 The interplay of HCMV with NK cells through LILRB1/UL18

UL18 was first discovered when researchers noticed an HCMV glycoprotein protein can bind β2 microglobulin (β2m) normally bound with the MHC-I α chain. However, the amino acid

sequence of UL18 shares just over 20% similarity with MHC-I molecules [230]. Similar to MHC-I, UL18 also contains a peptide-binding groove that can be occupied by cellular peptides [231]. However, it is difficult to express UL18 *in vitro* in the absence of the HCMV genome [232, 233].

As mentioned above, NK cells play a crucial role in the early defense of HCMV infection and UL18 is an immune evasion protein of HCMV targeting NK cell receptor LILRB1. The bulk of the UL18 is shielded by the extensive glycosylation. This glycosylation blocks the binding site for TCR or killer-cell immunoglobulin-like receptors (KIRs) but leaves the contact region with LILRB1 exposed [230, 234]. To date, although it has been shown that the NK activating receptor NKG2C/CD94 can weakly interact with UL18 [235], LILRB1 signaling can still be dominant due to its a 1000-fold higher binding affinity with UL18 than NKG2C/CD94 when the two receptors are co-expressed. Many studies suggested that the interaction of LILRB1 with UL18 is important in the immune response of NK cells to HCMV and most of them supported an inhibitory role of UL18 (or its mouse counterpart m144) in NK cells functions [61, 192, 236-239]. However, one early study suggested that UL18 enhanced NK cell killing [233]. Notably, UL18 has also been shown to inhibit LILRB1-positive NK cells but activate LILRB1-negative NK cells through an unknown mechanism [191], implying the activating or inhibitory effect of UL18 on NK cells is influenced by LILRB1 expression. The aforementioned activating receptor NKG2C/CD94 may be mediating the activating role of UL18 on LILRB1-negative NK cells. The shielding from TCR binding and maintaining a high-affinity binding with LILRB1 but a much lower affinity with NKG2C, suggests that UL18 is a highly evolved evasion protein that captured the MHC-I structure but acquired lots of alteration upon interplay with NK cells.

HCMV infection can modulate the NK cell receptor repertoire including LILRB1. A higher proportion of LILRB1-positive NK cells and also T cells was observed in HCMV seropositive donors compared with the seronegative donors [203, 240, 241]. Consistently, LILRB1 expression is increased on recently expanding NK cells during acute HCMV infection [79].

LILRB1 surface expression on NK cells was higher in renal transplant patients with active HCMV infection [242]. In lung transplant patients, an early increase of LILRB1-positive lymphocytes, particularly NK and T cells, was detected prior to the onset of HCMV disease [203, 243]. All these studies above indicate that HCMV infection leaves a significant imprint of LILRB1 expression on NK cells and T cells, and in turn, LILRB1 expression on NK cells and T cells could potentially be exploited as a marker for predicting the development of HCMV disease in transplant patients. Considering the immunosuppressive treatment in transplant patients largely impairs antiviral immunity of T cells while leaving NK cells less affected [244-247], our lab focuses on the NK cell response in transplant patients. In the following sections, I will describe what is known about the regulation of LILRB1 gene expression and our group's recent study on the association of LILRB1 gene polymorphisms with HCMV infection in transplant patients.

1.5.4 Lineage-specific transcriptional regulation of LILRB1 gene expression

LILRB1 has broad expression in the immune system but it also exhibits dramatic heterogeneity of expression patterns in diverse types of immune cells and different individuals. It was demonstrated by several groups that LILRB1 is expressed ubiquitously at high-density on circulating myeloid cells and at a relatively low level on only subsets of T cells and NK cells, and B cells have a LILRB1 expression pattern similar to myeloid cells [60, 186, 248]. These results suggest that LILRB1 gene expression involves cell-type-specific mechanisms. The study of transcriptional regulation for the LILRB1 gene was initiated in 2003 by characterizing a promoter close to the translation start codon (currently known as the proximal promoter). Strong transcriptional activity of a ~1kb sequence upstream of the transcription start site was observed in a myeloid cell line THP-1 while only mild activity was documented in a T cell line Jurkat and 293 cells. The core promoter mapped from -101 to -155 relative to the transcription start site was found to associate with transcription factors Sp1 and PU.1 binding [249]. This was the first

study to provide evidence that the LILRB1 gene has lineage-specific regulation. With the discovery of a distal exon (currently known as exon 1) located ~13 kb upstream of the translation start codon in 2010, researchers uncovered that lymphocytes primarily initiated LILRB1 gene transcription using a promoter up to 2000 bp from this distal exon [248]. Notably, almost all the transcripts from monocytes do not contain this distal exon, which strongly indicates that lymphocytes and monocytes use the distal and proximal promoter, respectively, to transcribe the LILRB1 gene. They further observed that the distal exon exhibited an effect in repressing the translation of LILRB1 protein, which provides an explanation for the relatively low LILRB1 density expressed on lymphocytes relative to monocytes, especially if they have similar levels of transcript [248]. Nevertheless, the LILRB1 protein translated from lymphocytes and monocytes are identical since the distal exon belongs to the 5'-untranslated region (UTR). Our group later defined a 126 bp (-14086 to -13966 from the ATG) core region for the distal promoter and with a functional JunD binding site that is required for expression in NK cells [250].

1.5.5 Heterogeneous LILRB1 expression in NK cells

The heterogeneous expression pattern in a single individual is another level of LILRB1 expression heterogeneity. Take NK cells as an example, individual NK cells are highly heterogeneous and consist of LILRB1-negative NK cells and LILRB1-positive NK cells with different surface densities. Moreover, the frequency of LILRB1-positive NK cells differs among individuals ranging from 20% to 80% positive [3]. Both of LILRB1 protein and mRNA level correlates well with the frequency of LILRB1-positive NK cells among individuals, indicating the heterogeneous LILRB1 expression patterns on NK cells are mainly derived from the transcription level [3]. It is unclear why NK cells in one person have subsets with different LILRB1 expression

This indicates the differences are mainly derived from the transcription level. It is unclear why NK cells in one person have subsets with different LILRB1 expression While the mechanism underlying heterogeneous LILRB1 expression in NK cells and the variation in the LILRB1-positive NK cell frequency is unknown, our group and others have linked particular haplotypes with the frequency of LILRB1-positive NK cells [3, 251], a feature reminiscent of the expression patterns of the highly related and syntenic KIRs. Similarly, KIR has allele-specific expression patterns of variegation [252] and KIR expression is acquired at a late stage of NK differentiation as is LILRB1 [253]. The KIR expression patterns are correlated with DNA methylation at the promoter region [254-256] and the DNA methylation is believed to keep LILR genes quiescent [249]. Given that NK cells primarily use the distal promoter to transcribe the LILRB1 gene, and previous data from our group showed that the proximal promoter was active in NK cell lines using a luciferase reporter assay [257], the repressed activity of the proximal promoter in NK cells is likely mediated by epigenetic mechanisms. Indeed, our group previously observed that multiple CpGs located in the proximal regulatory region (not CpG islands) of the LILRB1 gene have a higher DNA methylation rate in NK and B cells than in monocytes as illustrated in Figure 1.5, which might explain the low activity of the proximal promoter in lymphocytes [257]. Without CpG island in the promoter region of some KIR genes, our group found that a single CpG site in the core distal promoter of the LILRB1 gene exhibited a very low extent of methylation in NK and B cells as compared to the prominent methylation in monocytes, suggesting this methylation might prevent the transcript from the distal promoter in monocytes. It also fits with our previous observations that the monocytic cell line THP-1 cells can transcribe from the distal promoter when introduced by a plasmid *in vitro* [257].

During NK cell development, a probabilistic switch controls expression of KIR through a bidirectional promoter for which the relative strength of the forward activity over the reverse activity correlates with the frequency that a particular KIR gene will progress to the permanent expression [258, 259]. Polymorphisms within the bidirectional promoter are associated with

allele-specific frequencies of expression for a given KIR gene [252, 260]. Although multiple KIR genes can be expressed in a single NK cell, typically only one allele for each KIR gene is expressed, and a piwi-like system arising from the antisense transcript may silence the other allele of a KIR gene that has initiated reverse transcription [261]. Previous work from our group using a bioinformatics prediction tool and a reporter assay showed some evidence for a bi-directional promoter in the LILRB1 gene. Specifically, the proximal promoter has reverse activity and the activity was relatively weak in an NK cell line compared with that in a monocytic cell line [257]. It is possible that the reverse activity occurs during a developmental stage for NK cells or monocytes. Our group also tested the possibility of whether the proximal promoter could work as an enhancer to regulate the activity of the distal promoter in NK cells, and the reporter assay results appeared to indicate a negative regulatory role if any [257].

1.5.6 Dynamic regulation of LILRB1 by cytokines and disease

Our group has previously tracked LILRB1 expression from several healthy donors for a whole year and observed fluctuations of LILRB1-positive cell frequency for both NK and T cells over time. This made our group ask whether cytokines could influence LILRB1 expression of NK and T cells. LILRB1 expression was examined on *ex-vivo* NK cells and, of many cytokines tested, only IL-2 and IL-15, which are both important cytokines in NK cell development, were found to up-regulate both the frequency of LILRB1-positive NK cells and the surface intensity of LILRB1 on NK cells. The further reporter assay revealed that IL-2 increased the activity of the proximal promoter but inhibited the activity of the distal promoter in NK cells [262]. These results strongly suggest that LILRB1 expression can be modulated by the cell microenvironment *in vivo*. Figure 1.5 gives a comparison of currently known regulations of LILRB1 gene transcription in NK cells and monocytes.

The change of LILRB1 expression has been associated with a wide range of diseases. As mentioned above, HCMV infection is associated with the expansion of LILRB1-positive NK

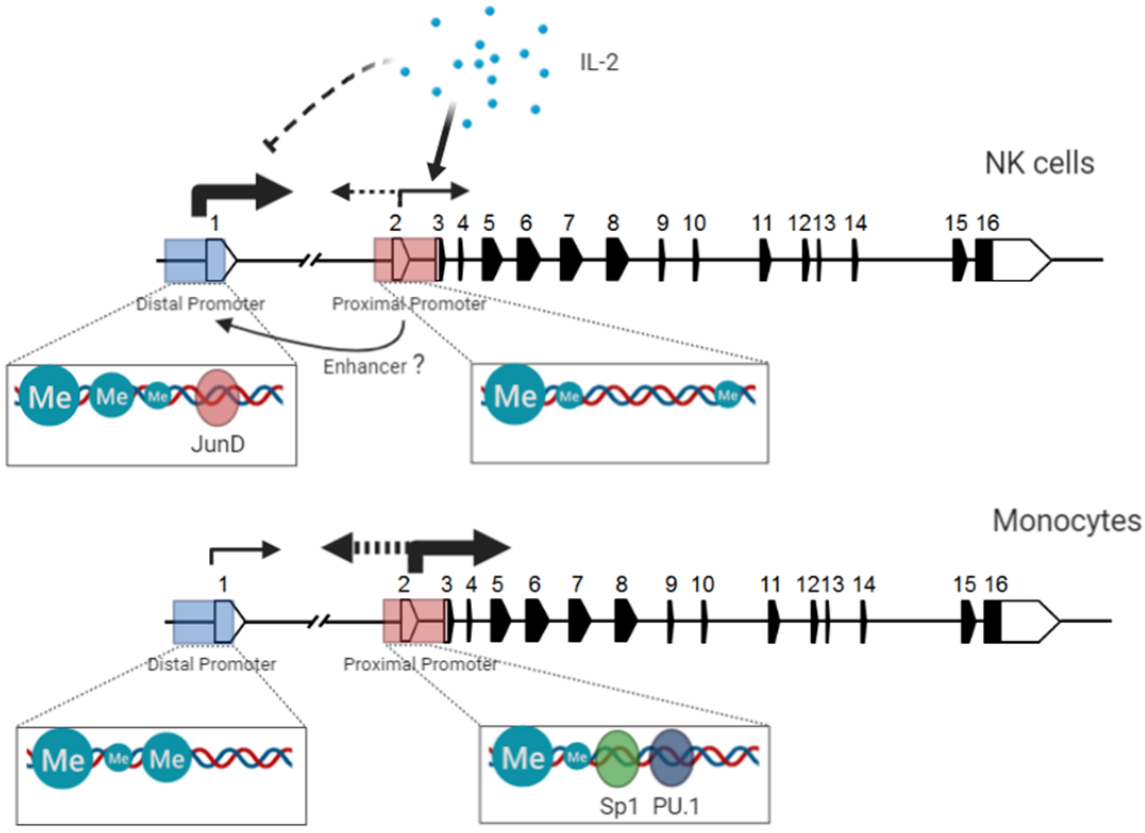

Figure 1.5 Transcriptional regulation of the LILRB1 gene in NK cells and monocytes. Schematics of LILRB1 gene transcription regulation in NK cells and monocytes are shown. Exons are numbered above and black filled parts indicate the protein-coding region. The distal and proximal promoters were highlighted by blue and red, respectively. Arrows suspended on promoters indicate the transcriptional direction. Arrows with dotted lines indicate the reverse transcription activity. The thickness of the arrows indicates the relative strength of transcriptional activity. CpG methylation is represented by an aquamarine circle with "Me" inside, and the circle size indicates the relative percentage of methylation.

cells and LILRB1 expression on other lymphoid cells can fluctuate with time particularly in response to HCMV replication [203, 241-243, 251]. It has been shown that the frequency of LILRB1-positive NK cells was increased in long-term non-progressor HIV patients [263]. LILRB1 expression was also found to be up-regulated on NK cells in patients with breast cancer [264]. It was demonstrated that the frequency of LILRB1-positive B cells and DCs from peripheral blood was significantly decreased in systemic lupus erythematosus (SLE) patients [265, 266], and a recent study found that LILRB1 transcript level was up-regulated in inflammatory $CD163^+$ DC3s in SLE patients [267]. The transcript level of LILRB1 and the increased frequency of LILRB1-positive cells of PBMCs are also associated with rheumatoid arthritis (RA), and autoimmune thyroid disease, respectively [268, 269]. For cardiovascular diseases, the proportions of LILRB1-positive circulating NK and T cells were increased in patients with atherosclerotic diseases, and LILRB1 protein expression was found to be expressed in the muscle lesions of idiopathic inflammatory myopathies [241, 270]. In addition, the expansion of LILRB1-positive circulating B cells in people infected by malaria has been reported [271]. Besides the association with diseases, the frequency of the LILRB1-positive decidual NK cells is also decreased in the first trimester of pregnancy [272]. To date, the cause and effect of LILRB1 heterogeneity and dynamic regulation in the immune system are poorly understood and more studies are necessary to gain knowledge of the basic molecular mechanisms involved in regulating LILRB1 gene expression in various cell types.

1.5.7 LILRB1 gene polymorphisms and the association with HCMV susceptibility in transplant patients

1.5.7.1 A general overview of LILRB1 gene polymorphisms

LILRB1 gene is highly polymorphic and has SNPs located in both the protein-coding region and the regulatory region [3]. Besides synonymous SNPs distributed along with the whole LILRB1 gene, there are four non-synonymous SNPs in the coding regions of D1 and D2

domains. Based on the data drawn from the 1000 Genomes Project [273], there are one major and several minor LILRB1 haplotypes involving the four non-synonymous SNPs (Figure 1.6A). Several non-synonymous SNPs are also found in the coding regions of D3, D4, the transmembrane domain, and the cytoplasmic tail [3].

We previously defined several haplotypes and their relationship to LILRB1 expression on NK cells in healthy individuals [3]. More specifically, individuals with SNPs rs1004443-A, rs3760860-G, and rs3760861-G located in the proximal regulatory region of the LILRB1 gene have a higher frequency of LILRB1-positive NK cells and a higher surface expression level on NK cells. However, a previous study from another group demonstrated the haplotype "AGG" was associated with lower surface expression of LILRB1on lymphocytes or monocytes from Japanese donors [274]. Both their and our group revealed strong linkage disequilibrium (LD) between the SNPs in the protein-coding region and that in the proximal regulatory region (Table 1). We denote the haplotype "AGG" and its counterpart "GAA" as the "high" and "low" haplotype, respectively, with respect to their association with the frequency of LILRB1-positive NK cells. We further extended these haplotypes to the distal regulatory region as illustrated in Figure 1.6B. The haplotype "AGG" mentioned above has been associated with the susceptibility to RA in Japanese [274] and better control of respiratory syncytial virus infection in infants [275]. Moreover, the genotype of the non-synonymous SNP rs1061680 was reported to be associated with HCMV-disease in Caucasian HIV patients [276].

1.5.7.2 LILRB1 polymorphisms and HCMV susceptibility in transplant patients

Given the ability of UL18 to inhibit NK cell responses and the apparent importance of NK cells in controlling HCMV replication, our group genotyped transplant patients for the LILRB1 gene to test the original hypothesis that individuals with a higher frequency of LILRB1-positive NK cells would exhibit worse control of HCMV replication. Details for patients' information and experimental design can be found in our recently published paper [277]. We selected five

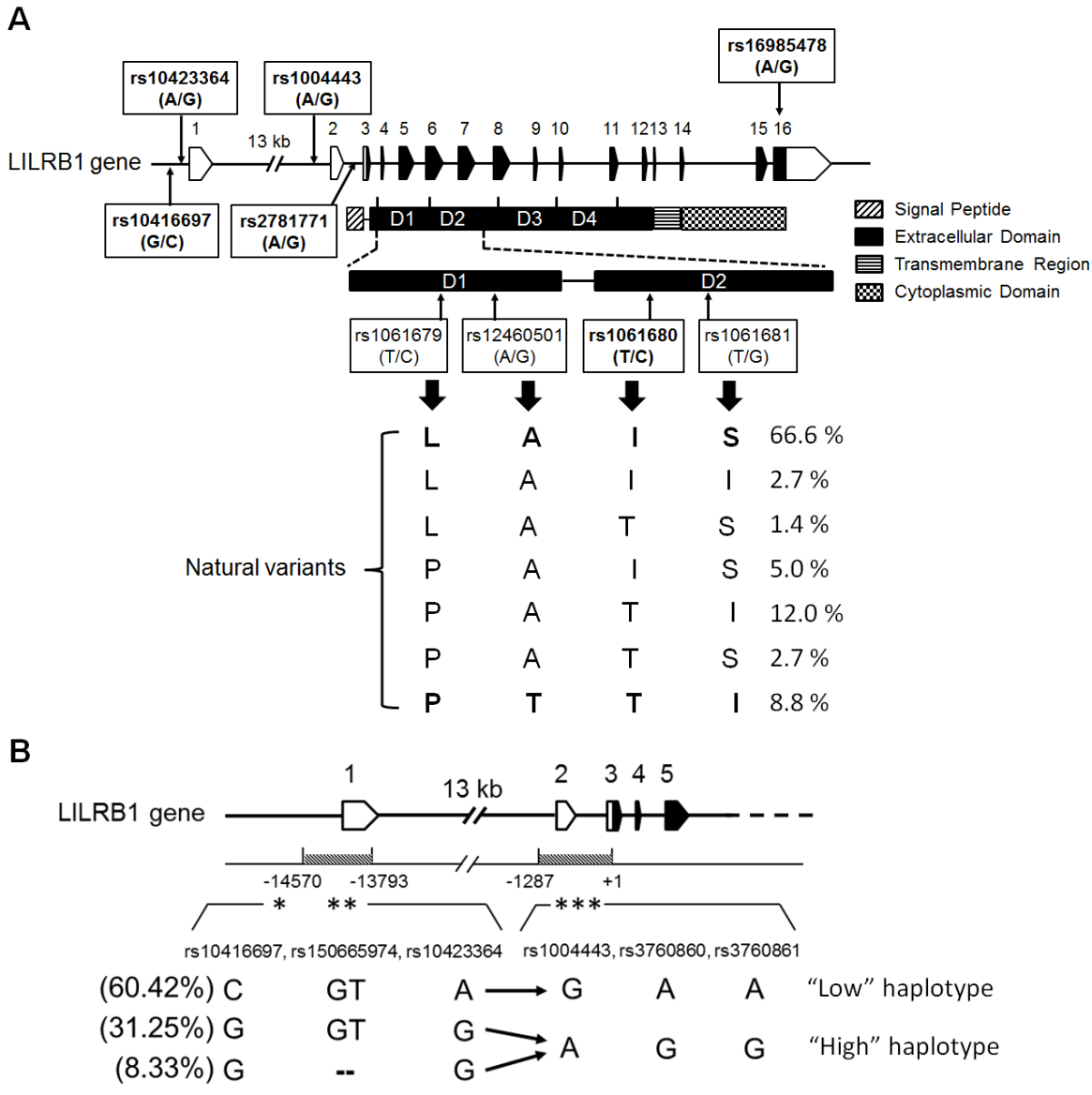

Figure 1.6 LILRB1 gene polymorphisms and haplotypes focused on in this study.
(A) Schematic of the LILRB1 gene with the location of SNPs that are focused on in this study. The protein-coding region is filled with black and the corresponding protein structure was mapped underneath. SNPs highlighted in bold indicate the ones focused on in the study of transplant patients. Natural protein variants resulted from the non-synonymous SNPs located in the D1, D2 domains, and their frequency in the European population are shown. Uppercase letters indicate the possible amino acid in each position. (B) A schematic diagram of the SNPs used to define the "low" and "high" haplotypes and the extended haplotypes in the distal regulatory region. Distal and proximal promoters are marked by the shaded regions and the location is indicated by the distance from the LILRB1 translational start site.

Table 1 LD values acquired from the 1000 Genomes Project phase 1 on European populations. (Published in Yu et. al. Table 1 [277])

LD (r^2)	***rs10416697***	***rs10423364***	***rs1004443***	**rs1061679**	**rs12460501**	***rs1061680***	**rs1061681**
rs10416697	-	0.98	0.98	0.91	0.22	0.76	0.50
rs10423364		-	**1.00**	**0.92**	**0.22**	**0.76**	**0.50**
rs1004443			-	0.92	0.22	0.76	0.50
rs1061679				-	**0.24**	**0.68**	**0.53**
rs12460501					-	0.29	0.28
rs1061680						-	**0.65**
rs1061681							-

Bold indicates SNPs analyzed in transplant patients.

SNPs for analysis spreading throughout the LILRB1 (Figure 1.6A). In detail, we used rs10416697 at -14895 from the translational start site in the distal promoter region and rs1004443 (-1026) that form extended haplotypes in the regulatory domains (Figure 1.6B). The third SNP (rs2781771) is at -225 relative to the start codon in intron 2. The fourth SNP (rs1061680) causes a non-synonymous substitution in the second immunoglobulin domain of the receptor previously examined in the context of HIV and HCMV as mentioned above [276]. The final and most 3' SNP tested is at position +5724 relative to the translational start site (rs16985478), with a second non-synonymous change in the cytoplasmic tail that encodes a potential ubiquitination site [3]. In a small cohort with 67 Canadian transplant patients [278], we found that the patients, particularly the kidney transplant patients, homozygous of the minor allele at rs10416697 and rs1061680 which linked with the "low" haplotype and were more prone to presenting HCMV disease (Figure 1.7A and 1.7B), which is counter to our prediction that patients with more LILRB1-positive NK cells ("high" haplotype) would have a higher incidence of HCMV disease.

The putative association of the SNP rs1061680 and rs10423364 which is a potential surrogate of rs10416697 (r^2=0.98) (Table 1) with HCMV asymptomatic infection and/or disease was then validated in a larger cohort from the Swiss Transplant Cohort Study (STCS) which includes 1080 Caucasian STCS solid organ transplant (SOT) recipients [279]. We found that kidney transplant patients, particularly the HCMV-positive ones, homozygous for the minor alleles of rs10423364 and rs1061680 which linked with the "low" haplotype were associated with a higher incidence of HCMV infection (Figure 1.7C and 1.7D). Altogether, these results reveal a possible role of genetic variation in LILRB1 in influencing the control of HCMV in transplant patients, and the patients with homozygous "low" haplotypes are proposed to have poorer outcomes.

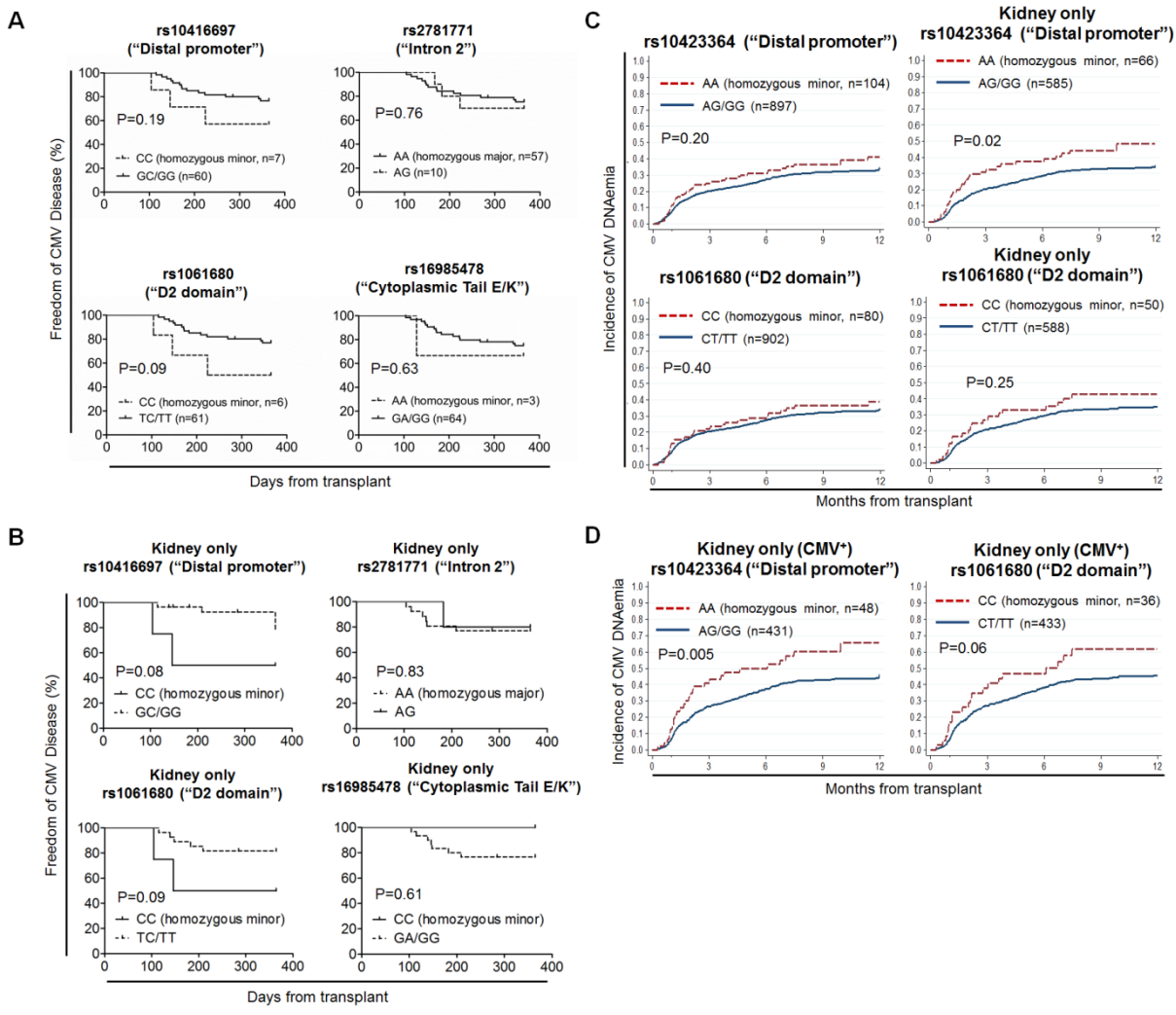

Figure 1.7 LILRB1 genotype and control of HCMV replication in transplant patients. (A) Disease-free survival rates for HCMV disease of 67 D+/R– Canadian transplant patients genotyped for the indicated SNPs. The P values indicated in each graph were determined by log-rank (Mantel-Cox) test. (B) Incidence of HCMV disease in kidney transplant patients from the Canadian cohort genotyped for the indicated SNPs. (C) Incidence of HCMV DNAemia genotyped for rs10423364 and rs1061680 of all the SOT patients or kidney patients from the STCS. (D) Incidence of HCMV DNAemia of D+/R– or R+ STCS kidney transplant patients genotyped for the indicated SNPs. (Published in Yu et. al. Figure 1, Supplemental Figure 2 and 3. [277])

1.6 Research focus and objectives

Our group and others have demonstrated differential LILRB1 expression patterns on NK cells are associated with LILRB1 polymorphisms as introduced above. To address the question regarding how the polymorphisms influence LILRB1 expression on NK cells, our group previously performed a luciferase reporter assay to compare the activity of the distal promoters from the "high" and "low" haplotypes but did not detect a significant difference [277] (Figure 1.8A). Considering that the DNA methylation status is different at the promoter regions among different lineages, we were wondering whether or not the "high" and "low" haplotype have differential DNA methylation status at the distal promoter in NK cells which may lead to differential promoter activity. Our lab previously examined the DNA methylation of the distal promoter from the two haplotypes within isolated individual NK cell clones and found that only one CpG site showed different percentages of methylation (Figure 1.8B). Given that the DNA methylation at the promoter region of KIR genes repressed the gene expression in NK cells [254], it is possible that a negative regulator occupies the under-methylated site or a positive regulator requires the methylation. However, this result does not fit well with the silencing role of DNA methylation for KIRs. Considering that enhancers are crucial elements controlling the cell-type-specific and spatial-temporal gene expression, in Chapter 3, I tested the hypothesis that the LILRB1 has additional regulatory regions besides the promoters.

Data from the transplant patients study shown in Figure 1.7 described an association of LILRB1 gene polymorphisms in the regulatory regions and a ligand-binding domain with the control of HCMV in transplant patients. Based on the results that transplant patients with the particular genotype (homozygous "low" haplotype) conferring relatively lower LILRB1 expression on NK cells showed worse control of HCMV, I accordingly modified our original hypothesis to that the LILRB1 protein variants produced from the "low" haplotype have stronger functional inhibition to NK cells compared with that produced from the "high" haplotype (Figure 1.9). The test of this new hypothesis is elaborated in Chapter 4. Furthermore, based on a

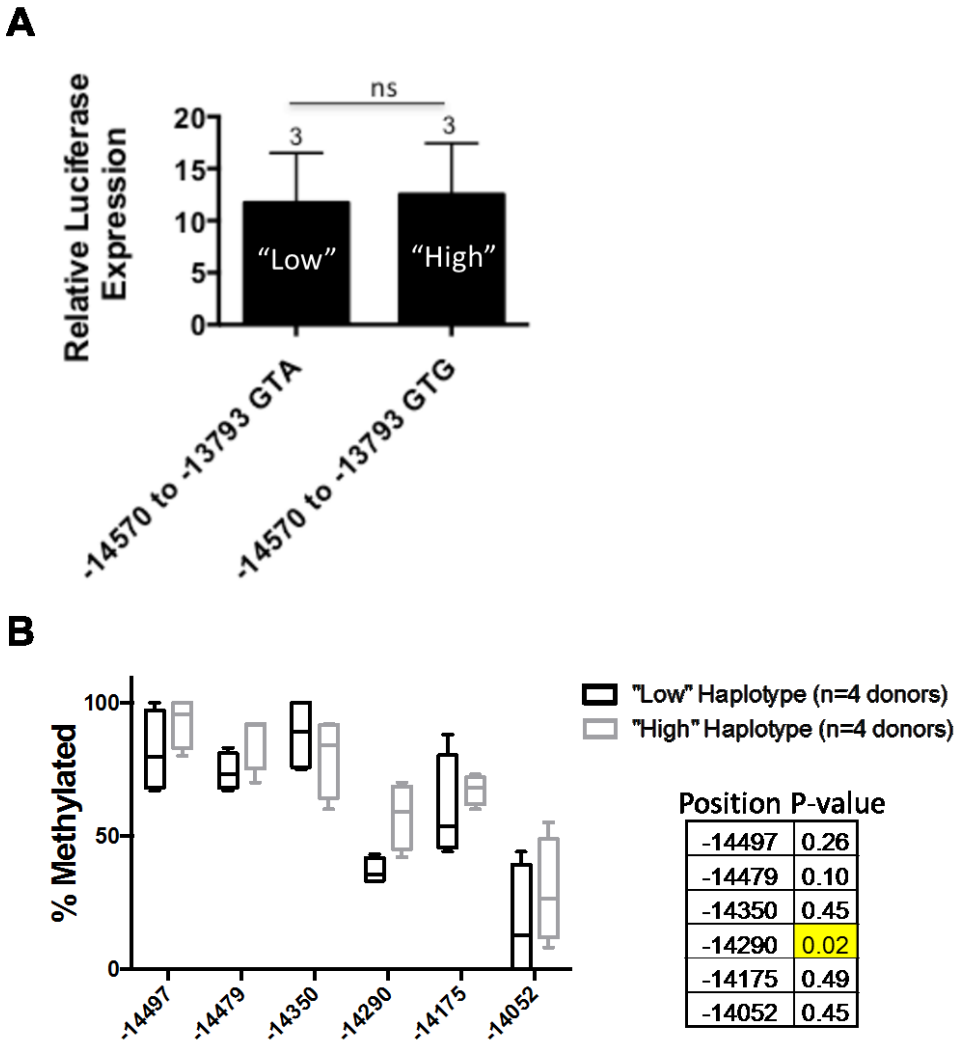

Position	P-value
-14497	0.26
-14479	0.10
-14350	0.45
-14290	0.02
-14175	0.49
-14052	0.45

Figure 1.8 Comparison of transcriptional activity and DNA methylation of the LILRB1 distal promoter from the "high" and "low" haplotype.

(A) Transcriptional activity of the distal promoter in NK92 cells. The number of independent experimental tests for each haplotype is indicated above the error bar [277]. The position of the distal promoter is relative to the translational start site of the gene. Student's T-test was used to determine the significance and "ns" indicates the P-value ≥ 0.05. Work was performed by Chelsea L. Davidson and published in [277] (B) DNA methylation analysis on the LILRB1 distal promoter in primary NK cells. For each donor, 20 clones or more were analyzed to calculate the DNA methylation percentage at each CpG position. The haplotype of each clone was determined and grouped into "low" and "high" haplotype. The x-axis indicates the position of the CpG, relative to the translational start site of the gene. The table indicates the P-values for each CpG site examined as determined by Student's T-test. The site that reached statistically significant between the two groups is highlighted by yellow. This work was performed by Chelsea L. Davidson [257].

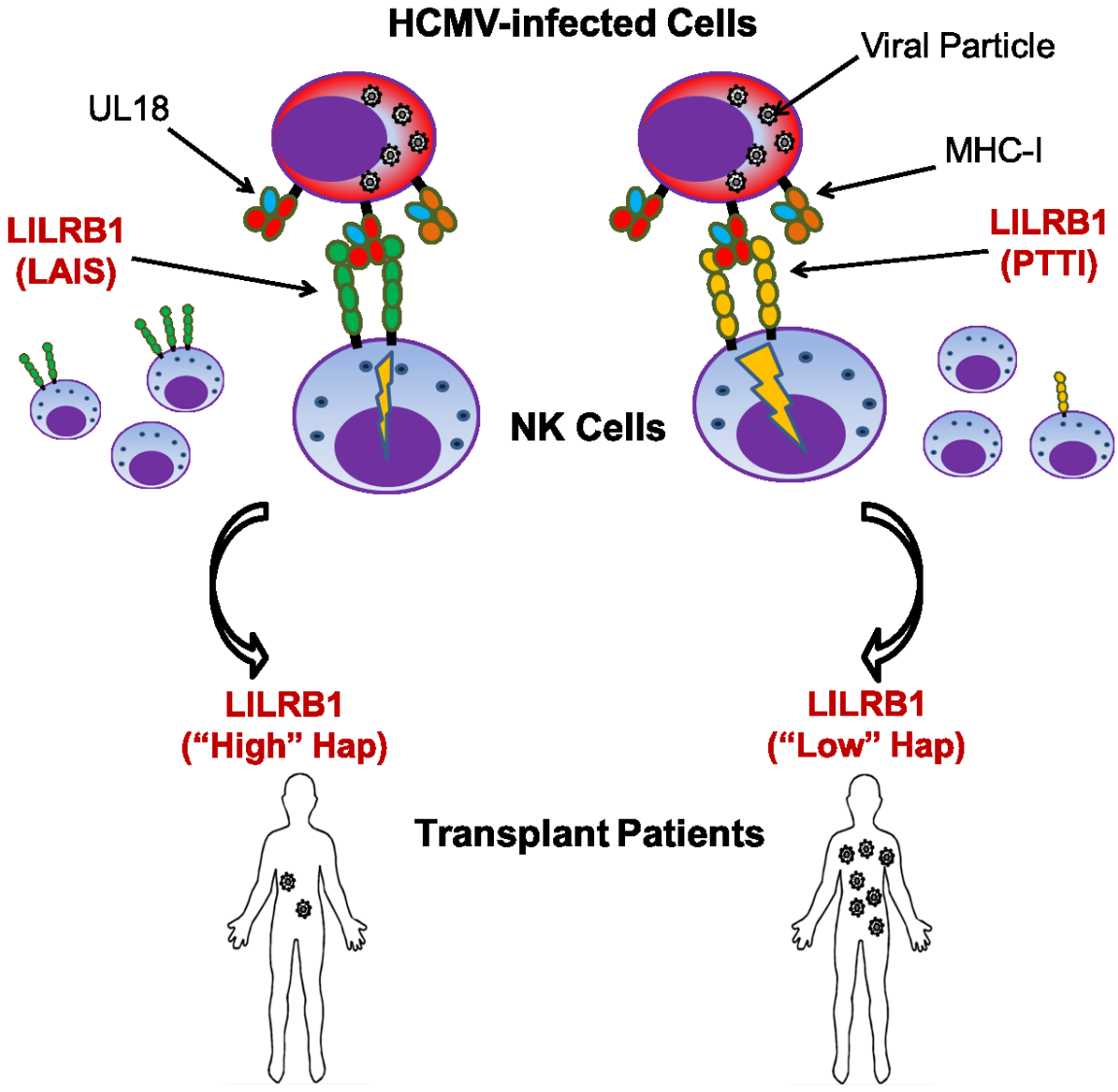

Figure 1.9 Model illustrating the influence of LILRB1 gene polymorphisms on HCMV susceptibility in transplant patients through differential LILRB1/UL18 interactions.

serendipitous finding in a model cell line expressing UL18 generated for Chapter 4, I investigated the consequence of UL18 expression on the phenotypic change of that LILRB1-positive cell line and explored the underlying mechanism in Chapter 5.

CHAPTER 2
Materials and Methods

Parts of this chapter were adapted from *Yu, et. al. "LILRB1 polymorphisms influence posttransplant HCMV susceptibility and ligand interactions." The Journal of clinical investigation 128.4 (2018): 1523-1537.[277]*

2.1 Donors, primary cells, and cell lines

2.1.1 Blood donors

Blood samples were collected from healthy individuals in this study with written informed consent, and the experiments were performed as approved by the Health Research Ethics Board at the University of Alberta (Edmonton, Canada). Blood sampling was done by Bara'ah Azaizeh.

2.1.2 PBMCs and primary NK cells

PBMCs were isolated from peripheral blood using Lympholyte-H Cell Separation Media (Cedarlane, Burlington, ON, Canada). NK cells were then isolated from the PBMCs using the EasySep Human NK Cell Isolation kit (STEMCELL Technologies, Vancouver, BC, Canada) following the manufacturer's protocol. PBMC and purified NK cells were stained using antibodies targeting CD3, CD56, and LILRB1 to determine the NK cell purity and LILRB1 expression on NK cells. Purified NK cells were plated at 3, 1 and 0.3 cells/well with 10^4 irradiated 721.221 feeder cells/well in V-bottom 96-well plates to generate single clones using limiting dilution and cultured in Iscove's Modified Dulbecco's Medium (IMDM) (Thermo Fisher Scientific, Waltham, MA, USA) with 10% human serum (Gemini Bio Products, West Sacramento, CA, USA), 1 mM L-glutamine, supplemented with 0.5 µg/mL PHA-P (Sigma-Aldrich, St. Louis, MO, USA) and 100 U/mL recombinant human IL-2 as previously described [262]. Clones were derived from plates with growth in less than 30 wells after 30 days.

2.1.3 Cell lines

The human NK cell line NKL was cultured in IMDM supplemented with 10% characterized FBS (Thermo Fisher Scientific), 1 mM L-glutamine, and 200 U/mL recombinant human IL-2 (Tecin, supplied by Biological Resources Branch, NCI at Frederick, USA). The human B cell lymphoma cell line 721.221 and 721.221 cells stably expressing HLA-B58,

HLA-Cw15, and HLA-G, respectively, originally obtained through Dr. Eric Long (NIH, Bethesda, Maryland, USA) were maintained in IMDM supplemented with 10% FBS (Thermo Fisher Scientific) and 1 mM L-glutamine. The medium for 721.221 cells expressing HLA-B58, HLA-Cw15, and HLA-G was also supplemented with 0.5 mg/ml G418 sulfate (Life Technologies, Grand Island, NY, USA). A clone of 721.221 cells expressing HA-HLA-B58-YFP was generated by Dr. Li Fu and cultured in the medium of 721.221 cells with 1 μg/ml puromycin (Bioshop Canada Inc, Burlington, ON, Canada) as described in her thesis [280]. YTS cells were obtained from Dr. Eric Long (National Institutes of Health, Maryland, USA) as a gift and cultured in IMDM with 15% characterized FBS with 50 μM β-mercaptoethanol and 1 mM L-glutamine. Phoenix and Cos-7 cells were purchased from ATCC (Manassas, VA, USA) and cultured in Dulbecco's Modified Eagle Medium (DMEM) (Thermo Fisher Scientific) with 10% FBS. RBL cells expressing HA-PTTI or HA-LAIS variant were generated by Chelsea L. Davidson and maintained in Minimum Essential Media (MEM) (Thermo Fisher Scientific) medium containing 10% FBS and 0.8 mg/mL of G418 [257].

2.2 Genotyping of blood donors

The blood donors were all genotyped for LILRB1 gene by Chelsea L. Davidson or Bara'ah Azaizeh. The protocol of the TaqMan Genotyping was detailed previously in the thesis of Chelsea Davidson [257]. Briefly, the genomic DNA was isolated from blood samples using the illustra blood genomicPrep Mini Spin Kit (GE Healthcare, Chicago, IL, USA). TaqMan genotyping for each of the SNPs (rs10416697, rs1004443, rs2781771, and rs1061680) was performed using10 ng of DNA per reaction in duplicate. For each genotyping assay, a positive control sample with known genotypes and a negative control without DNA was included. Each PCR reaction was prepared using the 2X universal master mix (Applied Biosystems, Waltham, MA, USA), primer-probe mix (Thermo Fisher Scientific), genomic DNA, and proper volume of

water. The PCR reaction was run on the StepOne PCR Machine (Applied Biosystems) and the genotype calling was analyzed using the StepOne software.

2.3 Antibodies

Purified unconjugated Mouse α-Human CD85j (clone: HP-F1, IgG1κ) [186] was kindly provided by Dr. Miguel López-Botet (Pompeu Fabra University, Barcelona, Spain). Alexa Fluor 647 conjugated α-HA (clone: 16B12) and Mouse IgG1κ isotype (clone: MOPC-21) were purchased from Biolegend (San Diego, CA, USA). Unconjugated and APC-conjugated Mouse α-Human CD85j (clone: HP-F1, IgG1κ) and Mouse IgG1κ isotype control APC-conjugated antibody were purchased from eBioscience (San Diego, CA, USA). PE-conjugated Mouse α-Human CD56 (clone: CMSSB, IgG1κ) was also purchased from eBioscience. FITC-conjugated Mouse α-Human CD3 (clone: HIT3a, IgG2aκ) was purchased from BD Biosciences (San Jose, CA, USA). Mouse IgG1κ isotype control (clone: MOPC-21) was purchased from Sigma-Aldrich. α-Human HLA-I (clone: W6/32) and α-Human CD8 (clone: 51.1) were purified from hybridoma supernatants (ATCC). Goat α-Human IgG Fc and alkaline phosphatase-conjugated $F(ab')_2$ Goat α-Mouse IgG or IgM antibody were purchased from Jackson ImmunoResearch (West Grove, PA, USA). PE-conjugated Mouse α-Human IgG Fc (catalog: 9042-09) was from SouthernBiotech (Birmingham, AL, USA). PE-Cy5 Mouse α-Human CD85j (clone: GHI/75) and PE-Cy5 Mouse IgG2bκ Isotype control were purchased from BD Biosciences. ChIP grade α-Human YY1 (clone: D5D9Z) was obtained from Cell Signaling Technology (CST) and the Normal Rabbit IgG control was included in the SimpleChIP® Enzymatic Chromatin IP Kit (CST: #9003, Danvers, MA, USA). α-Human LFA-1 α subunit (ATCC: HB202, clone: TS1/22, IgG1κ) and α-Human LFA-1 β subunit (ATCC: HB203, clone: TS1/18, IgG1κ) were purified from hybridoma supernatants. APC-conjugated Mouse α-Human CD11a/CD18 (LFA-1, clone: m24, IgG1κ) and PE-conjugated Mouse α-Human CD18 (clone: TS1/18, IgG1κ) were purchased from Biolegend.

2.4 Allele-specific expression assay

Ex-vivo NK cell clones were first stained by α-Human CD85j (clone: HP-F1) for surface LILRB1 expression using flow cytometry. For each LILRB1-positive clone, 8 x 10^4 cells were lysed using the SingleShot™ Cell Lysis Kit (Bio-Rad, Hercules, CA, USA) following manufacturer's protocol and immediately subjected to reverse transcription using iScript™ Advanced cDNA Synthesis Kit (Bio-Rad). A custom TaqMan genotyping assay (ID: ANGZE69) was used to differentiate the expression of alleles specific for rs1061079 (C/T) and designed using the online tool (https://www.thermofisher.com/order/custom-genomic-products/tools/genotyping/). The sequences of primers and probes are listed in Table 2. Each Droplet Digital™ PCR (ddPCR) reaction was prepared by mixing amount of cDNA template equivalent to 1000 input cells for every single clone (assuming 100% lysis), Taqman primers probes mix and ddPCR Supermix for Probes (no dUTP, Bio-Rad), and then subjected to droplet generation using QX200 Droplet Generator (Bio-Rad) following the instruction manual. The ddPCR reactions were amplified in a thermal cycler according to the kit instructions and the fluorescence signals were detected and recorded using the QX200 Droplet Reader (Bio-Rad). The copy number per sample of the two alleles for the SNP rs1061079 (C/T) was determined using QuantaSoft™ Software (Bio-Rad).

2.5 CRISPR-Cas9-based knockout

2.5.1 Knockout of the putative enhancer fragment in NKL cells

The putative enhancer region was amplified using iProof™ Hi-Fi DNA Polymerase (Bio-Rad) with the primers listed in Table 2. CRISPR guide RNAs were designed using the online software CHOPCHOP (http://chopchop.cbu.uib.no/). Both boundaries of the 3 kbp region encompassing the entire putative enhancer were targeted by two single guide RNAs

(AATCAGTACTAAAAATCTTC and AAAGACAAGCACATTGGGAC), respectively. The fragment knockout in NKL cells was achieved using Alt-R CRISPR-Cas9 System (Integrated DNA Technologies, Coralville, IA, USA) combined with the 4D-Nucleofector system (Lonza, Basel, Switzerland) according to the manufacturers' protocol and all the materials used were RNase-free. Briefly, the CRISPR guide RNAs and tracrRNA (conjugated with ATTO 550) were adjusted to 200 µM and pre-incubated in equimolar concentrations in a microcentrifuge tube to a final duplex concentration of 100 µM (25% for each guide RNA and 50% for tracrRNA). The duplex formation protocol was 95°C for 5 min and then cooling down to room temperature. Next, 120 pM RNA duplex was mixed with 106 pM Cas9 nuclease in PBS and incubated at room temperature for 10–20 min to form ribonucleoprotein complex. 2 x 10^5 PBS-washed NKL cells were suspended in the reagents from SF Cell Line 4D-Nucleofector™ X Kit S and mixed with the ribonucleoprotein complex supplemented with 4 µM Alt-R Cas9 electroporation enhancer. The mix was then transferred into one well of the Nucleocuvette and electroporated with the CM150 program. Nucleofection efficiency was determined by flow cytometry after 24 hours and the NKL cells were further incubated for two days and assessed for LILRB1 surface expression with antibody staining (clone: GHI/75) by flow cytometry. The population with decreased LILRB1 expression was sorted and followed with single-cell sorting to generate clones using BD FACSAria™ III sorter (Becton Dickinson, Franklin Lakes, NJ, USA). The genomic DNA of the clones was isolated using QuickExtract™ DNA Extraction Solution (Lucigen, Middleton, WI, USA), and the knockout of the putative enhancer was validated using PCR and Sanger sequencing.

2.5.2 Knockout of LILRB1 gene in 721.221 cells

Two independent CRISPR guide RNAs (g1: GTGACCCTCAGGTGTCAGGG and g2: GGGGGTCACTGCTCTCTGAG) targeting LILRB1 gene exon5 were designed using CHOPCHOP software. For the LILRB1 gene knockout in 721.221 cells, two guide RNAs were

used to control each other while only g1 guide RNA was used to knock out the LILRB1 gene in 221-UL18 cells and a negative control crRNA for human (Integrated DNA Technologies) was also included in the assay. The knockout of the LILRB1 gene in 721.221 cells and 221-UL18 cells was also achieved using Alt-R CRISPR-Cas9 System combined with the 4D-Nucleofector system according to the manufacturers' protocol. The same protocol for the preparation of the ribonucleoprotein complex and nucleofection was applied as described above. Nucleofection efficiency was determined by flow cytometry after 24 hours. LILRB1- 721.221 cells were sorted after about one week after the nucleofection using BD FACSAria™ III sorter. The cells were then expanded and with which single-cell sorting was applied. The knockout was confirmed by Sanger sequencing as described above. The 221-UL18 cells with LILRB1 knocked out were only sorted for the LILRB1-negative population.

2.6 Quantitative chromosome conformation capture (3C-qPCR)

The 3C-qPCR assay was performed following the protocol essentially as described by Hegage et. al. [281] with some minor modifications. NKL cells were cross-linked in complete media supplemented with 1% formaldehyde for 10 minutes at room temperature and quenched by 0.125 M glycine. The cells were then washed twice with ice-cold PBS and lysed with lysis buffer containing 10 mM Tris-HCl (pH= 8.0), 10 mM NaCl, and 0.2% Nonidet P-40 with protease inhibitor mixture (CST) for 45 minutes on ice. Nuclei were collected and resuspended in 1.2X restriction enzyme buffer supplemented with 0.3% SDS and then incubated at 37°C with shaking for 1 hour. 2% Triton X-100 was added to the nuclei to sequester the SDS and incubated at 37°C with shaking for 1 hour. Cross-linked genomic DNA within the nuclei was digested by EcoRI overnight at 37°C with shaking. 1.6% SDS was then added to the sample and the restriction enzyme was inactivated by incubating at 65°C for 25 minutes. The digested DNA was diluted into the 1.15x ligation buffer supplemented with 1% Triton X-100 and incubated for 1 hour at 37°C with gentle shaking. T4 DNA ligase (Thermo Fisher Scientific) was added to ligate

the DNA fragments and the reaction was incubated at 16°C for 4 hours followed with 30 minutes at room temperature. The cross-linking was reversed by adding proteinase K and incubating at 65°C overnight. After treatment with RNase for 45 minutes at 37°C, the sample was purified by phenol-chloroform extraction and ethanol precipitation. The concentration of the 3C library was determined using Qubit Fluorometric Quantitation System (Thermo Fisher Scientific). Digest efficiency for each of the restriction sites involved in the 3C analysis was accessed using the primers listed in Table 2 and the digest efficiencies tested were all over 80% for the samples used in the assay. Specific ligation products were detected by Taqman qPCR with the primers and probe listed in Table 2. To generate a reference control library, we purchased the bacterial artificial chromosome (BAC) clone (WI2-1436-K15) which contains the whole LILRB1 gene from BACPAC Resources (Oakland, CA, USA), and performed parallel digestion, ligation and purification steps as described above. The values presenting the relative cross-linking frequency was calculated using the formula of $10^{(Ct-b)/a}$ (b=intercept; a=slope) where the parameters were from the standard curves generated using the BAC reference control library.

2.7 Chromatin immunoprecipitation (ChIP) and ChIP-loop assay

ChIP assay was performed using SimpleChIP® Enzymatic Chromatin IP Kit (CST) following the manufacturer's protocol. Briefly, the chromatin of NKL cells was cross-linked as described for the 3C assay. Nuclei were isolated and incubated with Micrococcal Nuclease to digest the chromatin to fragments of between 150-900 bp. The nuclei were sonicated using the Sonic Dismembrator Model 100 (Thermo Fisher Scientific) to break down the nuclear membrane. The digested chromatin was collected and then incubated with α-human YY1 (1:50 dilution) or Normal Rabbit IgG overnight at 4°C with rotation. Protein G magnetic beads were added to each immunoprecipitated sample and incubated at 4°C for 2 h with rotation. The beads were washed and the chromatin was eluted at 65°C for 30 minutes with vortexing in a

thermomixer (Thermo Fisher Scientific). The cross-linking was reversed by incubating with Proteinase K overnight at 65°C. Predicted YY1 binding loci were assessed by standard PCR using the purified ChIP DNA and then analyzed in agarose gel. The primers used for ChIP and ChIP-loop were designed based on the transposase-accessible chromatin using sequencing (ATAC-Seq) results (Figure 3.3B) and listed in Table 2.

The ChIP-Loop assay was performed as described previously [282] combined with the SimpleChIP® Enzymatic Chromatin IP Kit. The digested and ligated chromatin was generated as described above before proceeding to the immunoprecipitation using the YY1 or Normal Rabbit IgG antibody. The purified ChIP-Loop library was subjected to PCR analysis.

2.8 Receptor Constructs and Transfections

2.8.1 YTS transfection

HA-tagged LILRB1 PTTI and LAIS variant were sub-cloned from pDisplay vectors constructed by Chelsea L. Davidson [257] into the pMXs-puro vector (gift from Dr. Lewis Lanier, University of California, San Francisco, USA) using ClaI and NotI restriction sites. The sequences were confirmed by sequencing before transfection. The retroviral transduction of YTS cells was performed as previously described [283]. Basically, 2.5 x 10^6 Phoenix cells were seeded in a 60 mm culture dish 12-16 hours before transfection. On the day of transfection, the media was replaced with fresh media supplemented with 25 μM chloroquine. The transfection mixture containing 10 μg DNA, 50 μl 2.5M $CaCl_2$, 500 μl 2 x HBS (50 mM HEPES, pH=7.05; 10 mM KCl; 12 mM Dextrose; 280 mM NaCl; 1.5 mM Na_2HPO_4) and 450 μl sterile water was added dropwise to the Phoenix cells and then incubated at 37°C/5% CO2 for 8-10 hours. Next, the media of the Phoenix cells was replaced with 3 ml YTS media and incubated cells at 32°C/5% CO2 for 48 hours. The supernatant containing retrovirus was supplemented with 8 μg/ml working concentration of polybrene (Sigma-Aldrich) and then added to 5 x 10^5 YTS cells. The cell suspension was plated in a 24-well plate with 0.5 ml per well, spun at room temperature for

90 minutes at 1500 rpm and incubated 3 hours at 37°C/5% CO2. The cells were pelleted and cultured with fresh YTS medium in a T25 flask for 48 hours and then selected with 1 μg/ml puromycin replacing with fresh medium every 3-4 days. When cultures returned to confluence, LILRB1 surface expression was assessed by flow cytometry. Single-cell clones were obtained by cell-sorting and surface expression was detected using α-HA antibody or α-LILRB1 (HP-F1) by flow cytometry.

2.8.2 721.221 cells with stable expression of HA-UL18-YFP

HCMV strain AD169-derived UL18 gene sequence in a plasmid was kindly provided by Dr. Lewis Lanier. The coding sequence was amplified with primers that replaced the stop codon with an in-frame join to fuse YFP using BamH1 and the pEYFP-N1 plasmid (Takara Bio, Mountain View, CA, USA) with a linker sequence RDPPVAT. UL18-YFP was amplified by PCR with appropriate restriction sites and sub-cloned into pDisplay in-frame with the N-terminal HA-tag generating a linker of GAQPARSPGIRGCRSS. The resulting construct was sequenced, and an apparent PCR error in the linker between the HA tag and UL18 was corrected by site-directed mutagenesis. The construct was sub-cloned into pMXs-puro (pMXs-HA-UL18-YFP) using the EcoRI restriction site. The retroviral transduction of 721.221 cells was performed as described in 2.8.1 except for the using 721.221 media as opposed to YTS media and using 1 ml per well for the plating in the 24-well plate. When cultures returned to confluence after the selection by puromycin, UL18 surface expression was assessed by flow cytometry. Single-cell clones were obtained by the limiting dilution and surface expression was detected using the α-HA antibody by flow cytometry.

2.8.3 LILRB1-Fc fusions and variants

The construct of the expression vector for "LAIS" LILRB1-D1D2-Fc has been previously described [226, 280]. For more efficient protein production, Li Fu generated a new plasmid by

moving the CD5 leader sequence and Fc region from CD5neg1 (gift from Dr. Eric Long) to the pEGFP (Takara Bio) backbone and removing the EGFP-cassette (Fc-simple) [280]. The "PTTI" LILRB1-D1D2 domains were moved into the Fc-simple plasmid using PCR to generate an in-frame fragment with EcoR1 sites. The plasmids encoding the other LILRB1 mutants including “PTII”, “LTTI”, “PATI”, and “PTTS” were generated based on Fc-simple-“PTTI” by site-directed mutagenesis. The insert including in the Fc tag of all those constructs were fully sequenced to ensure no additional mutations were introduced.

2.9 Cytotoxicity Assay

Effector cells were counted by TC20™ Automated Cell Counter (Bio-Rad Laboratories, Hercules, CA, USA) and diluted to 10^6 cells/mL with RPMI 1640 medium supplemented with 10% FBS. Calcein-AM (Life technologies) was dissolved in anhydrous DMSO (Life technologies) at 100 μM and stored for up to one week. Target cells were adjusted to 5 x 10^6 cells/mL and labeled in the medium with 3.5 μM Calcein for 30 minutes at 37°C/5% CO2. Calcein-labeled cells were washed twice with 10 ml RPMI medium and counted and diluted to 5 x 10^4 cells/mL. For a 10:1 E: T ratio reaction, 50 μL 10^6 cells/mL effector cells and 100 μL 5 x 10^4 /mL target cells were added in triplicate in each well of a V-bottom 96-well plate (Corning, Corning, NY, USA) containing 50 μL RPMI 1640/10% FBS.

Where indicated to block receptor function, 50 μL of 10 μg/ml HP-F1 or MOPC-21 or medium were pre-aliquoted into the V-bottom 96-well plate. 100 μL RPMI media and or RPMI containing 2% Triton X-100 were added to target cells for the spontaneous and maximum release, respectively. The plate was incubated at 37°C/5% CO2 for 4 hours, spun at 200 rpm for 2 minutes. 100μL of supernatant was transferred to the black flat-bottom 96-well plate (Corning) and calcein release was measured in the EnSpireTM 2300 Multilabel Reader (PerkinElmer, Waltham, MA, United States). The specific lysis was calculated based on the formula for each well: 100 x (experimental release – spontaneous release)/ (maximum release – spontaneous

release). For analysis of significance, the means of the calculated specific lysis rates were compared by two-tailed paired-samples T-Test with the significance of a P value less than 0.05. Statistical analysis in this study was performed with SPSS Statistics 20 (IBM). Except as otherwise indicated, all the experimental data set are presented as mean ± SD.

2.10 Purification of LILRB1 D1D2-Fc fusion protein

Plasmids containing the variants and artificial mutants of LILRB1 D1D2 domains were amplified in E.coli and extracted by GenElute HP Plasmids Midi prep kit (Sigma-Aldrich). Cos-7 cells seeded in T150 flasks were transfected with 20 μg DNA per flask. Cells were washed with DMEM for three times 12 hours post-transfection and then maintained in the serum-free DMEM medium with 1% NEAA (Thermo Fisher Scientific). The medium was collected and changed every three days for three times and filtered for the affinity purification. The medium was loaded to a column filled with Protein A/G beads (Millipore, Billerica, MASS, USA) at 4°C, and the column was washed with PBS and then eluted by 0.05M Glycine. Eluted protein was neutralized by 1M Tris buffer and dialyzed into PBS with Amicon centrifugal filters (Millipore). Protease inhibitors cocktail (Roche, Basel, Switzerland) was subsequently added to the purified protein. Concentration was determined using the Micro BCA kit (Thermo Fisher Scientific). Purity and specificity were verified by Coomassie staining and Western blotting using α-human IgG Fc respectively. Purified human IgG Fc fragment control has been previously described [283].

2.11 Capture-based ELISA

Capture-based ELISA was used to check the conformation consistency of the purified LILRB1 variants and artificial mutants. ELISA Medium Binding plate (Corning, Corning, NY, USA) were coated at 4°C overnight using 25 μg/ml Goat α-Human IgG Fc diluted in 0.1M $NaHCO_3$ (pH=9.6). The coated plate was incubated with the blocking buffer (2% BSA /0.05%

Tween-20/PBS) at room temperature for 1 hour. Then, the plate was washed four times with the washing buffer (0.05% Tween-20/PBS) before adding the Fc-fusion proteins for 1-hour incubation at room temperature. The plate was washed three times to remove the unbound proteins and then incubated at room temperature for 1 hour with 1.25 μg /ml HP-F1 antibody which is conformationally sensitive to the folding of D1 and D2 domains of LILRB1. Next, the plate was washed three times prior to adding the alkaline phosphatase-conjugated $F(ab')_2$ Goat α-Mouse IgG and IgM secondary antibody and incubating for 1-hour incubation at room temperature. The plate was then washed five times and incubated with PNPP substrate (Thermo Fisher Scientific) for about 20 minutes. The plate was read at OD 405 nm using SpectraMax 384 Plus Microplate Reader (Marshall Scientific, Hampton, NH, USA).

2.12 LILRB1 binding assay

721.221 cells were counted and adjusted the concentration to 2 x 10^7/mL with FACs buffer (2% FBS and 1mM EDTA in PBS). 10 μL of Fc-fusion protein was added to 10 μL of cells in a 1.5 mL microfuge tube and incubated 1 hour at 4°C with rotation, washed with 4 ml FACs buffer and then incubated with 100 μL 5 μg/mL PE mouse α-human IgG Fc for 30 minutes at 4°C. Cells were washed again, fixed with 4% formaldehyde, and analyzed on the LSRFortessa analyzer (Becton Dickinson). Compensation was required for the YFP spill into the PE channel for binding to UL18 expressing cells. Where indicated, 100 μL 10 μg/ml W6/32 or isotype control was pre-incubated with the cells at 4°C for 10 minutes, and the cells washed with FACs buffer prior to adding the Fc-fusion proteins.

The UL18-Fc fusion was generated as previously described [284]. To account for the difference in the expression of LILRB1 PTTI and LAIS variants on RBL cells, the binding was normalized by staining LILRB1 with α-HA or HP-F1. For the statistical analysis, each MFI value was corrected by subtraction of the MFI of the Fc control and then divided by arithmetic average MFI of the entire sample MFIs in one independent test. The results of the binding assay

were aggregated from at least three independent tests and one-way ANOVA was used to compare the binding of different purified proteins with a specific ligand. The differences were considered significant when a P value was less than 0.05.

2.13 De-glycosylation

Potential N-linked glycosylation sites were predicted with "GlycoEP" (http://www.imtech.res.in/raghava/glycoep/index.html). For enzymatic de-glycosylation, the volume of 2 μg purified proteins were adjusted to 43 μL with 250 mM NaHPO4 buffer (pH=7.5) and then mixed with 2.5 μL denaturing buffer containing 2% SDS, 1 M β-mercaptoethanol and incubated at 100°C for 5 minutes. The mixture was cooled to room temperature and 2.5 μL 10% Triton X-100 detergent was added with 2 μL of N-Glycosidase F from *Elizabethkingia meningosepticum* (Millipore) and incubated for 3 hours at 37°C. Samples were separated by 10% SDS-PAGE and stained by Coomassie Blue.

2.14 Quantification of cell clustering size

Cells were counted and seeded into a 48-well plate (3×10^5 cells/well) with three parallel repeats for each cell line. The cells were cultured for 24 hours and the cell photos were taken automatically using the Time Lapse Mode (1s/well) from the EVOS® FL Auto Cell Imaging System (Life technologies). The cell photos were loaded into ImageJ software for analysis. The process for quantifying average clustering size for each photo is as following: 1) Switch the type of the image to 8-bit; 2) Adjust the threshold of the image by the auto mode to highlight the cells and cell clusters; 3) Select the unsaturated region with a circle (x-scale factor=1.2; y-scale factor=1.2); 4) Quantify the clustering size using the Analyze Particles tool with the parameter size (pixel^2) set from 400 to infinity. The cutoff of particle size (400) to exclude the non-aggregated cells was determined by two people who were blind to all the samples.

2.15 Imaging flow cytometry

To examine and analyze the distribution of UL18 protein in the 721.221 cell line stably expressing UL18, imaging flow cytometry was performed. 721.221, 221-UL18 and 221-B58 cells were fixed in 4% paraformaldehyde (PFA) and then washed by FACs buffer. 5 mg/mL DAPI stock solution was diluted 1:1000 with FACs buffer. 300 µL of the working solution was used for 1 x 10^6 cells and incubated for 1 hour at room temperature. The cells were then washed again with FACs buffer and transferred to 1.5 mL microcentrifuge tubes for detection in the ImageStreamx Mark II (Amnis Corporation, WA, USA) flow cytometer. The unstained 721.221, 721.221 stained by DAPI and unstained 221-B58 are used as double negative and single positive controls, respectively to set up the compensation. Data were visualized and analyzed using IDEAS® v6.2 software (Amnis Corporation). The YFP signal derived from the plasma membrane and cytosol was discriminated using the connected component masks from the software, and then the membrane/cytosol ratio was calculated based on the geometric mean fluorescence intensity (Geom.MFI) of the YFP signal.

2.16 Quantitative Real-Time PCR

Total RNA was extracted using the RNeasy Mini kit (Qiagen, Mississauga, ON, Canada) with on-column DNase digestion to remove genomic DNA. cDNA was synthesized using the iScript™ Advanced cDNA Synthesis Kit (Bio-Rad). Primers for quantitative Real-Time PCR are listed in Table 2. RPL24 gene was used as the internal reference control for all the samples. All the PCR reactions were prepared using PerfeCTa SYBR Green SuperMix (Low ROX) (Quantabio, Beverly, MA, USA) according to the manufacturer's instructions and run on a Bio-Rad C1000 Touch Thermal Cycler. The results were analyzed using the 2^-ΔΔCt method [285].

Table 2 Sequence of the primers and probes used in this thesis.

Primers and probe used in ddPCR		
Name	Sequence (5' to 3')	
rs1061679-F	ACCCAGGAGTACCGTCTATATAGAGA	
rs1061679-R	CTGGCCCTTCTTCACAAGCT	
Taqman-C-VIC	CGTGTAATCCAGGGTGCTG	
Taqman-T-FAM	CGTGTAATCCAGAGTGCTG	
Amplification of bisulfite converted DNA		
Name	Forward Primers (5' to 3')	Reverse Primers (5' to 3')
Distal-BS	GGGGTTTATTGAAAGTTTTTAGGAT	CCCACAAAAAAATCACTCTTCTTAC
Amplification of putative enhancer		
Name	Forward Primers (5' to 3')	Reverse Primers (5' to 3')
LILRB1-Enh	TCTTCGTTGTGTATATGGCAAATTTCG	CGTGGGACCCTAGAGAGACTGTTGTTCT
Detection of putative enhancer knockout		
Name	Forward Primers (5' to 3')	Reverse Primers (5' to 3')
Enh-KO	GCTTTAGGAATTACATAGTTTCAGGT	CGTGGGACCCTAGAGAGACTGTTGTTCT
LILRB1-RT-qPCR		
Name	Forward Primers (5' to 3')	Reverse Primers (5' to 3')
Total LILRB1	ATCCTGATCGCAGGACAGTT	GGAAAGTTTGCATCCATCCCTG
Primers used in YY1 ChIP assay		
Name	Forward Primers (5' to 3')	Reverse Primers (5' to 3')
YY1-Neg	CACAGCTGGAGTGCTTCTCTCTAA	GAGACGTGCTGTGAATCATTCCCT
YY1-D1	CACATTAAAATGTGGGCAAACGAC	TCCTGAGAACATGTGTCCCTTGAC
YY1-D2	GGATCCTACTTCTAGTTGGGAGAT	ATTTTGGCTGGGAGGAGCAAAATG
YY1-D3	TGGGAAGTGATGAGGGGTGCTTGT	TCTCTCGGAAGGTCTAAACACCTC
YY1-D4	ATCTAAGAATGAGGAGAAAGCAAG	GAGAAAGAGAGAACTTAGGAACTC
YY1-D5	TGACTCATGTGAGATCAGGAGTTC	TCACTGCAACCTACATCTCCCATG
YY1-E1	TTCTCCTTTTTTTGGTTAGTGTAG	ATATTGTGGCACCACCAAAGGATC
YY1-E2	TTGCCCACAGATATCCCAGTGATG	TAGGGAGACAGACAACGTTCCTCC
YY1-E3	TGACGTGGTAGCTGCTTCATGTAG	AACTACCTGCCCTTTCCTACCCTG
YY1-E4	GGACAGCGTGTGTGAGTCCTGAAG	TGTGATCTGCCGCAGGCTCTACCA
YY1-E5	AGCATTGGACTTTCAGAGGGCACT	GAATAAGTATGACAGCTGGGGCAC
YY1-P1	TCAGTATTTCCTCCCACAAGGAAC	ACATTGGCTGTGTTAGGCCTTAGG
YY1-P2	CCCTAAGGCCTAACACAGCCAATG	AGCAAGGATTACAATCTGGAGTGC
YY1-P3	TGCGAGATGCGTCTCTGCTGATCT	TTCCTTCTCACAGCCTCCCACATG
Primers and probe used in the 3C-qPCR and ChIP-Loop assay		
Name	Sequence (5' to 3')	
3C Taqman probe	CGTTGGTTGTAATGTCAACTTTATCATTTC	
3C--17925	CCATGGTGTATATGTGAAAGTTAG	
3C--16483	TACGTTGAACCAATTTCAGGCTC	
3C--11214	CATAGCTCTAATTACTGGAGAGAG	
3C--7667 (Anchor)	AGAGATGGCTGACTACACTAAC	
3C--3504	AGAGCTGCTTAGAAACAGAGTTC	
3C--1972	GAAAAGTCTGCCGTTCATATACAC	
3C--1474	AAGTTCCCAAGTGTAGATGGAT	
3C-+2125	GACTTTGAGCTCAGAGAGGACAG	
3C-+5523	ACTCACCTCAGTGTCCATCTGC	
DE--17925	TATCACTCAAACTGACACCTTC	
DE--16483	GTAAATTCTCAGACACGTGCAGCCT	
DE--11214	TACCAAACTACATGAAACAGCT	
DE--7667	GCAAATTTCGACTGTGAATCCATC	
DE--3504	CCTCCTGCTTTGACGAGGTTTAT	
DE--1792	GTATCACAACATCACACTTCCCT	
DE--1474	GAACACCCTGGTGTTTAGTGCTTC	
DE-+2125	CCCATGGCGTCTAAGATCAACGTAC	
DE+5523	CAGTGACGTATGCCGAGGTGAAACA	

CHAPTER 3

Characterization of an intronic enhancer of LILRB1 gene

Parts of this chapter have been accepted to be published in The Journal of Immunology titled "LILRB1 intron 1 has a polymorphic regulatory region that enhances transcription in NK cells and recruits YY1"

3.1 Background

LILRB1 is the only LILR receptor expressed on NK cells and its expression is heterogeneous in a single person. Moreover, the frequency of LILRB1-positive NK cells differs among individuals [3, 104]. The genetic variation appears to explain the heterogeneity of LILRB1 expression on NK cells since previous work from our lab demonstrated a correlation of the frequency of LILRB1-positive NK cells with LILRB1 haplotypes. The haplotypes span from the distal regulatory region to the protein-coding region. However, the mechanisms modulating the differential LILRB1 expression in and among individuals are poorly understood, and based on our current knowledge, it is hard to explain why some individuals with the same haplotype, for example, the heterozygous "high" and "low", are exceptions in terms of the proportion of LILRB1-positive NK cells [3]. Moreover, it is also unknown if the LILRB1 gene employs allele-specific regulation similar to some KIR genes [255] which could further increase the heterogeneity of NK cells. This chapter will first focus on investigating the allelic expression of the LILRB1 gene in primary NK cell clones.

Aside from being expressed in NK cells, LILRB1 is widely expressed on other lymphoid lineages and myeloid lineages, and the expression patterns differ in both the frequency of LILRB1-positive cells and the LILRB1 surface density. For a long time after the discovery of LILRB1, researchers only knew of the existence of the proximal promoter. Uncovering the distal exon and promoter which is mainly used by lymphocytes partially explained why monocytes have the ubiquitous and relatively higher surface expression of LILRB1 compared to lymphocytes [248]. Our lab subsequently determined the core region of the distal promoter and found the binding of JunD in this region positively regulates LILRB1 gene transcription in NK cells [250].

To examine if the distal promoter of the "high" and "low" haplotypes have different activities, a luciferase reporter assay was applied in an NK cell line, NK92. However, there was no significant difference in the activity of the distal promoter between the two haplotypes [277]. Considering the important role of DNA methylation in regulating the expression of KIR genes in

NK cells [255] and the evidence from an earlier study that DNA methylation is also involved in regulating LILR genes transcription in a monocyte and a B cell line [249], our lab then investigated whether there is a difference between the two haplotypes in terms of CpG DNA methylation status using isolated primary NK cell clones. The results of the bisulfite sequencing assay indicated there was only one CpG site in the distal promoter with different percentages of methylation. Intriguingly, the "high" haplotype is associated with the higher methylation percentage at this CpG site which is opposite to the repressing role of DNA methylation reported for KIRs gene transcription. It also should be noted that this experiment did not distinguish between LILRB1-positive or LILRB1-negative cells which may be associated with different DNA methylation patterns in the distal promoter. Thus, it could not be concluded that the methylation of the distal promoter causes different LILRB1 expression patterns between the two haplotypes. All these data led me to speculate that LILRB1 gene transcription is also regulated by polymorphic cis-acting elements other than the promoter in NK cells.

Given that enhancers are crucial elements controlling the cell-type-specific gene expression and associated with different types of histone modifications [286-288], in this chapter, I identified a putative enhancer within the first intron of LILRB1 gene through histone modification data from primary NK cells. I also did predictions of the binding sites for transcription factors in this putative enhancer and tested the binding of Yin Yang 1 (YY1) by ChIP. In addition, physical contact between the putative enhancer and the distal promoter was also examined. Last but not least, the function of the putative enhancer was tested by applying CRISPR-based deletion.

3.2 Results

3.2.1 NK clones express both LILRB1 alleles to varying degrees

Our previous work showed that both alleles of LILRB1 are expressed in a mixed population of *ex vivo* NK cells [3]. To examine the relative expression of each allele within

single NK cells, I selected three individuals with varying LILRB1-positive NK cell profiles as shown in Figure 3.1 known to be heterozygous at SNP rs1061679. I initially performed a single-cell analysis of *ex-vivo* NK cells to determine the relative expression of each allele for rs1061679 but the sensitivity was not sufficient to draw conclusions. Therefore, I grew out clones from purified NK cells and analyzed the relative rs1061679 expression in at least 8 clones from each donor. The clones had varying surface staining of LILRB1 as shown in Figure 3.1 and I included a clone without detectable surface expression for each donor in the analysis. As expected, detection of LILRB1 transcript was correlated with surface expression, however, in each donor, I found a different pattern of expression for the two alleles. For D183, two clones expressed only rs1061679-C, and three clones expressed both alleles while three clones had no detectable transcript. For D185 and D500, I detected both alleles in 5/12 and 8/11 clones respectively. In contrast to D183, I detected the rs1061679-T variant alone in several clones for both D185 and D500. For those clones where both alleles were detected, the ratio was variable with either allele being dominant (Figure 3.2).

The trend that there is a more frequent expression of the rs1061079-T allele in two out of three donors fits with our earlier observation of a correlation between the frequency of LILRB1-positive NK cells and LILRB1 gene polymorphisms in the regulatory regions of the gene [3]. The SNP rs1061679 is in the coding domain but in strong linkage disequilibrium with the SNPs within the distal promoter (r2= 0.92) and proximal promoter (r2= 0.91) which we showed to correlate with the frequency of LILRB1 expression on NK cells [277]. Therefore, it is fitting that the rs1061079-T allele was detected more frequently and on its own in two donors. Although D183 showed the opposite trend, it also had the fewest clones to analyze and suggests there may be additional polymorphic regulatory regions.

3.2.2 Prediction of an enhancer in LILRB1 intron 1

Given that enhancers are elements that typically control the cell type-specific gene

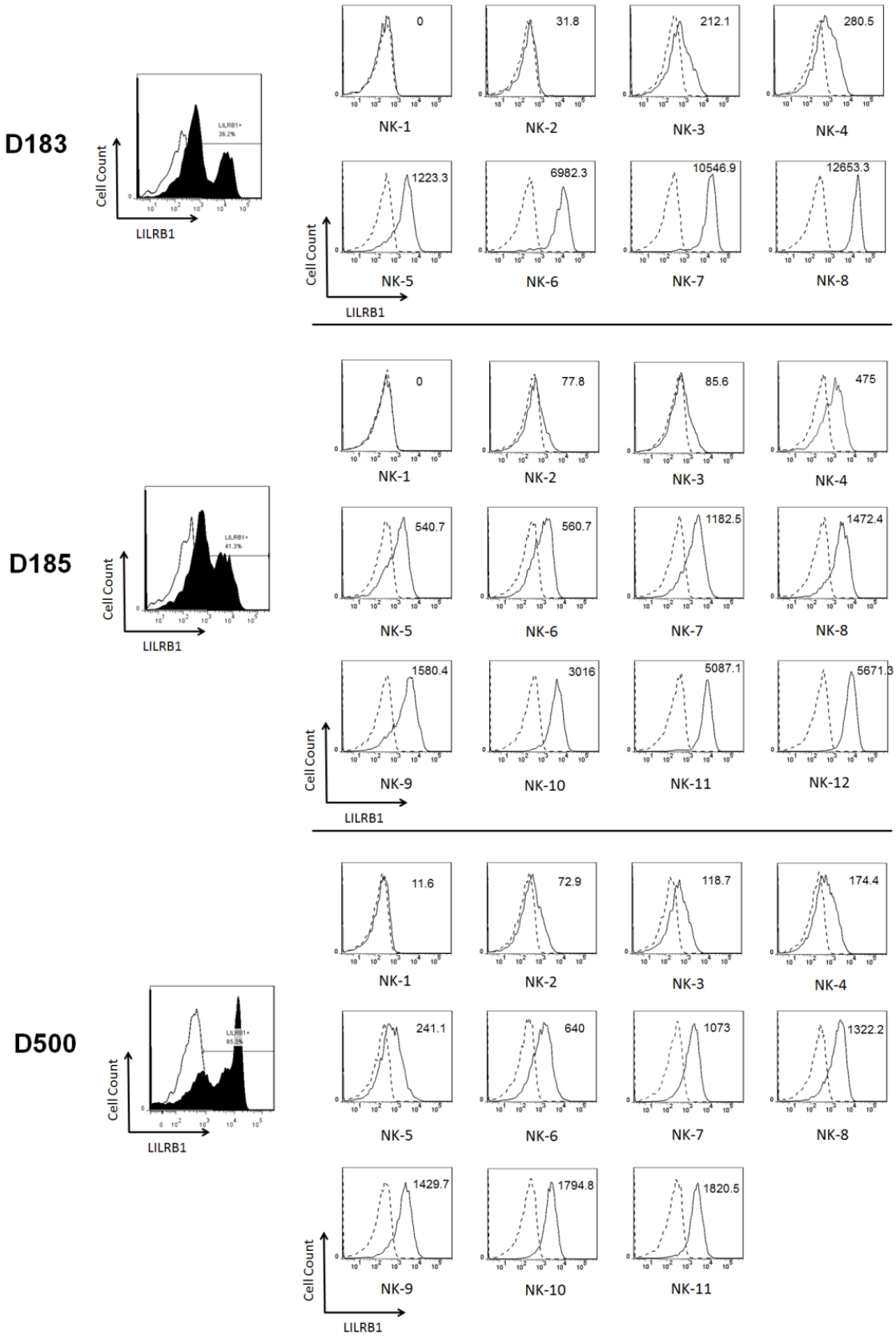
D183
LILRB1+
36.2%
Cell Count
LILRB1
0
31.8
212.1
280.5
NK-1
NK-2
NK-3
NK-4
1223.3
6982.3
10546.9
12653.3
NK-5
NK-6
NK-7
NK-8
Cell Count
LILRB1
D185
LILRB1+
41.3%
Cell Count
LILRB1
0
77.8
85.6
475
NK-1
NK-2
NK-3
NK-4
540.7
560.7
1182.5
1472.4
NK-5
NK-6
NK-7
NK-8
1580.4
3016
5087.1
5671.3
NK-9
NK-10
NK-11
NK-12
Cell Count
LILRB1
D500
LILRB1+
65.3%
Cell Count
LILRB1
11.6
72.9
118.7
174.4
NK-1
NK-2
NK-3
NK-4
241.1
640
1073
1322.2
NK-5
NK-6
NK-7
NK-8
1429.7
1794.8
1820.5
NK-9
NK-10
NK-11
Cell Count
LILRB1

Figure 3.1 Surface LILRB1 expression patterns of primary NK cells from three donors. Primary NK cells were isolated from three donors (D183, D185, and D500) and LILRB1 expression was determined by flow cytometry plotted on the left side. The white and black filled peaks indicate the unstained control and the staining using the LILRB1 antibody (HP-F1), respectively. The frequency of the LILRB1-positive subsets was shown inside of each plot. The LILRB1 expression of *ex-vivo* NK clones from each donor is shown correspondingly on the right. Dotted lines indicate the staining using isotype antibody and the black lines indicate using the LILRB1 antibody (HP-F1). The Geom.MFI value with background subtracted is shown inside of each plot.

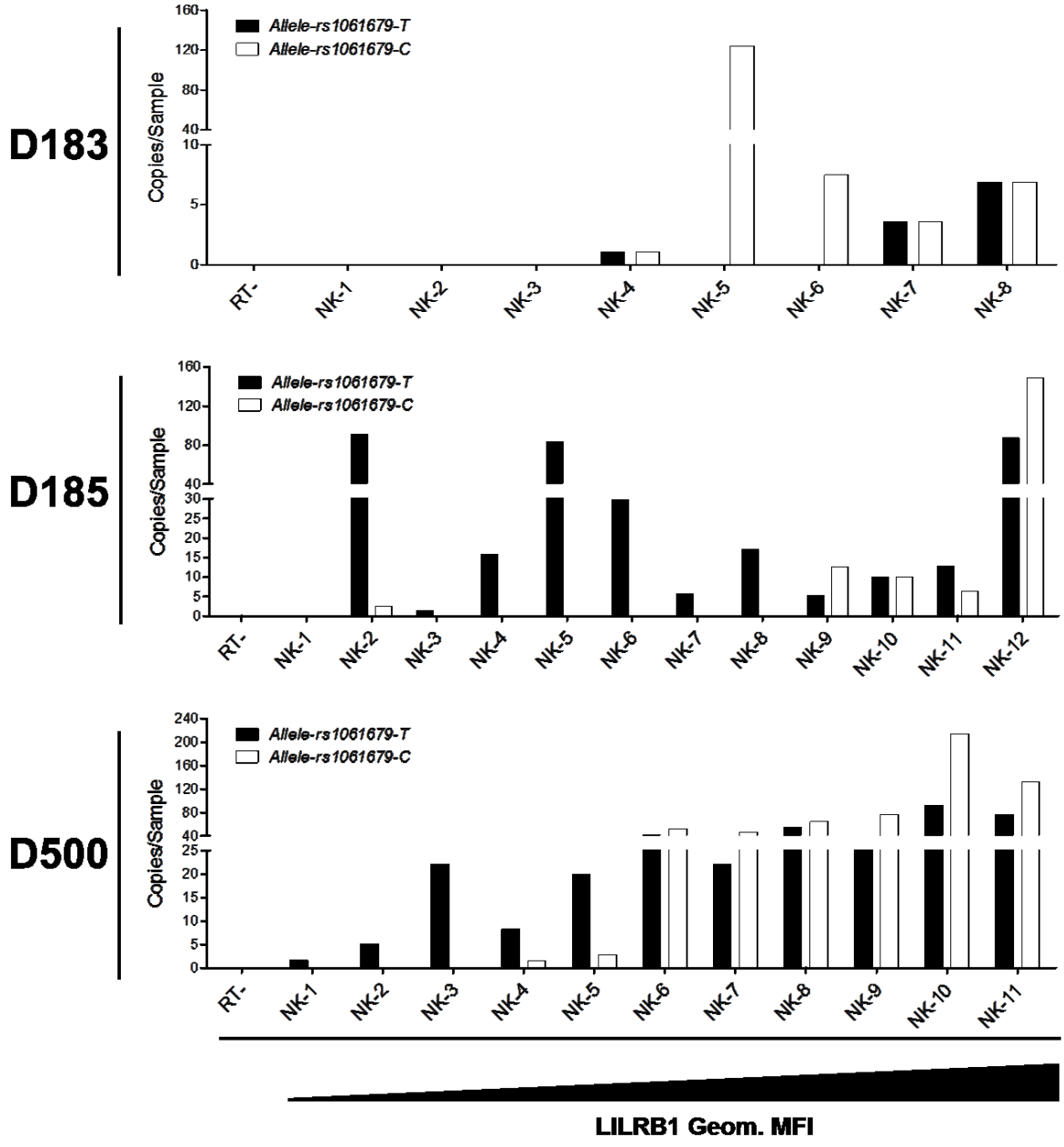

Figure 3.2 LILRB1 gene allelic expression of ex-vivo single NK clones.
Histogram corresponding to each donor in Figure 3.1 shows the copy number per sample of LILRB1 transcript from the rs1061679-T and rs1061679-C allele determined using ddPCR in *ex-vivo* NK cell clones. NK cells of different clones are plotted from low to high of LILRB1 surface expression as measured by flow cytometry (see Figure 3.1). RT- indicates the negative control without adding reverse transcriptase. Detailed values shown in the histogram are listed in Appendix A1.

expression that could mediate allele-specific effects, I looked for evidence of additional regulatory elements in the LILRB1 gene using data from the Roadmap Epigenomics project (http://www.roadmapepigenomics.org/) [289]. The dataset includes patterns of histone modifications and DNase sensitivity for populations of cells denoted as CD56, CD3, CD19, and CD14 markers for NK, T, B, and monocyte cells. First, I examined the patterns of DNA accessibility and histone modification at the known promoters in the various cell populations (Figure 3.3A). Active promoters are marked by DNase hypersensitivity (green) and H3K4me3 (blue) and H3K27ac (orange). The region upstream of the distal promoter showed both H3K4me3 and H3K27ac in CD56, CD3, and CD19 cells but not CD14 cells (Figure 3.3A). This pattern of histone modification is consistent with the fact that only lymphocytes use the distal promoter to transcribe LILRB1. A reciprocal situation is found at the proximal promoter which is marked as an active promoter only for the CD14 cells.

In the three lymphoid cell types, there is a 3 kb region within intron 1 with high sensitivity to DNase and three peaks densely marked by H3K4me1 (red) and H3K27ac (region boxed in Figure 3.3A), a pattern of modifications associated with active enhancers [288]. The intensity of the signal is greatest for CD19, followed by CD56 and then CD3, which corresponds to the expected proportion of cells that would express LILRB1 for each lineage and the region does not exhibit the modifications in CD14 cells. Published ATAC-Seq data from decidual NK cells [290] also showed the 3 kb region has high accessibility further supporting a role for this region in regulating transcription (Figure 3.3B). In addition, analysis of available ChIP-Seq data from the ENCODE (https://www.encodeproject.org/) or GEO (https://www.ncbi.nlm.nih.gov/geo/) datasets [291, 292], also contains histone modifications indicative of an active enhancer at the same region in three lymphoblastoid cell lines and Jurkat cells, further supporting the 3 kb region as a regulatory site in lymphoid cells (Figure 3.5). The region starts at 55135000 and ends at 55137700 (Human hg19) and, as expected for an intron, has a high degree of variability with many SNPs recorded in the SNP and the 1000 genomes databases (Figure 3.4A).

To characterize the putative enhancer region and the relationship with the promoter

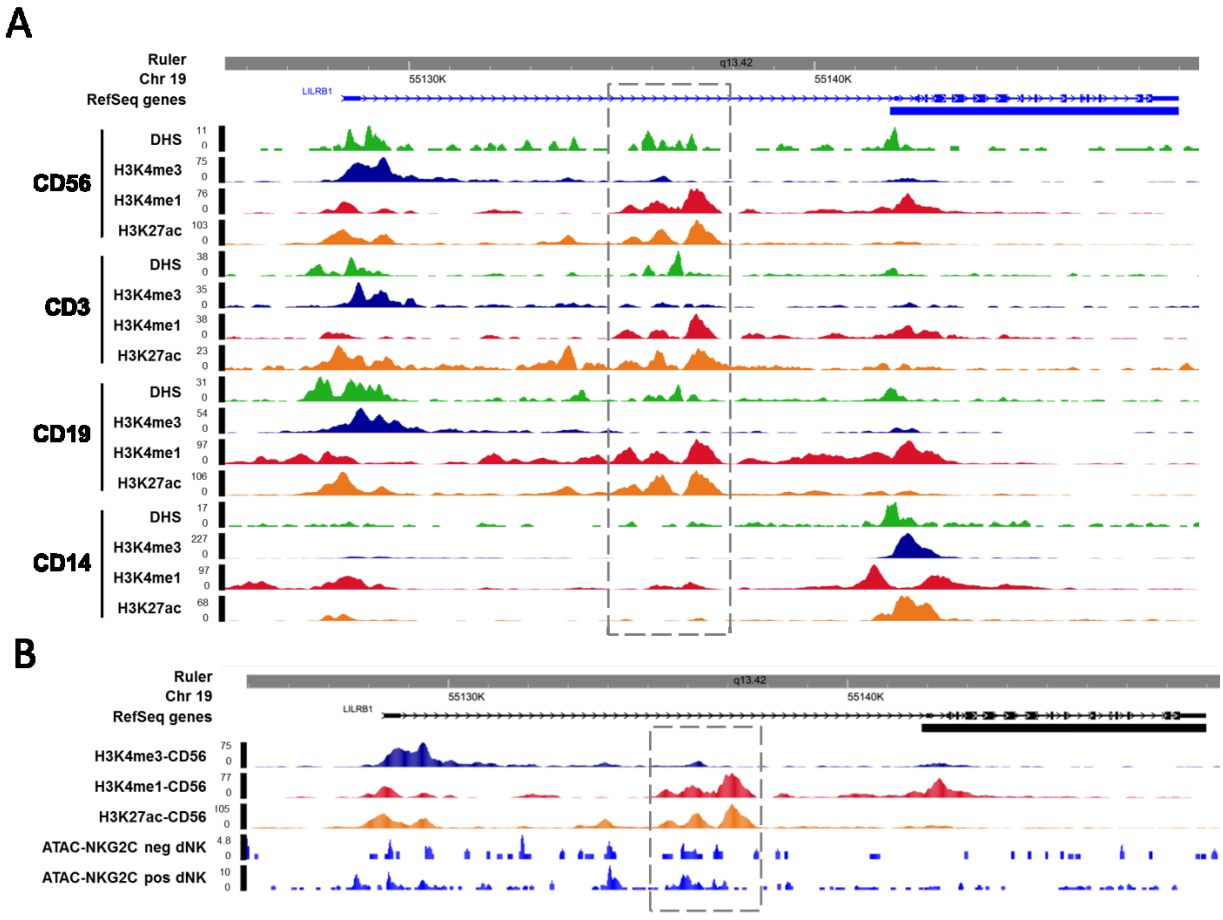

Figure 3.3 Prediction of a putative enhancer region in the intron 1 of the LILRB1 gene. (A) Histone modification markers at LILRB1 gene locus in different types of immune cells. DNase I hypersensitivity sites (DHS) and histone modifications ChIP-Seq data of CD56, CD3, CD19 and CD14 primary cells shown above was achieved from the "NIH Roadmap Epigenomics Project" (http://www.roadmapepigenomics.org/). The GEO database (https://www.ncbi.nlm.nih.gov/geo/) accession number for each track is listed as following: CD56 (DHS-GSM665836; H3K4me3-GSM1027301; H3K4me1-GSM1027297; H3K27ac-GSM1027288), CD3 (DHS-GSM701526; H3K4me3-GSM1058782; H3K4me1-GSM1058778; H3K27ac-GSM1058764), CD19 (DHS-GSM701492; H3K4me3-GSM537632; H3K4me1-GSM1027296; H3K27ac-GSM1027287), CD14 (DHS-GSM701503; H3K4me3-GSM1102797; H3K4me1-GSM1102793; H3K27ac-GSM1102782). The grey dotted box indicates the location of the lymphoid-specific putative enhancer. (B) ATAC-Seq at the LILRB1 gene locus in decidual NK cells. H3K4me3, H3K4me1, and H3K27ac ChIP-Seq data are the same as what is shown in panel A to indicate the region of the promoter and putative enhancer (grey dotted box). The ATAC-Seq data from human NKG2C- and NKG2C+ decidual NK cells was acquired from GEO DataSets (GSE100636) [290].

haplotypes, I amplified the predicted enhancer region from NKL cells that have both promoter haplotypes as well as two donors D230 and D258 which are homozygous for the promoter haplotypes [277]. The alignment of a portion of the sequence is shown in Figure 3.4B. Despite being heterozygous for the promoter haplotypes, only one sequence was derived from NKL for the entire 3 kb region. Only one sequence was derived from D258 as well, however, it differs from NKL's in a number of places, 4 of which are shown in Figure 3.4B. I obtained two alleles from D230 and while the sequence is more similar to that of NKL for the region shown in the left panel of Figure 3.4B, it differs in other regions as shown in the right panel of Figure 3.4B. As will be discussed in more detail below, algorithms to predict transcription factor binding sites indicate a large number of potential sites for factors known to be expressed by lymphoid cells such as STAT4, Pax5, and c-Ets-1 (Table 3). The sequence variation in this putative enhancer region suggests alleles could differentially recruit transcription factors. In addition, the region has predicted YY1 sites, and YY1 is a factor that has been implicated in enhancer function.

3.2.3 YY1 interacts with the enhancer and the LILRB1 promoters

The physical interaction of enhancers with promoters can be mediated by certain cofactors including the mediator, cohesin, and DNA-binding proteins such as YY1 that facilitate and stabilize the DNA looping structure by forming dimers [293-296]. YY1 is also a factor that can promote or prevent transcription and several YY1 binding sites are predicted in the putative enhancer region as well as in the distal and proximal promoters. There is also evidence YY1 binds to the putative enhancer region and the two promoters in three lymphoblastoid cell lines and Jurkat cells from the published ChIP-Seq data from the ENCODE and GEO datasets (Figure 3.5) [291, 292]. These observations suggest YY1 could mediate physical interaction between the enhancer and the two promoters. To test if YY1 also binds to the putative enhancer and/or the two promoter elements of the LILRB1 gene in NK-type cells, I applied YY1-chromatin immunoprecipitation (ChIP) in NKL cells. I analyzed 13 YY1 sites within the putative enhancer

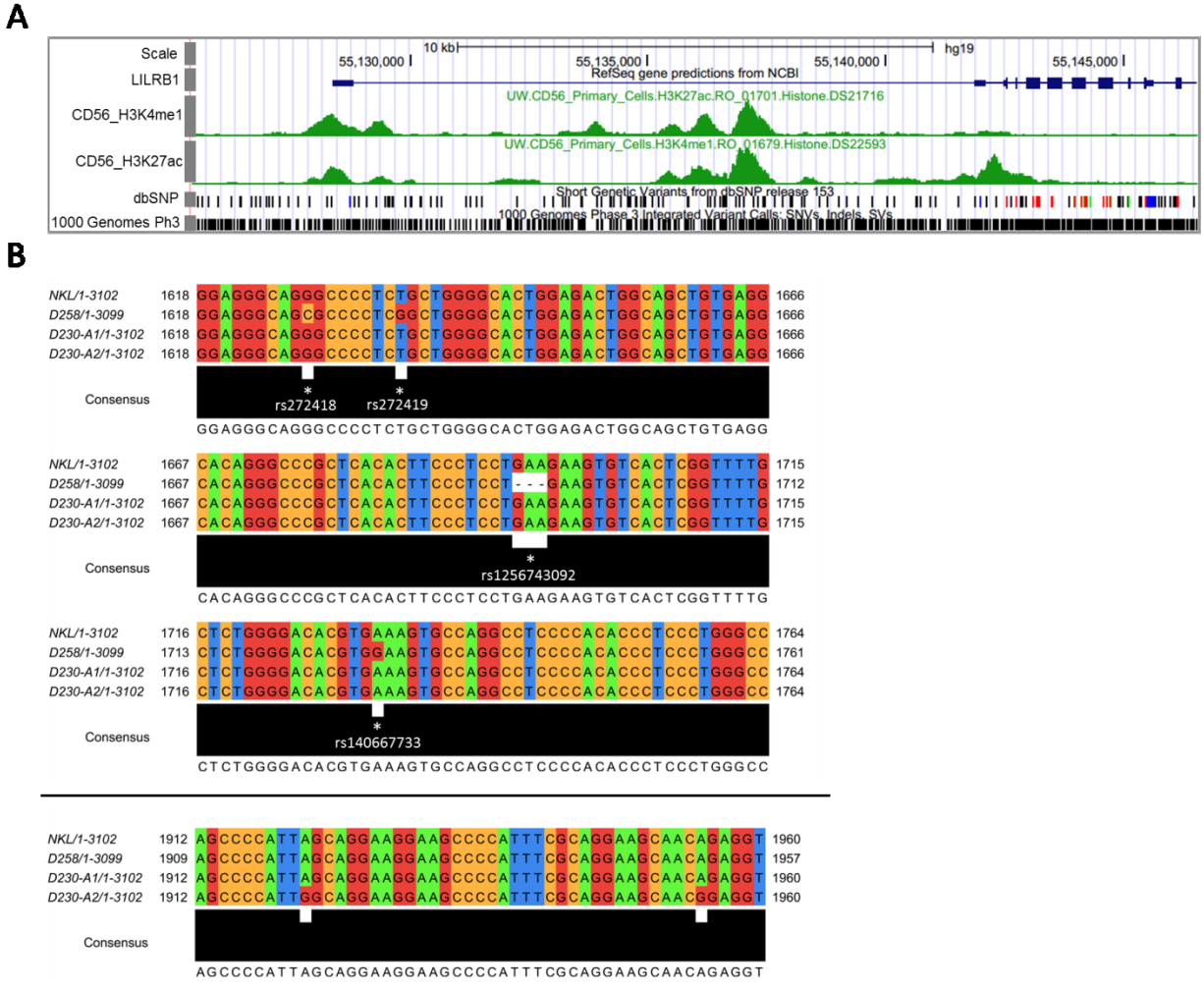

Figure 3.4 Polymorphisms of the putative enhancer region.
(A) Sequence variation data at the LILRB1 gene locus shown is from the SNP database and the 1000 genomes project (Phase 3). Signals of H3K4me1 and H3K27ac in CD56 primary cells are also shown to indicate the position of the putative enhancer. (B) A partial region of the alignment of the amplified putative enhancer from NKL, the homozygous "high" donor (D258), and the homozygous "low" donor (D230). Several SNPs are marked by white asterisks in the upper panel. D230-A1 and A2 indicate the two alleles sequenced from the genomic DNA of donor D230 which can be differentiated by the alignment shown in the lower panel. Numbers after each name indicates the size of the putative enhancer sequenced. The alignment was done using the Mafft program.

Table 3 Prediction of transcription factor binding sites in the region of the putative enhancer.

			Predicted Binding Sites		
TFs	Expression in NK	Transcriptional Activity	D258	D230-A1	D230-A2
C/EBPbeta	Y	Activator	74	73	73
C/EBPalpha	N	Activator	9	8	8
c-Ets-1	Y	Activator/Repressor	11	9	9
EBF1	N	Activator/Repressor	3	4	4
GCFC2	Y	Repressor	1	0	0
GR-alpha	Y	Activator/Repressor	45	45	44
GR-beta	Y	Dependent on GR-alpha expression	68	67	67
HIF-1	Y	Activator	0	1	1
NF-kappaB1	Y	Activator/Repressor	0	1	0
NF-Y	Y	Activator/Repressor	3	3	4
p53	Y	Activator	29	28	28
Pax-5	N	Activator	30	31	31
RelA	Y	Activator	0	1	1
RXR-alpha	?	Activator/Repressor	34	33	33
STAT4	Y	Activator	29	27	27
USF1	?	Activator	4	3	3
YY1	Y	Activator/Repressor	23	23	23

The prediction was done using the ALGGEN-PROMO program (http://alggen.lsi.upc.es/cgi-bin/promo_v3/promo/promoinit.cgi?dirDB=TF_8.3) with the sequenced genomic sequence from homozygous "high" donor (D258) and the homozygous "low" donor (D230). In the "Expression in NK" lane, "Y" and "N" indicates yes or no, respectively, while "?" means unknown, and the information was acquired from Proteomics DB (https://www.proteomicsdb.org/proteomicsdb/#overview). The information about the transcriptional activity for the listed factors was acquired from the NCBI-Gene database (https://www.ncbi.nlm.nih.gov/gene/), GeneCards (https://www.genecards.org/) and Wikipedia (https://en.wikipedia.org/wiki/Main_Page). There are two lanes of prediction for enhancer allele 1 and 2 sequenced from the genomic DNA of donor D230. The number listed indicates the number of predicted binding sites in the putative enhancer for each specific transcription factor.

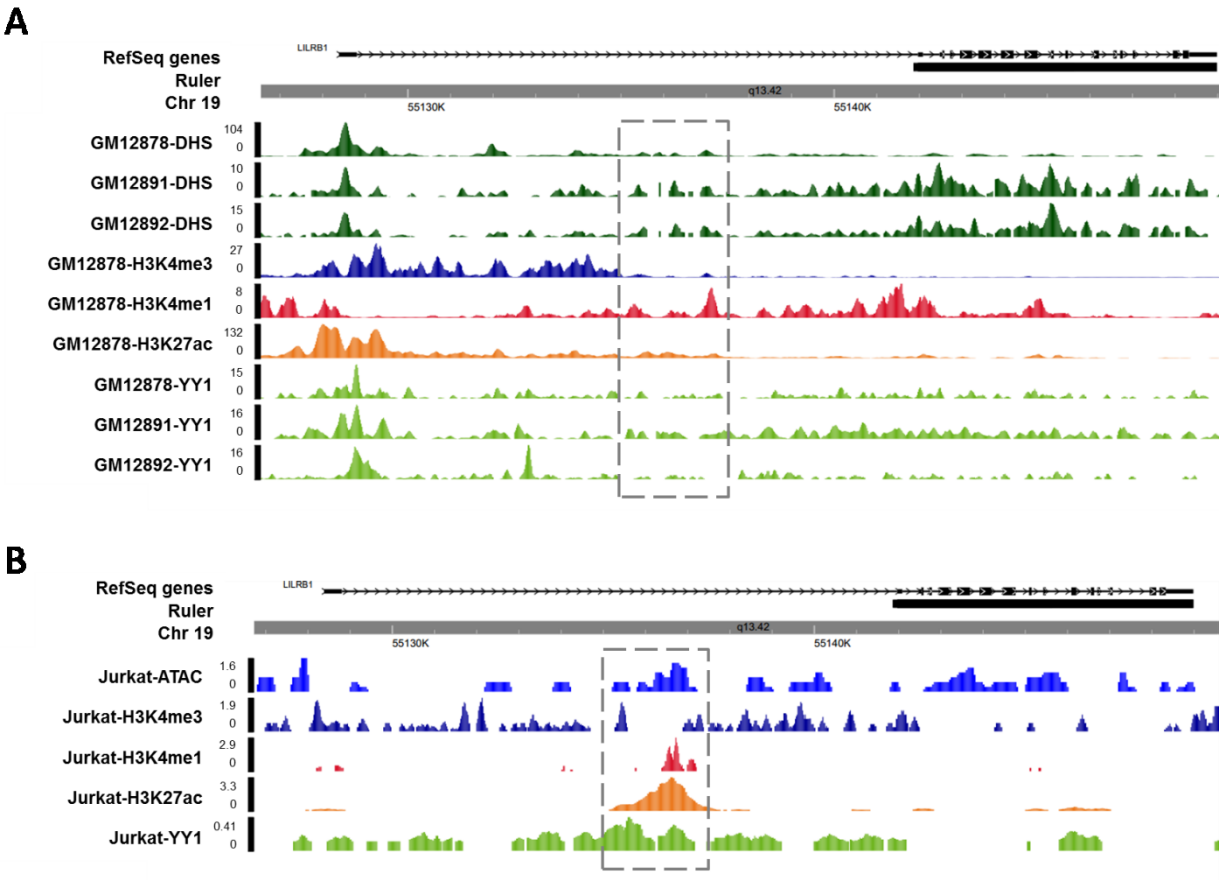

Figure 3.5 Histone modification markers and YY1 ChIP at LILRB1 gene locus in lymphoblastoid cell lines and Jurkat cells.

(A) Histone modification ChIP-Seq data of GM12878 cell line, DHS, and YY1 ChIP-Seq data of GM12878, GM12891, and GM12892 at LILRB1 gene locus. The GEO accession number for each track is listed as following: GM12878 (DHS-GSM736620; H3K4me3-GSM733708; H3K4me1-GSM733772; H3K27ac-GSM733771; YY1-GSM803406), GM12891 (DHS-GSM816656; YY1-GSM803535), GM12892 (DHS-GSM816657; YY1-GSM803516). (B) Histone modification ChIP-Seq, ATAC-Seq, and YY1 ChIP-Seq data of Jurkat cells. The GEO accession number for each track is listed as following: ATAC-GSM3693103; H3K27ac-GSM1697882; H3K4me1-GSM3374691; H3K4me3-GSM945267; YY1-ChIP-GSM2773998. In both panel A and B, The grey dotted box indicates the putative enhancer region.

region and two promoter regions and detected YY1 binding at 10 sites (Figure 3.6). Two of the sites were excluded due to high background for the negative control (E1 and D5) and all the remaining 11 sites shown except D3 have YY1 association (Figure 3.6). The D1 and P3 sites consistently provided the most intense signal suggesting the highest occupancy with YY1 for these sites. The ChIP results indicate YY1 is present at the promoter and enhancer regions and support the possibility YY1 scaffolds these regulatory elements together.

3.2.4 The putative enhancer and the two promoters form DNA-loops

Given genome-wide high throughput chromosome conformation capture by sequencing (HiC-Seq) assay is a powerful tool used to identify chromatin interactions across the whole genome [297], I first examined the chromatin interacting pattern at the LILRB1 gene locus using HiC data in the 4D Nucleome Data Portal [298] available for several lymphoblastoid cell lines. I visualized the data using the HiGlass browser that provides a two-dimensional heat map with the mirrored organization of chromatin. Signals inside of the heat map indicate the richness of the sequencing counts derived from the interactions between the fragments in horizontal and vertical axes. The analysis reveals signals indicting the interaction between the putative enhancer and both of the LILRB1 promoters in most cell lines (boxed regions) (Figure 3.7B). However, the dilution HiC data available is all derived from HindIII libraries which did not provide the best resolution for the fragments we are interested in (Figure 3.7A).

Therefore, I went on to test if the putative enhancer is in direct physical contact with the LILRB1 gene promoters in NK cells by performing 3C-qPCR on NKL cells. I used EcoRI to generate suitable fragments to resolve the putative enhancer from the LILRB1 promoters and specify their interaction (Figure 3.8A). The probe and the anchoring primer were designed within the enhancer fragment close to the EcoRI site at -7667 from the translational start codon and all the test primers for the fragments were designed close to the upstream restriction end (Figure 3.8A). Among the three distal fragments examined, the -16483-fragment encompassing

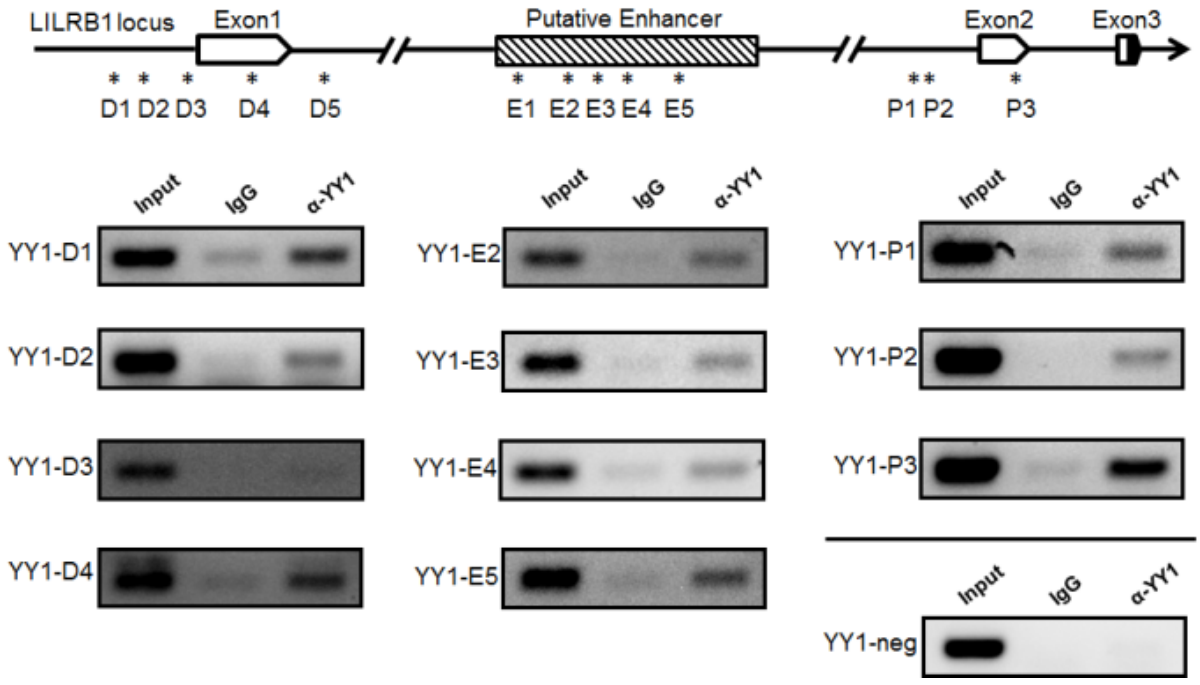

Figure 3.6 YY1-ChIP analysis on the region of the putative enhancer, and the LILRB1 gene distal and proximal promoters in NKL cells.

Schematic of partial LILRB1 gene locus and location of the tested predicted YY1 binding sites marked by asterisks. The protein-coding region starts in exon 3 and is filled with black. The primers used for each predicted site shown above are listed in Table 2. ChIP results are shown as electrophoresis of the PCR products detecting YY1 binding at different sites in NKL cells. Input and IgG worked as a positive and negative control for the ChIP assay, respectively, and the YY1-neg was a negative control detecting a non-YY1 binding site for the ChIP antibody targeting human YY1. The results of YY1-D5 and YY1-E1 are excluded due to their high background with IgG control. The results shown are representative of 3 independent experiments.

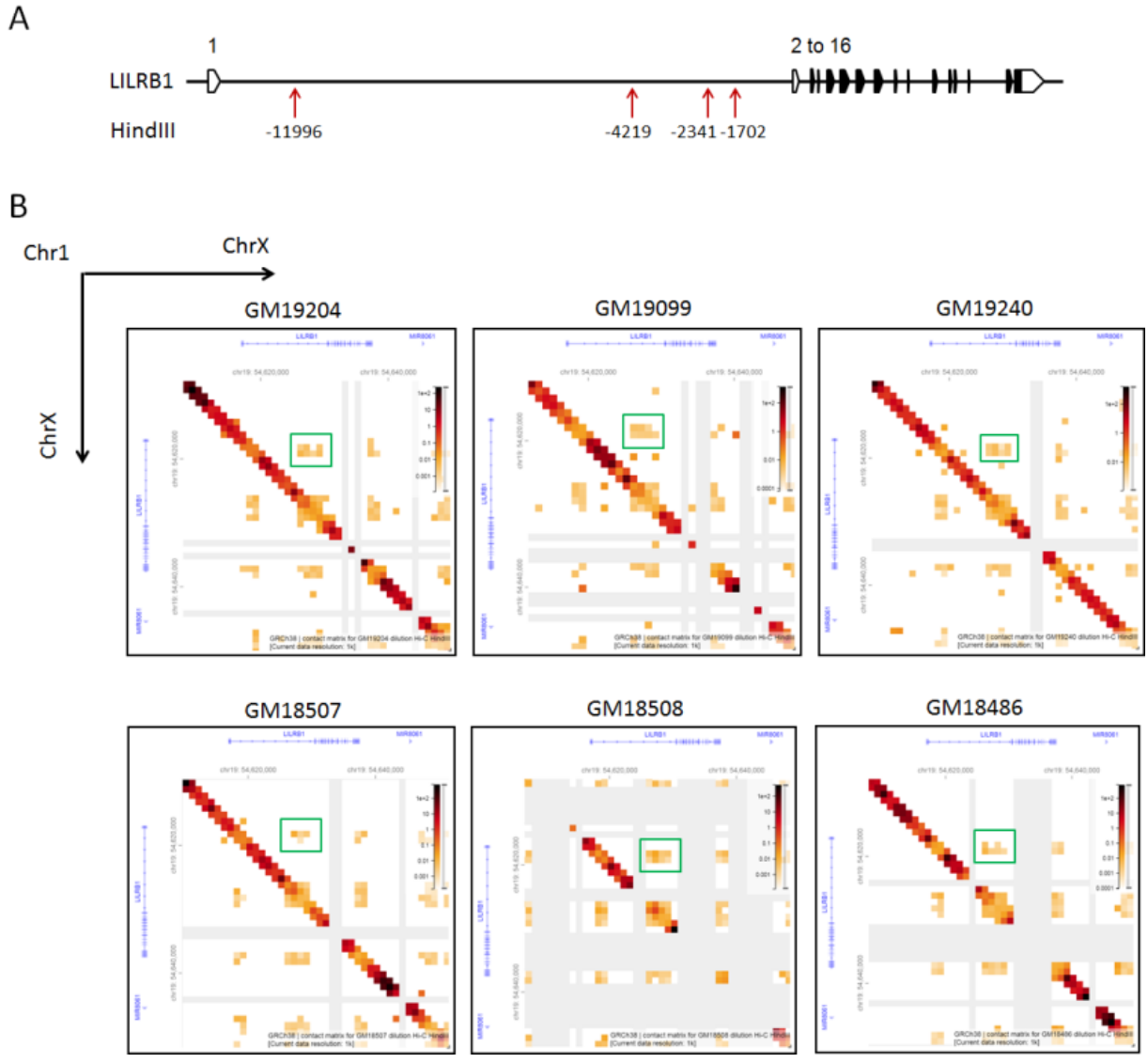

Figure 3.7 Dilution HiC map at LILRB1 gene locus of lymphoblastoid cell lines.
(A) Schematic showing the HindIII cutting sites at LILRB1 gene locus. (B) 1kb resolution zoom-in view at LILRB1 gene locus in Dilution HiC 2-D map of 6 different lymphoblastoid cell lines acquired from 4D Nucleome (4DN) Data Portal and displayed by Hi-Glass browser. All the Dilution HiC results shown above were using the HindIII enzyme to build the assay library. The interaction between the fragment containing the distal promoter and the putative enhancer on the upper right phase is gated by a green box in each plot. 4DN accession numbers for the HiC experiments shown above are listed as following: GM19204-4DNFI78T9N5Y; GM19099-4DNFIKAC7MSF; GM19240-4DNFIM8KVPS6; GM18507-4DNFIEYSPGU1; GM18508-4DNFI6SJZVXZ; GM18486-4DNFI7N72M2A.

the distal promoter has a significantly stronger interaction with the anchor in the enhancer than fragments on either side (Figure 3.8A). There were two additional major and minor interactions observed with -1972 and -1474 in the proximal region respectively, where the proximal promoter and the YY1 site denoted as P3 in Figure 3.6 are included in the latter fragment (Figure 3.8A). The stronger signal for the -1972-fragment suggests the region upstream of the previously defined "core promoter" is involved.

To investigate if YY1 is part of the complexes that contain the enhancer and promoter in the 3C assay, I used ChIP-loop, a technique that combines ChIP and 3C. In brief, the chromatin-capture procedure was initiated and then, the YY1-associated complexes were immunoprecipitated and subsequently analyzed by PCR for the ligation products. As shown in Figure 3.8B, specific ligation products with the three fragments denoted as -16483, -1972 and -1474, were detected in the α-YY1-immunoprecipitated samples relative to an IgG control and the negative control region at -17925. Collectively, the 3C and ChIP-loop data are consistent with the YY1-ChIP placing YYI at the site of the enhancer and promoters in complex with each other in NKL cells.

3.2.5 Deletion of the putative enhancer decreases LILRB1 expression

I tested the ability of the 3.2 kb region to enhance the distal promoter using the pGL3-basic luciferase system. However, the region actually repressed transcription and its size made it difficult to pursue this approach. To more directly test the role of the putative enhancer in LILRB1 gene expression in the context of chromatin, I applied CRISPR-Cas9 technology to delete the 3.2 kb region in NKL cells as illustrated in Figure 3.9A. I sorted single-cell clones with lower LILRB1 expression by flow cytometry and analyzed by PCR to more readily ascribe the relative LILRB1 expression to the deletion and assess the variability of LILRB1 expression in un-manipulated but cloned NKL cells. I selected clones with decreased surface LILRB1 expression compared with the NKL control. In these six clones, detected bands corresponding to

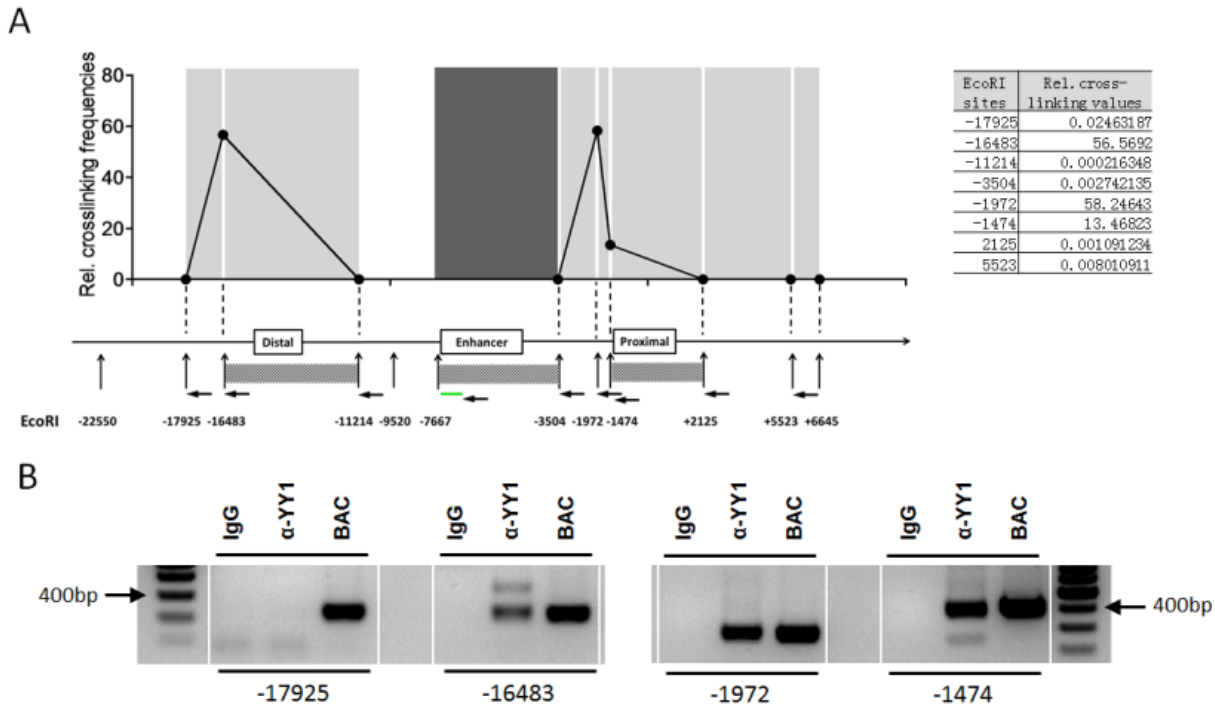

Figure 3.8 Physical contact between the putative enhancer and LILRB1 gene promoters involving YY1 in NK cells.

(A) Analysis of physical contact between the putative enhancer and the LILRB1 gene promoters by 3C-qPCR assay in NKL cells. The chromatin was digested by EcoRI, and the EcoRI sites are marked by vertical arrowheads. All the numbers below the EcoRI sites are indicating the distance to the translational start site of LILRB1 gene. Dark grey shading indicates the anchor fragment and the light grey shading indicates the fragments tested for the cross-linking frequency with the anchor fragment. The green bar represents the Taqman probe and the horizontal arrowheads indicate the positions of primers. Asterisks indicate the 10 sites with YY1 binding shown in Figure 3.6. The exact relative cross-linking values listed on the right were calculated referring to the method described previously (42). The results shown are representative of 3 independent experiments. (B) Involvement of YY1 in the enhancer/promoter physical interaction tested by ChIP-loop assay (ChIP+3C) shown as electrophoresis of the PCR products using 3C primers. The fragment -17925 was used as a negative control validated in panel A. Library build using BAC DNA encompassing the whole LILRB1 gene was used as a positive control. Target PCR products were sequenced to verify the specificity. The results shown are representative of 3 independent experiments.

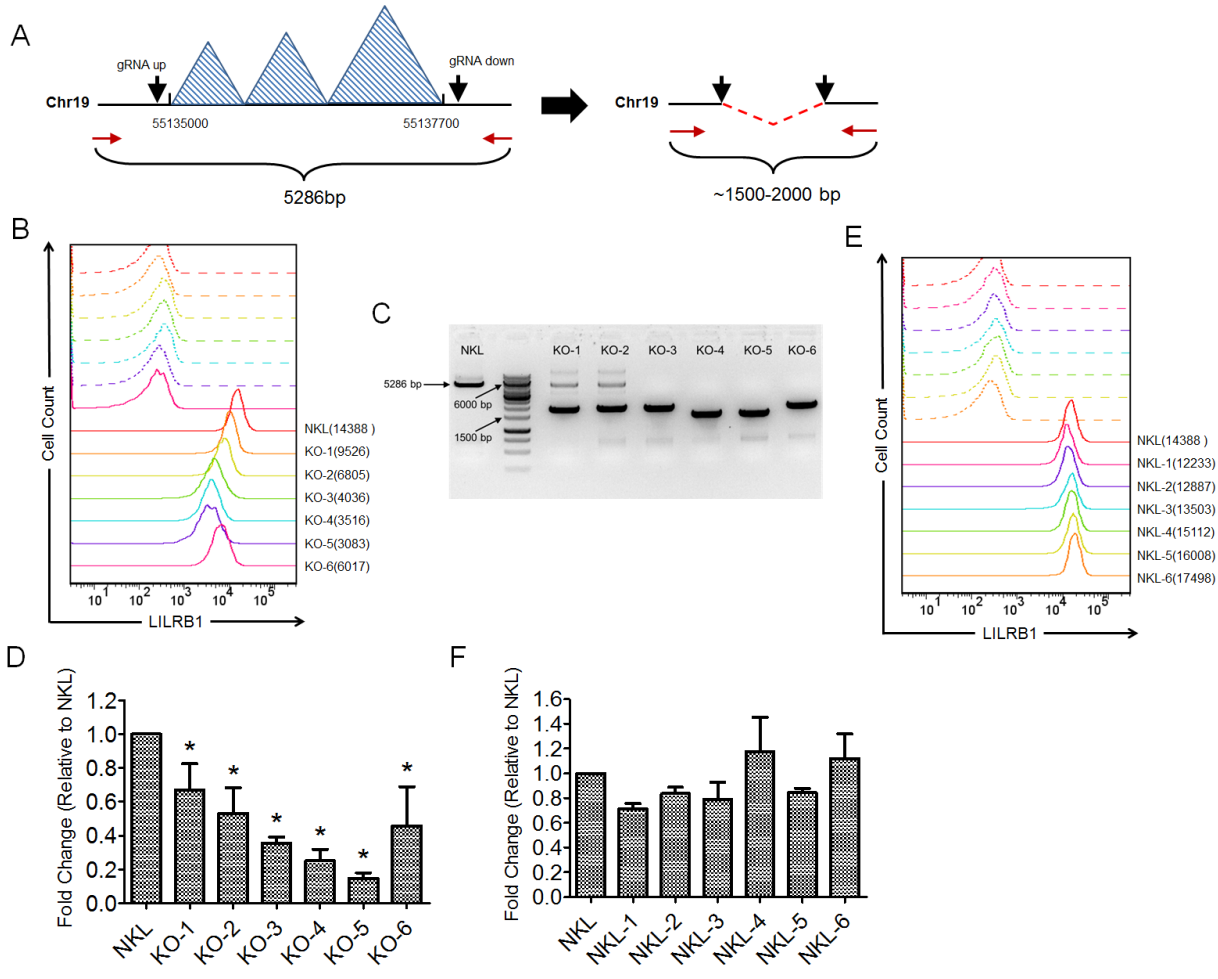
A
gRNA up
gRNA down
Chr19
55135000
55137700
5286bp
Chr19
~1500-2000 bp
B
Cell Count
LILRB1
NKL(14388)
KO-1(9526)
KO-2(6805)
KO-3(4036)
KO-4(3516)
KO-5(3083)
KO-6(6017)
C
NKL
KO-1
KO-2
KO-3
KO-4
KO-5
KO-6
5286 bp
6000 bp
1500 bp
E
Cell Count
LILRB1
NKL(14388)
NKL-1(12233)
NKL-2(12887)
NKL-3(13503)
NKL-4(15112)
NKL-5(16008)
NKL-6(17498)
D
Fold Change (Relative to NKL)
NKL
KO-1
KO-2
KO-3
KO-4
KO-5
KO-6
F
Fold Change (Relative to NKL)
NKL
NKL-1
NKL-2
NKL-3
NKL-4
NKL-5
NKL-6

Figure 3.9 CRISPR-based knockout of the putative enhancer in NK cells.
(A) Schematic depicts the knockout of the putative enhancer represented by three peaks of H3K4me1 and H3K27ac signals using the CRISPR-Cas9 system in NKL cells. Black arrowheads indicate the location of the guide RNAs. Red arrowheads indicate the positions of primers to validate the fragment knockout. (B) Surface LILRB1 level on parental NKL cells and the knockout NKL clones (KO-1 to KO-6) tested by flow cytometry using the HP-F1 antibody. Different clones stained using the HP-F1 antibody are indicated by different colors and the dotted peak in the same color indicates the corresponding clones stained using isotype antibody. Each Geom.MFI value with background subtracted is shown beside the plot. (C) Electrophoresis detecting the knockout fragments in NKL clones shown in panel B. Parental NKL cells was used as a negative control. Sanger-sequencing was used to confirm the knockout sequence. (D) Total LILRB1 transcript level was detected in the knockout NKL cells using real-time quantitative PCR (RT-qPCR). Fold change values of the knockout cell lines relative to parental NKL cells were calculated using the 2^-ΔΔCt method. Means of the fold change calculated from three independent experiments were compared using Student's T-test, and "*" indicates the P-value<0.05. (E) Surface LILRB1 expression on six NKL sub-clones (NKL-1 to NKL-6) ranged from low to high MFI tested by flow cytometry using the HP-F1 antibody. Different clones stained using the HP-F1 antibody are indicated by different colors and the dotted peak in the same color indicates each clone stained using isotype antibody. Each Geom.MFI value with background subtracted is shown beside the plot. (F) Total LILRB1 transcript level was detected in the six NKL sub-clones using real-time quantitative PCR (RT-qPCR). Fold change values of the NKL cell clones relative to parental NKL cells were calculated using the 2^-ΔΔCt method.

the intact locus at 5286 bp from NKL control and to the expected deletion at around 1500 to 2000 bp and sequenced the product to ensure the deletion was of the correct locus. Among the 6 clones, KO-3, KO-4, KO-5, KO-6 with two alleles knocked out showed lower surface LILRB1 expression than that of KO-1 and KO-2 with one allele knocked out (Figure 3.9B and C). To investigate whether the decreased surface LILRB1 expression was due to the decreased LILRB1 transcription, I isolated total RNA from the 6 knockout clones and did quantitative real-time PCR to detect the change of LILRB1 transcript. Consistent with the flow cytometry data shown in Figure 3.9B, the LILRB1 mRNA level of the 6 knockout clones was all significantly decreased compared with the NKL control (Figure 3.9D). Importantly, the LILRB1 mRNA levels of those 6 clones were well matched with the LILRB1 MFIs detected by flow cytometry (Figure 3.9B and D), which suggested the knockout of the putative enhancer inhibited the LILRB1 gene transcription.

To ensure the lower LILRB1 transcript was not an artifact of sub-cloning the NKL line, I also isolated 19 NKL clones from the parental NKL cells. Although these NKL sub-clones have slightly different LILRB1 surface expression, they were all close to the parental level (Figure 3.9E). The mRNA was also analyzed for six of these clones showing minimal changes in the transcript level (Figure 3.9F). These results indicate the intronic putative enhancer plays a positive role in regulating LILRB1 gene transcription.

3.3 Summary

In this chapter, I explored a new transcriptional regulatory mechanism of LILRB1 in NK cells with a view to uncovering how lineage-specific patterns of expression are generated and how polymorphisms selectively control the expression patterns in NK cells. I used the features of KIR transcriptional regulation and publicly available epigenomic data as a guide. I investigated the allelic expression of LILRB1 in *ex-vivo* NK clones from heterozygous individuals and I showed that individual NK cells can express one or both alleles at the same

time and there is a correlation between the high cell surface density and the expression of both alleles. As indicated by the public ChIP-Seq data of histone modifications, I observed a region within the first intron of the LILRB1 gene and highly marked with active enhancer signals in primary NK cells. Amplification and alignment of this putative enhancer from two donors indicate it is a polymorphic element that is consistent with the data from the SNP database. Using software predicting transcription factor binding sites, I found that the polymorphisms in the putative enhancer may influence the binding of transcription factors expressed in NK cells. I also found some binding sites of YY1, a transcription factor reported as a structural protein in terms of enhancer/promoter physical interaction. Notably, I detected the association of YY1 with the putative enhancer as well as the distal and the proximal promoter of the LILRB1 gene by ChIP. Moreover, I demonstrated that the enhancer and the LILRB1 promotors were in physical contact using 3C assay and the complex can be pulled down by the YY1 antibody, implicating YY1 may work as a scaffold. Finally, I provide evidence that the deletion of the putative enhancer reduces the amount of LILRB1 transcript and protein in an NK cell line.

In conclusion, the LILRB1 gene is expressed by either or both alleles in NK clones and the newly identified intronic enhancer positively regulates LILRB1 gene expression presumably through interacting with the distal promoter mediated by YY1. The identification of this regulatory element provides new insight into the LILRB1 regulation mechanism in NK cells and may help better understand the formation of the heterogeneous LILRB1 expression patterns in NK cells.

CHAPTER 4

Influence of LILRB1 gene polymorphisms on NK cell function and interaction with ligands

A version of this chapter has been published in *Yu, K., Davidson, C. L., Wójtowicz, A., Lisboa, L., Wang, T., Airo, A. M., ... & Humar, A. (2018). LILRB1 polymorphisms influence posttransplant HCMV susceptibility and ligand interactions. The Journal of clinical investigation, 128(4), 1523-1537.*

4.1 Background

Our lab previously investigated the relationship of LILRB1 gene polymorphisms with the LILRB1 expression patterns on NK cells and defined two main haplotypes, involving a series of strongly-linked SNPs in both regulatory region and protein-coding region, associating with the relatively "high" and "low" frequency of LILRB1-positive NK cells (Figure 1.4) [3, 277]. In Chapter 3, I described that NK cells expressed the LILRB1 transcripts from the allele associated with the "high" haplotype more frequently than the allele associated with the "low" haplotype. As introduced in Chapter 1, HCMV infection is correlated with increased frequency of LILRB1-positive NK cells and the viral MHC-I mimic UL18 inhibits NK cells through binding to LILRB1. Thus, our group studied LILRB1 polymorphisms in the context of HCMV infection of transplant patients in two separate cohorts based on the hypothesis that patients with the "low" haplotype can better control HCMV. Unexpectedly, we observed that the patients with homozygous "low" genotype were in turn more susceptible to HCMV infection (Figure 1.5). A possible explanation for this finding is that the non-synonymous polymorphisms strongly linked with the promoter haplotypes influence the function of the LILRB1 protein variants such that the "low" haplotype is actually the one associated with greater NK cell inhibition.

Given the ability of UL18 to inhibit NK cell responses and the apparent importance of NK cells in controlling HCMV replication, I investigated the effect of only 4 known non-synonymous SNPs in the coding region of ligand-binding domains (D1 and D2) of the LILRB1 gene on modulating NK cell function and binding to the viral ligand UL18. I hypothesized that the LILRB1 variants linked with the "low" haplotype have stronger inhibition to NK cell function and interaction with UL18. To this end, I selected the major protein variant "LAIS" and one of the minor variants "PTTI" which has all the four mutated amino acids different to the major variant to test my hypothesis (Figure 1.4). I also included several MHC-I molecules as the control as UL18 binds to the D1 and D2 domains of LILRB1 in a manner that parallels the interaction of LILRB1 with MHC-I [221].

4.2 Results

4.2.1 LILRB1 variants differ for functional inhibition of NK cells

To test potential functional differences between the LILRB1 variants, I established an *in-vitro* system with conventional 721.221 tumor targets expressing surface UL18. The 721.221 cell line was transduced with a retroviral vector encoding UL18 with hemagglutinin (HA) tag at the N-terminus and YFP at the C-terminus. UL18 expression levels are shown as measured with anti-HA and the intrinsic YFP expression relative to the parental cell line (Figure 4.1A).

To directly compare the function of the two LILRB1 variants that differ at all four polymorphic positions in D1D2, I expressed the two variants denoted as LAIS and PTTI in a LILRB1-negative NK cell line. I transduced YTS cells with HA-tagged LAIS-LILRB1 and HA-tagged PTTI-LILRB1, and selected sub-clones with similar surface expression levels of LILRB1 by flow cytometry using HP-F1 and α-HA (Figure 4.1B). A similar ratio of HA to HP-F1 suggests that the four amino acid differences do not lead to major changes in the conformation of the receptor. I confirmed the function of the receptors in YTS cells using 221 cells expressing HLA-G (Figure 4.1C) and the antibody W6/32 to block the recognition and prevent inhibition (Figure 4.5D). Lysis of 221 cells by YTS-LAIS and YTS-PTTI was similarly and reproducibly reduced compared to parental YTS cells (Figure 3E, top panel), but the difference does not reach a measurable level of significance in aggregated data (Figure 3E, bottom panel). The lower lysis of the MHC-I deficient target is likely due to the expression of LILRB1 tempering signaling in YTS cells in a cell-intrinsic manner. The lysis of 221 cells bearing HLA-Cw15 (Figure 4.1C) or UL18 was lower for YTS-PTTI compared to YTS-LAIS (Figure 4.1E) suggesting a better interaction by PTTI and there was with no significant difference between the two LILRB1 variants with the more potent ligand HLA-G (Figure 4.1E, lower panel). Treatment with HP-F1 antibody to block LILRB1 function increases the lysis of Cw15, UL18, and HLA-G target cells to the same level as YTS cells demonstrating the receptor interaction with the ligand is indeed inhibiting the YTS cells (Figure 4.1F).

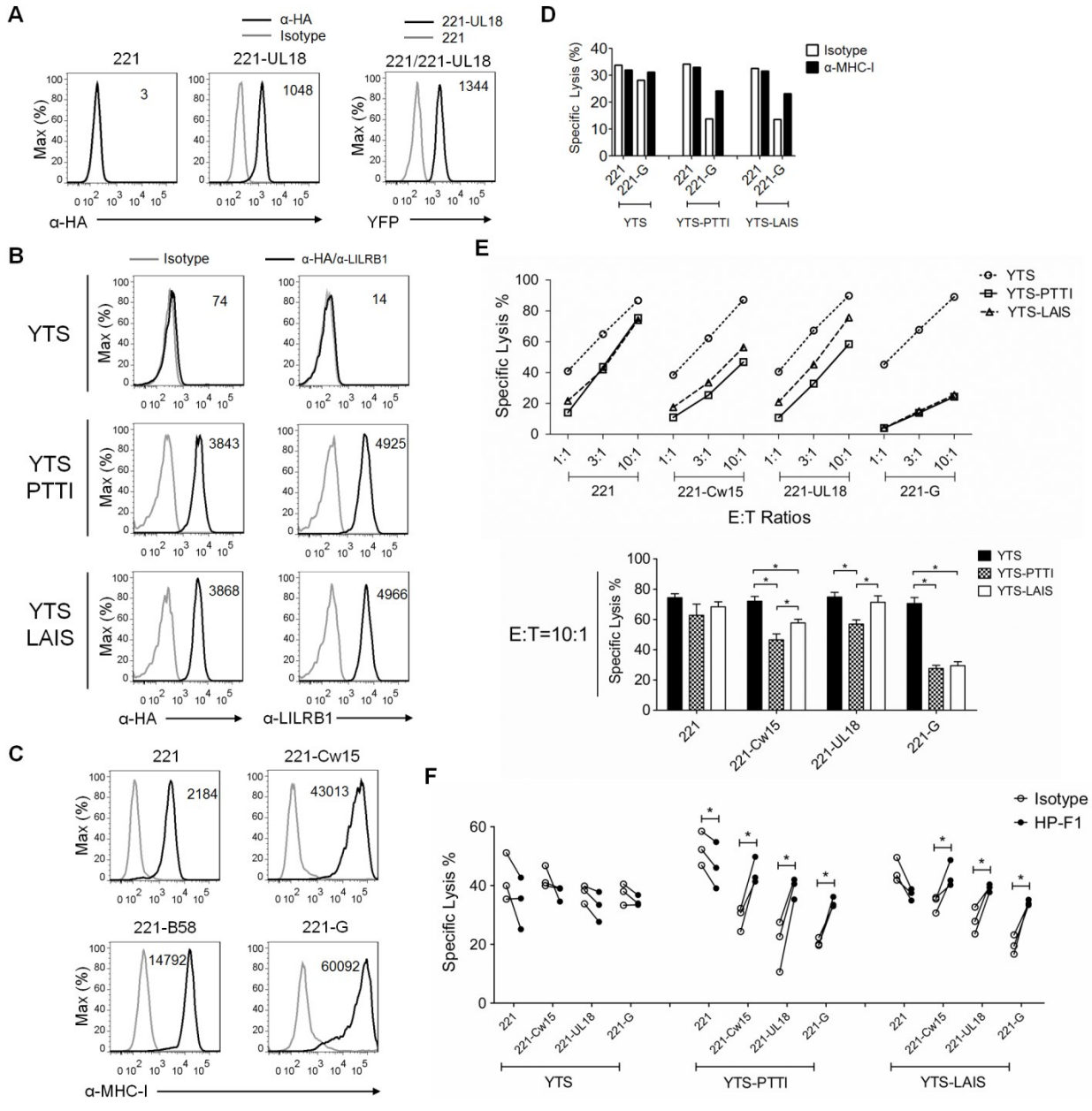
A
α-HA
Isotype
221-UL18
221
221
221-UL18
221/221-UL18
3
1048
1344
Max (%)
α-HA
YFP
D
Isotype
α-MHC-I
Specific Lysis (%)
221
221-G
YTS
YTS-PTTI
YTS-LAIS
B
Isotype
α-HA/α-LILRB1
YTS
YTS PTTI
YTS LAIS
74
14
3843
4925
3868
4966
Max (%)
α-HA
α-LILRB1
E
YTS
YTS-PTTI
YTS-LAIS
Specific Lysis %
1:1
3:1
10:1
221
221-Cw15
221-UL18
221-G
E:T Ratios
E:T=10:1
C
221
221-Cw15
221-B58
221-G
2184
43013
14792
60092
Max (%)
α-MHC-I
F
Isotype
HP-F1
Specific Lysis %
YTS
YTS-PTTI
YTS-LAIS

Figure 4.1 Functional activity of LILRB1-PTTI and -LAIS variants.
(A) Expression of HA–UL18-YFP on transduced 721.221 cells (left). MFIs are corrected for background staining in each case. (B) Surface expression of LILRB1 on YTS cells and LILRB1-transduced YTS cells detected with α-HA or α-LILRB1 (HP-F1). (C) Surface expression of MHCI on transduced 721.221 cells detected with W6/32. (D) Anti-MHC-I blocking of the killing of 721.221 cells expressing HLA-G by YTS cells expressing LILRB1 variants. The lysis was determined in the presence of 10μg/ml α-MHC-I (W6/32) or isotype control at an E: T of 10: 1. The figure shows the representative result of 3 independent tests. (E) Specific lysis of 721.221 cells; 721.221 cells presenting HLA-Cw15, HLA-G, and UL18 by YTS; and YTS cells expressing LILRB1. Upper panel: representative result from 6 independent assays with 3 E/T ratios. Lower panel: aggregated result of 6 experiments at an E/T of 10:1; error bars indicate SD. *$P < 0.05$ determined by paired-samples t-test. (F) The lysis was determined in the presence of 10 μg/ml α-LILRB1 (HP-F1) or isotype control IgG1κ at an E/T of 10:1. Results are aggregated from 3 independent tests. Error bars indicate SD. *$P < 0.05$ as determined by paired-samples t-test.

4.2.2 LILRB1 binding with HLA-I molecules and viral UL18

To probe the relationship of polymorphisms with the binding properties of the variants, I generated Fc-tagged versions of the D1-D2 domains of the two LILRB1 variants. The LAIS variant migrated slightly faster than the PTTI variant by SDS-PAGE analysis (Figure 4.2A). The two variants bind equally well to the antibody HP-F1 as previously reported [274] (Figure 4.2B). I compared the binding of the Fc-fusion protein to 221 cells expressing MHC-I ligands (Figure 4.1C) over a range of concentrations at 4°C detected by flow cytometry. The raw binding data are illustrated in Appendix A2. The signal was higher at all concentrations for the PTTI-Fc variant compared to the LAIS-Fc variant with HLA-Cw15 and with HLA-B58 (Figure 4.2C). Consistent with the functional assays (Figure 4.1), binding of the two variants to cells expressing HLA-G was similar. The binding was not saturated which precludes formal comparison of half-maximal binding concentrations. The binding specificity was demonstrated by blocking the antibody W6/32 (Figure 4.2D). I next compared the binding of the LILRB1 variants to 221 cells expressing UL18. I observed lower binding of LAIS-Fc compared to PTTI-Fc (Figure 4.3A), although the difference in binding to UL18 is less pronounced than with HLA-Cw15 and HLA-B58. I performed a reciprocal binding assay using purified UL18-Fc fusion protein and HA-tagged full-length LILRB1-PTTI and LAIS expressed on RBL cells normalized to the receptor levels using α-HA and HP-F1 respectively (Figure 4.3B). Again, LILRB1-PTTI bound better to UL18-Fc than LILRB1-LAIS most clearly at the highest concentration tested (900 nM), although the assay was limited by the amount of UL18-Fc available (Figure 4.3C). The results of the binding assays are consistent with the differences observed in the functional assays, although it is unclear why differences in binding with MHC-I were not observed by *Kuroki et. al* [274]. According to the published three-dimensional structures, none of the residues affected by the polymorphisms make direct contact with UL18 or HLA-A2, although they do all align on the same face of the receptor. The residues proline/leucine and threonine/alanine corresponding to rs1061679 and rs12460501, respectively, are located near the interface, whereas the residues threonine/isoleucine and isoleucine/serine corresponding to rs1061680 and rs1061681,

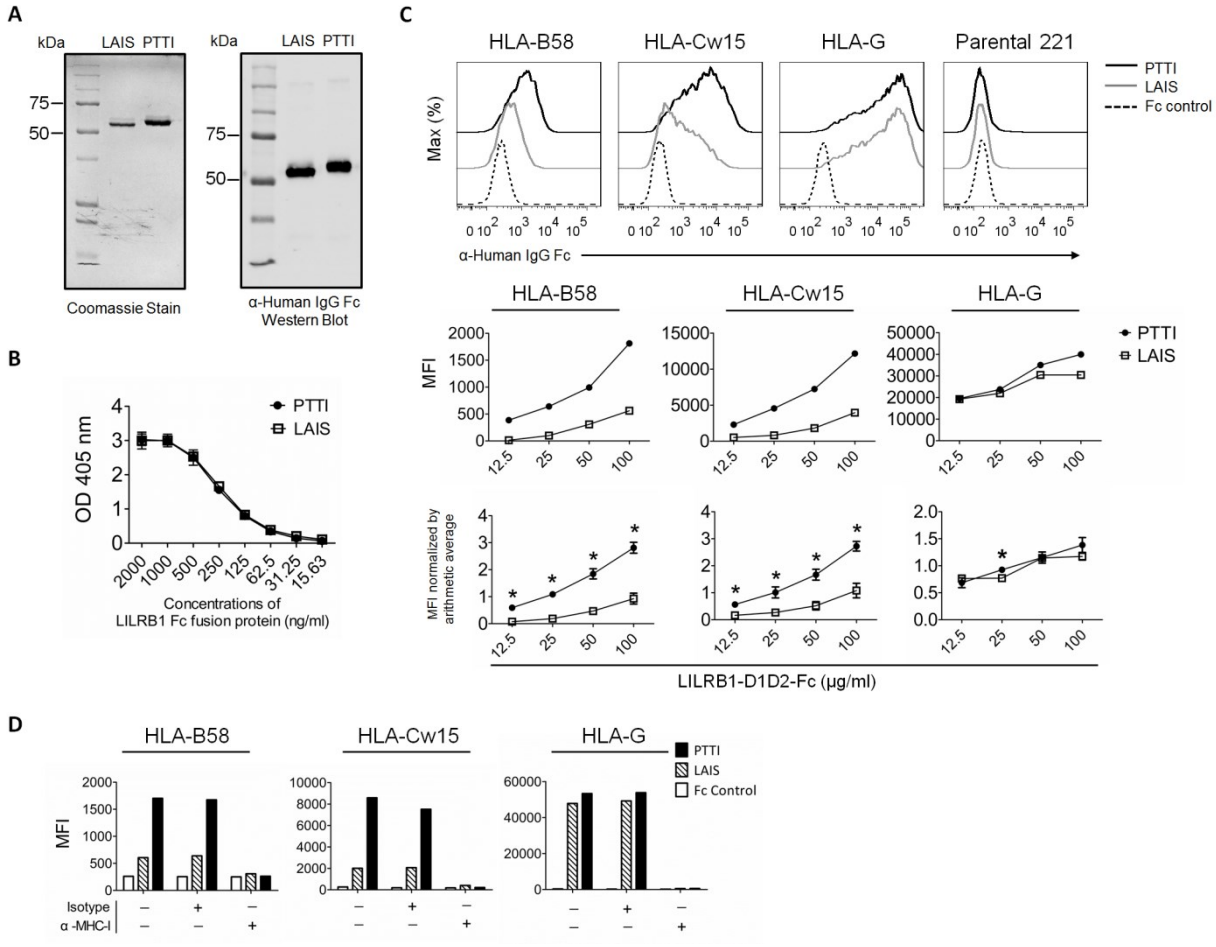

Figure 4.2 Binding of soluble LILRB1 variants to HLA-I molecules.
(A) Representative analysis of purified LILRB1 D1D2-Fc fusion proteins by Coomassie blue staining (left) and α-human IgG Fc Western blot (right). (B) Reactivity with α-LILRB1 (HP-F1) was determined by ELISA over the indicated range of concentration of the LILRB1-Fc protein. Results shown are the average of 3 independent tests for the same batch of protein; error bars represent SD. (C) The top histograms illustrate the binding of purified LILRB1-Fc to 221 cells with HLA-B58, HLA-Cw15, and HLA-G by flow cytometry at 50 μg/ml. The middle panels show 1 representative titration plotted as the MFI. The bottom series of plots show the normalized binding results aggregated from 3 independent tests. *$P < 0.05$ using 1-way ANOVA. (D) Cells expressing HLA-I were incubated with 10 μg/ml α-MHCI (W6/32) or the isotype antibody before the addition of 50 μg/ml LILRB1 variants or Fc control. The binding was measured by flow cytometry. The plots shown are a representative result of 3 independent tests.

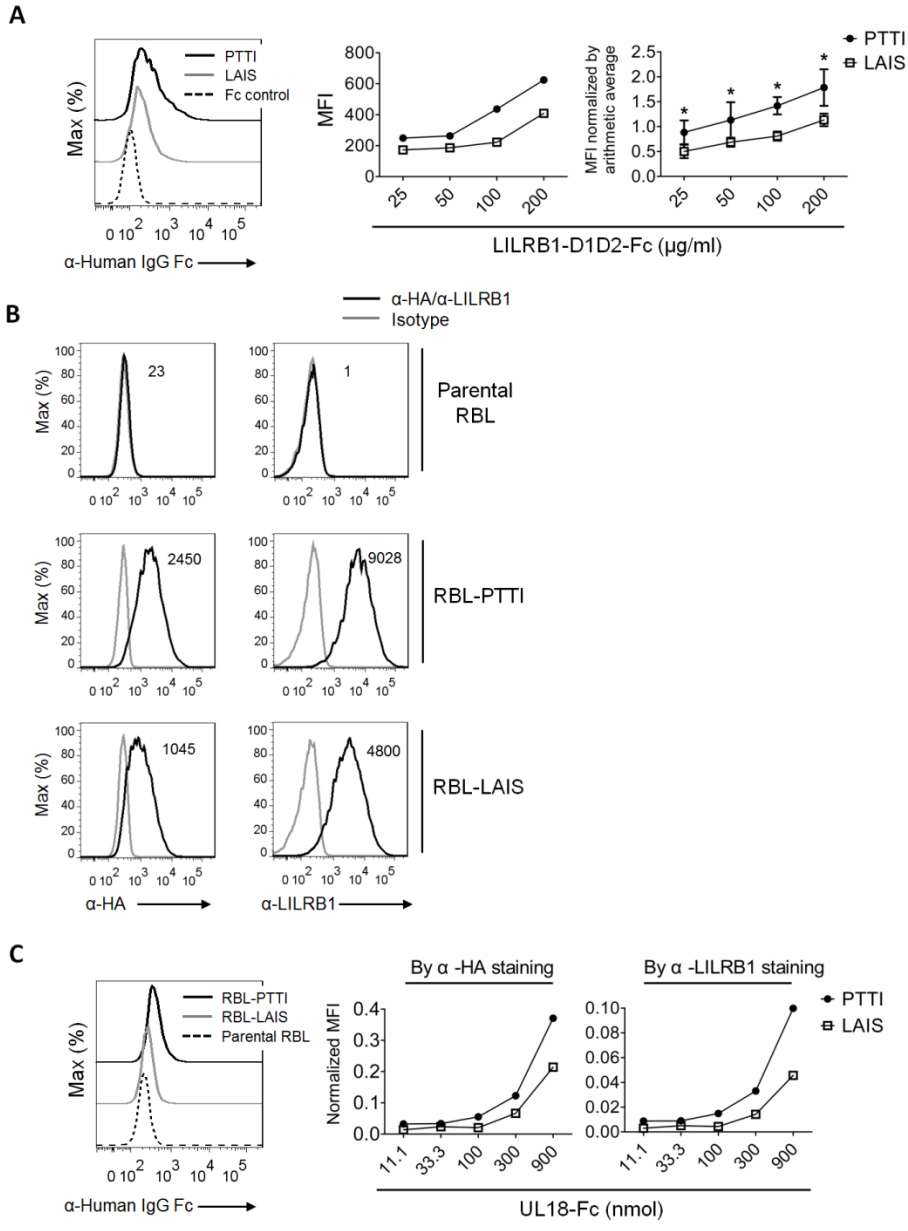

Figure 4.3 Binding of soluble LILRB1 variants to HCMV UL18.
(A) Binding of LILRB1–D1D2-Fc variants to UL18 expressed on 721.221 cells. The flow histogram on the left shows the binding of UL18 with 100 μg/ml Fc fusion proteins. The middle plot shows a representative experiment across 4 concentrations. The far-right graph shows the aggregate data for 3 experiments normalized as described in Methods (*$P < 0.05$ using 1-way ANOVA). (B) Expression of the LILRB1-PTTI and -LAIS variants on transduced RBL cells was measured by α-HA or α-LILRB1 (HP-F1) staining (representative of 3 independent tests). (C) UL18-Fc binding to LILRB1 variants expressed on RBL cells shown in F with a representative histogram shown on the left at 300 nmol. The binding data are normalized by the MFI for α-HA (middle) or α-LILRB1 (HP-F1) (far right). The results are representative of 3 independent tests.

respectively, are localized quite far away (Figure 4.4). Furthermore, the leucine to proline change can have a significant impact on protein structure and conformational dynamics because proline introduces rigidity into the backbone and leucine is a larger hydrophobic residue. Residue N117 is predicted to be glycosylated in LILRB1-PTTI but not LILRB1-LAIS due to the presence of a threonine residue at position 119 ([274] and Figure 4.4). An additional N-linked carbohydrate in PTTI at residue 117 would also explain the difference in migration I observed between the LAIS and PTTI variants on SDS-PAGE (Figure 4.2A) and if important for binding could explain the discrepancy with the previous report due to their production of the receptors in E. coli [274].

4.2.3 Residue T119 is required for glycosylation of N117 and differentially influences ligand binding

To test if glycosylation of PTTI was responsible for the difference in migration, I treated the purified Fc-fusion proteins with N-glycosidase. Treatment with N-glycosidase under denaturing conditions resulted in the two LILRB1 variants running at a similar size (Figure 4.5B). To investigate if the N-linked glycosylation plays a role in the binding of LILRB1-PTTI, I mutated the asparagine residue at position 117 to glutamine (N117Q). The N117Q-PTTI-Fc receptor co-migrated with LAIS-Fc, and the N117Q mutation in LAIS-Fc did not alter its mobility in a gel (Figure 4.5C). The N117Q mutation in the two mutants also did not change the reactivity with HP-F1 as detected by ELISA (Figure 4.5D). As predicted, the binding of N117Q-PTTI to HLA-Cw15 was diminished to a level similar to LAIS (Figure 4.5E). N117Q-LAIS-Fc binding with Cw15 was unchanged compared with LAIS-Fc and close to the limit of detection (Figure 4.5E). Somewhat unexpectedly, mutation of residue 117 to a glutamine in PTTI and LAIS reduced binding to HLA-G, however, the two mutants still bound similarly to HLA-G (Figure 4.5E). These observations suggest that in addition to being a site for the glycosylation in PTTI, residue N117 in LAIS influences the interaction with HLA-G without

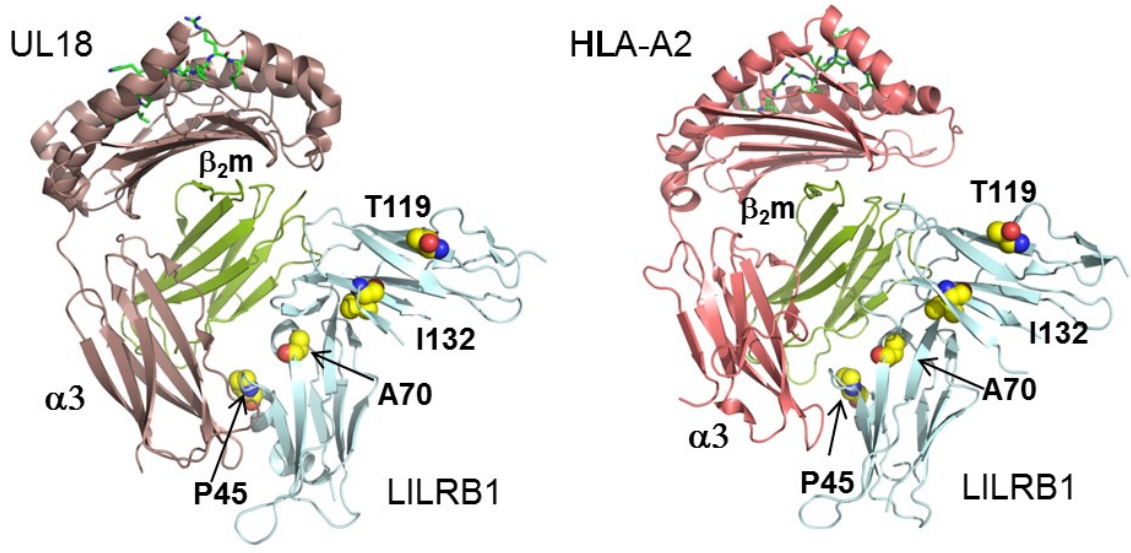

Figure 4.4 Comparison of the co-crystallization complex of LILRB1 with HLA-I and HCMV UL18.

The crystal structures of the LILRB1/UL18 (PDB code 3D2U) and LILRB1/HLA-A2 (PDB code 4NO0) complexes reveal significant overall similarities. The positions of the four LILRB1 variable residues Pro45, Ala70, Thr119, and Ile132 are indicated. The figure is adapted from *Yu et. al*, supplemental Figure 4A [277].

being glycosylated. Surprisingly, N117Q substitution enhanced the binding of both LILRB1 variants to UL18 with similar binding curves (Figure 4.5E). These results point to the importance of residue 117 and its modification being important in the interaction of LILRB1 with various endogenous and viral ligands even if there is not an obvious explanation for the enhanced binding of the N117Q mutant.

4.2.4 All four residues contribute significantly to the interactions between UL18 and MHC-I

To directly test if residue T119 influences binding and is involved in the glycosylation of PTTI, I used site-directed mutagenesis to generate the variant PTII, and at the same time LTTI to test the role of residue P45 in this interaction. PTII co-migrates with LAIS confirming the effect of T119 on migration and glycosylation (Figure 4.6A) but does not alter reactivity with HP-F1 (Figure 4.6B). Consistent with our prediction that T119 influences the interaction, binding of PTII-Fc to Cw15 and UL18 was reduced compared to PTTI (Figure 4.6C). In addition, the substitution of the proline residue at position 45 to leucine also significantly reduced the interaction with UL18 and Cw15 almost as much as the T119I mutation. These two mutations also reduced binding to HLA-G.

To address the role of T90 and I132, I generated the corresponding versions of the D1D2 domains with the combinations of PATI and PTTS as Fc-fusion proteins. As expected, PATI-Fc and PTTS-Fc migrated more slowly than LAIS-Fc similar to PTTI-Fc (Figure 4.6D) and there was no difference in reactivity with HP-F1 (Figure 4.6E). PATI bound to all ligands with similar efficiency as LAIS with reduced binding to both HLA-Cw15 and UL18 (Figure 4.6F). These results suggest only NK cells with the PTTI variant would be well inhibited by UL18 and predicts PATI behaves similarly to LAIS although it is associated with polymorphisms in the promoter region leading to the low frequency of expression on NK cells. The presence of a serine at position 132 in the context of a receptor with PTT in the first three variable positions

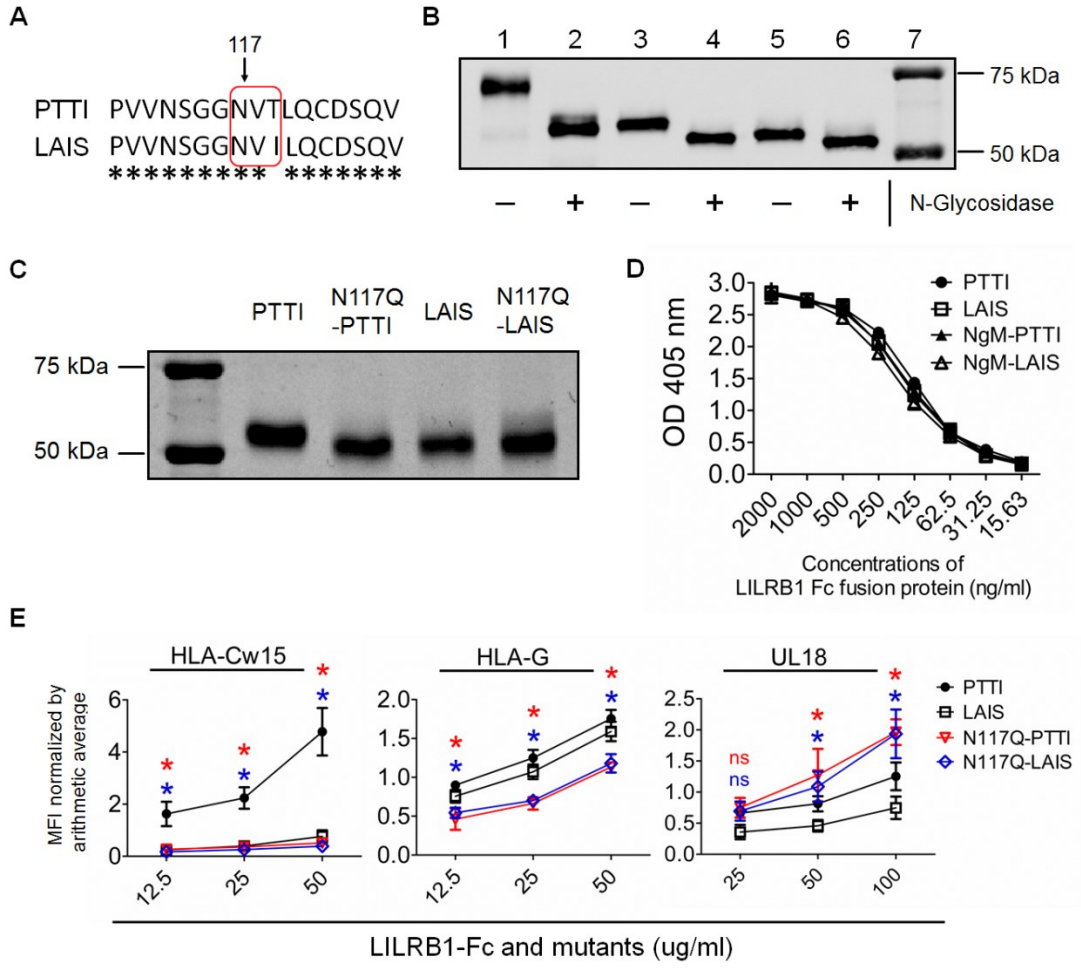

Figure 4.5 Mutation of the putative glycosylation site alters binding.
(A) The sequence surrounding the putative N-linked glycosylation site NVT at position 117 is shown for both variants. The region boxed in red illustrates the target sequence NVT, present only in the variants with T at position 119. (B) LILRB1-PTTI and -LAIS variants treated with N-glycosidase analyzed by SDS-PAGE and Western blot. Lanes 1–2 are KIR3DL1-Fc, 3–4 are LILRB1-PTTI-Fc, 5–6 are LILRB1-LAIS-Fc, and 7 is the molecular weight marker. (C) Representative SDS-PAGE and Coomassie blue staining of the LILRB1-Fc N117Q-PTTI and N117Q-LAIS mutants. Lanes from left to right indicate the protein ladder, LILRB1-PTTI-Fc, N117Q-PTTI-Fc, LILRB1-LAIS-Fc, and N117Q-LAIS-Fc. (D) Reactivity with α-LILRB1 (HP-F1) for the mutated LILRB1 by ELISA. Results shown are the average of 3 independent tests for the same batch of protein; error bars represent SD. (E) Fc fusion protein binding to cells expressing the ligands at the top was measured by flow cytometry as before. Significance testing was performed between the binding of each artificial mutants and PTTI. *$P < 0.05$, ns = $P \geq 0.05$ using 1-way ANOVA. The plots are the normalized binding results aggregated from at least 3 independent tests (4 and 5 independent tests for HLA-G and UL18, respectively).

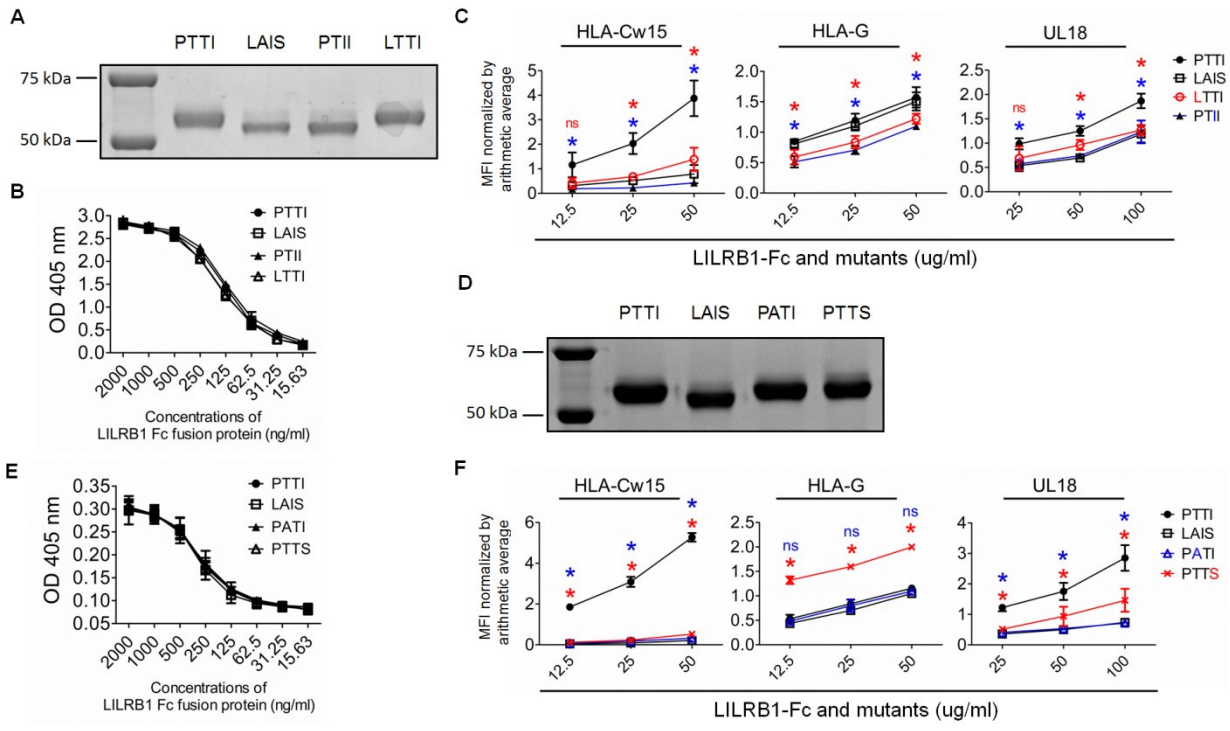

Figure 4.6 Contributions of each residue to binding.
(A and D) Migration of LILRB1–D1D2-Fc fusion protein mutants as detected by Coomassie blue staining. (B and E) Reactivity of the LILRB1–D1D2-Fc fusion proteins with α-LILRB1 (HP-F1) measured by ELISA. Results shown are the average of 3 independent tests for the same batch of protein; error bars represent SD. (C and F) Normalized binding aggregated from 3 independent tests. Significance testing was performed between the binding of each artificial mutant and PTTI. *P < 0.05 using 1-way ANOVA.

reduces the binding with UL18 relative to PTTI and remarkably has a dramatic enhancing effect on HLA-G binding (Figure 4.6F).

4.3 Summary

In this chapter, I investigated whether the LILRB1 protein variants involving the 4 non-synonymous SNPs in the D1 and D2-coding region differentially inhibit NK cells. I generated model NK cell lines stably expressing the "PTTI" variant or "LAIS" variant which is correlated with the "low" and "high" haplotype, respectively. I detected different cytotoxic responses of those two NK cell lines to the target cells expressing UL18 or classical MHC-I, but not with HLA-G. Accordingly, I purified the D1-D2 domains of those two LILRB1 variants and demonstrated that the "PTTI" variant has a significantly stronger binding with either UL18 or MHC-I molecules but not HLA-G compared with the "LAIS" variant, which is consistent with the observed stronger inhibition mediated by the "PTTI" variant on NK cells. Then, I showed that each of four non-synonymous substitutions in the ligand-binding domains alters significantly the physical interaction of the LILRB1 receptor with all the ligands tested. Of note, I also verified that the amino acid at position 119 controls the addition of an N-linked glycan and the glycosylation in the "PTTI" variant is crucial to maintain its stronger ligand binding capacity than the "LAIS" variant. Remarkably, compared with the classical MHC-I molecules examined, the LILRB1 variants tested maintain stronger interaction with HLA-G which is fitting with a principal role of LILRB1 in fetal tolerance. Together, these data indicate that, whereas alleles with higher affinity for UL18 have adapted through selective regulation of LILRB1 expression on NK cells to limit the evasion of NK responses by HCMV.

CHAPTER 5

Investigating the effects of UL18 in cell adhesion

5.1 Background

Our lab has been using 721.221 cells as a model to study the interaction of NK receptors with different HLA-I molecules [226, 277, 283]. Similar to primary human B cells from peripheral blood, tonsil, or germinal center [299-302], in our typical culture conditions, 721.221 cells are dispersed suspension cells with a minority of cells forming small-size cell aggregates. Compared with the parental 721.221 cells or 721.221 cells expressing classical HLA-I, I observed that 721.221 cells expressing UL18 (221-UL18) formed macroscopic cell clusters, implying that UL18 might influence the cell adhesion. Particularly in screening single-cell clones of 221-UL18 cells, only the clones showing big cell clusters had a relatively high level of UL18 surface expression. The clustering phenotype was recapitulated upon repeating the retroviral transduction of UL18. The phenotype of clustering cells has been previously described as homotypic adhesion (HTA) on human B cells mediated by various stimulators [299, 300, 303-306]. Thus, we hypothesized that UL18 could induce the HTA of 721.221 cells.

Dynamic intercellular cell adhesion is very essential in many biological processes including cell development, cell homing or extravasation, and immune recognition [307]. In this chapter, I aimed to characterize the HTA phenotype observed on 221-UL18 cells and explore the underlying mechanism causing the aggregation of 721.221 cells after transducing HCMV UL18. This study was divided into three sections including the characterization of the HTA phenotype of UL18-221 cells, examining the role of LILRB1 in the formation of the HTA phenotype, and investigating the involvement of the adhesion molecule LFA-1 in maintaining the HTA phenotype. Our lab previously reported a *cis*-interaction of LILRB1 with MHC-I molecules expressed on 721.221 cells which could impact the detection of surface LILRB1 by flow cytometry [226]. Thus, I also examined whether there is a *cis*-interaction between UL18 and LILRB1 on 221-UL18 cells.

5.2 Results

5.2.1 Characterization of the HTA phenotype of 721.221 cells transduced with UL18

To unbiasedly compare the HTA cluster formation in 721.221 cell lines expressing different surface molecules, I used a microscope-based assay to automatically take the cell photos and then quantify the size of cells clusters using ImageJ software. To exclude the potential influence of cell adhesion from the retroviral transduction and drug selection alone, I used the pMXs-puro empty vector to transduce 721.221 cells as a control (221-puro). In addition, to make sure the HTA phenotype was due to UL18, I also used 721.221 cells expressing HLA-B58 (221-B58) fused with the same tags of 221-UL18 (an HA tag at the N-terminus and a YFP tag at the C-terminus) as a comparison. With this assay, I found that the size of cell clusters of 221-UL18 cells was significantly larger than that of parental 721.221 cells, 221-puro and 221-B58, which is consistent with the hypothesis that UL18 can induce HTA of 721.221 cells (Figure 5.1). Since I noticed that the clones with small cell clusters express lower surface UL18 than those that formed large clusters when I was screening the clones of 221-UL18 cells, it appeared that the size of aggregates was related to UL18 surface expression level. To test this hypothesis, I sorted 221-UL18 cells into two subpopulations with relatively “high” and “low” surface expression of UL18. The YFP signal was correlated with the UL18 surface expression on the two sorted populations. Not surprisingly, I observed bigger cell clusters with cells expressing a higher level of surface UL18 (Figure 5.2).

To exclude the possibility that UL18-mediated HTA is dependent on the intracellular YFP-tag at the C-terminus, I deleted the YFP sequence from the original plasmid and added stop codon at the end of UL18 sequence to generate a pMXs-HA-UL18 vector for 721.221 cell transduction. The results demonstrated that 721.221 cells transduced the YFP-deleted vector had comparable surface expression level of UL18 with the ones transduced with the YFP tag. In addition, without the YFP tag, 221-UL18 also formed the HTA phenotype which did not show a significant change in the size of cell clusters (Figure 5.3). Thus, it appears that the YFP tag is not

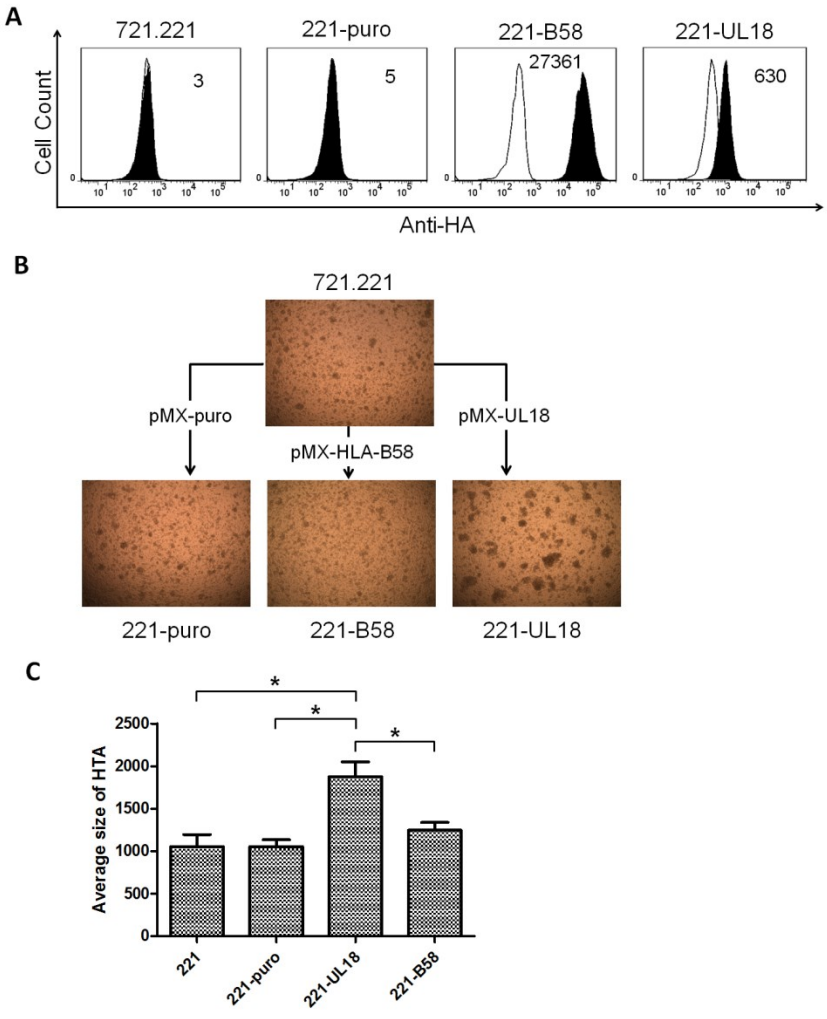

Figure 5.1 HTA phenotype of 721.221 cells transduced with HCMV UL18.
(A) Flow cytometry staining of HA tag on 721.221, 221-puro, 221-B58, and 221-UL18 cells. The Geom. MFI value with the background subtracted is shown inside of each plot. White and black filled curves indicate the isotype control and the antibody against the HA tag, respectively. The flow cytometry data is representative of results from three independent experimental repeats (for 221-B58, one time of anti-HA staining and two times of anti-HLA-I staining, clone W6/32). (B) Representative cell photos of 721.221, 221-puro, 221-B58, and 221-UL18. Both 221-B58 and 221-UL18 cells are expressing an HA tag at the N-terminus and YFP tag at the C-terminus of the target protein. All the cell types were counted and the same amount of cells were seeded in 48-well plate with fresh media 24 hours before taking photos. All photos were taken in the bright field with 40X magnification. Photos shown are representatives from three independent experimental repeats. (C) Quantification of cell clusters of the four cell lines shown in panel A using ImageJ. Average cluster sizes were calculated using data collected from three independent experiments. Statistical analysis comparing transduced cell lines to parental 721.221 cells was done using 1-way ANOVA, "*" indicates P-value < 0.05.

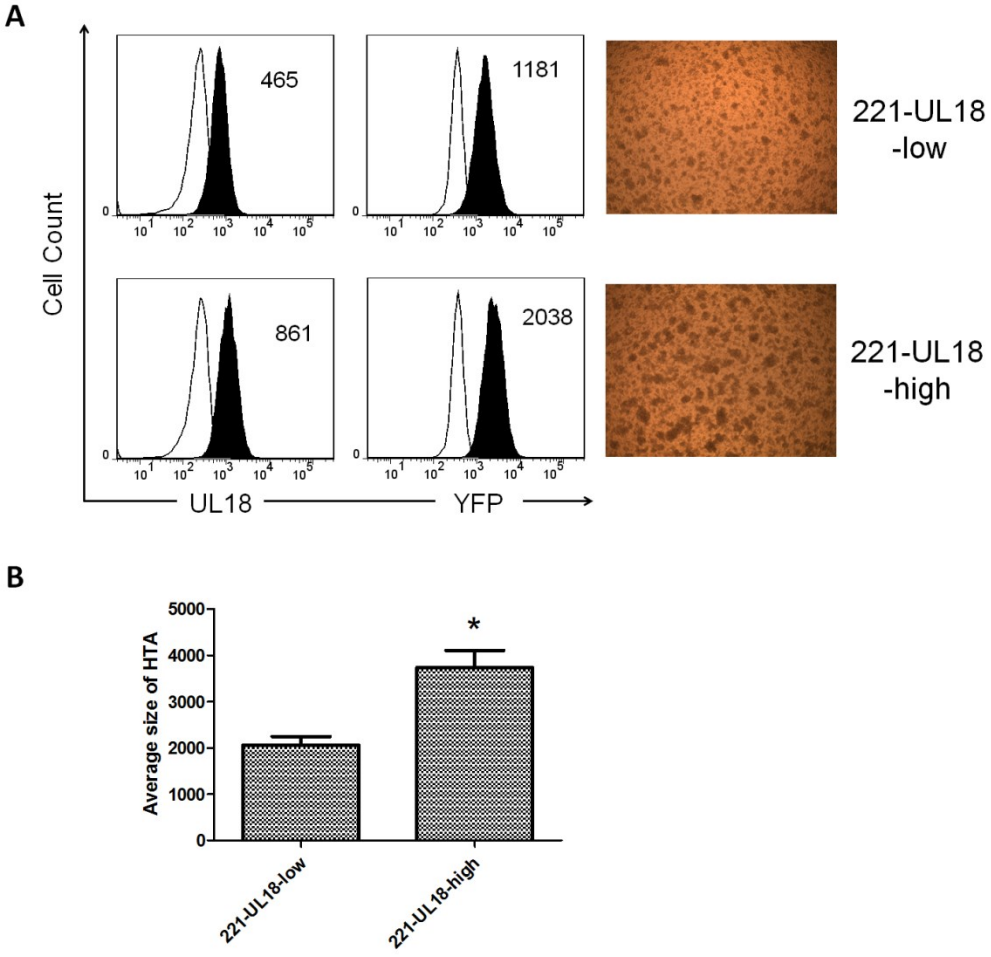

Figure 5.2 Correlation of clustering size of 221-UL18 cells with UL18 surface expression level.

(A) Comparison of the clustering size of 221-UL18 cells with relatively high and low UL18 surface expression. Flow cytometry staining of surface UL18 shown is representative of results from two independent experiments. The Geom. MFI value with the background subtracted is shown inside of each plot. White and black filled curves indicate the isotype control and the antibody against the HA tag or YFP signal, respectively. YFP background was determined using unstained 721.221 cells. The corresponding photos are representative of three independent experiments and were taken in the bright field with 40X magnification. (B) Quantification of the clustering size of the two cell lines shown in panel A using ImageJ. The average clustering sizes were calculated using data collected from three independent experiments. Statistical analysis was done using Student's t-test, "*" indicates P-value < 0.05.

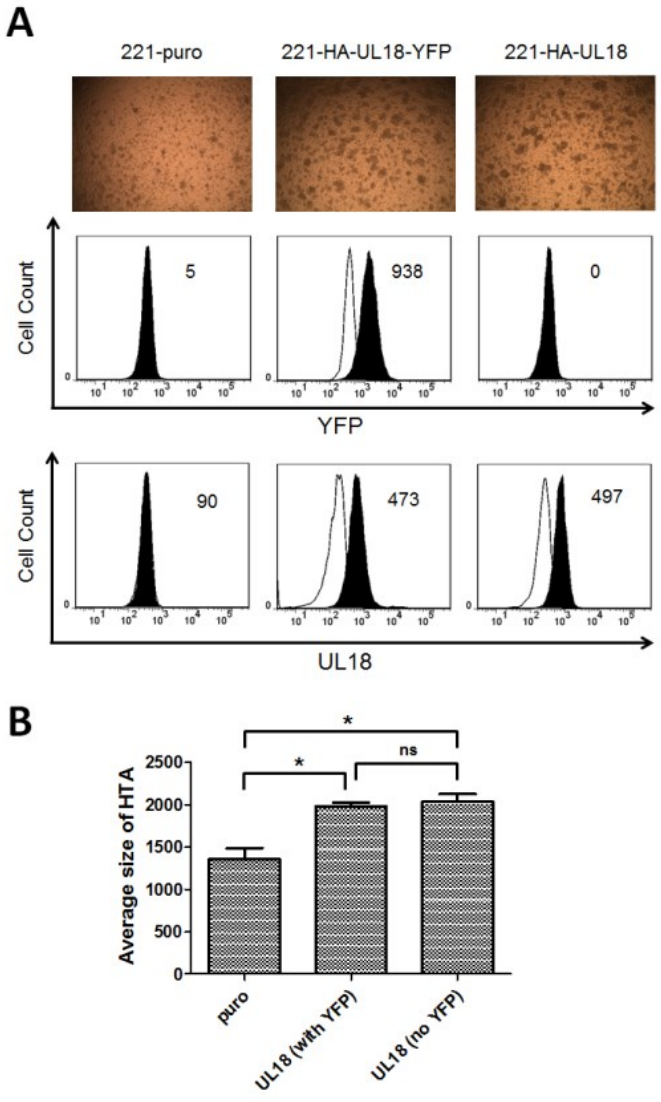

Figure 5.3 Effect of YFP tag on UL18 expression and HTA phenotype of 221-UL18 cells. (A) Comparison of UL18 surface expression and HTA phenotype of 221-UL18 cells with (221-HA-UL18-YFP) and without (221-HA-UL18) expressing YFP tag. Flow cytometry staining of surface UL18 shown is representative of results from two independent experiments. The Geom. MFI values with background subtracted are shown inside of each plot. White and black filled curves indicate the isotype control and the antibody against the HA tag or YFP signal, respectively. YFP background was determined using unstained 721.221 cells. The corresponding photos are representative of three independent experiments and were taken in the bright field with 40X magnification. (B) Quantification of the clustering size of the three cell lines shown in panel A using ImageJ. The average clustering sizes were calculated using data collected from three independent experiments. Statistical analysis comparing the three groups was done using 1-way ANOVA, "*" indicates P-value < 0.05, ns indicates P-value ≥ 0.05.

necessary to maintain UL18 surface expression and the HTA phenotype of 221-UL18 cells. Together, these experimental results provide evidence for the role of UL18 in mediating aggregation of 721.221 cells.

5.2.2 Effects of UL18 on the proliferation of 721.221 cells

I noticed that the color change of the media from 221-UL18 culture was slower compared with 721.221 cells during the regular cell culturing, which implies UL18 may repress the cell proliferation or even cell metabolism. 721.221 cells have a high surface expression level of LILRB1. Transduction of UL18, a strong ligand for LILRB1, may dynamically interact with LILRB1 on 721.221 cells and the signaling of LILRB1 may have an impact on the cell proliferation. As mentioned in Chapter 1, considering LILRB1 is not a strict inhibitory receptor for immune cell functions and UL18 was also reported to play activating roles on T and NK cells, there are several potential ways UL18 expression could change 721.221 cell proliferation. In addition, the UL18-induced change in cell-cell adhesion on 721.221 cells may also influence cell proliferation [308, 309]. To examine if the UL18 transduction changed the proliferation of 721.221 cells, I generated growth curves by counting the density of the live cells and applied CellTrace Violet (CTV) staining assay to assess the cell division rate using 221-puro cells as a control. Both the growth curve and the CTV dilution curve reveal a trend of decreased proliferation of 221-UL18 cells compared with 221-puro, although the change was mild and did not reach statistical significance (Figure 5.4). This result indicates that UL18 expression in our model does not significantly change the proliferation of 721.221 cells but it cannot be excluded that UL18 may show an impact on cell proliferation with higher UL18 expression levels.

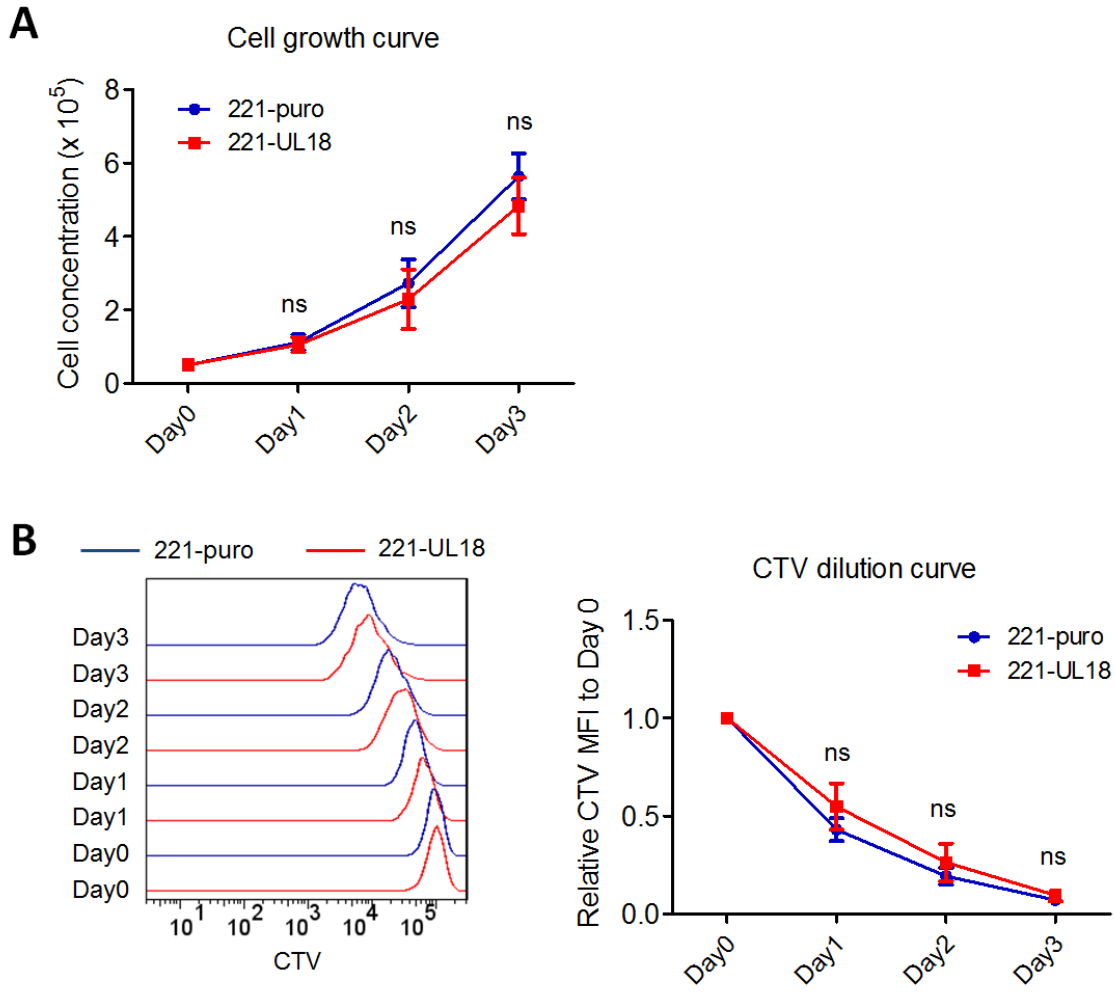

Figure 5.4 Comparison of cell proliferation between 221-puro and 221-UL18.
(A) Cell growth curves of the two cell lines. Each cell line was seeded in a 12-well plate at a concentration of $0.5x10^5$ cells / mL on Day 0. Concentrations for live cells were measured using TC20 automated cell counter from three wells per cell line on a single day, and average concentrations were calculated and plotted in the line chart. Data shown is the averaged result from three independent experimental repeats. Statistical analysis was done using Student's t-test, "ns" indicates P-value ≥ 0.05. (B) CTV dilution of the two cell lines. Each cell line was counted, stained with CTV at a concentration of 5μM, and then seeded in three wells of 12-well plate. The CTV MFIs from Day 0 to Day 3 for each cell line were assessed by FACs. The left plot shows one representative flow cytometry result. The right plot shows the CTV dilution curves. The Y-axis indicates the MFI values normalized to the value measured on Day 0 for each of the cell lines. Data shown is the averaged result from three independent experimental repeats. Statistical analysis was done using Student's t-test, "ns" indicates P-value ≥ 0.05.

5.2.3 Effect of the LILRB1 functional blocking antibody in the HTA formation of 721.221 cells transduced with UL18.

To test my first assumption and address the question of whether LILRB1/UL18 *trans*-interaction causes the HTA phenotype of 221-UL18 cells, I did antibody-blocking assay that two 221-UL18 clonal cell lines with relatively high UL18 surface expression were cultured by adding the LILRB1 antibody (clone: HP-F1) which targets the D1 and D2 domains and has been used to functionally block LILRB1 by us and others [186, 193, 199, 277]. However, compared with the isotype control, the formation of cell clumps was not altered tracking up to 24 hours after adding the blocking antibody to both cell lines. Additionally, even at the concentrations equal and above what is required to prevent receptor function in NK cells [277], the blocking antibody did not show any trend to slow down the clumping formation (Figure 5.5). These results suggest that blocking the LILRB1/UL18 *trans*-interaction in cell culture did not affect the HTA formation of 221-UL18 cells.

5.2.4 LILRB1 is cis-interacting with UL18 on 221-UL18 cells

A previous study from our lab demonstrated that LILRB1 *cis*-interacts with MHC-I molecules expressed on a same 721.221 cell and the complexed receptor has differential accessibility to two LILRB1 antibodies. Specifically, HP-F1 tends to bind free (not binding to MHC-I) LILRB1, while another LILRB1 antibody clone, GHI/75, preferentially binds LILRB1 interacting *in cis* with MHC-I [226]. Thus, as an MHC-I homolog, UL18 is probably also able to *cis*-interact with LILRB1 on a same 721.221 cell which limits the recognition of the HP-F1 antibody that I used in the blocking assay. To test this possibility, I applied GHI/75 and HP-F1 staining on 221-UL18 cells using flow cytometry and then used the ratio of MFI between the two antibodies to assess the *cis*-interaction of LILRB1 as described before [226]. As shown in Figure 5.6A, both the GHI/75 and HP-F1 staining was dramatically decreased on 221-UL18 cells compared with 721.221. The Geom. MFI ratio of GHI/75 to HP-F1 staining on 221-UL18

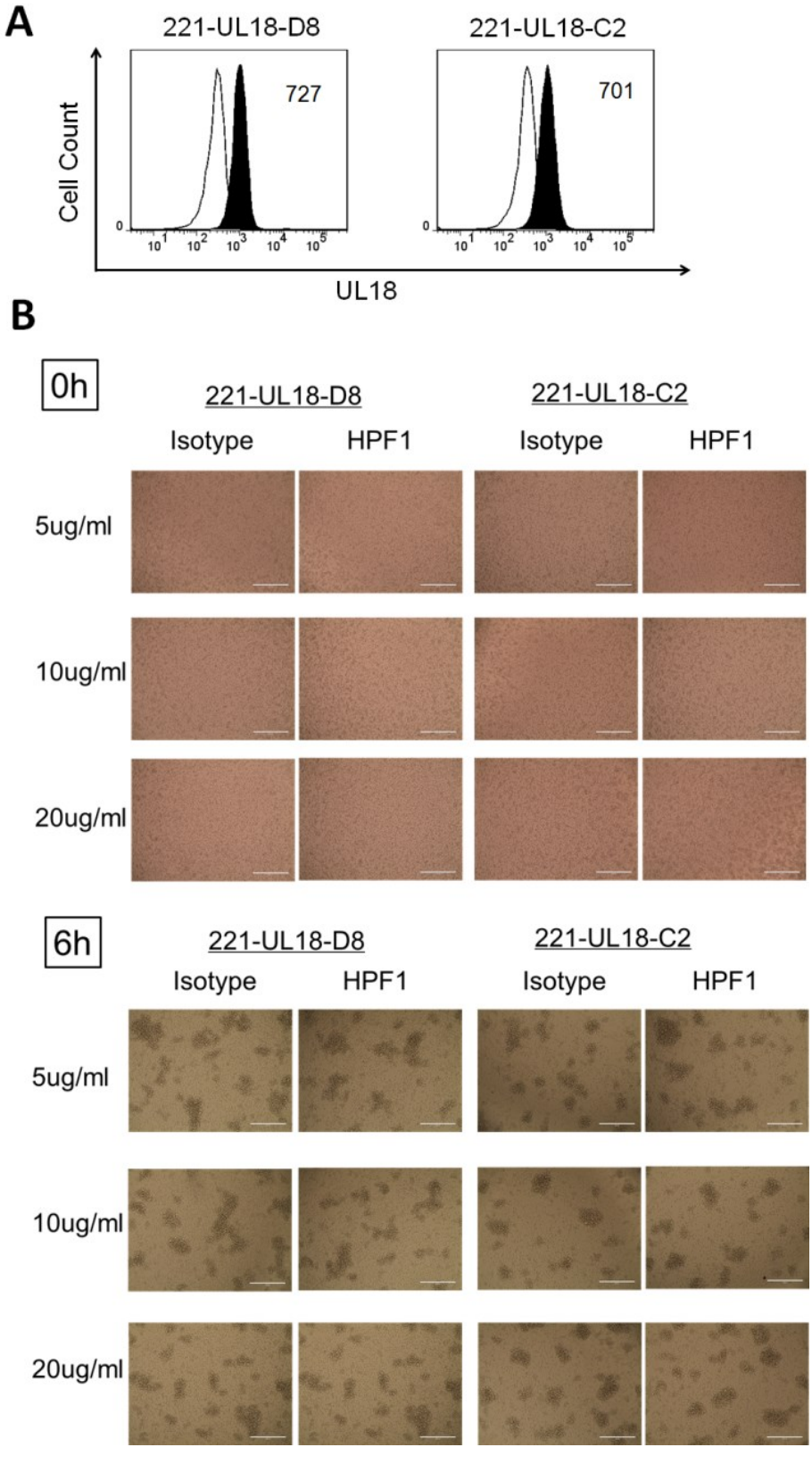
A
221-UL18-D8
221-UL18-C2
727
701
Cell Count
UL18
B
0h
221-UL18-D8
221-UL18-C2
Isotype
HPF1
Isotype
HPF1
5ug/ml
10ug/ml
20ug/ml
6h
221-UL18-D8
221-UL18-C2
Isotype
HPF1
Isotype
HPF1
5ug/ml
10ug/ml
20ug/ml

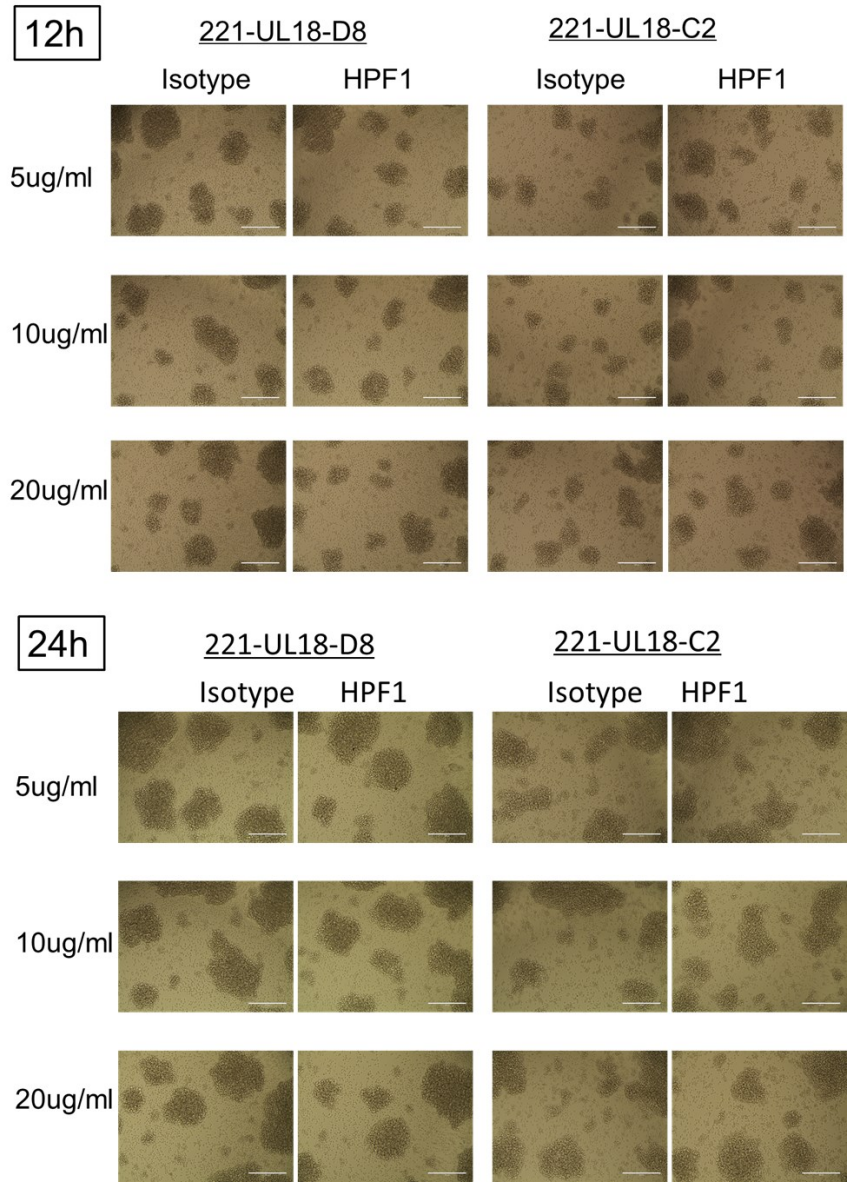

Figure 5.5 Effect of LILRB1 blocking antibody on HTA phenotype formation.
(A) Flow cytometry staining of surface UL18 on two clones of 221-UL18 cells named D8 and C2. The Geom. MFI value with the background subtracted is shown inside of each plot. White and black filled curves indicate the isotype control and the antibody against the HA tag, respectively. Flow cytometry data is representative of results from two independent experiments. (B) LILRB1 antibody blocking assay on two clones of 221-UL18 cells. The HTA formation was tracked from 0 h to 24 h after seeding the cells. Three working concentrations of the LILRB1 antibody (HP-F1) and isotype control were used. All photos were taken in the bright field with 100X magnification. Photos shown are representatives from two independent experimental repeats.

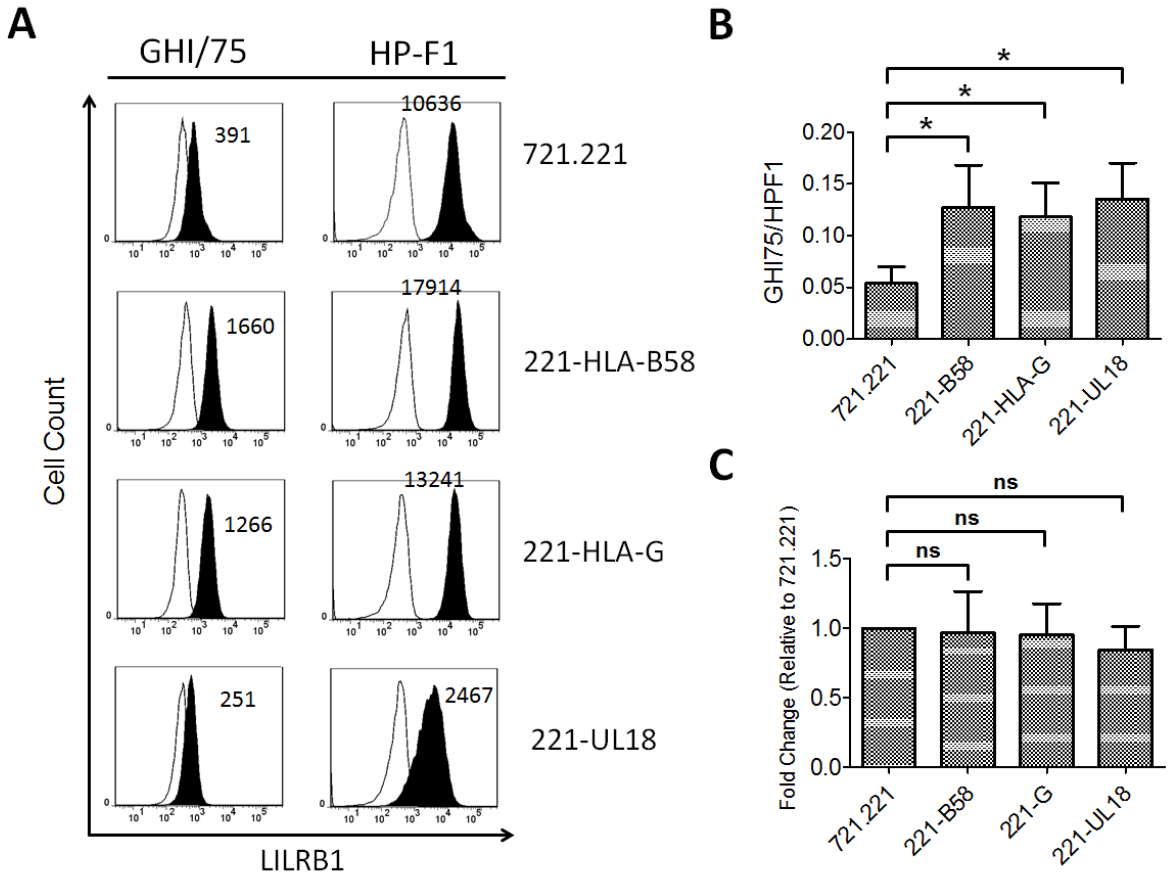

Figure 5.6 Evidence for the cis-interaction between UL18 and LILRB1 on 221-UL18 cells. (A) Flow cytometry staining of LILRB1 on 721.221, 221-B58, 221-G, and 221-UL18 (clone D8) cells using two different LILRB1 antibodies GHI/75 and HP-F1. The Geom. MFI value with the background subtracted is shown inside of each plot. White and black filled curves indicate the isotype control and the antibody against LILRB1, respectively. Flow cytometry data is representative of results from three independent experiments. (B) The Geom. MFI ratios of GHI/75 staining to HP-F1 staining of the four cell lines in panel A averaged from three independent experiments. Statistical analysis comparing 721.221 cells with each of three other cell lines was done using Student's t-test, * indicates P-value < 0.05. (C) Comparison of LILRB1 mRNA levels in the four cell lines shown in panel A and B. LILRB1 Average mRNA level relative to 721.221 cells is shown and the data was aggregated from three independent experimental repeats. The internal reference control used in the RT-qPCR was the RPL24 gene. Statistical analysis comparing 721.221 cells with each of three other cell lines was done using Student's t-test, ns indicates P-value ≥ 0.05.

cells was higher than that on 721.221 which is similar to the positive control 221-B58 and 721.221 cells expressing HLA-G (221-G) and indicates the *cis*-interaction is occurring (Figure 5.6B). However, since the *cis*-interacting LILRB1 is preferred to be recognized by GHI/75, the much lower GHI/75 staining on 221-UL18 cells compared with that on 221-B58 and 221-G did not support a large amount of *cis*-interactions. A possible explanation for the low GHI/75 staining on 221-UL18 cells is that some LILRB1 proteins were arrested in the ER by UL18 because of its ER retention [232], which reduces the surface LILRB1 expression. To examine the cellular distribution of UL18, I applied imaging flow cytometry on 221-UL18-YFP and used 221-B58-YFP for comparison. Indeed, a large proportion of UL18 was located intracellularly of 221-UL18 cells. In comparison, 221-B58 has very intense surface expression relative to the intracellular expression (Figure 5.7A). Analysis of the ratio between the YFP signal detected on the plasma membrane and intracellular space by the software reveals that UL18 has a much lower surface expression relative to the intracellular pool compared with HLA-B58 (Figure 5.7B). This result strongly supports the possibility that a proportion of LILRB1 is stuck intracellularly by UL18 in 221-UL18 cells.

To exclude that LILRB1 transcription was down-regulated in 221-UL18 cells, I did RT-qPCR assay comparing the LILRB1 mRNA level in 721.221, 221-B58, 221-G, and 221-UL18 cells. Similar to 221-B58 and 221-G cells, there was no significant change in the LILRB1 mRNA level in 221-UL18 cells compared with the parental 721.221 cells (Figure 5.6C), which indicates the expression of UL18 or MHC-I molecules does not affect LILRB1 gene transcription in 721.221 cells. Together, these data provide evidence that UL18 can *cis*-interact with LILRB1 on the surface of 221-UL18 cells and some LILRB1 proteins are likely engaged by UL18 intracellularly.

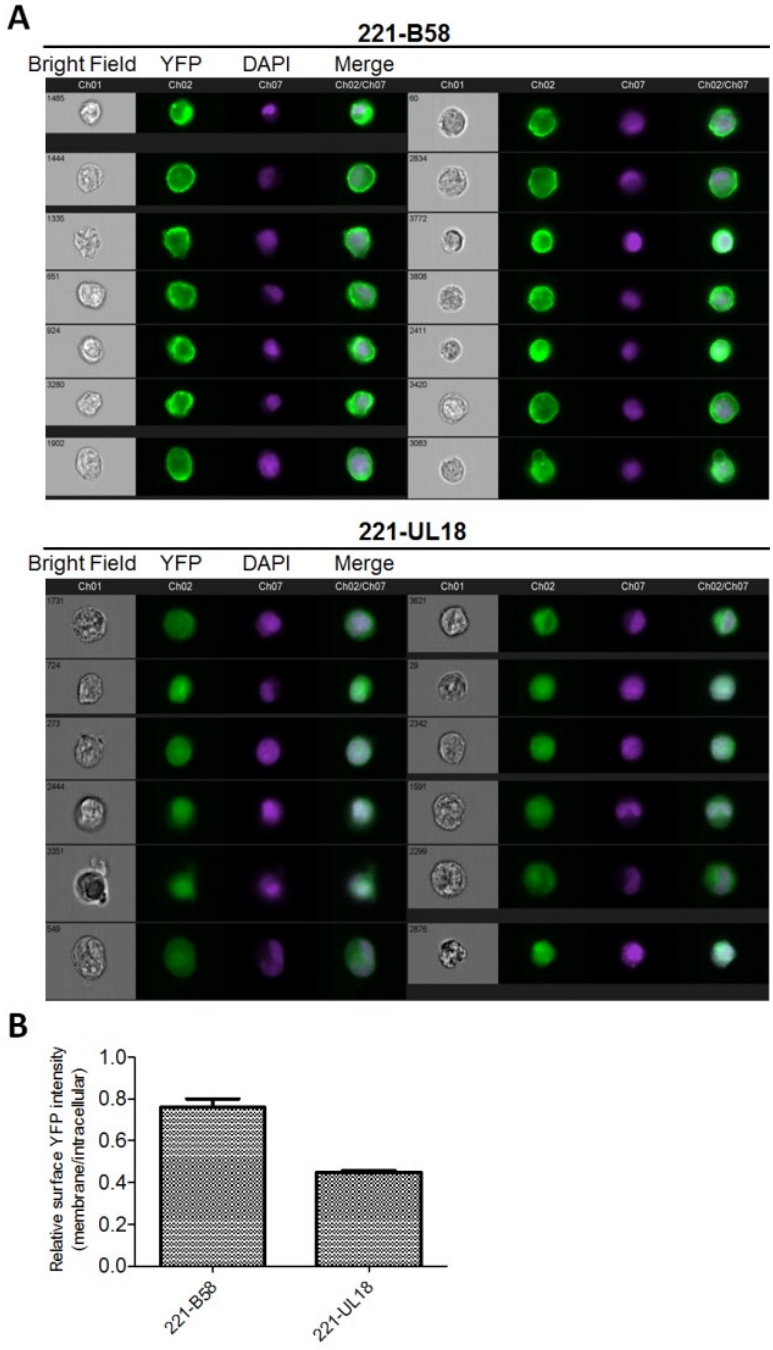

Figure 5.7 Imaging flow cytometry of 221-B58 and 221-UL18 cells determining the relative surface expression of the transduced protein.

(A) Visualization of the fluorescent signals from the two cell lines where the YFP represents the HLA-B58 or UL18 position and DAPI indicates the nucleus position. (B) Analysis of the YFP ratio between the plasma membrane and cytosol in the two cell lines using IDEAS® v6.2 software. Results are aggregated from two independent experiments.

5.2.5 A cell-intrinsic role of LILRB1 in UL18-induced aggregation of 721.221 cells

There is evidence that *cis*-interaction of LILRB1 with MHC-I molecules plays a role in regulating cell biologies, such as activation of mast cells [224] and osteoclast development [225]. Although it appears that the formation of the HTA phenotype is not a result of the LILRB1/UL18 *trans*-interaction, LILRB1 still may play a role in this phenotype through the signaling derived from the *cis*-interaction with UL18. To clarify if LILRB1 is required for the HTA phenotype of 221-UL18 cells, I applied CRISPR technology to knock out the LILRB1 gene in 721.221 cells and then did UL18 retroviral transduction. I designed two guide RNAs (g1 and g2) to knock out the LILRB1 gene (Figure 5.8A) independently and screened two clones without any surface LILRB1 expression determined by flow cytometry (Figure 5.8B). The successful knockout of the LILRB1 gene in these two clones was confirmed by sequencing and both contained frameshift mutations. Following retroviral transduction, UL18 was successfully expressed on 221-g1-KO and 221-g2-KO cells, and a notably higher expression level was detected on wild type 721.221 cells in parallel by surface staining (Figure 5.8B). Unlike wild type 721.221 cells, neither of LILRB1 gene knockout cell lines formed a significant HTA phenotype (Figure 5.8B and C). From these results, LILRB1 appeared to be important for 721.221 cells in developing the UL18-induced HTA. However, I noticed that the UL18 surface expression was lower on the two LILRB1-knockout cell lines compared with the parental 721.221 cells (Figure 5.8B). Furthermore, the proportion of the surface UL18 to total UL18 protein of the LILRB1-knockout cell lines represented by the ratio of anti-HA staining to YFP intensity was also decreased over 50% compared to the parental 721.221 cells (Figure 5.8D), which suggests more UL18 stays intracellular if there is no LILRB1 expressed. This change raised a possibility that LILRB1 may not be the direct factor causing the UL18-induced HTA but may act through facilitating enough UL18 surface expression to establish the HTA phenotype.

To further investigate the contribution of LILRB1 in the UL18-induced HTA, I applied CRISPR again to knock out the LILRB1 gene using g1 guide RNA in a clone of 221-UL18 cells (clone D8) which is able to form big cell clusters (Figure 5.5 and Figure 5.9A). A guide RNA

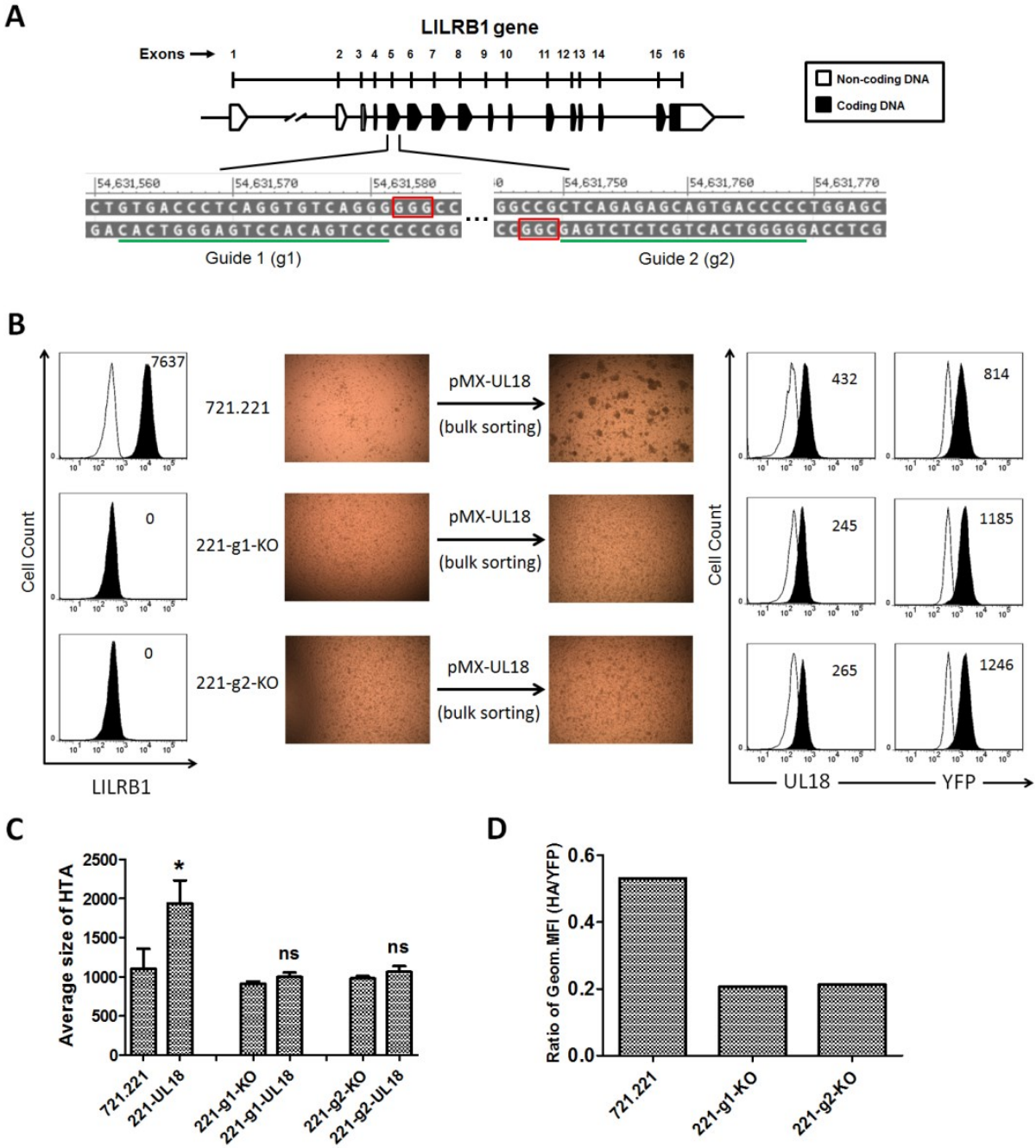
A
LILRB1 gene
Exons
1
2 3 4 5 6 7 8 9 10 11 12 13 14 15 16
Non-coding DNA
Coding DNA
54,631,560
54,631,570
54,631,580
54,631,750
54,631,760
54,631,770
CTGTGACCCTCAGGTGTCAGGGGGGCC
GACACTGGGAGTCCACAGTCCCCCCGG
GGCCGCTCAGAGAGCAGTGACCCCCTGGAGC
CCGGCGAGTCTCTCGTCACTGGGGGACCTCG
Guide 1 (g1)
Guide 2 (g2)
B
Cell Count
LILRB1
7637
721.221
pMX-UL18
(bulk sorting)
0
221-g1-KO
0
221-g2-KO
432
814
245
1185
265
1246
UL18
YFP
C
Average size of HTA
2500
2000
1500
1000
500
0
*
ns
ns
721.221
221-UL18
221-g1-KO
221-g1-UL18
221-g2-KO
221-g2-UL18
D
Ratio of Geom.MFI (HA/YFP)
0.6
0.4
0.2
0.0
721.221
221-g1-KO
221-g2-KO

Figure 5.8 LILRB1 is involved in the UL18-induced HTA formation of 721.221 cells.
(A) Schematic showing the targeting sites of the two CRISPR guide-RNAs (g1 and g2). Protospacer adjacent motif (PAM) sequences are highlighted by red boxes, and the guide RNA sequences are underlined in green. The chromosome location shown in the ruler refers to the GRCh38.p12 version of the human genome. (B) LILRB1 gene was knocked out in 721.221 cells using two different guide RNAs (g1 and g2) and then the cells were transduced with UL18 followed by cell sorting to enrich UL18 and YFP double-positive population. Flow cytometry analysis of LILRB1 (HP-F1) and UL18 (anti-HA and YFP) are shown on the left and right, respectively. With the exception of the YFP background determined by unstained 721.221 cells, white and black filled curves indicate the isotype control and the antibody to LILRB1 or HA tag, respectively. The Geom. MFI value with the background subtracted is shown inside of each plot. All photos were taken in the bright field with 40X magnification. The results of a representative of two experiments are shown. (C) Comparison of aggregate size before and after UL18 transduction and sorting of the three cell lines shown in panel A. The average clustering sizes were calculated using data collected from three independent experimental repeats. Statistical analysis comparing each pair of cells was done using Student's t-test, "*" indicates P-value < 0.05, ns indicates P-value ≥ 0.05. (D) The Geom. MFI ratio of surface UL18 and YFP corresponding to the flow cytometry data shown in panel A.

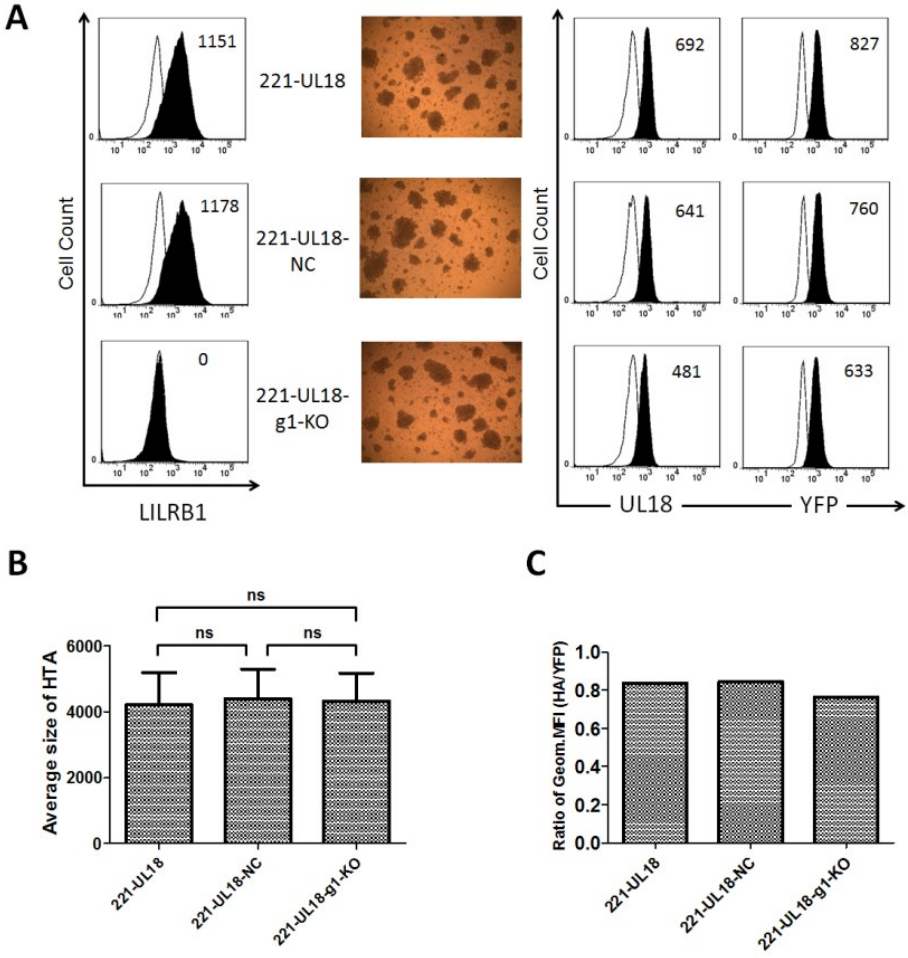

Figure 5.9 LILRB1 is not required to sustain the UL18-induced HTA phenotype.
(A) LILRB1 gene was knocked out in a clone of 221-UL18 cells (clone D8) using the g1 guide RNA and then the cells were bulk sorted to enrich the LILRB1-negative population. A guide RNA that does not have a specific target in humans was used as a negative control (NC). Flow cytometry staining of LILRB1 (HP-F1) and UL18 (anti-HA and YFP) are shown on the left and right, respectively. With exception of YFP signal shown by black filled curves and background determined using unstained 721.221 cells shown by white filled curves, other white and black filled curves indicate the isotype control and the antibody to LILRB1 or HA tag, respectively. The Geom. MFI value with the background subtracted is shown inside of each plot. All photos were taken in the bright field with 40X magnification. LILRB1 gene knockout and flow cytometry analyses were done once and the cell photos shown are representative of three experimental repeats. (B) Comparison of the size of the aggregates of the three cell lines shown in panel A. The aggregate sizes of the three cell lines were measured three times independently. Statistical analysis comparing each pair of cells was done using Student's t-test, ns indicates P-value ≥ 0.05. (C) The Geom. MFI ratio of surface UL18 and YFP corresponding to flow cytometry data shown in panel A.

(NC) that does not have any specific target in humans was used as a negative control in parallel and LILRB1 gene expression on 221-UL18-NC cells was comparable with parental 221-UL18 cells. 221-UL18-g1 cells were sorted to enrich the LILRB1-negative population by flow cytometry (Figure 5.9A). Then, the HTA phenotype was assessed on parental 221-UL18, 221-UL18-NC, and 221-UL18-g1 cells. Surprisingly, compared with 221-UL18 cells, 221-UL18-g1 cells maintained the HTA phenotype without apparent change and measurement of aggregate size did not reveal any significant reduction (Figure 5.9B). This finding strongly suggested that LILRB1 was not necessary to maintain the UL18-induced HTA phenotype in 721.221 cells. It seems that this result is inconsistent with the reciprocal assay by knocking out the LILRB1 gene in 721.221 cells before UL18 transduction as described above. However, compared with the parental cells, I noticed that the reduction of surface UL18 on 221-UL18-g1 cells was not as dramatic as 221-g1-UL18 and 221-g2-UL18, and the proportion of surface UL18 in 221-UL18-g1 cells as indicated by the ratio of HA to YFP was not decreased remarkably (Figure 5.8C and Figure 5.9C). Nonetheless, the HTA phenotype can be maintained for 221-UL18 cells even if there is no interaction between UL18 and LILRB1.

From those two reciprocal LILRB1 gene knockout assay, I found LILRB1 is required to establish the HTA phenotype upon transduction of UL18 in 721.221 cells but not necessary to maintain the HTA phenotype in 721.221 cells already expressing UL18. In addition, LILRB1 appears to improve the surface expression of UL18 on 721.221 cells. These results raise new questions that how UL18 is able to facilitate the cell-cell adhesion of 721.221 cells and how LILRB1 affects UL18 surface expression.

5.2.6 Involvement of LFA-1 in the UL18-induced HTA phenotype of 721.221 cells.

In order to further characterize the process of how UL18 influences the adhesion system, I went on to consider pathways that are known to be directly involved in cell-cell adhesion. As reviewed previously [310, 311], integrin family proteins are crucial transmembrane receptors

and considered as the most versatile adhesion molecules in the immune system, such as mediating cell adhesion, proliferation, activation, and migration. Lymphocyte function-associated antigen 1 (LFA-1), which belongs to the β2 integrin subfamily and is expressed on most types of leukocytes [312, 313], could be an obvious candidate because it has been reported to mediate HTA in different types of immune cells [300, 314-318]. LFA-1 is composed of the αL and β2 chain, and the specific ligands for LFA-1 are known as members of intercellular adhesion molecules (ICAMs) [310, 319]. Therefore, I asked if LFA-1 which is highly expressed on 221-UL18 cells (Figure 5.10A) was required in forming the aggregation phenotype.

To determine whether the UL18-induced HTA involves LFA-1 interacting with its ligands, I incubated 221-UL18 cells with LFA-1 blocking antibodies targeting either the α-chain (clone: HB202) or the β-chain (clone: HB203). First, I titrated the two antibodies using 221-UL18-D8 clone which forms big aggregates. Surprisingly, 1 μg/mL working concentration was enough to dramatically inhibit the formation of HTA during an incubation of 24h. Then, I added 1 μg/mL blocking antibody to the medium of 221-puro cells and 221-UL18 cells and examined the HTA formation after 24h. Consistently, I found anti-LFA-1 targeting either the α-chain or β-chain could completely block the formation of the cell aggregation of 221-UL18 cells (Figure 5.10B and C), which strongly demonstrated that LFA-1 is necessary to form the HTA phenotype on 221-UL18 cells. The size of the cell aggregates for the 221-puro cells was also significantly reduced when incubated with the LFA-1 blocking antibody, indicating the small cell clusters formed by 221-puro cells are also LFA-1-mediated. These results provide solid evidence that LFA-1 is required to form the HTA of 721.221 cells and UL18 expression is able to enhance the LFA-1-mediated HTA.

It seems that 221-UL18 had slightly elevated LFA-1 expression on the surface compared to 221-puro cells (Figure 5.10A), but this difference is unlikely to result in a significant change of HTA, so I investigated whether the LFA-1 activation level was different. Similar to other

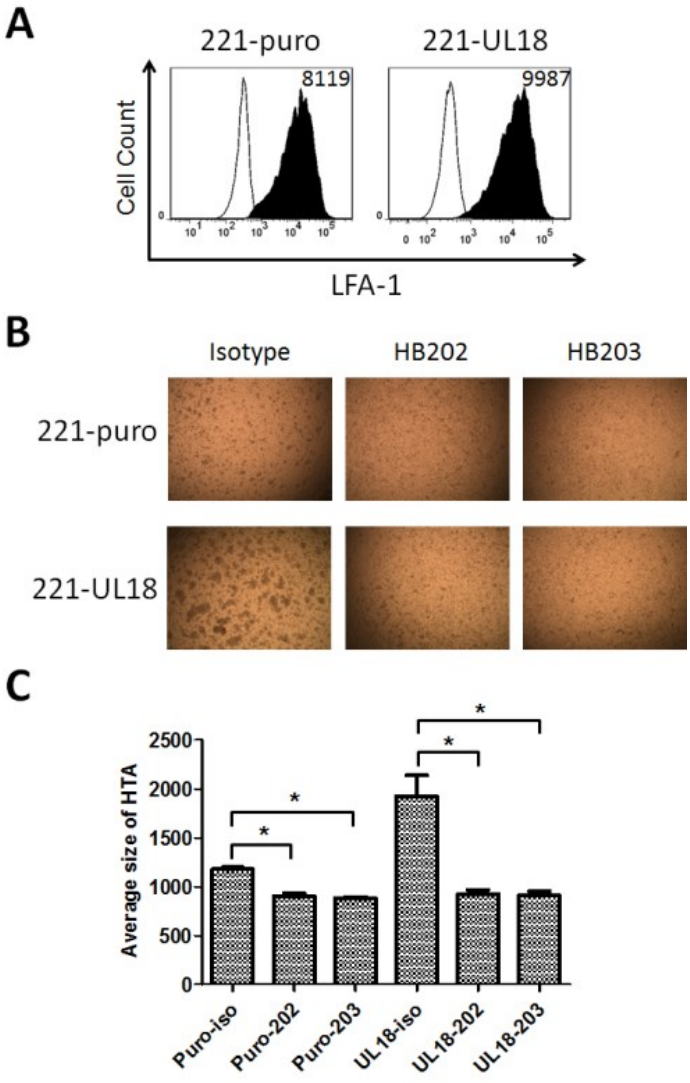

Figure 5.10 UL18-induced HTA on 721.221 cells can be reversed by anti-LFA-1 blocking. (A) Flow cytometry staining of LFA-1 on 221-puro and bulk-sorted 221-UL18 cells using an anti-LFA-1 antibody (clone: HB202). The Geom. MFI value with the background subtracted is shown inside of each plot. White and black filled curves indicate unstained control and the antibody against LFA-1, respectively. (B) Blocking of the HTA on 221-UL18 cells using two LFA-1 antibodies in parallel (clone: HB202 and HB203). Cells were seeded with 1μg/mL of HB202, HB203, or the isotype control antibody, respectively, 24 h prior to HTA assessment. 221-puro cells were used as a negative control. Cell photos were taken in the bright field with 40X magnification. The experiment was repeated three times and one time of representative results are shown. (C) Comparison of aggregates size after the incubation using LFA-1 blocking antibody or isotype control shown in panel B. The average clustering sizes were calculated using data collected from three independent experimental repeats. Statistical analysis comparing each pair of cells was done using Student' s t-test, "*" indicates P-value < 0.05.

integrins, LFA-1 has three distinct folding conformations including bent with a closed headpiece, extended with a closed headpiece, and extended with an open headpiece, from which the extended-open is the active conformation and has the highest ligand-binding affinity [320]. Generally, LFA-1 with a closed headpiece has a low affinity to bind the ligands on resting immune cells. Upon engagement with the target cells, immune cells receive activating signals through activating receptors and promote a conformational change of LFA-1 to the active conformation which has a much higher affinity to bind its ligands. This process is known as the "inside-out signaling" which involves the help by some cytoskeletal proteins such as talin and kindling [321-324]. Therefore, it is also possible that UL18 may induce a conformation switch of LFA-1 on the cell surface of 721.221 cells which then enhances the HTA formation. Since these three conformations can be differentiated by specific antibodies [325], I did flow-cytometry using the LFA-1 antibody specific for the active conformation with high affinity (clone: m24) and the conformation with a low and intermediate affinity (clone: TS1/18) to compare whether 221-UL18 cells display more active LFA-1 on the cell surface than 221-puro control. Mn^{2+} treatment which can abundantly induce the active conformation of LFA-1 was used as a positive control [326] (Figure 5.11A). However, compared with 221-puro cells, m24 staining on 221-UL18 was only slightly enhanced and also for TS1/18 (Figure 5.11B), which may be due to the slightly up-regulated total LFA-1 expression on 221-UL18 cells as shown in Figure 5.8A. Therefore, UL18-induced HTA on 721.221 cells is unlikely to result from a change in the activation state of LFA-1. How UL18 is able to enhance LFA-1-dependent HTA requires further investigation.

5.3 Summary

In this chapter, I first characterized the HTA phenotype that I observed on 221-UL18 cells. I found 221-UL18 cells could form a significantly larger size of HTA than 221-B58 and the mock-transduced 221-puro cells. Importantly, the size of the aggregates of 221-UL18 is

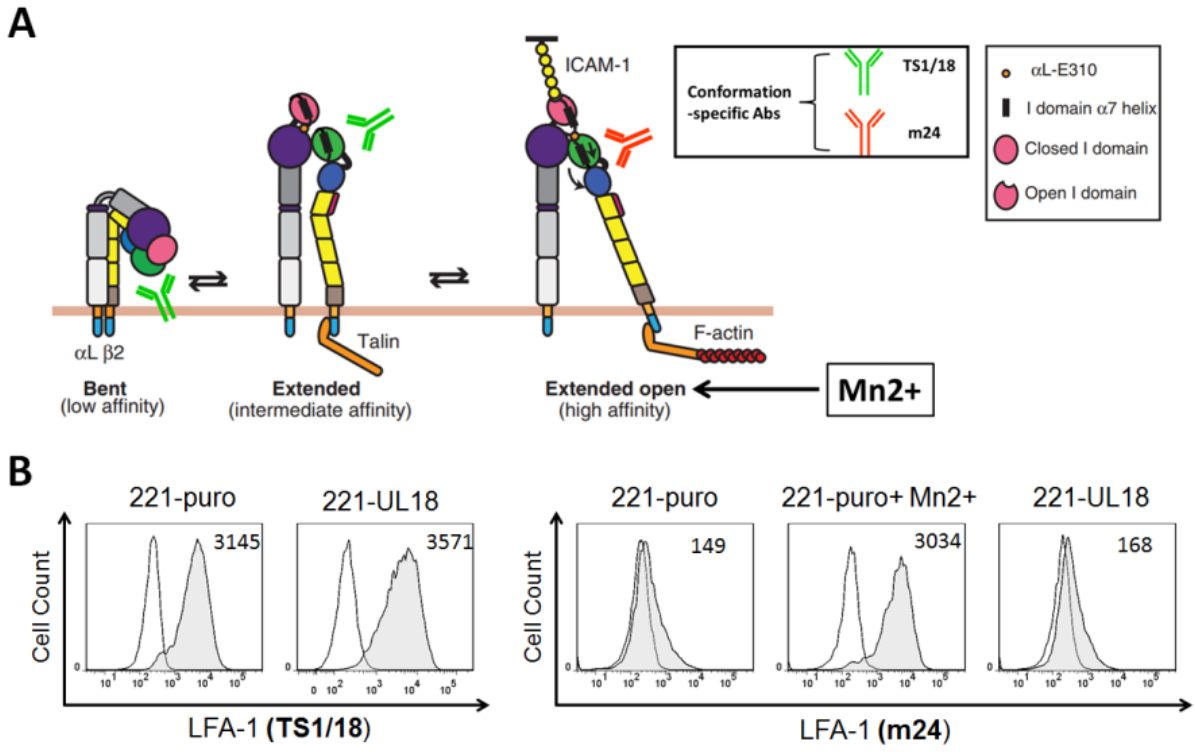

Figure 5.11 Comparison of LFA-1 conformational states on 221-puro cells and 221-UL18 cells by flow cytometry.

(A) Schematic diagram of the three conformational states of LFA-1with different ligand binding affinities and the target sites of the antibodies used. *The figure is adapted from Pflugfelder SC. et al, 2017* [327]. (B) Flow cytometry staining of 221-puro and UL18-positive bulk sorted 221-UL18 cells using LFA-1 antibodies recognizing different conformational states. The 221-puro cells pre-treated with Mn^{2+} were used as a positive control. The Geom. MFI value background subtracted is shown inside of each plot. White and light grey filled curves indicate background and antibody against LFA-1, respectively. TS1/18 staining was only done once while m24 staining is representative data from two independent experimental repeats.

correlated with the surface expression level of UL18, which suggests this phenotype is UL18-dependent. I also showed that the HTA phenotype is independent of the YFP tag fused at the C-terminus of UL18.

Then I moved forward to figure out the potential mechanism leading to the formation of UL18-induced HTA phenotype on 721.221 cells. In the beginning, I tested whether the *trans*-interaction between UL18 and LILRB1 which is highly expressed on 721.221 cells directly leads to the cell aggregation. However, the addition of a LILRB1 functional blocking antibody HP-F1 failed to reverse the HTA phenotype of 221-UL18 clones, which indicates the HTA phenotype is not a result of the *trans*-interaction of LILRB1 with UL18. This is supported by evidence that some LILRB1 molecules might be trapped by UL18 in the cytoplasm and the surface LILRB1 was also occupied by UL18 through *cis*-interaction, which limited free LILRB1 on the cell surface for *trans*-interaction. To examine the role of LILRB1 in the HTA formation, I applied CRISPR technology to knock out the LILRB1 gene in 721.221 cells then followed by UL18 transduction. The HTA formation was dramatically inhibited on those 221-UL18 without expressing LILRB1. However, if I knocked out the LILRB1 gene in a 721.221 cell clone that already expressing UL18 and had the HTA phenotype, the HTA phenotype was sustained. This apparent contradictory result suggested that LILRB1 is important for the establishment of UL18-induced HTA but not necessary for maintaining it. A possible reason to explain this might be that LILRB1 played a role in driving a process of cell differentiation that favors the HTA phenotype induced by UL18.

As LILRB1/UL18 *trans*-interaction is not involved in forming the cell aggregation of 221-UL18 cells, we went on to determine if LFA-1 which is a pivotal adhesion molecule expressed on leukocytes plays a role in the HTA phenotype formation. Surprisingly, using an antibody to block either the α-chain or β-chain was able to totally inhibit the HTA formation on 221-UL18 cells. Given that LFA-1 was only slightly up-regulated on 221-UL18 compared with 221-puro cells, we tested whether the activation status of LFA-1 was increased on 221-UL18. However, I did not detect any increase of the high-affinity conformation of LFA-1 on 221-UL18

compared with 221-puro on the cell surface. So far, since the HTA phenotype of 221-UL18 is directly LFA-1-dependent, there are still several questions to answer: 1) is the slight up-regulation of LFA-1 on the surface of 221-UL18 cells enough to induce the HTA phenotype? 2) Is the expression of LFA-1 ligands such as ICAMs changed on 221-UL18 cells? 3) What other mechanisms are there for UL18 to influence the LFA-1/ICAM axis?

CHAPTER 6

Discussion and future directions

Parts of this chapter are adapted from the published article *Yu, K., Davidson, C. L., Wójtowicz, A., Lisboa, L., Wang, T., Airo, A. M., ... & Humar, A. (2018). LILRB1 polymorphisms influence posttransplant HCMV susceptibility and ligand interactions. The Journal of clinical investigation, 128(4), 1523-1537.* and the article titled "LILRB1 intron 1 has a polymorphic regulatory region that enhances transcription in NK cells and recruits YY1" which has been accepted to be published in The Journal of Immunology.

6.1 Summary of the findings in this study

In Chapter 3, I first examined LILRB1 allelic expression patterns in human NK cell clones and extended our understanding of LILRB1 expression in NK cells to a single-cell level. Then, I characterized a 3 kb putative enhancer element in the LILRB1 gene intron 1. I cloned the whole enhancer element from donors with "high" or "low" *LILRB1* haplotypes and analyzed the sequence for polymorphisms and potential transcription factor binding sites. I detected the binding of YY1 in the putative enhancer, distal promoter, and proximal promoter of LILRB1 gene. I further showed that the putative enhancer had physical interactions with both of the two LILRB1 gene promoter regions and YY1 was involved in those interactions. Next, I examined the functional importance of the putative enhancer on LILRB1expression in NK cells using CRISPR technology. I found this putative enhancer played a positive role in regulating LILRB1 gene transcription in an NK cell line by knocking out the whole 3 kb element.

In the second part of my study, I tested functional differences of two natural LILRB1 protein variants arising from polymorphisms in the coding region of D1 and D2 domain in terms of inhibiting natural cytotoxicity. I found that the "PTTI" variant induced stronger inhibition than the "LAIS" variant on NK cell killing of target cells expressing UL18 or classical MHC-I molecules. Then, I compared the binding capacity of those two protein variants with MHC-I ligands and HCMV UL18 using purified soluble Fc-tagged receptors and ligands expressed on model cell lines. The results of the binding assays were consistent with the functional assay. I used mutagenesis on those two protein variants and figured out that all four amino acids contributed to the differential binding I observed and that the one polymorphism altered an N-linked glycosylation site that also appears to influence the receptor binding. Combined with the relationship of LILRB1 genetic variation with the LILRB1 surface expression pattern on NK cells, and the differences in the inhibitory signal, I proposed a molecular mechanism to explain the different responses to HCMV infection in transplant patients we observed before (Figure 1.7).

The third part of my study was derived from an unexpected finding I observed when I was generating the 221-UL18 stable cell line in that 221-UL18 formed big cell clusters compared with the parental 721.221 cells, which is termed the HTA phenotype. As LILRB1 is highly expressed on 721.221 cells, I examined the potential role of LILRB1 mediating the adhesion by binding to UL18 and found such a LILRB1/UL18 trans-interaction was not responsible for causing the clustering phenotype of 221-UL18 cells. However, I found that the phenotype was prevented if the LILRB1 gene was knocked out in 721.221 cells before UL18 transduction, but not after. Finally, I showed that LFA-1 was the essential adhesion molecule mediating the clustering phenotype of 221-UL18 cells.

6.2 LILRB1 heterogeneous expression in NK cells

The heterogeneity of LILRB1 expression in NK cells is reflected in two different ways: a. different people have different frequencies of LILRB1-positive NK cells; b. individual NK cells have different amounts of cell surface LILRB1. To understand what determines the frequency of LILRB1-positive NK cells, our lab has been focused on characterizing the NK-specific regulation of LILRB1 transcription and the influence of allelic variation on LILRB1 expression in NK cells. We have characterized two main haplotypes that are associated with different frequencies of LILRB1-positive subsets in NK cells [3]. However, the amount of transcript from those two haplotypes was not determined and we did not know if both alleles could be expressed at the same time in the same cell. To this end, I investigated the allelic expression of LILRB1 in NK clones from heterozygous individuals. Considering the advantages of ddPCR including high precision, absolute quantification, and high sensitivity on low-concentration samples, I used ddPCR and a SNP in the coding region to differentiate and quantify the transcripts derived from the two alleles. I detected transcript for the allele in strong linkage disequilibrium with the "high haplotype" (r^2=0.92, Table 1) at a higher frequency as it is detectable in more clones from two of the three individuals examined. This correlates well with our previous results that individuals

with the “high haplotype” associate with more frequent LILRB1-positive NK cells [257] and is reminiscent of the allele-specific expression patterns of KIRs. However, the expression of LILRB1 alleles differs from KIR in several aspects. First, a substantial proportion of NK clones express both alleles whereas, for most KIR, a minority express both alleles [255]. Second, there is significant variability in the number of transcripts among the NK clones examined which correlates imperfectly to the surface expression. This might be explained by the limitation of ddPCR that it is hard to equalize the template amount in different samples. Including reference gene expression for normalization is a feasible way by using the amplitude multiplexing and probe-mixing strategies of ddPCR. Nevertheless, the current result is enough to demonstrate the bi-allelic expression of LILRB1 at the single-cell level. Curiously, for the majority of clones that express both alleles, the amount of transcript which is associated with the “high haplotype” is the higher one. It may be helpful to verify this finding by testing more donors. Previously, we showed that the distal promoter variants provide similar levels of transcription when tested ectopically in an NK cell line indicating polymorphisms in the core promoter do not directly explain the expression patterns [277]. Together, the results suggest the mechanism that leads to differential expression of LILRB1 in NK cells is not simply due to the probability of initiating transcription and limiting the expression to one allele during a tight developmental window similar to KIRs. Nor does it appear to be a result of different promoter activities caused by the genetic variations as the promotors have similar activity in reporter assays. Rather, it may involve other levels of regulation that could be other regulatory elements affected by epigenetic mechanisms as epigenetic modifications may be mapped differentially on the alleles at a clonal level.

For one possible explanation, we considered that variation in the DNA methylation status of the distal promoter could lead to differential recruitment of transcription factors and influence the expression level. Indeed, in the case of KIRs, methylation of CpG islands in the promoter mediated by PIWI-like RNA that leads to the closing of the locus has been proposed as a mechanism to differentially silence alleles [261]. The LILRB1 distal promoter region lacks

obvious CpG islands, none-the-less, our previous DNA methylation analysis suggests one CpG site in the distal promoter needs to be de-methylated for expression in NK cells. Another upstream CpG site in the distal promoter showed differential methylation between the two haplotypes, however, the methylation percentage correlated with the frequency of LILRB1-positive NK cells [257]. Although most methyl-CpG binding proteins are regarded to play a repressive role in gene transcription by recruiting transcriptional co-repressor protein, certain methyl-CpG binding proteins can activate transcription which indicates DNA methylation may not always be a repressing marker [328-332]. Therefore, if this CpG site is playing a role in the different LILRB1 expression between the two haplotypes, it is likely by promoting methylation-dependent binding of an activating transcription factor or preventing the association of a negative regulatory factor.

I discovered that a polymorphic intronic enhancer exists that may contribute to heterogeneous LILRB1 expression in NK cells. I described above that this enhancer forms physical contact with the distal promoter presumably through the help of the scaffold protein YY1 which was detected binding to both the enhancer and the distal promoter. Coincidently, the proximal promoters of KIR genes also bind YY1, and a polymorphic mutation at the YY1 site increases promoter activity and the ratio between the reverse and forward transcripts [252, 260, 333]. However, in the cell lines and blood donors we analyzed, the YY1 sites are conserved and therefore unlikely to directly influence the allele-specific expression patterns of LILRB1. None-the-less, polymorphisms do alter the prediction of other transcription factor binding sites in the enhancer region (Table 3), which could lead to differential levels of transcription between alleles. Future directions can be focused on testing whether and how the polymorphisms in this intronic enhancer may modulate its regulation on LILRB1 expression.

While this thesis has illustrated an additional polymorphic regulatory sequence within the LILRB1 gene, additional layers of regulation might also be involved in the steady-state expression of the transcript. Along these lines, the differential amount of specific transcription factors could possibly influence the LILRB1 expression in NK cells due to genetic or epigenetic

regulation. A very recent report showed that NF90 associated with the LILRB1 transcript in THP-1 cells and PBMCs, and inhibits LILRB1 protein expression in THP-1 cells [334]. It is interesting to examine whether NK cells express NF90 and whether NK clones express different levels of NF90. Single-cell RNA-Sequencing is a powerful assay that could be used to screen transcription factors and micro-RNAs with differential expression in NK cell clones. Genetic variation may also influence the regulation of LILRB1 transcription or translation by micro-RNAs as the 3'UTR of LILRB1 gene is also polymorphic [3]. In addition, exogenetic factors, such as HCMV, HIV, and pregnancy, may also contribute to the LILRB1 heterogeneity in NK cells as introduced above.

With regards to heterogeneous LILRB1 expression on NK cells in a single person, we have previously shown that the pattern of LILRB1 expression on peripheral NK cells remains quite stable in healthy individuals over the course of one year [262]. As previously reported, LILRB1 starts to be expressed during later stages of NK development close to the appearance of KIRs [253, 335, 336], but the signals that initiate LILRB1 transcription in NK cells are unknown. We were not able to identify any additional promoters for the LILRB1 gene. However, previous analysis from our lab indicates the proximal promoter does display some elements suggesting a transcript could arise in reverse (TATA box and poly-A site) and reporter assay did show a weak reverse activity of the proximal but not the distal promoter in NKL cells [257]. Therefore, it remains possible that the proximal promoter has reverse activity during NK cell development to regulate the activation or repression of the LILRB1 locus similar to KIRs. It will also be important to examine the DNA methylation status of the distal promoter and histone modification status of the intronic enhancer in LILRB1-positive and negative subsets of NK cells separately, and at different stages of NK cell development. Little is known about the mechanisms for the frequency change of LILRB1-positive NK cells in an individual in responding to infections, diseases, or particular physiological situations. Previous work from our lab sheds light on this question showing that the LILRB1 profile on NK cells can be changed by IL-2 and IL-15 *in vitro*, and IL-2 can regulate LILRB1 promoter activities [262], which implies

the LILRB1 gene transcription can also be modulated in addition to the expansion of particular LILRB1-positive NK subsets in response to stimuli. Although it appears that the microenvironment *in vivo* matters in relation to the dynamic LILRB1 phenotype on NK cells, more investigations are needed to understand the mechanisms in NK cells, such as identifying the transcription factors and the epigenetic modifications of *cis*-regulatory elements that contribute to LILRB1 expression changes during development or other situations.

6.3 The function of the newly discovered intronic enhancer

In Chapter 3, I predicted a new regulatory region in intron 1 of the LILRB1 gene by active enhancer specific histone modification patterns in CD56+ cells. Of note, we also observed similar profiles in T cells and B cells, but not monocytes indicating the putative enhancer is lymphoid-specific. I used a transcription factor prediction tool (ALGGEN-PROMO program) and found this region possesses many potential sites to recruit transcription factors known to be expressed by lymphoid cells including some that are more T and NK (e.g. STAT5 [337, 338]), or B lineage-specific (e.g. Pax5 [339]). Interestingly, I also observed multiple transcription factors including Foxp3, Smad3, NF-AT, AP-1, ETS-1, C-Rel, STAT5, and cAMP response element-binding protein (CREB) that are involved in the development of regulatory T cells [340]. In addition, and also found the 3.2 kb sequence contains the binding sites for Ccaat enhancer-binding proteins (C/EBPs). C/EBPs and CREB could recruit the co-activator CREB-binding protein (CBP) that is regarded as markers to predict potential enhancers by ChIP-sequencing [341-344]. Among the many transcription factors predicted to associate with the enhancer element, we focused on YY1 because YYI was shown recently to be a structural regulator mediating enhancer/promoter interactions [296]. Importantly, I also searched for the binding sites of 25 more candidate enhancer-promoter structuring transcription factors including CTCF that were identified by a previous study [296] but did not get any hits. Our results demonstrate YY1 is bound to the enhancer region as well as both promoters and can pull down

the ligated 3C products with each promoter suggesting YY1-dimers bridge the elements together (Figure 6.1).

The 3C interaction I detected and the results of the CRISPR experiment indicate the whole 3kb region is a positive regulator of the distal promoter in NK cells. In future, it would be worth doing a 3C experiment with NK cells expressing different levels of LILRB1 as I predict one would detect more frequent physical interactions between this putative enhancer and the distal promoter in LILRB1-positive NK cells than LILRB1- ones. I also detected a 3C interaction of the enhancer with the proximal promoter but the biological relevance of the interaction is not understood. Despite the ability of NKL cells to support transcription from the proximal promoter in a luciferase reporter plasmid, the transcription of LILRB1 from the proximal promoter is negligible in *ex-vivo* NK cells although it can be increased by cytokine stimulation [248, 250, 262]. It is tempting to speculate that the enhancer also has a silencing effect on the proximal promoter, for example, by blocking the formation of the transcription preinitiation complex (Figure 6.1). Such a repressive activity could be an explanation of why the enhancer makes contact with the proximal promoter and why the proximal promoter is not used by NK cells. Future work can be done to better understand the role of the enhancer on both LILRB1 promoters, for instance, to uncover the trans-acting factors involved in the promoter/enhancer interaction. Besides, considering the similar histone modification signals in B and T cells, further investigation is warranted to test the function of the enhancer in other types of immune cells to verify it is active in other lymphocytes. It is predicted that the function of this enhancer may be different depending on the cell types as discussed above that some transcription factors predicted to bind the enhancer are lineage-specific or may have different expression levels in different immune cells.

6.4 A possible origin of the intronic enhancer

The presence of this regulatory region may explain why the LILRB1 gene maintains a 13

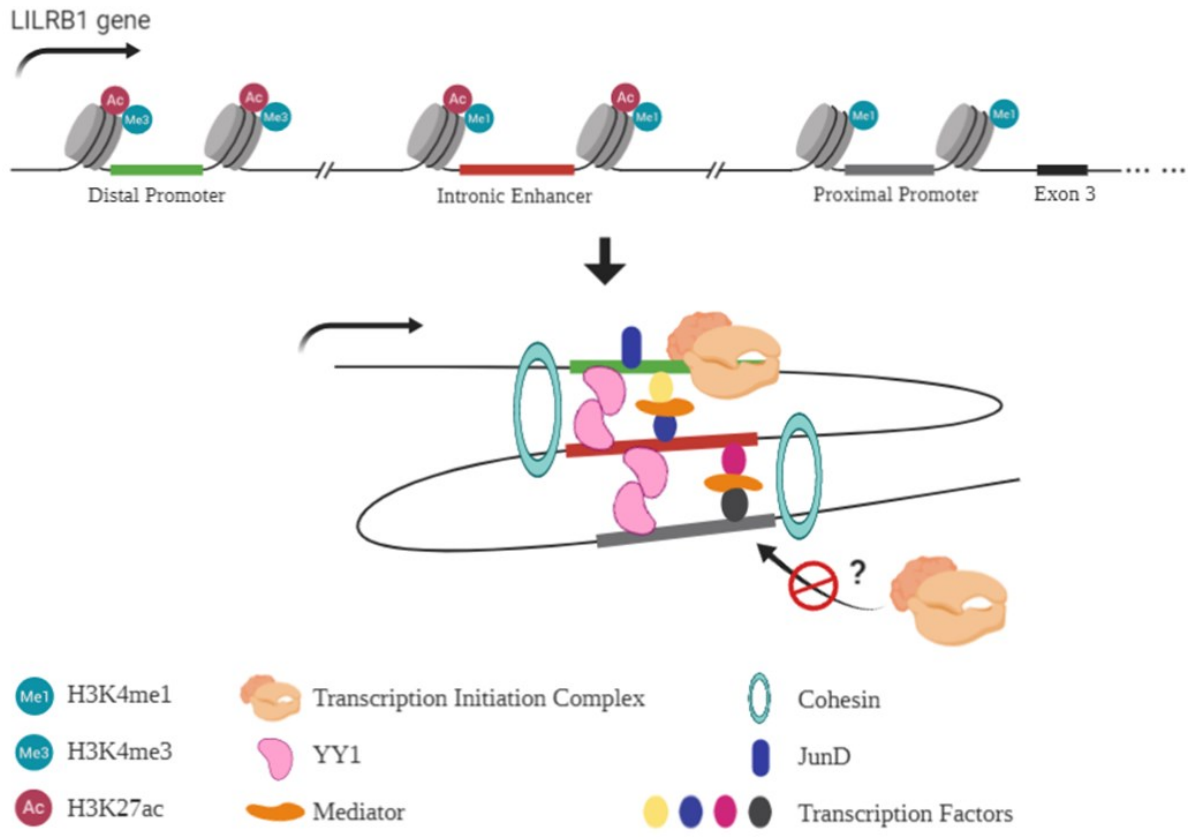

Figure 6.1 Model of the intronic enhancer-mediated regulation of the LILRB1 gene transcription in human NK cells.

The upper schematic shows the upstream *cis*-element of the LILRB1 gene and corresponding histone modification in NK cells. The arrow indicates the transcriptional direction. The lower schematic shows the physical interaction between the intronic enhancer and the promoters through forming loops mediated by YY1 dimer and other cofactors including cohesion and mediators.

kb long intron 1 whereas most other LILR genes tend toward very compact structures. Analysis with RepeatMasker annotations [345] reveals that the putative enhancer region is inside of a long interspersed nuclear element (LINE) named by L1PA15-16 (Figure 6.2A). LINE is a group of transposable elements and makes up about one-fifth of the human genome [346, 347] and its presence is supportive of the enhancer's formation by a transposable element. L1PA15-16 belongs to the type of LINE1 which is the main active LINE type in the human genome [347, 348]. The distal promoter and the flanking sequences are annotated by another LINE, several long terminal repeat retrotransposons (LTRs), and short interspersed nuclear elements (SINEs) which are also different groups of transposable elements [349] (Figure 6.2A). Intriguingly, a report published in the same year when the proximal promoter was characterized proposed that an endogenous retrovirus-like element (ERV) could work as an alternative promoter for LILRB1 gene [350]. For now, we know that the distal promoter may originate from an LTR through analysis with RepeatMasker annotations [345] (Figure 6.2A). The presence of the LINE, SINE, and LTR suggests the distal promoter and first exon were acquired through multiple insertion events and this may explain how the locus evolved to differentially regulate the LILRB1 gene in myeloid and lymphoid cells. Multiple alignments of the LILRB1 gene in different species reveals differences between primates and non-primates not only at the level of sequence conservation but also in retaining all or partial sequences upstream of the proximal promoter, although some primates such as gorilla and rhesus do not have exon1. Not surprisingly, compared to human sequence, the missing regions from primates including chimpanzee and gibbon are well-matched with some repeated elements annotated (Figure 6.2B). These findings suggest that LILRB1 gene may undergo extensive recombination with transposons during evolution, which could dramatically change the gene regulation mechanism and might directly cause the formation of the distal exon1 and the long intron1 that are regulated in a cell type or tissue-specific manner [351].

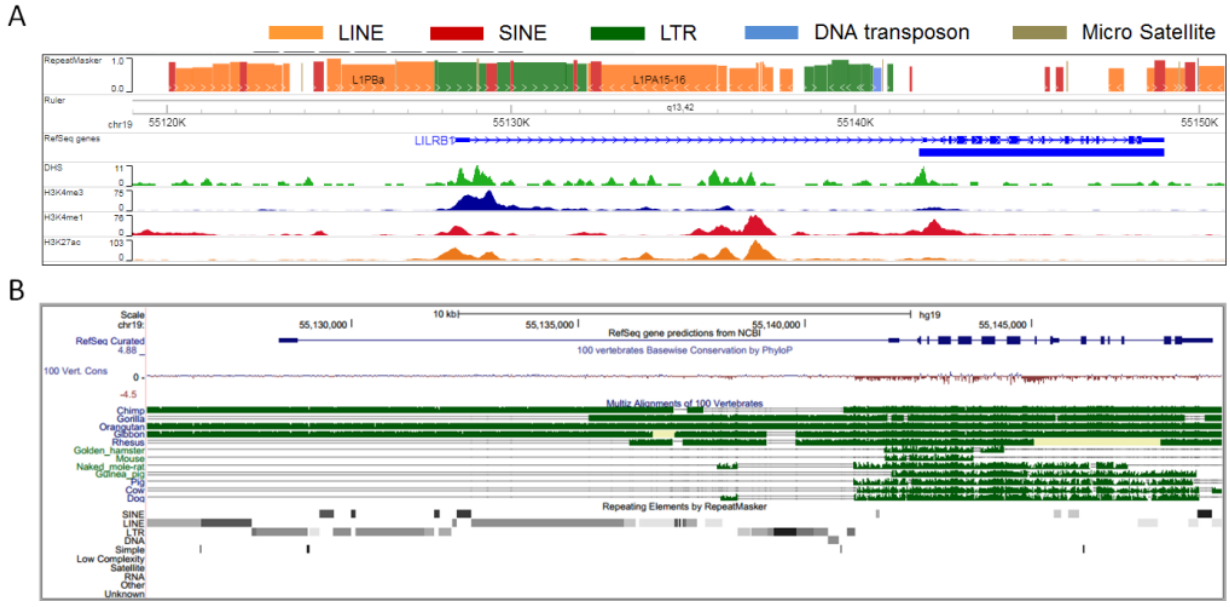

Figure 6.2 Tracking of different types of repeating elements at human LILRB1 gene locus and multiple alignments of LILRB1 genes or homologs from vertebrates.

(A) RepeatMasker tracking of the human LILRB1 gene locus. Different types of repeating elements are represented by different colors shown above the figure. LINE-long interspersed nuclear element; SINE-short interspersed nuclear element; LTR-long terminal repeat element. Histone modification markers in CD56 primary cells are also shown to indicate the location of the regulatory regions. (B) Multiple alignments of LILRB1 genes or homologs in different species of vertebrates. RepeatMasker tracking for the human sequence is also shown to indicate the location of the repeated elements.

6.5 Differential interaction of MHC-I molecules and UL18 with LILRB1 variants

In Chapter 4, I showed that the two LILRB1 protein variants (PTTI and LAIS) differentially inhibited NK cell cytotoxicity to the target cells expressing classical MHC-I or HCMV UL18. Instead of using surface plasmon resonance to examine binding affinity as done by others [274], I performed a flow cytometry-based binding assay to test the binding of LILRB1 variants with ligands expressed on model cell lines which is closer to what likely to occur *in vivo*. Indeed, the results of the binding assay were consistent with the functional assay. Further investigation demonstrated that the substitution of each of the four residues influences the binding significantly to both classical MHC-I molecules and the UL18. The rather dramatic effect of introducing an isoleucine at position 119 to generate PTII suggests that glycosylation influences binding, and likely explains why an earlier study did not detect any differences in affinity using proteins generated in bacteria [274]. The glycan could directly influence the interaction with classical MHC-I and UL18 but the molecular mechanism is unclear (Figure 6.3). It is likely to contribute by stabilizing a particular conformation that favors binding perhaps influencing the angle of the hinge. This possibility is discussed in section 6.6. What remains difficult to explain is that the introduction of glutamine into position 117 disrupted binding to Cw15 and HLA-G, while simultaneously enhancing binding to UL18 for both variants. There may be a steric hindrance between LILRB1 with UL18 due to UL18's glycosylation, not found on MHC-I. Another and not mutually exclusive possibility is that the residues are part of a second functional interface of the receptor because all of the polymorphic residues are located on the same face. The near-total coverage by glycosylation of the UL18 surface outside the area of known LILRB1 interaction likely precludes additional points for contact. An additional possibility is that the residues influence the receptor dimerization as has been suggested for the related KIR inhibitory receptors where the formation of higher-order complexes may be involved in signal transduction [352]. However, it is somewhat difficult to imagine how the formation of higher-order complexes would have such similar effects for MHC-I and UL18 but not HLA-G.

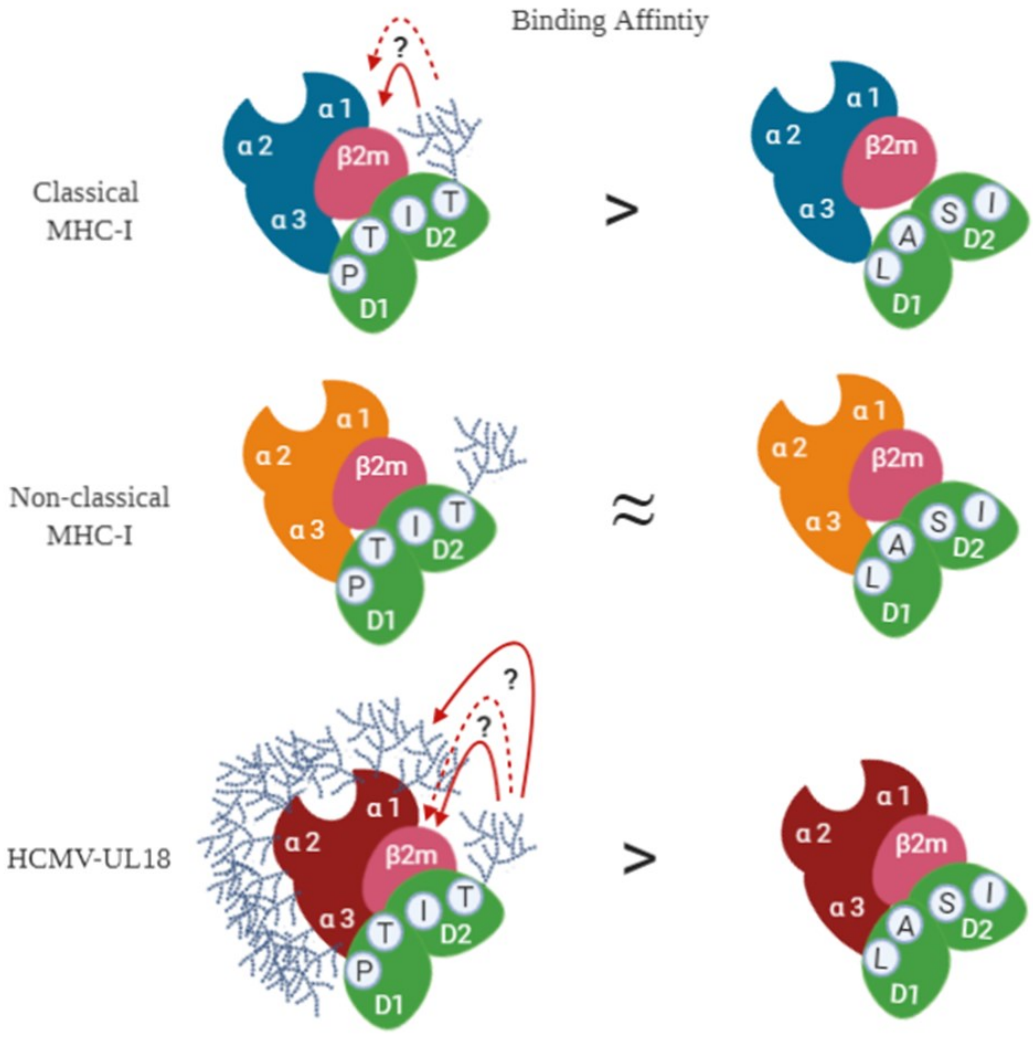

Figure 6.3 Model depicting the role of N-glycosylation on the D2 domain of LILRB1 in binding with MHC-I molecules and HCMV-UL18.
Classical MHC-I, non-classical MHC-I, and UL18 are indicated by blue, orange, and red, respectively. Relative positions of the four amino acids in the D1 and D2 domains that are influenced by the non-synonymous SNPs are shown. Binding affinity comparison between the PTTI and LAIS variant is proposed based on the results of the flow cytometry-based binding assay shown in Chapter 4. The possible roles of the N-glycan modified on the PTTI variant are indicated by solid (direct) and dotted (indirect) red arrows.

The similar binding with HLA-G we observe with natural variants compared to the artificial combinations we generated suggests that maintaining interaction with HLA-G within a particular threshold provides selective pressure on diversification of LILRB1. HLA-G is best known for its expression in the placenta where it is presumed to modulate the environment to prevent immune-mediated fetal rejection [353]. The introduction of a serine at position 132 into the PTTI variant significantly augmented binding to HLA-G, but this combination does not occur at any appreciable frequency as a natural variant [273] (Figure 1.6A). 2.7% of the European population carries the LAII haplotype, a variant likely to have a lower affinity for HLA-G and could influence reproduction. LILRB1 polymorphism may be relevant in the response of cancer as HLA-G expression on cancer cells is associated with poor outcomes [354, 355].

It should be noted that the results of the protein binding data shown in Chapter 4 were from the assay using 4°C as the binding temperature. It may be useful to test the binding at 37°C to mimic *in-vivo* conditions. There are also a couple of cell-based reporter assays that could be useful and more sensitive than the 721.221 system I used. For example, A GFP reporter cell system was applied to screen the malaria-encoded ligands for LILRB1 [229] and another LacZ gene reporter system was reported to investigate the binding of mouse NKR-P1B receptor to mouse CMV ligands [356].

6.6 Predicted structural consequences of LILRB1 polymorphisms

To evaluate the structural consequences of the LILRB1 polymorphisms on the interactions with each MHC/peptide complex, our collaborator, Adnane Achour lab, created three-dimensional models for several MHC/peptide in complex with the LILRB1 variants, respectively, based on the released co-crystallized LILRB1/HLA-A2 and LILRB1/UL18 [277]. It was thought that the inter-domain angle of D1D2 increases by 10~15 ^{o} upon the formation of the complex with MHC-I suggesting the importance of the flexibility of the D1D2 angle in the

binding [214]. Superposition of the crystalized D1D2 LILRB1 variants (PATI, PTTI, LAIS) reveals the polymorphisms notably influence the inter-domain angle (Figure 6.4) which may cause the change of contact interface with ligands. The flexibility of the inter-domain angle may also have an effect on the role of the N-glycan at T119 (Figure 4.4) contributing to the interaction. The structurally modeled complexes of LILRB1 with HLA-Cw15 and HLA-G appear to be highly similar to the LILRB1/UL18 complex (Figure 6.5 A, B, and C) but the details in the interface may explain the detected differential binding affinity.

For the comparison between UL18 and HLA-I binding with LILRB1-PATI, there are obvious differences in the conformation of the loops in the inter-domain region that has parts of the sites for the direct interaction (Figure 6.5 A, B and C). For comparison between HLA-Cw15 (or HLA-A2) and HLA-G, the residues (S195F and H197Y) have a big difference in the side chain and significantly alter the conformation of a loop between the two β-strands in the α3 domain (Figure 6.5 E, F). This potentially explains the differential affinity among UL18, HLA-G, and classical HLA-I in binding with LILRB1.

The results of the mutagenesis experiment in Chapter 4 indicate that P45 residue is important for the stronger binding with UL18 of PTTI variant. The co-crystallized LILRB1/UL18 complex reveals that a smaller residue P45 may influence the binding indirectly through facilitating the formation of two hydrogen bonds between UL18-N199, N201, and the LILRB1-T43, L37, respectively, compared with L45. In addition, a salt bridge is formed between UL18-D202 and LILRB1-R84 when the residue is P45 (Figure 6.5D).

The residue A70T also plays a role in influencing the binding of LILRB1 with either UL18 or classical MHC-I as shown above. First, the location of A70T is in the hinge region of D1 and D2 domain which directly alters the inter-domain angle between the PTTI and the PATI variant as shown in Figure 6.4. This may involve the formation of a hydrogen bond between the hydroxyl group of T70, but not A70, and the residue E184 in the D2 domain (Figure 6.6A). Second, A70T can influence the binding indirectly through residue E184. As shown in Figure 6.5A, there is a hydrogen bond between E184 and the β2m residue K91 in the PATI variant but

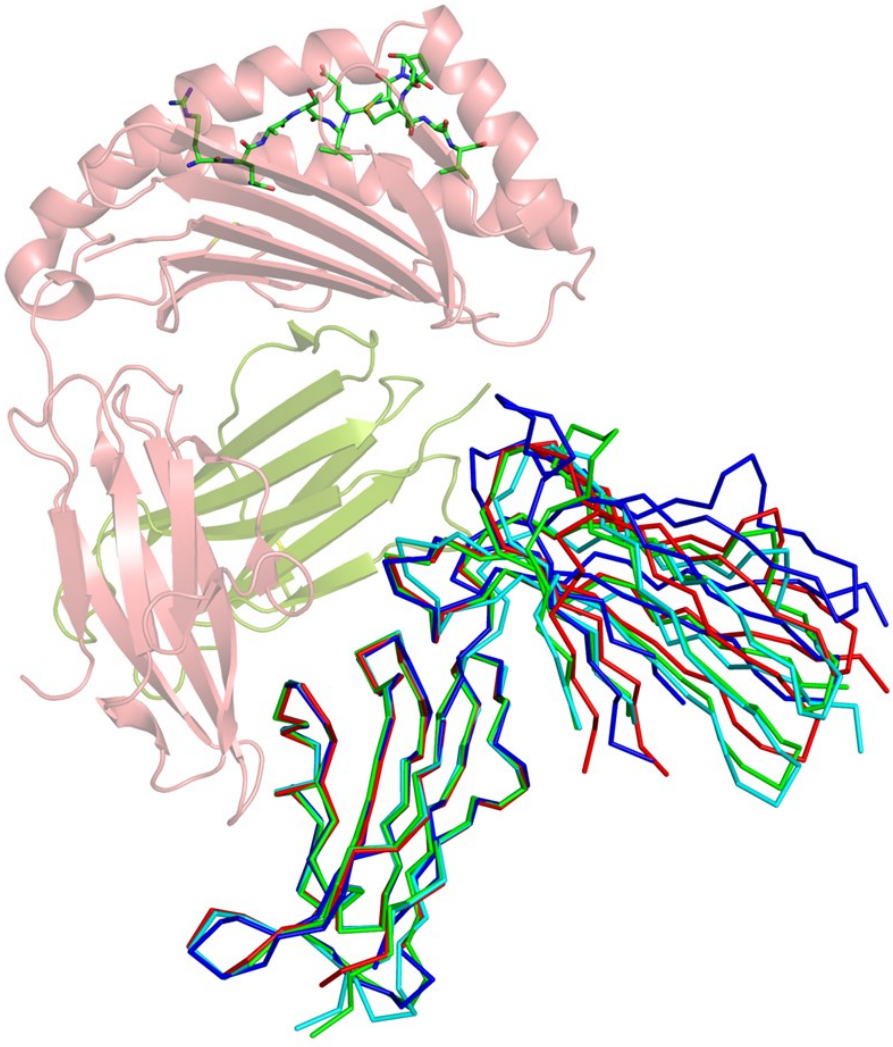

Figure 6.4 Change of the D1-D2 inter-domain angle of LILRB1 variants.
Superposition of the D1 domain of the four crystal structures of LILRB1 reveals significant flexibility in the angle formed between the D1 and D2 domains. The free LILRB1-PATI (PDB code 1G0X), free LILRB1-PTTI (PDB code 1UGN), free LILRB1-LAIS (PDB code 1VDG) and the LILRB1-PATI/HLA-A2 complex (PDB code 4NO0) are colored in red, cyan, green and blue, respectively. The figure is adapted from *Yu et. al*, supplemental Figure 4B [277].

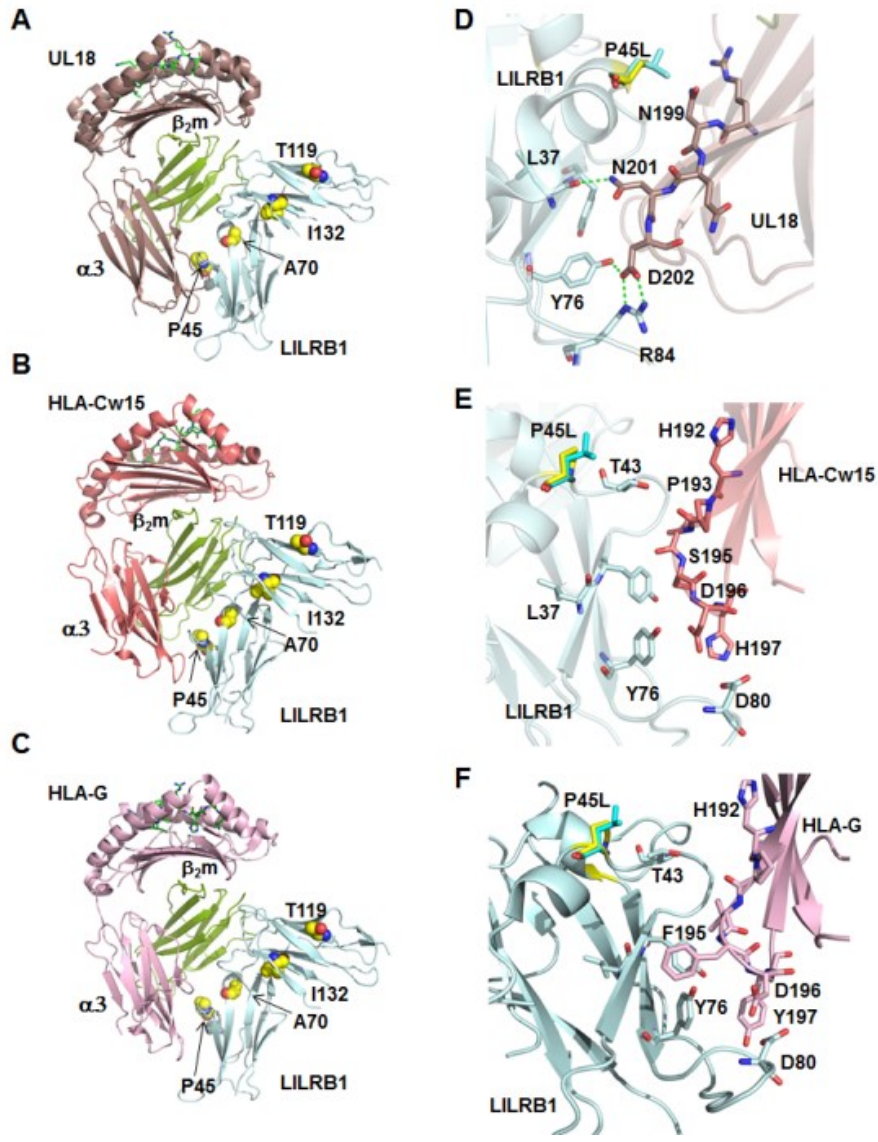

Figure 6.5 P45L has larger effects on the UL18/LILRB1 interaction compared with MHCI/LILRB1.

Comparison of the 3D structures of 3 complexes, including the crystal structure of UL18/LILRB1 (A) and the molecular models of HLA-Cw15/LILRB1 (B) and HLA-G/LILRB1 (C), illustrates the similarity of their binding modes as well as important differences in the details of these interactions. Proteins are displayed as cartoons with heavy chains of UL18 and HLA molecules in different pink colors, the β2m subunit in green, and LILRB1 in light cyan. The 4 residues that differ between the LILRB1 alleles are shown as yellow spheres. (D) Conformation of P45L in LILRB1 interacting with UL18 compared with the complexes formed with HLA-Cw15 (E) or HLA-G (F). LILRB1 is in light cyan, and the chains of UL18 or HLA are pink. Residues important for the interactions are displayed as sticks. The figure is adapted from *Yu et. al*, Figure 7 [277].

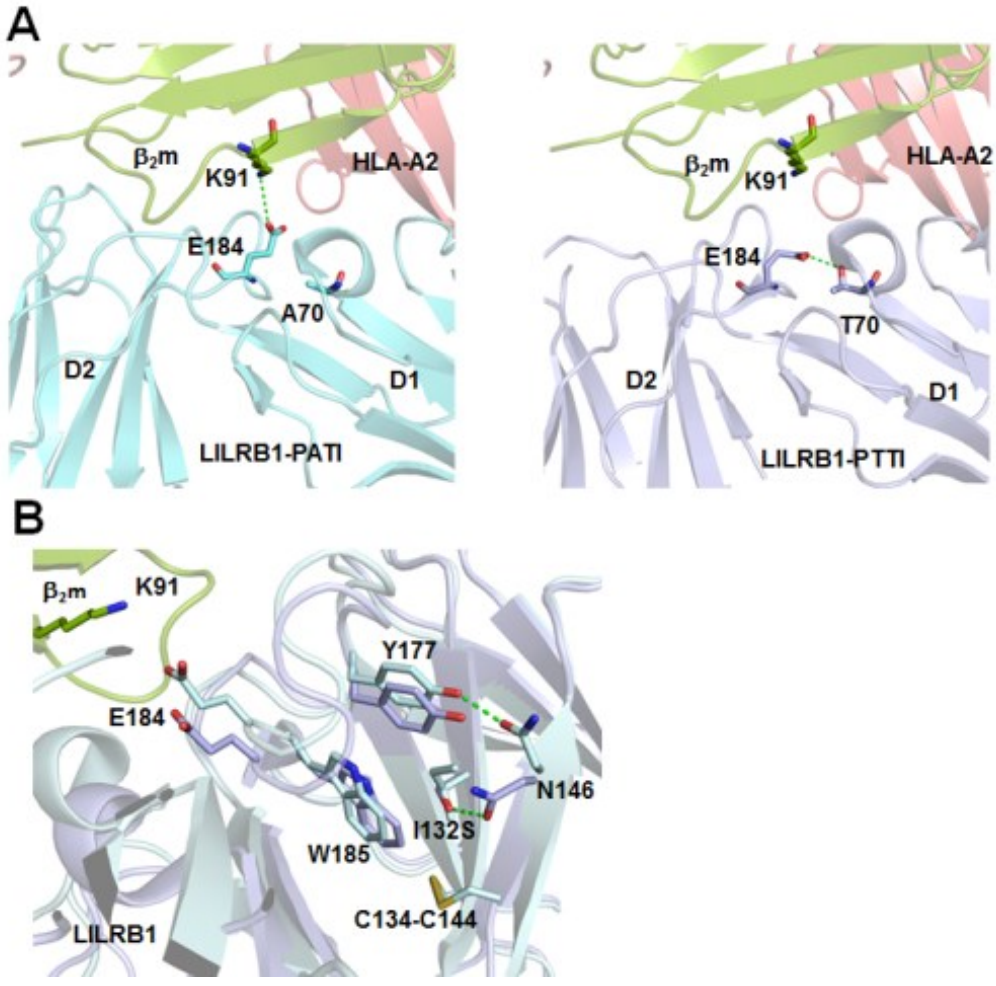

Figure 6.6 LILRB1 residues 70 and 132 impact indirectly on MHC binding.
(A) The indirect effect of the A70T polymorphism, shown for the HLA-A2/LILRB1 complex, is due to the conformation modification of the side chain of residue E184 and the removal of a hydrogen bond formed with residue K91 in β2m. (B) The S132I modification in the PATI variant (light blue) abrogates the hydrogen bond formed between the side chain of S132 and the residue N146 in the LAIS variant (purple). As a result of this modification, the side chains of the residues Y177 and W185 are also affected, changing the shape of the section of LILRB1 that connects the D1 and D2 domains and thus the interface that contacts LILRB1. Furthermore, the S132I modification results in a movement of residue E184, which is localized closer to the β2m subunit, resulting in favorable interactions. The figure is adapted from *Yu et. al*, supplemental Figure 7 [277].

not PTTI. Similarly, the residue E184 of the PATI variant forms a hydrogen bond with the K91 when binding to UL18 [218].

The I132S substitution also indirectly influences the binding although it is not in the interface. As shown in Figure 6.6B comparing the crystal structures of the PATI and LAIS variants, N146 in the D2 domain forms a hydrogen bond with Y177 of the PATI variant but with S132 of the LAIS variant, which results in a significant change in the conformation of a loop. The I132S substitution allows residues W185 and Y177 to move closer with the C134-C144 disulfide bridge leading to a smaller cavity within the hydrophobic core of the D2 domain in the LAIS variant. The result of this movement makes the residue E184 further away from the K91 and reduces the interface of the LAIS variant with HLA-I/UL18.

Together, the analysis of the structural modeling explains how the non-synonymous SNPs influence the binding of different LILRB1 variants with the ligands tested in the binding assay to some extent. Some questions are hard to answer through the modeling such as why the PTTI and LAIS variants have a comparable binding with HLA-G while the I132S substitution leads to a dramatic increase in the binding of the PTTS variant, and why the T70 is important in maintaining the strong binding of the PTTI variant with HLA-Cw15 but not HLA-G.

6.7 Implication of LILRB1 gene polymorphisms for the clinical relevance of HCMV

The overall effect of the LILRB1 genotype on control of HCMV is relatively mild and the SNP with the highest significance differs between the two cohorts although they both map the same extended haplotype that correlates with less frequent LILRB1 expression on NK cells. Further dissecting which SNPs control expression in NK cells and which influence binding should refine any further examinations of the genetic association with HCMV replication. Our results are in agreement with the higher rates of HCMV disease in a subgroup of HIV+ patients with a threonine at position 119 [276]. Future studies that assess SNPs within the interval between rs1004443 and rs1061680 may locate the most predictive SNP. For example, a stronger

association may be revealed with removal of the variants with encoding alanine at rs12460501, for example, the PATI variant which has weak binding to UL18 and the frequency is 12% in the population. Thus, in the future, more natural variants including PAIS and PATS should be tested in the NK cytotoxic assay and the binding assay with UL18.

It is not entirely clear why the correlation between LILRB1 genotype and susceptibility to HCMV infection is pronounced in STCS kidney transplant patients and a similar skewing for viremia was observed in the D+/R- group from the Canada cohort. The results of this study need to be viewed with the standard qualification for analysis of subgroups as well as the reduction of the sample size, but they also are strengthened by the similarity of the results between the two cohorts in terms of the extended haplotype in the distal regulatory region that associates with more HCMV (disease or viremia). In both cohorts, kidneys are the predominant organ type with liver recipients being the second most frequent organ type. The organ distribution has obvious implications since liver recipients are typically at a lower risk for HCMV infection and disease, likely decreasing the strength of the association between HCMV replication and the genotypes when the overall cohorts (i.e. all organ types) are taken into consideration. HCMV infection in kidney recipients was 33.79% vs. 28.32% in the other organ types in the Swiss cohort dataset genotyped for rs10423364. The Canadian patients were all HCMV D+/R-, with a much higher incidence of HCMV disease (25% vs. <6%) than what is seen in the Swiss cohort in which ~76% were HCMV recipient seropositive. The difference may explain why in the latter we saw a genotype effect only for viremia. In a previous study using STCS patients, the association with the KIR genotype was predominantly in patients receiving the highest level of immune suppression, specifically heart and lung recipients as well as the kidney recipients given anti-thymocyte globulin (ATG) which depletes T cells [357]. However, we found KIR and LILRB1 to be independent variables in STCS samples despite their proximity to one another within the LRC.

The two LILRB1 variants (PTTI and LAIS) I examined showed functional inhibition to NK cell killing. Two previous studies might provide an alternative explanation for my results as they

suggest a potential protective influence of LAIS and the related variants. A recent study showed that certain UL18 variants that differ from AD169 not only fail to inhibit NK cells but stimulate LILRB1-positive NK cells [192]. However, the study did not take into account the LILRB1 variants, but it did show that the stimulation required LILRB1. As mentioned in Chapter 1 that the activating receptor NKG2C can weakly bind to UL18, it is interesting to test whether UL18 variants differentially bind to NKG2C because the activation of NKG2C signaling may override the inhibition of NK cells by LILRB1. There is another earlier study that demonstrated LILRB1-positive T cells are stimulated through UL18 [204] even though LILRB1 inhibits T cells in other situations suggesting the signal transmitted by LILRB1 may be context-dependent, [199, 222, 358-360], but NKG2C expression was not accessed [204]. Since many HCMV-specific effector/memory T cells are LILRB1-positive, the role of LILRB1 variation in T cell responses should be considered as well. The contribution of LILRB1 interaction with MHC-I may also be a factor and in our earlier study, we found few if any LILRB1-positive NK cells respond to classical MHC-I, however, it is unlikely a rare PTTI homozygous donor was tested at that time [361].

The significance of the association of LILRB1 SNPs with HCMV disease is that it may be useful as part of a collection of biomarkers used to determine the relative risk for patients post-transplant and to guide prophylactic use of antivirals in these patients. Many studies have investigated genetic influences on the immune response to HCMV; the genes implicated in modulating the control of HCMV post-transplant include IL-28B, CCL8, several microRNAs, CLTA4, TLR9, DC-SIGN and most relevant to NK cells, NKG2C and KIRs [240, 243, 362-376]. Further studies with additional cohorts could be useful to pinpoint the SNPs with the best correlation and to explore the relationship to the sequence of UL18 within each patient.

Another interesting implication of the present work relates to prenatal and perinatal infection with HCMV. HCMV is the leading cause of birth defects caused by infection and estimates of permanent damage are as high as 0.1% of births with deafness as the most frequent problem and more prevalent for a primary infection [377]. LILRB1 is expressed by myeloid

cells within the decidua as well as the NK cells [206], and it seems possible that the variation in the interaction of UL18 or HLA-C and LILRB1 might be a factor in controlling transmission of the virus to the fetus or infants. Due to the sequelae of congenital infection, there is a significant effort to generate an HCMV vaccine, and consideration of the UL18 sequence might be important for generating the optimal immune response as strategies were tested based on chimeric viruses with distinct UL18 sequences [378, 379].

6.8 Biological relevance of the HTA phenotype of 221-UL18

In Chapter 5, I described a novel function of UL18 in enhancing the LFA-1-dependent cell aggregation using a model B cell line 721.221. However, it is unknown whether this UL18-induced HTA phenotype is a specific response from 721.221 cells. It will be very interesting to express UL18 in other immune cells, especially monocytes which are infectable cells for HCMV and implicated in the latency and systemic spread of the virus [12, 380, 381], to test if this effect of UL18 will act in a cell-type-specific fashion. I have tried UL18 transduction in K562 cells which is another MHC-I-deficient myeloid leukemia cell line. I observed intracellular expression of UL18 whereas the surface expression was very low. However, I didn't see an obvious effect on cell aggregation. Compared with 721.221 cells, K562 does not express any LILRB1. These could be possible reasons why I failed to get much UL18 surface expression as I described in Chapter 5 that LILRB1 appears to help UL18 express on the cell surface and was required in 721.221 for the phenotypic change. Co-expressing LILRB1 with UL18 is an alternative way to examine whether this will induce cell aggregation and more cell types can be tested. Another interesting question is what it means to HCMV pathogenesis if UL18 would induce the cell aggregation of monocytes. In immunocompetent individuals, acute HCMV infection does not lead to productive extracellular viruses in the blood, but the viruses seem to move directly between leukocytes, endothelial cells, and fibroblasts to spread throughout the body [7, 382]. It has been proposed that the cell-cell transmission events may play an important

role in CMV dissemination *in vivo* through partial cell-cell fusion [382-385]. Therefore, it is interesting to test if UL18 contributes to HCMV dissemination using wild-type HCMV and UL18-deficient HCMV *in vitro*. Moreover, it has been demonstrated that productive infection of peripheral blood monocytes by HCMV was not permissive unless the cells are differentiated into macrophages [386-388], and the terminally differentiated tissue macrophages are likely the initial sites of local HCMV reactivation [21]. Despite the short life-span of monocytes, previous studies revealed that HCMV infection of monocytes could promote trans-endothelial migration and induce differentiation into long-lived macrophages [381]. If UL18 expression could enhance LFA-1-dependent cell adhesion of the peripheral monocytes, it might be involved in promoting trans-endothelial migration and tissue residency of those infected cells [389, 390].

Aside from the effect on cell adhesion, I also showed that UL18 slightly inhibited the proliferation of 721.221 cells. Similarly, it has been revealed that the CD19 monoclonal antibody can induce LFA-1-dependent HTA of human tonsillar B cells and inhibit cell proliferation without increasing LFA-1 and ICAM-1expression [299]. Later studies uncovered that the inhibitory or activating role of CD19 monoclonal antibody on B cell proliferation is dependent on the mitogenic stimulus added and the degree of the antibody cross-linking [391]. A monoclonal antibody targeting CD40, an important co-stimulatory receptor expressed on B cells [392], can also induce B cell HTA in an LFA-1-dependent manner. In contrast to what I observed for UL18, they found the aggregated cells had stronger DNA synthesis than the non-aggregated cells, and the DNA synthesis induced by CD40 antibody was suppressed if LFA-1 was blocked [393]. Their data suggested a positive role of the HTA phenotype in cell proliferation but it seemed the stimulatory role of CD40 was dependent on the HTA phenotype. The slight inhibition of cell proliferation by UL18 is presumably due to UL18 binding to the inhibitory receptor LILRB1, which can be tested using 221-UL18 cells with LILRB1 gene knocked out. To figure out if the clustering phenotype is also required for the inhibitory effect of UL18 on cell proliferation, the LFA-1 blocking antibody can be added in the culture before the CTV dilution assay or generating the growth curve.

Another aspect of change I noticed for 221-UL18 cells was the delayed color change of the phenol red in the medium of 221-UL18 cells compared with 721.221 cells, which implies that UL18 might influence cell metabolism. This is consistent with the down-regulated genes related to mitochondrial metabolic activities that I observed in the preliminary RNA-Sequencing data. Considering the cellular waste product including acidic metabolites (mainly L-lactate in human cells [394, 395]) or CO2 could change the medium pH, future works can examine the extracellular oxygen consumption, glucose uptake and glycolysis to explore the effect of UL18 in different aspects of the cellular respiration and energy metabolism. It is noteworthy that 221-G cells, but not the ones expressing classical MHC-I, also exhibit some similarities with 221-UL18 cells including the HTA phenotype and delayed color change of the medium. As mentioned in Chapter 1, although with much lower binding affinity than UL18, HLA-G is the relatively strong ligand for LILRB1 among MHC-I molecules and the 221-G cells we used had a very high surface expression of HLA-G as determined using W6/32 antibody (Figure 4.1C). It can be expected that HLA-G and UL18 may influence cell adhesion and metabolism using similar mechanisms. However, prior to going deep into the molecular mechanisms changing the cell metabolism, more solid studies in the future should be done to carefully examine the reproducibility of the delayed color change and verify whether it is a real effect mediated by UL18 and HLA-G.

The current main question for the role of UL18 is how UL18 expression drives the change of LFA-1-mediated cell adhesion of 721.221 cells. I found LILRB1 is involved in the original establishment of the HTA phenotype but not necessary to maintain this phenotype in the subsequent culturing. This suggests that, as opposed to a tonic signaling to trigger the HTA formation, UL18/LILRB1 interaction might induce a process of cell differentiation which would cause epigenetic changes in 721.221 cells that are able to maintain the phenotype. An efficient and unbiased way to approach this question is to examine the transcriptome change of 721.221 cells caused by UL18 expression. I did a pilot RNA-Sequencing on 221-HA-UL18-YFP (221-UL18, clone D8) cells using 721.221 cells and 221-HA-HLA-B58-YFP (221-B58) as

controls for the possibility that puromycin selection and the peptide tags may also have an impact on cell transcriptome (APPENDIX A3). It needs to be noted that this is a very preliminary assay with only one sample from each cell line that was intended to acquire a sketchy view of the cell transcriptome impacted by UL18, and most of the sequencing data were analyzed by Dr.Arun Kommadath from Dr. Paul Stothard's group. Indeed, we observed that either HLA-B58 or UL18 significantly changed the transcriptome of 721.221 cells while the transcriptomes of 221-B58 and 221-UL18 also exhibit extensive differences (APPENDIX A4) even though those two molecules are homologs with each other. Gene Ontology and KEGG pathway term enrichment analysis revealed that the genes with differential expression (DE) in 221-B58 and 221-UL18 comparing to 721.221 cells are involved in many different biological processes. Unexpectedly, we did not observe any enriched process related to cell adhesion in 221-UL18 cells (APPENDIX A5). One concern for this RNA-Sequencing experiment was that there was no experimental repeat for each sample to obtain reliable DE genes. APPENDIX A6 lists some genes that have obvious differences between 221-UL18 and 221-B58 comparing to 721.221 cells in terms of expression fold change. Comparing to HLA-B58, it is intriguing that UL18 has a bigger impact on downregulating some pattern recognition receptors [396, 397], cytokine receptors, chemokines, and chemokine receptors. Meanwhile, UL18 increased the expression of some inhibitory receptors or ligands [398-400]. Consistently, as described in Chapter 5 that UL18 transduction slightly increased surface LFA-1 expression on 721.221 (Figure 5.10A), the RNA-Sequencing data indicates an up-regulated mRNA level of the ITGB2 gene (encoding LFA-1 β2 subunit) in 221-UL18 cells. I did not see up-regulation of ICAMs genes by UL18 which fits the result of a previous study using AD169 HCMV lab strain or the UL18-deficient counterpart to infect human fibroblasts but did not find changes in ICAM-1 surface expression [203]. However, it is hard to explain why the mRNA level of Cyclin D1 (CCND1 gene) was higher in 221-UL18 cells than 721.221 cells since we observed slightly inhibited proliferation in 221-UL18 cells compared with 221-puro control (Figure 5.4). Last but not least, we observed that the expression of some genes playing important roles in cell

metabolic processes has been changed in 221-UL18 cells, such as ACADS, ACAD11 which are involved in mitochondrial fatty acid beta-oxidation [401, 402], pyruvate carboxylase (PC) which is involved in gluconeogenesis [403]. This supports the speculated role of UL18 in influencing cell metabolism. Furthermore, we found UL18 had a broad effect on decreasing the expression of 20 out of 22 mitochondrial transfer RNAs (Mt-tRNAs) (Figure 6.7B). Mt-tRNAs are important components of mitochondrial protein synthesis machinery, thus, down-regulation of most of those tRNAs may have global effect on translation of the essential subunits of respiratory complexes in mitochondria [404] and then cause significant change in cell metabolism and perhaps a slower cell proliferation. To summarize, there were no genes that are directly involved in LFA-1 signaling substantially changed by UL18 in the RNA-Sequencing data, it is still a mystery how UL18 enhanced the LFA-1-mediated cell adhesion. We did observe interesting changes in the expression of many genes related to immune recognition and activation, chemotaxis, and cell metabolism, but it is unclear whether this was due to the LILRB1 signaling. Future work could use LILRB1-deficient suspension cell lines for UL18 transduction to see if the gene expression changes will be recapitulated. On the other hand, it cannot be excluded that the altered gene expression I showed above was due to UL18 alone. A study using human PBMCs to co-culture with human fibroblasts infected by HCMV AD169 or UL18-deficient AD169 and observed differential IFNγ production, however, the UL18 expression was not detectable on the surface of infected fibroblasts, which suggests UL18 can function intracellularly and independent of LILRB1 during infection [203]. The RNA-Sequencing experiment shown above lacks the necessary experimental repeats for statistical analysis and the 221-UL18 and 221-B58 cells used were derived from single clones which might mislead the results due to clonal variation. Thus, it is worth re-designing an experiment using more biological repeats for each sample and substituting the clonal 221-UL18 and 221-B58 cells with sorted ones.

6.9 Concluding remarks

HCMV disease is a prevalent and life-threatening complication in patients after receiving grafts. Many studies have revealed changes of the LILRB1 expression on NK cells in HCMV-infected individuals, even before developing into HCMV disease, which implies LILRB1-positive NK cells could be an indicator of HCMV infection. Our studies with two transplant patient cohorts uncovered the association of LILRB1 polymorphisms with the susceptibility of transplant patients to HCMV infection. Given that LILRB1 is an NK cell inhibitory receptor, we assumed that the reason for the patients with weak control of HCMV infection is due to a higher amount of LILRB1 receptors on NK cell surface so that the NK cells response is highly repressed by UL18 which is an HCMV-encoded immune evasion protein targeting LILRB1. Meanwhile, our lab elaborated on the correlation of the related LILRB1 gene haplotypes with the frequency of LILRB1-positive NK cells in individuals. In contrary to our assumption, transplant patients with the haplotype linked with a higher frequency of LILRB1-positive NK cells is related to better control of HCMV. This drove my interest to ask if the polymorphisms influence the LILRB1 function in NK cells. Indeed, I detected differential cytotoxic responses to target cells expressing UL18 from NK cells expressing the two most different LILRB1 natural variants, respectively, which was supported by further exanimation of the binding ability of those two variants to UL18. This is the first research to compare the function of LILRB1 variants and the results linked with our previous study which leads to a model in which the specific LILRB1 alleles that allow for superior immune evasion by HCMV are restricted by mutations that limit LILRB1 expression selectively on NK cells (Figure 6.8). This study also sheds light on exploiting particular LILRB1 haplotypes for predicting the development of HCMV disease. Furthermore, during the experiment generating the model cell line stably expressing UL18, I noticed and characterized a novel role of UL18 in triggering cell-cell adhesion. I demonstrated this effect was dependent on LFA-1 but how UL18 influences the LFA-1-mediated cell adhesion is not understood. It may be attributed to the interaction with LILRB1 or some unexplored intracellular role of UL18, and further investigation should be done

to figure out this question. As illustrated in Figure 6.8, the relationship of UL18 with cell adhesion may facilitate the virus spread and pathogenesis of HCMV. To understand the mechanisms under the relationship of LILRB1 expression in NK cells with gene polymorphisms, our lab tested the role of the genetic variation on LILRB1 promoter activity and DNA methylation but did not come up with a convincing answer. I followed up and discovered a polymorphic enhancer located in the intron 1 of the gene that plays a positive role in LILRB1 gene transcription presumably through YY1 to interact with the distal promoter. The current study provides a new perspective to understand the heterogeneity of human NK cells and it is anticipated to examine in the future that whether the polymorphisms influence the function enhancer on the distal promoter (Figure 6.8). Beyond the role of LILRB1 targeted by HCMV and in decidual NK cells, there many associations of LILRB1 in other infections, autoimmune diseases, and cardiovascular diseases. Mounting evidence also supports the immune checkpoint function of LILRB1 in viral chronic infection and cancer. How LILRB1 is regulated in each of these contexts will require further characterization of the regulatory mechanisms for LILRB1 gene expression concerning developmental programs and differentiation into effector states.

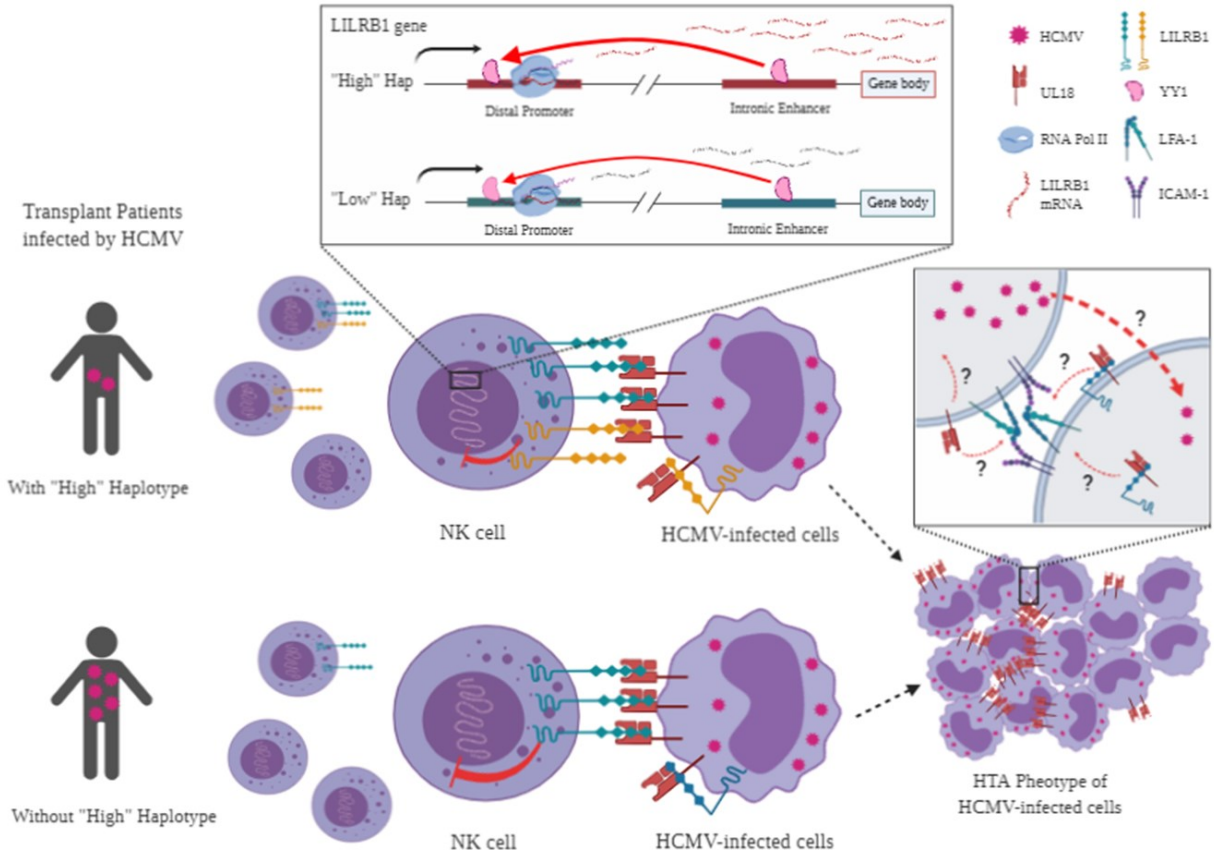

Figure 6.7 Model highlighting the findings in this thesis.
A proposed role of NK cells in differential HCMV susceptibility of transplant patients with different LILRB1 genotypes. LILRB1 gene in the "high" haplotype has stronger transcription than that in the "low" haplotype, which involves the regulation of the intronic enhancer on the distal promoter. However, the LILRB1 protein transcribed from the "low" haplotype has a stronger binding with HCMV-UL18 compared with that from the "high" haplotype, and this leads to worse control of HCMV infection by NK cells. The right side illustrates how UL18 might induce LFA-1-dependent aggregation of HCMV-infected cells and viral dissemination, but the mechanism of how UL18 and LILRB1 influence the LFA-1-ICAM axis is unclear as noted by "?". Solid red arrows and blunt end curves indicate the promoting and inhibiting effect, respectively. Dashed black curves indicate the formation of the HTA phenotype of the HCMV-infected cells. Dashed red curves indicate the possible functions of UL18 in LFA-1-dependent adhesion and viral spread.

Bibliography

1. Lisnić, B., V.J. Lisnić, and S. Jonjić, *NK cell interplay with cytomegaloviruses.* Current opinion in virology, 2015. **15**: p. 9-18.
2. Savoy, S.K. and J.E. Boudreau, *The Evolutionary Arms Race between Virus and NK Cells: Diversity Enables Population-Level Virus Control.* Viruses, 2019. **11**(10): p. 959.
3. Davidson, C.L., N.L. Li, and D.N. Burshtyn, *LILRB1 polymorphism and surface phenotypes of natural killer cells.* Human immunology, 2010. **71**(10): p. 942-949.
4. Myerson, D., et al., *Widespread presence of histologically occult cytomegalovirus.* Human pathology, 1984. **15**(5): p. 430-439.
5. Sinzger, C. and G. Jahn, *Human cytomegalovirus cell tropism and pathogenesis.* Intervirology, 1996. **39**(5-6): p. 302-319.
6. Toorkey, C.B. and D.R. Carrigan, *Immunohistochemical detection of an immediate early antigen of human cytomegalovirus in normal tissues.* Journal of Infectious Diseases, 1989. **160**(5): p. 741-751.
7. Sweet, C., *The pathogenicity of cytomegalovirus.* FEMS microbiology reviews, 1999. **23**(4): p. 457-482.
8. Gandhi, M.K. and R. Khanna, *Human cytomegalovirus: clinical aspects, immune regulation, and emerging treatments.* The Lancet infectious diseases, 2004. **4**(12): p. 725-738.
9. Desai, R., et al., *Impact of cytomegalovirus on long-term mortality and cancer risk after organ transplantation.* Transplantation, 2015. **99**(9): p. 1989-1994.
10. Ljungman, P., P. Griffiths, and C. Paya, *Definitions of cytomegalovirus infection and disease in transplant recipients.* Clinical infectious diseases, 2002. **34**(8): p. 1094-1097.
11. Meyers, J.D., N. Flournoy, and E.D. Thomas, *Risk factors for cytomegalovirus infection after human marrow transplantation.* Journal of Infectious Diseases, 1986. **153**(3): p. 478-488.
12. Söderberg-Nauclér, C., K.N. Fish, and J.A. Nelson, *Reactivation of latent human cytomegalovirus by allogeneic stimulation of blood cells from healthy donors.* Cell, 1997. **91**(1): p. 119-126.
13. Stagno, S., et al., *Primary cytomegalovirus infection in pregnancy: incidence, transmission to fetus, and clinical outcome.* Jama, 1986. **256**(14): p. 1904-1908.
14. Sinzger, C., M. Digel, and G. Jahn, *Cytomegalovirus cell tropism*, in *Human cytomegalovirus*. 2008, Springer. p. 63-83.
15. Martinez-Martin, N., et al., *An unbiased screen for human cytomegalovirus identifies neuropilin-2 as a central viral receptor.* Cell, 2018. **174**(5): p. 1158-1171. e19.
16. Gerna, G., A. Kabanova, and D. Lilleri, *Human cytomegalovirus cell tropism and host cell receptors.* Vaccines, 2019. **7**(3): p. 70.
17. Kalejta, R., *Functions of human cytomegalovirus tegument proteins prior to immediate early gene expression*, in *Human cytomegalovirus*. 2008, Springer. p. 101-115.
18. Pari, G., *Nuts and bolts of human cytomegalovirus lytic DNA replication*, in *Human Cytomegalovirus*. 2008, Springer. p. 153-166.
19. Sissons, J., et al., *Cytomegalovirus—its cellular immunology and biology.* Immunology today, 1986. **7**(2): p. 57-61.

20. Gibson, W., *Structure and formation of the cytomegalovirus virion*, in *Human cytomegalovirus*. 2008, Springer. p. 187-204.
21. Sinclair, J. and P. Sissons, *Latency and reactivation of human cytomegalovirus.* Journal of General Virology, 2006. **87**(7): p. 1763-1779.
22. Lischka, P. and H. Zimmermann, *Antiviral strategies to combat cytomegalovirus infections in transplant recipients.* Current opinion in pharmacology, 2008. **8**(5): p. 541-548.
23. Ligat, G., et al., *The human cytomegalovirus terminase complex as an antiviral target: a close-up view.* FEMS microbiology reviews, 2018. **42**(2): p. 137-145.
24. Biron, C.A., K.S. Byron, and J.L. Sullivan, *Severe herpesvirus infections in an adolescent without natural killer cells.* New England Journal of Medicine, 1989. **320**(26): p. 1731-1735.
25. Gazit, R., et al., *Expression of KIR2DL1 on the entire NK cell population: a possible novel immunodeficiency syndrome.* Blood, 2004. **103**(5): p. 1965-1966.
26. Kuijpers, T.W., et al., *Human NK cells can control CMV infection in the absence of T cells.* Blood, The Journal of the American Society of Hematology, 2008. **112**(3): p. 914-915.
27. Iversen, A.-C., et al., *Human NK cells inhibit cytomegalovirus replication through a noncytolytic mechanism involving lymphotoxin-dependent induction of IFN-β.* The Journal of Immunology, 2005. **175**(11): p. 7568-7574.
28. Wu, Z., et al., *Natural killer cells can inhibit the transmission of human cytomegalovirus in cell culture by using mechanisms from innate and adaptive immune responses.* Journal of virology, 2015. **89**(5): p. 2906-2917.
29. Plotkin, S.A., et al., *Multicenter trial of Towne strain attenuated virus vaccine in seronegative renal transplant recipients.* Transplantation, 1994. **58**(11): p. 1176-1178.
30. Schoppel, K., et al., *Kinetics of the antibody response against human cytomegalovirus-specific proteins in allogeneic bone marrow transplant recipients.* The Journal of infectious diseases, 1998. **178**(5): p. 1233-1243.
31. Gerna, G., et al., *Human cytomegalovirus serum neutralizing antibodies block virus infection of endothelial/epithelial cells, but not fibroblasts, early during primary infection.* Journal of General Virology, 2008. **89**(4): p. 853-865.
32. Macagno, A., et al., *Isolation of human monoclonal antibodies that potently neutralize human cytomegalovirus infection by targeting different epitopes on the gH/gL/UL128-131A complex.* Journal of virology, 2010. **84**(2): p. 1005-1013.
33. Fouts, A.E., et al., *Antibodies against the gH/gL/UL128/UL130/UL131 complex comprise the majority of the anti-cytomegalovirus (anti-CMV) neutralizing antibody response in CMV hyperimmune globulin.* Journal of virology, 2012. **86**(13): p. 7444-7447.
34. Kabanova, A., et al., *Platelet-derived growth factor-α receptor is the cellular receptor for human cytomegalovirus gHgLgO trimer.* Nature microbiology, 2016. **1**(8): p. 1-8.
35. Anderholm, K., C.J. Bierle, and M.R. Schleiss, *Cytomegalovirus vaccines: current status and future prospects.* Drugs, 2016. **76**(17): p. 1625-1645.
36. Krishna, B.A., M.R. Wills, and J.H. Sinclair, *Advances in the treatment of cytomegalovirus.* British Medical Bulletin, 2019. **131**(1): p. 5-17.

37. Li, C.-R., et al., *Recovery of HLA-restricted cytomegalovirus (CMV)-specific T-cell responses after allogeneic bone marrow transplant: correlation with CMV disease and effect of ganciclovir prophylaxis.* 1994.
38. Watanabe, K., et al., *Restoration of viral immunity in immunodeficient humans by the adoptive transfer of T cell clones.* Science, 1992. **257**(5067): p. 238-241.
39. Ramirez, N. and E. Olavarria, *Viral-specific adoptive immunotherapy after allo-SCT: the role of multimer-based selection strategies.* Bone marrow transplantation, 2013. **48**(10): p. 1265-1270.
40. Feuchtinger, T., et al., *Adoptive transfer of pp65-specific T cells for the treatment of chemorefractory cytomegalovirus disease or reactivation after haploidentical and matched unrelated stem cell transplantation.* Blood, The Journal of the American Society of Hematology, 2010. **116**(20): p. 4360-4367.
41. Sellar, R.S. and K.S. Peggs, *Therapeutic strategies for cytomegalovirus infection in haematopoietic transplant recipients: a focused update.* Expert opinion on biological therapy, 2014. **14**(8): p. 1121-1126.
42. Davison, A.J., et al., *The human cytomegalovirus genome revisited: comparison with the chimpanzee cytomegalovirus genomeFN1.* Journal of General Virology, 2003. **84**(1): p. 17-28.
43. Murphy, E., et al., *Coding potential of laboratory and clinical strains of human cytomegalovirus.* Proceedings of the National Academy of Sciences, 2003. **100**(25): p. 14976-14981.
44. Zhu, H., Y. Shen, and T. Shenk, *Human cytomegalovirus IE1 and IE2 proteins block apoptosis.* Journal of virology, 1995. **69**(12): p. 7960-7970.
45. Cinatl, J., et al., *Persistent human cytomegalovirus infection induces drug resistance and alteration of programmed cell death in human neuroblastoma cells.* Cancer research, 1998. **58**(2): p. 367-372.
46. Skaletskaya, A., et al., *A cytomegalovirus-encoded inhibitor of apoptosis that suppresses caspase-8 activation.* Proceedings of the National Academy of Sciences, 2001. **98**(14): p. 7829-7834.
47. Goldmacher, V.S., *vMIA, a viral inhibitor of apoptosis targeting mitochondria.* Biochimie, 2002. **84**(2-3): p. 177-185.
48. McSharry, B.P., S. Avdic, and B. Slobedman, *Human cytomegalovirus encoded homologs of cytokines, chemokines and their receptors: roles in immunomodulation.* Viruses, 2012. **4**(11): p. 2448-2470.
49. Arnon, T.I., et al., *Inhibition of the NKp30 activating receptor by pp65 of human cytomegalovirus.* Nature immunology, 2005. **6**(5): p. 515-523.
50. Rölle, A., et al., *Effects of human cytomegalovirus infection on ligands for the activating NKG2D receptor of NK cells: up-regulation of UL16-binding protein (ULBP) 1 and ULBP2 is counteracted by the viral UL16 protein.* The Journal of Immunology, 2003. **171**(2): p. 902-908.
51. Dunn, C., et al., *Human cytomegalovirus glycoprotein UL16 causes intracellular sequestration of NKG2D ligands, protecting against natural killer cell cytotoxicity.* The Journal of experimental medicine, 2003. **197**(11): p. 1427-1439.
52. Chalupny, N.J., et al., *Down-regulation of the NKG2D ligand MICA by the human cytomegalovirus glycoprotein UL142.* Biochemical and biophysical research communications, 2006. **346**(1): p. 175-181.
53. Bennett, N.J., et al., *Intracellular sequestration of the NKG2D ligand ULBP3 by human cytomegalovirus.* The Journal of Immunology, 2010. **185**(2): p. 1093-1102.
54. Stern-Ginossar, N., et al., *Host immune system gene targeting by a viral miRNA.* Science, 2007. **317**(5836): p. 376-381.

55. Seidel, E., et al., *Dynamic co-evolution of host and pathogen: HCMV downregulates the prevalent allele MICA∗008 to escape elimination by NK cells.* Cell reports, 2015. **10**(6): p. 968-982.
56. Fielding, C.A., et al., *Two novel human cytomegalovirus NK cell evasion functions target MICA for lysosomal degradation.* PLoS pathogens, 2014. **10**(5).
57. Lin, A., H. Xu, and W. Yan, *Modulation of HLA expression in human cytomegalovirus immune evasion.* Cell Mol Immunol, 2007. **4**(2): p. 91-98.
58. Tomasec, P., et al., *Surface expression of HLA-E, an inhibitor of natural killer cells, enhanced by human cytomegalovirus gpUL40.* Science, 2000. **287**(5455): p. 1031-1033.
59. Ulbrecht, M., et al., *Cutting edge: the human cytomegalovirus UL40 gene product contains a ligand for HLA-E and prevents NK cell-mediated lysis.* The Journal of Immunology, 2000. **164**(10): p. 5019-5022.
60. Cosman, D., et al., *A novel immunoglobulin superfamily receptor for cellular and viral MHC class I molecules.* Immunity, 1997. **7**(2): p. 273-282.
61. Reyburn, H.T., et al., *The class I MHC homologue of human cytomegalovirus inhibits attack by natural killer cells.* 1997.
62. Takasugi, M., M.R. Mickey, and P.I. Terasaki, *Reactivity of lymphocytes from normal persons on cultured tumor cells.* Cancer research, 1973. **33**(11): p. 2898-2902.
63. Rosenberg, E.B., et al., *Lymphocyte cytotoxicity reactions to leukemia‐associated antigens in identical twins.* International journal of cancer, 1972. **9**(3): p. 648-658.
64. Herberman, R.B., M.E. Nunn, and D.H. Lavrin, *Natural cytotoxic reactivity of mouse lymphoid cells against syngeneic and allogeneic tumors. I. Distribution of reactivity and specificity.* International journal of cancer, 1975. **16**(2): p. 216-229.
65. Herberman, R.B., et al., *Natural cytotoxic reactivity of mouse lymphoid cells against syngeneic and allogeneic tumors. II. Characterization of effector cells.* International journal of cancer, 1975. **16**(2): p. 230-239.
66. Vivier, E., et al., *Functions of natural killer cells.* Nature immunology, 2008. **9**(5): p. 503-510.
67. Lanier, L., et al., *Human natural killer cells isolated from peripheral blood do not rearrange T cell antigen receptor beta chain genes.* The Journal of experimental medicine, 1986. **163**(1): p. 209-214.
68. Sun, J.C. and L.L. Lanier, *NK cell development, homeostasis and function: parallels with CD8+ T cells.* Nature Reviews Immunology, 2011. **11**(10): p. 645-657.
69. Raulet, D.H., R.E. Vance, and C.W. McMahon, *Regulation of the natural killer cell receptor repertoire.* Annual review of immunology, 2001. **19**(1): p. 291-330.
70. McQueen, K.L. and P. Parham, *Variable receptors controlling activation and inhibition of NK cells.* Current opinion in immunology, 2002. **14**(5): p. 615-621.
71. Bryceson, Y.T., et al., *Synergy among receptors on resting NK cells for the activation of natural cytotoxicity and cytokine secretion.* Blood, 2006. **107**(1): p. 159-166.
72. Fehniger, T.A., et al., *Acquisition of murine NK cell cytotoxicity requires the translation of a pre-existing pool of granzyme B and perforin mRNAs.* Immunity, 2007. **26**(6): p. 798-811.
73. Sun, J.C., J.N. Beilke, and L.L. Lanier, *Adaptive immune features of natural killer cells.* Nature, 2009. **457**(7229): p. 557-561.

74. O'Leary, J.G., et al., *T cell–and B cell–independent adaptive immunity mediated by natural killer cells.* Nature immunology, 2006. **7**(5): p. 507-516.
75. Paust, S., B. Senman, and U.H. Von Andrian, *Adaptive immune responses mediated by natural killer cells.* Immunological reviews, 2010. **235**(1): p. 286-296.
76. Fehniger, T.A. and M.A. Cooper, *Harnessing NK cell memory for cancer immunotherapy.* Trends in immunology, 2016. **37**(12): p. 877-888.
77. Cooper, M.A., et al., *Cytokine-induced memory-like natural killer cells.* Proceedings of the National Academy of Sciences, 2009. **106**(6): p. 1915-1919.
78. Romee, R., et al., *Cytokine activation induces human memory-like NK cells.* Blood, The Journal of the American Society of Hematology, 2012. **120**(24): p. 4751-4760.
79. Lopez-Vergès, S., et al., *Expansion of a unique CD57+ NKG2Chi natural killer cell subset during acute human cytomegalovirus infection.* Proceedings of the National Academy of Sciences, 2011. **108**(36): p. 14725-14732.
80. Foley, B., et al., *Cytomegalovirus reactivation after allogeneic transplantation promotes a lasting increase in educated NKG2C+ natural killer cells with potent function.* Blood, The Journal of the American Society of Hematology, 2012. **119**(11): p. 2665-2674.
81. Rölle, A. and P. Brodin, *Immune adaptation to environmental influence: the case of NK cells and HCMV.* Trends in immunology, 2016. **37**(3): p. 233-243.
82. Hwang, I., et al., *Identification of human NK cells that are deficient for signaling adaptor FcRγ and specialized for antibody-dependent immune functions.* International immunology, 2012. **24**(12): p. 793-802.
83. Zhang, T., et al., *Cutting edge: antibody-dependent memory-like NK cells distinguished by FcRγ deficiency.* The Journal of Immunology, 2013. **190**(4): p. 1402-1406.
84. Lee, J., et al., *Epigenetic modification and antibody-dependent expansion of memory-like NK cells in human cytomegalovirus-infected individuals.* Immunity, 2015. **42**(3): p. 431-442.
85. Orange, J.S., *Formation and function of the lytic NK-cell immunological synapse.* Nature Reviews Immunology, 2008. **8**(9): p. 713-725.
86. Zamai, L., et al., *Natural killer (NK) cell–mediated cytotoxicity: differential use of TRAIL and Fas ligand by immature and mature primary human NK cells.* The Journal of experimental medicine, 1998. **188**(12): p. 2375-2380.
87. Kang, S., H.M. Brown, and S. Hwang, *Direct antiviral mechanisms of interferon-gamma.* Immune network, 2018. **18**(5).
88. Orange, J.S. and Z.K. Ballas, *Natural killer cells in human health and disease.* Clinical immunology, 2006. **118**(1): p. 1-10.
89. Moretta, L., et al., *Effector and regulatory events during natural killer–dendritic cell interactions.* Immunological reviews, 2006. **214**(1): p. 219-228.
90. Walzer, T., et al., *Natural-killer cells and dendritic cells:"l'union fait la force".* Blood, 2005. **106**(7): p. 2252-2258.
91. Degli-Esposti, M.A. and M.J. Smyth, *Close encounters of different kinds: dendritic cells and NK cells take centre stage.* Nature Reviews Immunology, 2005. **5**(2): p. 112-124.

92. Morandi, B., et al., *NK cells of human secondary lymphoid tissues enhance T cell polarization via IFN - γ secretion.* European journal of immunology, 2006. **36**(9): p. 2394-2400.
93. Martín-Fontecha, A., et al., *Induced recruitment of NK cells to lymph nodes provides IFN-γ for TH 1 priming.* Nature immunology, 2004. **5**(12): p. 1260-1265.
94. Leibson, H.J., et al., *Role of γ-interferon in antibody-producing responses.* Nature, 1984. **309**(5971): p. 799-801.
95. Sidman, C.L., et al., *γ-Interferon is one of several direct B cell-maturing lymphokines.* Nature, 1984. **309**(5971): p. 801-804.
96. Zingoni, A., et al., *Cross-talk between activated human NK cells and CD4+ T cells via OX40-OX40 ligand interactions.* The Journal of Immunology, 2004. **173**(6): p. 3716-3724.
97. Blanca, I.R., et al., *Human B cell activation by autologous NK cells is regulated by CD40-CD40 ligand interaction: role of memory B cells and CD5+ B cells.* The Journal of Immunology, 2001. **167**(11): p. 6132-6139.
98. Lu, L., et al., *Regulation of activated CD4+ T cells by NK cells via the Qa-1–NKG2A inhibitory pathway.* Immunity, 2007. **26**(5): p. 593-604.
99. Takeda, K. and G. Dennert, *The development of autoimmunity in C57BL/6 lpr mice correlates with the disappearance of natural killer type 1-positive cells: evidence for their suppressive action on bone marrow stem cell proliferation, B cell immunoglobulin secretion, and autoimmune symptoms.* The Journal of experimental medicine, 1993. **177**(1): p. 155-164.
100. Johansson, S., et al., *NK cells: elusive players in autoimmunity.* Trends in immunology, 2005. **26**(11): p. 613-618.
101. Piccioli, D., et al., *Contact-dependent stimulation and inhibition of dendritic cells by natural killer cells.* The Journal of experimental medicine, 2002. **195**(3): p. 335-341.
102. van Dommelen, S.L., et al., *Perforin and granzymes have distinct roles in defensive immunity and immunopathology.* Immunity, 2006. **25**(5): p. 835-848.
103. Nedvetzki, S., et al., *Reciprocal regulation of human natural killer cells and macrophages associated with distinct immune synapses.* Blood, 2007. **109**(9): p. 3776-3785.
104. Martin, A.M., et al., *Leukocyte Ig-like receptor complex (LRC) in mice and men.* Trends in immunology, 2002. **23**(2): p. 81-88.
105. Lanier, L.L., *NK cell receptors.* Annual review of immunology, 1998. **16**(1): p. 359-393.
106. Colonna, M. and J. Samaridis, *Cloning of immunoglobulin-superfamily members associated with HLA-C and HLA-B recognition by human natural killer cells.* Science, 1995. **268**(5209): p. 405-408.
107. D'andrea, A., et al., *Molecular cloning of NKB1. A natural killer cell receptor for HLA-B allotypes.* The Journal of Immunology, 1995. **155**(5): p. 2306-2310.
108. Vely, F. and E. Vivier, *Conservation of structural features reveals the existence of a large family of inhibitory cell surface receptors and noninhibitory/activatory counterparts.* The Journal of Immunology, 1997. **159**(5): p. 2075-2077.
109. Olcese, L., et al., *Human and mouse killer-cell inhibitory receptors recruit PTP1C and PTP1D protein tyrosine phosphatases.* The Journal of Immunology, 1996. **156**(12): p. 4531-4534.

110. Fry, A.M., L.L. Lanier, and A. Weiss, *Phosphotyrosines in the killer cell inhibitory receptor motif of NKB1 are required for negative signaling and for association with protein tyrosine phosphatase 1C.* The Journal of experimental medicine, 1996. **184**(1): p. 295-300.
111. Biassoni, R., et al., *The HLA-C-specific "activatory" or "inhibitory" natural killer cell receptors display highly homologous extracellular domains but differ in their transmembrane and intracytoplasmic portions.* Human Immunology, 1996. **1**(47): p. 70.
112. Lanier, L.L., et al., *Immunoreceptor DAP12 bearing a tyrosine-based activation motif is involved in activating NK cells.* Nature, 1998. **391**(6668): p. 703-707.
113. Lanier, L.L., *On guard—activating NK cell receptors.* Nature immunology, 2001. **2**(1): p. 23-27.
114. Lanier, L.L., *Up on the tightrope: natural killer cell activation and inhibition.* Nature immunology, 2008. **9**(5): p. 495-502.
115. Long, E.O., *Regulation of immune responses through inhibitory receptors.* Annual review of immunology, 1999. **17**(1): p. 875-904.
116. Vivier, E., J.A. Nunès, and F. Vély, *Natural killer cell signaling pathways.* Science, 2004. **306**(5701): p. 1517-1519.
117. Rangarajan, S. and R.A. Mariuzza, *Natural Killer Cell Receptors*, in *Structural Biology in Immunology*. 2018, Elsevier. p. 101-125.
118. Freud, A.G., et al., *A human CD34 (+) subset resides in lymph nodes and differentiates into CD56brightnatural killer cells.* Immunity, 2005. **22**(3): p. 295-304.
119. Vosshenrich, C.A., et al., *A thymic pathway of mouse natural killer cell development characterized by expression of GATA-3 and CD127.* Nature immunology, 2006. **7**(11): p. 1217-1224.
120. Andrews, D.M. and M.J. Smyth, *A potential role for RAG‐1 in NK cell development revealed by analysis of NK cells during ontogeny.* Immunology and cell biology, 2010. **88**(2): p. 107-116.
121. Gunther, U., et al., *Phenotypic characterization of CD3− 7+ cells in developing human intestine and an analysis of their ability to differentiate into T cells.* The Journal of Immunology, 2005. **174**(9): p. 5414-5422.
122. Blom, B. and H. Spits, *Development of human lymphoid cells.* Annu. Rev. Immunol., 2006. **24**: p. 287-320.
123. Abel, A.M., et al., *Natural killer cells: development, maturation, and clinical utilization.* Frontiers in immunology, 2018. **9**: p. 1869.
124. Hao, Q.-L., et al., *Identification of a novel, human multilymphoid progenitor in cord blood.* Blood, The Journal of the American Society of Hematology, 2001. **97**(12): p. 3683-3690.
125. Haddad, R., et al., *Molecular characterization of early human T/NK and B-lymphoid progenitor cells in umbilical cord blood.* Blood, 2004. **104**(13): p. 3918-3926.
126. Bennett, I.M., et al., *Definition of a natural killer NKR-P1A+/CD56-/CD16-functionally immature human NK cell subset that differentiates in vitro in the presence of interleukin 12.* The Journal of experimental medicine, 1996. **184**(5): p. 1845-1856.
127. Miller, J.S. and V. McCullar, *Human natural killer cells with polyclonal lectin and immunoglobulinlike receptors develop from single hematopoietic stem cells with preferential expression of NKG2A and KIR2DL2/L3/S2.* Blood, The Journal of the American Society of Hematology, 2001. **98**(3): p. 705-713.

128. Sivori, S., et al., *Early expression of triggering receptors and regulatory role of 2B4 in human natural killer cell precursors undergoing in vitro differentiation.* Proceedings of the National Academy of Sciences, 2002. **99**(7): p. 4526-4531.
129. Colucci, F., M.A. Caligiuri, and J.P. Di Santo, *What does it take to make a natural killer?* Nature Reviews Immunology, 2003. **3**(5): p. 413-425.
130. Yu, J., A.G. Freud, and M.A. Caligiuri, *Location and cellular stages of natural killer cell development.* Trends in immunology, 2013. **34**(12): p. 573-582.
131. Cichocki, F.M., B. Grzywacz, and J.S. Miller, *Human NK cell development: one road or many?* Frontiers in immunology, 2019. **10**: p. 2078.
132. Mace, E.M., et al., *Mutations in GATA2 cause human NK cell deficiency with specific loss of the CD56bright subset.* Blood, 2013. **121**(14): p. 2669-2677.
133. Freud, A.G. and M.A. Caligiuri, *Human natural killer cell development.* Immunological reviews, 2006. **214**(1): p. 56-72.
134. Vosshenrich, C.A., et al., *Roles for common cytokine receptor γ-chain-dependent cytokines in the generation, differentiation, and maturation of NK cell precursors and peripheral NK cells in vivo.* The Journal of Immunology, 2005. **174**(3): p. 1213-1221.
135. Ikawa, T., et al., *Commitment to natural killer cells requires the helix–loop–helix inhibitor Id2.* Proceedings of the National Academy of Sciences, 2001. **98**(9): p. 5164-5169.
136. Jaleco, A.C., et al., *Differential effects of Notch ligands Delta-1 and Jagged-1 in human lymphoid differentiation.* The Journal of experimental medicine, 2001. **194**(7): p. 991-1002.
137. Beck, R.C., et al., *The Notch ligands Jagged2, Delta1, and Delta4 induce differentiation and expansion of functional human NK cells from CD34+ cord blood hematopoietic progenitor cells.* Biology of Blood and Marrow Transplantation, 2009. **15**(9): p. 1026-1037.
138. Vosshenrich, C.A., S.I. Samson-Villéger, and J.P. Di Santo, *Distinguishing features of developing natural killer cells.* Current opinion in immunology, 2005. **17**(2): p. 151-158.
139. Gascoyne, D.M., et al., *The basic leucine zipper transcription factor E4BP4 is essential for natural killer cell development.* Nature immunology, 2009. **10**(10): p. 1118.
140. Kamizono, S., et al., *Nfil3/E4bp4 is required for the development and maturation of NK cells in vivo.* Journal of Experimental Medicine, 2009. **206**(13): p. 2977-2986.
141. Kashiwada, M., et al., *IL-4-induced transcription factor NFIL3/E4BP4 controls IgE class switching.* Proceedings of the National Academy of Sciences, 2010. **107**(2): p. 821-826.
142. Höglund, P. and P. Brodin, *Current perspectives of natural killer cell education by MHC class I molecules.* Nature reviews immunology, 2010. **10**(10): p. 724-734.
143. Cudkowicz, G. and J. Stimpfling, *Induction of immunity and of unresponsiveness to parental marrow grafts in adult F1 hybrid mice.* Nature, 1964. **204**(4957): p. 450-453.
144. Cudkowicz, G., *GENETIC CONTROL OF BONE MARROW GRAFT REJECTION: I. Determinant-Specific Difference of Reactivity in Two Pairs of Inbred Mouse Strains.* The Journal of experimental medicine, 1971. **134**(1): p. 281-293.
145. Kärre, K., *Natural killer cell recognition of missing self.* Nature immunology, 2008. **9**(5): p. 477-480.

146. Kiessling, R., et al., *Evidence for a similar or common mechanism for natural killer cell activity and resistance to hemopoietic grafts.* European journal of immunology, 1977. **7**(9): p. 655-663.
147. Höglund, P., et al., *Natural resistance against lymphoma grafts conveyed by H-2Dd transgene to C57BL mice.* The Journal of experimental medicine, 1988. **168**(4): p. 1469-1474.
148. Ohlen, C., et al., *Prevention of allogeneic bone marrow graft rejection by H-2 transgene in donor mice.* Science, 1989. **246**(4930): p. 666-668.
149. Ciccone, E., et al., *Self class I molecules protect normal cells from lysis mediated by autologous natural killer cells.* European journal of immunology, 1994. **24**(4): p. 1003-1006.
150. Valiante, N.M., et al., *Functionally and structurally distinct NK cell receptor repertoires in the peripheral blood of two human donors.* Immunity, 1997. **7**(6): p. 739-751.
151. Karlhofer, F.M., R.K. Ribaudo, and W.M. Yokoyama, *MHC class I alloantigen specificity of Ly-49+ IL-2-activated natural killer cells.* Nature, 1992. **358**(6381): p. 66-70.
152. Kim, S., et al., *Licensing of natural killer cells by host major histocompatibility complex class I molecules.* Nature, 2005. **436**(7051): p. 709-713.
153. Anfossi, N., et al., *Human NK cell education by inhibitory receptors for MHC class I.* Immunity, 2006. **25**(2): p. 331-342.
154. Johansson, S., et al., *Natural killer cell education in mice with single or multiple major histocompatibility complex class I molecules.* The Journal of experimental medicine, 2005. **201**(7): p. 1145-1155.
155. Fernandez, N.C., et al., *A subset of natural killer cells achieves self-tolerance without expressing inhibitory receptors specific for self-MHC molecules.* Blood, 2005. **105**(11): p. 4416-4423.
156. Yawata, M., et al., *MHC class I–specific inhibitory receptors and their ligands structure diverse human NK-cell repertoires toward a balance of missing self-response.* Blood, The Journal of the American Society of Hematology, 2008. **112**(6): p. 2369-2380.
157. Bix, M., et al., *Rejection of class I MHC-deficient haemopoietic cells by irradiated MHC-matched mice.* Nature, 1991. **349**(6307): p. 329-331.
158. Höglund, P., et al., *Recognition of beta 2-microglobulin-negative (beta 2m-) T-cell blasts by natural killer cells from normal but not from beta 2m-mice: nonresponsiveness controlled by beta 2m-bone marrow in chimeric mice.* Proceedings of the National Academy of Sciences, 1991. **88**(22): p. 10332-10336.
159. Liao, N.-S., et al., *MHC class I deficiency: susceptibility to natural killer (NK) cells and impaired NK activity.* Science, 1991. **253**(5016): p. 199-202.
160. Zimmer, J., et al., *Activity and phenotype of natural killer cells in peptide transporter (TAP)-deficient patients (type I bare lymphocyte syndrome).* The Journal of experimental medicine, 1998. **187**(1): p. 117-122.
161. Brodin, P., et al., *The strength of inhibitory input during education quantitatively tunes the functional responsiveness of individual natural killer cells.* Blood, The Journal of the American Society of Hematology, 2009. **113**(11): p. 2434-2441.
162. Elliott, J.M., J.A. Wahle, and W.M. Yokoyama, *MHC class I–deficient natural killer cells acquire a licensed phenotype after transfer into an MHC class I–sufficient environment.* Journal of Experimental Medicine, 2010. **207**(10): p. 2073-2079.

163. Joncker, N.T., et al., *Mature natural killer cells reset their responsiveness when exposed to an altered MHC environment.* Journal of Experimental Medicine, 2010. **207**(10): p. 2065-2072.
164. Juelke, K., et al., *Education of hyporesponsive NK cells by cytokines.* European journal of immunology, 2009. **39**(9): p. 2548-2555.
165. Brodin, P., K. Kärre, and P. Höglund, *NK cell education: not an on-off switch but a tunable rheostat.* Trends in immunology, 2009. **30**(4): p. 143-149.
166. Joncker, N.T., et al., *NK cell responsiveness is tuned commensurate with the number of inhibitory receptors for self-MHC class I: the rheostat model.* The Journal of Immunology, 2009. **182**(8): p. 4572-4580.
167. Orr, M.T. and L.L. Lanier, *Natural killer cell education and tolerance.* Cell, 2010. **142**(6): p. 847-856.
168. He, Y. and Z. Tian, *NK cell education via nonclassical MHC and non-MHC ligands.* Cellular & molecular immunology, 2017. **14**(4): p. 321-330.
169. Wilson, M.J., et al., *Plasticity in the organization and sequences of human KIR/ILT gene families.* Proceedings of the National Academy of Sciences, 2000. **97**(9): p. 4778-4783.
170. Wende, H., et al., *Organization of the leukocyte receptor cluster (LRC) on human chromosome 19q13. 4.* Mammalian Genome, 1999. **10**(2): p. 154-160.
171. Hirayasu, K. and H. Arase, *Leukocyte Immunoglobulin-Like Receptor (LILR).* Encyclopedia of Signaling Molecules, 2017: p. 1-8.
172. Wende, H., A. Volz, and A. Ziegler, *Extensive gene duplications and a large inversion characterize the human leukocyte receptor cluster.* Immunogenetics, 2000. **51**(8-9): p. 703-713.
173. Yokoyama, W.M., *What goes up must come down: the emerging spectrum of inhibitory receptors.* The Journal of experimental medicine, 1997. **186**(11): p. 1803-1808.
174. Colonna, M., et al., *A novel family of Ig‐like receptors for HLA class I molecules that modulate function of lymphoid and myeloid cells.* Journal of leukocyte biology, 1999. **66**(3): p. 375-381.
175. Nakajima, H., et al., *Cutting edge: human myeloid cells express an activating ILT receptor (ILT1) that associates with Fc receptor γ-chain.* The Journal of Immunology, 1999. **162**(1): p. 5-8.
176. Young, N.T., et al., *Conserved organization of the ILT/LIR gene family within the polymorphic human leukocyte receptor complex.* Immunogenetics, 2001. **53**(4): p. 270-278.
177. Canavez, F., et al., *Comparison of chimpanzee and human leukocyte Ig-like receptor genes reveals framework and rapidly evolving genes.* The Journal of Immunology, 2001. **167**(10): p. 5786-5794.
178. Hirayasu, K. and H. Arase, *Functional and genetic diversity of leukocyte immunoglobulin-like receptor and implication for disease associations.* Journal of human genetics, 2015. **60**(11): p. 703-708.
179. Hudson, L.E. and R.L. Allen, *Leukocyte Ig-like receptors–a model for MHC class I disease associations.* Frontiers in immunology, 2016. **7**: p. 281.
180. Zhang, J., et al., *Leukocyte immunoglobulin‐like receptors in human diseases: an overview of their distribution, function, and potential application for immunotherapies.* Journal of leukocyte biology, 2017. **102**(2): p. 351-360.
181. Burshtyn, D.N. and C. Morcos, *The Expanding Spectrum of Ligands for Leukocyte Ig-like Receptors.* The Journal of Immunology, 2016. **196**(3): p. 947-955.
182. Brown, D., J. Trowsdale, and R. Allen, *The LILR family: modulators of innate and adaptive immune pathways in health and disease.* Tissue antigens, 2004. **64**(3): p. 215-225.

183. Takeda, K. and A. Nakamura, *Regulation of immune and neural function via leukocyte Ig-like receptors.* The Journal of Biochemistry, 2017. **162**(2): p. 73-80.
184. Katz, H.R., *Inhibition of inflammatory responses by leukocyte Ig‐like receptors.* Advances in immunology, 2006. **91**: p. 251-272.
185. Samaridis, J. and M. Colonna, *Cloning of novel immunoglobulin superfamily receptors expressed on human myeloid and lymphoid cells: structural evidence for new stimulatory and inhibitory pathways.* European journal of immunology, 1997. **27**(3): p. 660-665.
186. Colonna, M., et al., *A common inhibitory receptor for major histocompatibility complex class I molecules on human lymphoid and myelomonocytic cells.* Journal of Experimental Medicine, 1997. **186**(11): p. 1809-1818.
187. Zhao, J., et al., *The MHC class I‐LILRB1 signalling axis as a promising target in cancer therapy.* Scandinavian journal of immunology, 2019. **90**(5): p. e12804.
188. Bellón, T., et al., *Mutational analysis of immunoreceptor tyrosine-based inhibition motifs of the Ig-like transcript 2 (CD85j) leukocyte receptor.* The Journal of Immunology, 2002. **168**(7): p. 3351-3359.
189. Long, E.O., *Negative signaling by inhibitory receptors: the NK cell paradigm.* Immunological reviews, 2008. **224**(1): p. 70-84.
190. Vitale, M., et al., *The leukocyte Ig-like receptor (LIR)-1 for the cytomegalovirus UL18 protein displays a broad specificity for different HLA class I alleles: analysis of LIR-1+ NK cell clones.* International immunology, 1999. **11**(1): p. 29-35.
191. Prod'homme, V., et al., *The human cytomegalovirus MHC class I homolog UL18 inhibits LIR-1+ but activates LIR-1− NK cells.* The Journal of Immunology, 2007. **178**(7): p. 4473-4481.
192. Chen, K.C., et al., *LIR1 expressing human Natural Killer cell subsets differentially recognize isolates of human cytomegalovirus through the viral MHC Class I homolog UL18.* Journal of Virology, 2016: p. JVI. 02614-15.
193. Roberti, M.P., et al., *Overexpression of CD85j in TNBC patients inhibits Cetuximab‐mediated NK‐cell ADCC but can be restored with CD85j functional blockade.* European journal of immunology, 2015. **45**(5): p. 1560-1569.
194. Favier, B., et al., *ILT2/HLA-G interaction impairs NK-cell functions through the inhibition of the late but not the early events of the NK-cell activating synapse.* The FASEB Journal, 2010. **24**(3): p. 689-699.
195. Morel, E. and T. Bellón, *HLA class I molecules regulate IFN-γ production induced in NK cells by target cells, viral products, or immature dendritic cells through the inhibitory receptor ILT2/CD85j.* The Journal of Immunology, 2008. **181**(4): p. 2368-2381.
196. Godal, R., et al., *Natural killer cell killing of acute myelogenous leukemia and acute lymphoblastic leukemia blasts by killer cell immunoglobulin-like receptor–negative natural killer cells after NKG2A and LIR-1 blockade.* Biology of Blood and Marrow Transplantation, 2010. **16**(5): p. 612-621.
197. Gonen-Gross, T., et al., *Inhibitory NK receptor recognition of HLA-G: regulation by contact residues and by cell specific expression at the fetal-maternal interface.* PLoS One, 2010. **5**(1).
198. Fu, B., et al., *Natural killer cells promote fetal development through the secretion of growth-promoting factors.* Immunity, 2017. **47**(6): p. 1100-1113. e6.

199. Saverino, D., et al., *The CD85/LIR-1/ILT2 inhibitory receptor is expressed by all human T lymphocytes and down-regulates their functions.* The Journal of Immunology, 2000. **165**(7): p. 3742-3755.
200. Ketroussi, F., et al., *Lymphocyte cell-cycle inhibition by HLA-G is mediated by phosphatase SHP-2 and acts on the mTOR pathway.* PloS one, 2011. **6**(8).
201. Merlo, A., et al., *CD85/LIR-1/ILT2 and CD152 (Cytotoxic T Lymphocyte Antigen 4) Inhibitory Molecules Down-Regulate the Cytolytic Activity of Human CD4+ T-Cell Clones Specific forMycobacterium tuberculosis.* Infection and immunity, 2001. **69**(10): p. 6022-6029.
202. Gustafson, C.E., et al., *Immune checkpoint function of CD85j in CD8 T cell differentiation and aging.* Frontiers in immunology, 2017. **8**: p. 692.
203. Wagner, C.S., et al., *Increased expression of leukocyte Ig-like receptor-1 and activating role of UL18 in the response to cytomegalovirus infection.* The Journal of Immunology, 2007. **178**(6): p. 3536-3543.
204. Saverino, D., et al., *Specific recognition of the viral protein UL18 by CD85j/LIR-1/ILT2 on CD8+ T cells mediates the non-MHC-restricted lysis of human cytomegalovirus-infected cells.* The Journal of Immunology, 2004. **172**(9): p. 5629-5637.
205. Arnold, V., et al., *S100A9 protein is a novel ligand for the CD85j receptor and its interaction is implicated in the control of HIV-1 replication by NK cells.* Retrovirology, 2013. **10**(1): p. 122.
206. Li, C., et al., *HLA-G homodimer-induced cytokine secretion through HLA-G receptors on human decidual macrophages and natural killer cells.* Proceedings of the National Academy of Sciences, 2009. **106**(14): p. 5767-5772.
207. Shlapatska, L.M., et al., *CD150 association with either the SH2-containing inositol phosphatase or the SH2-containing protein tyrosine phosphatase is regulated by the adaptor protein SH2D1A.* The Journal of Immunology, 2001. **166**(9): p. 5480-5487.
208. Ostrakhovitch, E.A. and S.S.-C. Li, *The role of SLAM family receptors in immune cell signaling.* Biochemistry and cell biology, 2006. **84**(6): p. 832-843.
209. Merlo, A., et al., *Inhibitory receptors CD85j, LAIR-1, and CD152 down-regulate immunoglobulin and cytokine production by human B lymphocytes.* Clin. Diagn. Lab. Immunol., 2005. **12**(6): p. 705-712.
210. Fanger, N.A., et al., *The MHC class I binding proteins LIR‐1 and LIR‐2 inhibit Fc receptor‐mediated signaling in monocytes.* European journal of immunology, 1998. **28**(11): p. 3423-3434.
211. Barkal, A.A., et al., *Engagement of MHC class I by the inhibitory receptor LILRB1 suppresses macrophages and is a target of cancer immunotherapy.* Nature immunology, 2018. **19**(1): p. 76.
212. Young, N.T., et al., *The inhibitory receptor LILRB1 modulates the differentiation and regulatory potential of human dendritic cells.* Blood, The Journal of the American Society of Hematology, 2008. **111**(6): p. 3090-3096.
213. Tenca, C., et al., *CD85j (leukocyte Ig-like receptor-1/Ig-like transcript 2) inhibits human osteoclast-associated receptor-mediated activation of human dendritic cells.* The Journal of Immunology, 2005. **174**(11): p. 6757-6763.
214. Willcox, B.E., L.M. Thomas, and P.J. Bjorkman, *Crystal structure of HLA-A2 bound to LIR-1, a host and viral major histocompatibility complex receptor.* Nature immunology, 2003. **4**(9): p. 913-919.
215. Wang, Q., et al., *Structures of the four Ig-like domain LILRB2 and the four-domain LILRB1 and HLA-G1 complex.* Cell. Mol. Immunol, 2019.

216. Kuroki, K., et al., *Structural and Functional Basis for LILRB Immune Checkpoint Receptor Recognition of HLA-G Isoforms.* The Journal of Immunology, 2019. **203**(12): p. 3386-3394.
217. Dulberger, C.L., et al., *Human leukocyte antigen F presents peptides and regulates immunity through interactions with NK cell receptors.* Immunity, 2017. **46**(6): p. 1018-1029. e7.
218. Yang, Z. and P.J. Bjorkman, *Structure of UL18, a peptide-binding viral MHC mimic, bound to a host inhibitory receptor.* Proceedings of the National Academy of Sciences, 2008. **105**(29): p. 10095-10100.
219. Hee, C.-S., et al., *Dynamics of free versus complexed β 2-microglobulin and the evolution of interfaces in MHC class I molecules.* Immunogenetics, 2013. **65**(3): p. 157-172.
220. Mohammed, F., D.H. Stones, and B.E. Willcox, *Application of the immunoregulatory receptor LILRB1 as a crystallisation chaperone for human class I MHC complexes.* Journal of immunological methods, 2019. **464**: p. 47-56.
221. Chapman, T.L., A.P. Heikema, and P.J. Bjorkman, *The inhibitory receptor LIR-1 uses a common binding interaction to recognize class I MHC molecules and the viral homolog UL18.* Immunity, 1999. **11**(5): p. 603-613.
222. Shiroishi, M., et al., *Human inhibitory receptors Ig-like transcript 2 (ILT2) and ILT4 compete with CD8 for MHC class I binding and bind preferentially to HLA-G.* Proceedings of the National Academy of Sciences, 2003. **100**(15): p. 8856-8861.
223. Cerboni, C., et al., *Spontaneous mutations in the human CMV HLA class I homologue UL18 affect its binding to the inhibitory receptor LIR‐1/ILT2/CD85j.* European journal of immunology, 2006. **36**(3): p. 732-741.
224. Masuda, A., et al., *Cis binding between inhibitory receptors and MHC class I can regulate mast cell activation.* The Journal of experimental medicine, 2007. **204**(4): p. 907-920.
225. Mori, Y., et al., *Inhibitory immunoglobulin-like receptors LILRB and PIR-B negatively regulate osteoclast development.* The Journal of Immunology, 2008. **181**(7): p. 4742-4751.
226. Li, N.L., et al., *Cis association of leukocyte Ig‐like receptor 1 with MHC class I modulates accessibility to antibodies and HCMV UL18.* European journal of immunology, 2013. **43**(4): p. 1042-1052.
227. Chan, K.R., et al., *Leukocyte immunoglobulin-like receptor B1 is critical for antibody-dependent dengue.* Proceedings of the National Academy of Sciences, 2014. **111**(7): p. 2722-2727.
228. Nakayama, M., et al., *Paired Ig-like receptors bind to bacteria and shape TLR-mediated cytokine production.* The Journal of Immunology, 2007. **178**(7): p. 4250-4259.
229. Saito, F., et al., *Immune evasion of Plasmodium falciparum by RIFIN via inhibitory receptors.* Nature, 2017. **552**(7683): p. 101-105.
230. Beck, S. and B.G. Barrell, *Human cytomegalovirus encodes a glycoprotein homologous to MHC class-I antigens.* 1988.
231. Fahnestock, M.L., et al., *The MHC class I homolog encoded by human cytomegalovirus binds endogenous peptides.* Immunity, 1995. **3**(5): p. 583-590.
232. Maffei, M., et al., *Human cytomegalovirus regulates surface expression of the viral protein UL18 by means of two motifs present in the cytoplasmic tail.* The Journal of Immunology, 2008. **180**(2): p. 969-979.

233. Leong, C.C., et al., *Modulation of natural killer cell cytotoxicity in human cytomegalovirus infection: the role of endogenous class I major histocompatibility complex and a viral class I homolog.* The Journal of experimental medicine, 1998. **187**(10): p. 1681-1687.
234. Kuroki, K., A. Furukawa, and K. Maenaka, *Molecular recognition of paired receptors in the immune system.* Frontiers in microbiology, 2012. **3**: p. 429.
235. Kaiser, B.K., et al., *Structural basis for NKG2A/CD94 recognition of HLA-E.* Proceedings of the National Academy of Sciences, 2008. **105**(18): p. 6696-6701.
236. Farrell, H., et al., *Inhibition of natural killer cells by a cytomegalovirus MHC class I homologue in vivo.* Nature, 1997. **386**(6624): p. 510-514.
237. Browne, H., M. Churcher, and T. Minson, *Construction and characterization of a human cytomegalovirus mutant with the UL18 (class I homolog) gene deleted.* Journal of virology, 1992. **66**(11): p. 6784-6787.
238. Kim, J.-S., et al., *Human cytomegalovirus UL18 alleviated human NK-mediated swine endothelial cell lysis.* Biochemical and biophysical research communications, 2004. **315**(1): p. 144-150.
239. Valés-Gómez, M., et al., *Genetic variability of the major histocompatibility complex class I homologue encoded by human cytomegalovirus leads to differential binding to the inhibitory receptor ILT2.* Journal of virology, 2005. **79**(4): p. 2251-2260.
240. Gumá, M., et al., *Imprint of human cytomegalovirus infection on the NK cell receptor repertoire.* Blood, 2004. **104**(12): p. 3664-3671.
241. Romo, N., et al., *Association of atherosclerosis with expression of the LILRB1 receptor by human NK and T-cells supports the infectious burden hypothesis.* Arteriosclerosis, thrombosis, and vascular biology, 2011. **31**(10): p. 2314-2321.
242. Makwana, N.B., et al., *Asymptomatic CMV infections in long‐term renal transplant recipients are associated with the loss of FcR γ from LIR‐1+ NK cells.* European journal of immunology, 2016. **46**(11): p. 2597-2608.
243. Berg, L., et al., *LIR-1 expression on lymphocytes, and cytomegalovirus disease in lung-transplant recipients.* The Lancet, 2003. **361**(9363): p. 1099-1101.
244. Villard, J., *Immunity after organ transplantation.* Swiss medical weekly, 2006. **136**(5-6): p. 71-77.
245. Chiossone, L., et al., *Molecular analysis of the methylprednisolone-mediated inhibition of NK-cell function: evidence for different susceptibility of IL-2–versus IL-15–activated NK cells.* Blood, 2007. **109**(9): p. 3767-3775.
246. Wai, L.-E., et al., *Rapamycin, but not cyclosporine or FK506, alters natural killer cell function.* Transplantation, 2008. **85**(1): p. 145.
247. Wang, H., et al., *The unexpected effect of cyclosporin A on CD56+ CD16− and CD56+ CD16+ natural killer cell subpopulations.* Blood, The Journal of the American Society of Hematology, 2007. **110**(5): p. 1530-1539.
248. Lamar, D.L., C.M. Weyand, and J.J. Goronzy, *Promoter choice and translational repression determine cell type–specific cell surface density of the inhibitory receptor CD85j expressed on different hematopoietic lineages.* Blood, 2010. **115**(16): p. 3278-3286.
249. Nakajima, H., et al., *Transcriptional regulation of ILT family receptors.* The Journal of Immunology, 2003. **171**(12): p. 6611-6620.

250. Davidson, C.L., L.E. Cameron, and D.N. Burshtyn, *The AP-1 transcription factor JunD activates the leukocyte immunoglobulin-like receptor 1 distal promoter.* International immunology, 2014. **26**(1): p. 21-33.
251. Cadena‐Mota, S., et al., *Effect of cytomegalovirus infection and leukocyte immunoglobulin like receptor B1 polymorphisms on receptor expression in peripheral blood mononuclear cells.* Microbiology and immunology, 2018. **62**(12): p. 755-762.
252. Li, H., et al., *Genetic control of variegated KIR gene expression: polymorphisms of the bi-directional KIR3DL1 promoter are associated with distinct frequencies of gene expression.* PLoS genetics, 2008. **4**(11): p. e1000254.
253. Béziat, V., et al., *NK cell terminal differentiation: correlated stepwise decrease of NKG2A and acquisition of KIRs.* PloS one, 2010. **5**(8).
254. Santourlidis, S., et al., *Crucial role of DNA methylation in determination of clonally distributed killer cell Ig-like receptor expression patterns in NK cells.* The Journal of Immunology, 2002. **169**(8): p. 4253-4261.
255. Chan, H.-W., et al., *DNA methylation maintains allele-specific KIR gene expression in human natural killer cells.* Journal of Experimental Medicine, 2003. **197**(2): p. 245-255.
256. Chan, H.-W., et al., *Epigenetic control of highly homologous killer Ig-like receptor gene alleles.* The Journal of Immunology, 2005. **175**(9): p. 5966-5974.
257. Davidson, C.L., *Implications of genetic diversity on expression of LILRB1 in Natural Killer cells and susceptibility to HCMV infection in transplant patients.* 2016.
258. Cichocki, F., J.S. Miller, and S.K. Anderson, *Killer immunoglobulin-like receptor transcriptional regulation: a fascinating dance of multiple promoters.* Journal of innate immunity, 2011. **3**(3): p. 242-248.
259. Anderson, S.K., *Probabilistic bidirectional promoter switches: noncoding RNA takes control.* Molecular Therapy-Nucleic Acids, 2014. **3**: p. e191.
260. Davies, G., et al., *Identification of bidirectional promoters in the human KIR genes.* Genes and immunity, 2007. **8**(3): p. 245.
261. Cichocki, F., et al., *Cutting edge: KIR antisense transcripts are processed into a 28-base PIWI-like RNA in human NK cells.* The Journal of Immunology, 2010. **185**(4): p. 2009-2012.
262. Li, N.L., et al., *Modulation of the inhibitory receptor leukocyte Ig-like receptor 1 on human natural killer cells.* Frontiers in immunology, 2011. **2**.
263. O'Connor, G.M., et al., *Natural Killer cells from long-term non-progressor HIV patients are characterized by altered phenotype and function.* Clinical immunology, 2007. **124**(3): p. 277-283.
264. Mamessier, E., et al., *Human breast cancer cells enhance self tolerance by promoting evasion from NK cell antitumor immunity.* The Journal of clinical investigation, 2011. **121**(9): p. 3609-3622.
265. Monsivais-Urenda, A., et al., *Analysis of expression and function of the inhibitory receptor ILT2 (CD85j/LILRB1/LIR-1) in peripheral blood mononuclear cells from patients with systemic lupus erythematosus (SLE).* Journal of autoimmunity, 2007. **29**(2): p. 97-105.
266. Monsiváis-Urenda, A., et al., *Defective expression and function of the ILT2/CD85j regulatory receptor in dendritic cells from patients with systemic lupus erythematosus.* Human immunology, 2013. **74**(9): p. 1088-1096.

267. Dutertre, C.-A., et al., *Single-cell analysis of human mononuclear phagocytes reveals subset-defining markers and identifies circulating inflammatory dendritic cells.* Immunity, 2019. **51**(3): p. 573-589. e8.
268. Xiao, X., et al., *Genome-wide association studies and gene expression profiles of rheumatoid arthritis: An analysis.* Bone & joint research, 2016. **5**(7): p. 314-319.
269. Donız-Padilla, L., et al., *Analysis of expression and function of the inhibitory receptor ILT2 in lymphocytes from patients with autoimmune thyroid.* European journal of endocrinology, 2011. **165**: p. 129-136.
270. Schleinitz, N., et al., *Expression of the CD85j (leukocyte Ig‐like receptor 1, Ig‐like transcript 2) receptor for class I major histocompatibility complex molecules in idiopathic inflammatory myopathies.* Arthritis & Rheumatism: Official Journal of the American College of Rheumatology, 2008. **58**(10): p. 3216-3223.
271. Kalmbach, Y., et al., *Increase in annexin V-positive B cells expressing LILRB1/ILT2/CD85j in malaria.* European cytokine network, 2006. **17**(3): p. 175-180.
272. Marlin, R., et al., *Dynamic shift from CD85j/ILT-2 to NKG2D NK receptor expression pattern on human decidual NK during the first trimester of pregnancy.* PLoS One, 2012. **7**(1).
273. Consortium, G.P., *A global reference for human genetic variation.* Nature, 2015. **526**(7571): p. 68-74.
274. Kuroki, K., et al., *Extensive polymorphisms of LILRB1 (ILT2, LIR1) and their association with HLA-DRB1 shared epitope negative rheumatoid arthritis.* Human molecular genetics, 2005. **14**(16): p. 2469-2480.
275. Noyola, D.E., et al., *NK cell immunophenotypic and genotypic analysis of infants with severe respiratory syncytial virus infection.* Microbiology and immunology, 2015. **59**(7): p. 389-397.
276. Affandi, J.S., et al., *Can immune-related genotypes illuminate the immunopathogenesis of cytomegalovirus disease in human immunodeficiency virus–infected patients?* Human immunology, 2012. **73**(2): p. 168-174.
277. Yu, K., et al., *LILRB1 polymorphisms influence posttransplant HCMV susceptibility and ligand interactions.* The Journal of clinical investigation, 2018. **128**(4).
278. Manuel, O., et al., *Assessment of cytomegalovirus-specific cell-mediated immunity for the prediction of cytomegalovirus disease in high-risk solid-organ transplant recipients: a multicenter cohort study.* Clinical infectious diseases, 2013. **56**(6): p. 817-824.
279. Koller, M.T., et al., *Design and methodology of the Swiss Transplant Cohort Study (STCS): a comprehensive prospective nationwide long-term follow-up cohort.* European journal of epidemiology, 2013. **28**(4): p. 347-355.
280. Fu, L., *Investigating the role of the D0 domain of KIR3DL1 in ligand interaction and exploring the effect of LILRB1 on KIR3DL1 signaling.* 2013.
281. Hagège, H., et al., *Quantitative analysis of chromosome conformation capture assays (3C-qPCR).* Nature protocols, 2007. **2**(7): p. 1722.
282. Kim, T.H. and J. Dekker, *Generation of ChIP-loop libraries.* Cold Spring Harbor Protocols, 2018. **2018**(8): p. pdb. prot097857.
283. Fu, L., B. Hazes, and D.N. Burshtyn, *The first Ig domain of KIR3DL1 contacts MHC class I at a secondary site.* J Immunol, 2011. **187**(4): p. 1816-25.
284. Wagner, C.S., et al., *Structural elements underlying the high binding affinity of human cytomegalovirus UL18 to leukocyte immunoglobulin-like receptor-1.* Journal of molecular biology, 2007. **373**(3): p. 695-705.

285. Livak, K.J. and T.D. Schmittgen, *Analysis of relative gene expression data using real-time quantitative PCR and the 2− ΔΔCT method.* methods, 2001. **25**(4): p. 402-408.
286. Heintzman, N.D., et al., *Distinct and predictive chromatin signatures of transcriptional promoters and enhancers in the human genome.* Nature genetics, 2007. **39**(3): p. 311-318.
287. Heintzman, N.D., et al., *Histone modifications at human enhancers reflect global cell-type-specific gene expression.* Nature, 2009. **459**(7243): p. 108-112.
288. Shlyueva, D., G. Stampfel, and A. Stark, *Transcriptional enhancers: from properties to genome-wide predictions.* Nature Reviews Genetics, 2014. **15**(4): p. 272.
289. Bernstein, B.E., et al., *The NIH roadmap epigenomics mapping consortium.* Nature biotechnology, 2010. **28**(10): p. 1045.
290. Gamliel, M., et al., *Trained Memory of Human Uterine NK Cells Enhances Their Function in Subsequent Pregnancies.* Immunity, 2018. **48**(5): p. 951-962. e5.
291. Consortium, E.P., *An integrated encyclopedia of DNA elements in the human genome.* Nature, 2012. **489**(7414): p. 57.
292. Barrett, T., et al., *NCBI GEO: archive for functional genomics data sets—update.* Nucleic acids research, 2012. **41**(D1): p. D991-D995.
293. Allen, B.L. and D.J. Taatjes, *The Mediator complex: a central integrator of transcription.* Nature reviews Molecular cell biology, 2015. **16**(3): p. 155.
294. Kagey, M.H., et al., *Mediator and cohesin connect gene expression and chromatin architecture.* Nature, 2010. **467**(7314): p. 430.
295. Splinter, E., et al., *CTCF mediates long-range chromatin looping and local histone modification in the β-globin locus.* Genes & development, 2006. **20**(17): p. 2349-2354.
296. Weintraub, A.S., et al., *YY1 is a structural regulator of enhancer-promoter loops.* Cell, 2017. **171**(7): p. 1573-1588. e28.
297. Van Berkum, N.L., et al., *Hi-C: a method to study the three-dimensional architecture of genomes.* JoVE (Journal of Visualized Experiments), 2010(39): p. e1869.
298. Dekker, J., et al., *The 4D nucleome project.* Nature, 2017. **549**(7671): p. 219.
299. Smith, S., K. Rigley, and R. Callard, *Activation of human B cells through the CD19 surface antigen results in homotypic adhesion by LFA-1-dependent and-independent mechanisms.* Immunology, 1991. **73**(3): p. 293.
300. Zapata, J.M., et al., *B-cell homotypic adhesion through exon-A restricted epitopes of CD45 involves LFA-1/ICAM-1, ICAM-3 interactions, and induces coclustering of CD45 and LFA-1.* Blood, 1995. **86**(5): p. 1861-1872.
301. Su, K.-Y., et al., *Efficient culture of human naive and memory B cells for use as APCs.* The Journal of Immunology, 2016. **197**(10): p. 4163-4176.
302. Caeser, R., et al., *Genetic modification of primary human B cells generates translationally-relevant models of high-grade lymphoma.* bioRxiv, 2019: p. 618835.
303. Rothlein, R., et al., *A human intercellular adhesion molecule (ICAM-1) distinct from LFA-1.* The Journal of Immunology, 1986. **137**(4): p. 1270-1274.

304. Kansas, G.S. and T.F. Tedder, *Transmembrane signals generated through MHC class II, CD19, CD20, CD39, and CD40 antigens induce LFA-1-dependent and independent adhesion in human B cells through a tyrosine kinase-dependent pathway.* The Journal of Immunology, 1991. **147**(12): p. 4094-4102.
305. Evans, S., et al., *IFN-alpha induces homotypic adhesion and Leu-13 expression in human B lymphoid cells.* The Journal of Immunology, 1993. **150**(3): p. 736-747.
306. Alduaij, W., et al., *Novel type II anti-CD20 monoclonal antibody (GA101) evokes homotypic adhesion and actin-dependent, lysosome-mediated cell death in B-cell malignancies.* Blood, 2011. **117**(17): p. 4519-4529.
307. Singer, S.J., *Intercellular communication and cell-cell adhesion.* Science, 1992. **255**(5052): p. 1671-1677.
308. Aplin, A.E., A.K. Howe, and R. Juliano, *Cell adhesion molecules, signal transduction and cell growth.* Current opinion in cell biology, 1999. **11**(6): p. 737-744.
309. Schwartz, M.A. and R.K. Assoian, *Integrins and cell proliferation: regulation of cyclin-dependent kinases via cytoplasmic signaling pathways.* Journal of cell science, 2001. **114**(14): p. 2553-2560.
310. Springer, T.A., *Adhesion receptors of the immune system.* Nature, 1990. **346**(6283): p. 425.
311. Zhang, Y. and H. Wang, *Integrin signalling and function in immune cells.* Immunology, 2012. **135**(4): p. 268-275.
312. Harris, E.S., et al., *Minireview: the leukocyte integrins.* Journal of Biological Chemistry, 2000.
313. Springer, T.A., et al., *The lymphocyte function associated LFA-1, CD2, and LFA-3 molecules: cell adhesion receptors of the immune system.* Annual review of immunology, 1987. **5**(1): p. 223-252.
314. Larson, R.S. and T.A. Springer, *Structure and function of leukocyte integrins.* Immunological reviews, 1990. **114**(1): p. 181-217.
315. Van Kooyk, Y., et al., *Enhancement of LFA-1-mediated cell adhesion by triggering through CD2 or CD3 on T lymphocytes.* Nature, 1989. **342**(6251): p. 811.
316. Fan, X., P. Benz, and R.P. Wüthrich, *ICAM-1-,-2-and LFA-1-independent homotypic T cell aggregation induced by a novel activating monoclonal antibody targeting the murine Thy-1 molecule.* Inflammation, 1996. **20**(4): p. 401-411.
317. Wuthrich, R.P., *Monoclonal antibodies targeting murine LFA-1 induce LFA-1/ICAM-1-independent homotypic lymphocyte aggregation.* Cellular immunology, 1992. **144**(1): p. 22-31.
318. Giannoni, E., et al., *Lymphocyte function-associated antigen-1-mediated T cell adhesion is impaired by low molecular weight phosphotyrosine phosphatase-dependent inhibition of FAK activity.* Journal of Biological Chemistry, 2003. **278**(38): p. 36763-36776.
319. Luo, B.-H., C.V. Carman, and T.A. Springer, *Structural basis of integrin regulation and signaling.* Annu. Rev. Immunol., 2007. **25**: p. 619-647.
320. Schürpf, T. and T.A. Springer, *Regulation of integrin affinity on cell surfaces.* The EMBO Journal, 2011. **30**(23): p. 4712-4727.
321. Kim, M., C.V. Carman, and T.A. Springer, *Bidirectional transmembrane signaling by cytoplasmic domain separation in integrins.* Science, 2003. **301**(5640): p. 1720-1725.
322. Calderwood, D.A., I.D. Campbell, and D.R. Critchley, *Talins and kindlins: partners in integrin-mediated adhesion.* Nature reviews Molecular cell biology, 2013. **14**(8): p. 503-517.

323. Walling, B.L. and M. Kim, *LFA-1 in T cell migration and differentiation.* Frontiers in immunology, 2018. **9**: p. 952.
324. Abram, C.L. and C.A. Lowell, *The ins and outs of leukocyte integrin signaling.* Annual review of immunology, 2009. **27**: p. 339-362.
325. Nordenfelt, P., H.L. Elliott, and T.A. Springer, *Coordinated integrin activation by actin-dependent force during T-cell migration.* Nature communications, 2016. **7**: p. 13119.
326. Dransfield, I., et al., *Divalent cation regulation of the function of the leukocyte integrin LFA-1.* The Journal of cell biology, 1992. **116**(1): p. 219-226.
327. Pflugfelder, S.C., et al., *LFA-1/ICAM-1 interaction as a therapeutic target in dry eye disease.* Journal of Ocular Pharmacology and Therapeutics, 2017. **33**(1): p. 5-12.
328. Bird, A.P. and A.P. Wolffe, *Methylation-induced repression—belts, braces, and chromatin.* Cell, 1999. **99**(5): p. 451-454.
329. Chahrour, M., et al., *MeCP2, a key contributor to neurological disease, activates and represses transcription.* Science, 2008. **320**(5880): p. 1224-1229.
330. Kemme, C.A., et al., *Potential role of DNA methylation as a facilitator of target search processes for transcription factors through interplay with methyl-CpG-binding proteins.* Nucleic acids research, 2017. **45**(13): p. 7751-7759.
331. Klose, R.J. and A.P. Bird, *Genomic DNA methylation: the mark and its mediators.* Trends in biochemical sciences, 2006. **31**(2): p. 89-97.
332. Wischnewski, F., et al., *Methyl-CpG binding domain proteins and their involvement in the regulation of the MAGE-A1, MAGE-A2, MAGE-A3, and MAGE-A12 gene promoters.* Molecular Cancer Research, 2007. **5**(7): p. 749-759.
333. van Bergen, J., et al., *Structural and functional differences between the promoters of independently expressed killer cell Ig‐like receptors.* European journal of immunology, 2005. **35**(7): p. 2191-2199.
334. Idda, M.L., et al., *NF90 regulation of immune factor expression in response to malaria antigens.* Cell Cycle, 2019. **18**(6-7): p. 708-722.
335. Young, N.T. and M. Uhrberg, *KIR expression shapes cytotoxic repertoires: a developmental program of survival.* Trends in immunology, 2002. **23**(2): p. 71-75.
336. Björkström, N.K., et al., *Expression patterns of NKG2A, KIR, and CD57 define a process of CD56dim NK-cell differentiation uncoupled from NK-cell education.* Blood, 2010. **116**(19): p. 3853-3864.
337. Moriggl, R., et al., *Stat5 is required for IL-2-induced cell cycle progression of peripheral T cells.* Immunity, 1999. **10**(2): p. 249-259.
338. Gotthardt, D., et al., *STAT5 is a key regulator in NK cells and acts as a molecular switch from tumor surveillance to tumor promotion.* Cancer Discovery, 2016. **6**(4): p. 414-429.
339. Cobaleda, C., et al., *Pax5: the guardian of B cell identity and function.* Nature immunology, 2007. **8**(5): p. 463.
340. Lee, W. and G.R. Lee, *Transcriptional regulation and development of regulatory T cells.* Experimental & molecular medicine, 2018. **50**(3): p. e456-e456.
341. Chrivia, J.C., et al., *Phosphorylated CREB binds specifically to the nuclear protein CBP.* Nature, 1993. **365**(6449): p. 855.

342. Kovács, K.A., et al., *CCAAT/enhancer-binding protein family members recruit the coactivator CREB-binding protein and trigger its phosphorylation.* Journal of Biological Chemistry, 2003. **278**(38): p. 36959-36965.
343. Wang, Z., et al., *Genome-wide mapping of HATs and HDACs reveals distinct functions in active and inactive genes.* Cell, 2009. **138**(5): p. 1019-1031.
344. Visel, A., et al., *ChIP-seq accurately predicts tissue-specific activity of enhancers.* Nature, 2009. **457**(7231): p. 854.
345. Smit, A., R. Hubley, and P. Green, *RepeatMasker Open-4.0. 2013–2015*, 2015.
346. Schumann, G.G., et al., *Unique functions of repetitive transcriptomes*, in *International review of cell and molecular biology*. 2010, Elsevier. p. 115-188.
347. Consortium, I.H.G.S., *Initial sequencing and analysis of the human genome.* nature, 2001. **409**(6822): p. 860.
348. Brouha, B., et al., *Hot L1s account for the bulk of retrotransposition in the human population.* Proceedings of the National Academy of Sciences, 2003. **100**(9): p. 5280-5285.
349. Hancks, D.C. and H.H. Kazazian Jr, *Active human retrotransposons: variation and disease.* Current opinion in genetics & development, 2012. **22**(3): p. 191-203.
350. van de Lagemaat, L.N., et al., *Transposable elements in mammals promote regulatory variation and diversification of genes with specialized functions.* Trends in Genetics, 2003. **19**(10): p. 530-536.
351. Trizzino, M., A. Kapusta, and C.D. Brown, *Transposable elements generate regulatory novelty in a tissue-specific fashion.* BMC genomics, 2018. **19**(1): p. 468.
352. Kumar, S., et al., *Zinc-Induced Polymerization of Killer-Cell Ig-like Receptor into Filaments Promotes Its Inhibitory Function at Cytotoxic Immunological Synapses.* Molecular cell, 2016. **62**(1): p. 21-33.
353. Hunt, J.S., et al., *HLA-G and immune tolerance in pregnancy.* The FASEB Journal, 2005. **19**(7): p. 681-693.
354. Rouas-Freiss, N., et al., *HLA-G proteins in cancer: do they provide tumor cells with an escape mechanism?* Cancer research, 2005. **65**(22): p. 10139-10144.
355. Carosella, E.D., et al., *HLA-G: from biology to clinical benefits.* Trends in immunology, 2008. **29**(3): p. 125-132.
356. Aguilar, O.A., et al., *A viral immunoevasin controls innate immunity by targeting the prototypical natural killer cell receptor family.* Cell, 2017. **169**(1): p. 58-71. e14.
357. Gonzalez, A., et al., *KIR-associated protection from CMV replication requires pre-existing immunity: a prospective study in solid organ transplant recipients.* Genes and immunity, 2014. **15**(7): p. 495-499.
358. Ince, M.N., et al., *Increased expression of the natural killer cell inhibitory receptor CD85j/ILT2 on antigen‐specific effector CD8 T cells and its impact on CD8 T‐cell function.* Immunology, 2004. **112**(4): p. 531-542.
359. Saverino, D., et al., *Dual effect of CD85/leukocyte Ig-like receptor-1/Ig-like transcript 2 and CD152 (CTLA-4) on cytokine production by antigen-stimulated human T cells.* The Journal of Immunology, 2002. **168**(1): p. 207-215.
360. Costa, P., et al., *Differential disappearance of inhibitory natural killer cell receptors during HAART and possible impairment of HIV-1-specific CD8 cytotoxic T lymphocytes.* Aids, 2001. **15**(8): p. 965-974.
361. Kirwan, S.E. and D.N. Burshtyn, *Killer cell Ig-like receptor-dependent signaling by Ig-like transcript 2 (ILT2/CD85j/LILRB1/LIR-1).* The Journal of Immunology, 2005. **175**(8): p. 5006-5015.

362. Manuel, O., et al., *Influence of IFNL3/4 polymorphisms on the incidence of cytomegalovirus infection after solid-organ transplantation.* J Infect Dis, 2015. **211**(6): p. 906-14.
363. Egli, A., et al., *Immunomodulatory Function of Interleukin 28B during primary infection with cytomegalovirus.* J Infect Dis, 2014. **210**(5): p. 717-27.
364. Corrales, I., et al., *IL28B genetic variation and cytomegalovirus-specific T-cell immunity in allogeneic stem cell transplant recipients.* J Med Virol, 2017. **89**(4): p. 685-695.
365. Cook, M., et al., *Donor KIR genotype has a major influence on the rate of cytomegalovirus reactivation following T-cell replete stem cell transplantation.* Blood, 2006. **107**(3): p. 1230-2.
366. Hadaya, K., et al., *Natural killer cell receptor repertoire and their ligands, and the risk of CMV infection after kidney transplantation.* Am J Transplant, 2008. **8**(12): p. 2674-83.
367. Jones, D.C., et al., *Killer immunoglobulin-like receptor gene repertoire influences viral load of primary human cytomegalovirus infection in renal transplant patients.* Genes Immun, 2014. **15**(8): p. 562-8.
368. Loeffler, J., et al., *Polymorphisms in the genes encoding chemokine receptor 5, interleukin-10, and monocyte chemoattractant protein 1 contribute to cytomegalovirus reactivation and disease after allogeneic stem cell transplantation.* J Clin Microbiol, 2006. **44**(5): p. 1847-50.
369. Niknam, A., et al., *The Association Between Viral Infections and Co-stimulatory Gene Polymorphisms in Kidney Transplant Outcomes.* Jundishapur J Microbiol, 2016. **9**(8): p. e31338.
370. Fernandez-Ruiz, M., et al., *Association between individual and combined SNPs in genes related to innate immunity and incidence of CMV infection in seropositive kidney transplant recipients.* Am J Transplant, 2015. **15**(5): p. 1323-35.
371. Misra, M.K., et al., *Cytotoxic T-lymphocyte antigen 4 gene polymorphism influences the incidence of symptomatic human cytomegalovirus infection after renal transplantation.* Pharmacogenetics and genomics, 2015. **25**(1): p. 19-29.
372. Saadi, M.I., et al., *Association of the costimulatory molecule gene polymorphisms and active cytomegalovirus infection in hematopoietic stem cell transplant patients.* Mol Biol Rep, 2013. **40**(10): p. 5833-42.
373. Redondo-Pachon, D., et al., *Adaptive NKG2C+ NK Cell Response and the Risk of Cytomegalovirus Infection in Kidney Transplant Recipients.* J Immunol, 2017. **198**(1): p. 94-101.
374. Lisboa, L., et al., *CCL8 and the Immune Control of Cytomegalovirus in Organ Transplant Recipients.* American Journal of Transplantation, 2015. **15**(7): p. 1882-1892.
375. Xiao, H., et al., *Donor TLR9 gene tagSNPs influence susceptibility to aGVHD and CMV reactivation in the allo-HSCT setting without polymorphisms in the TLR4 and NOD2 genes.* Bone marrow transplantation, 2014. **49**(2): p. 241-247.
376. Mezger, M., et al., *Investigation of promoter variations in dendritic cell-specific ICAM3-grabbing non-integrin (DC-SIGN)(CD209) and their relevance for human cytomegalovirus reactivation and disease after allogeneic stem-cell transplantation.* Clinical microbiology and infection, 2008. **14**(3): p. 228-234.
377. Buxmann, H., et al., *Primary Human Cytomegalovirus (HCMV) Infection in Pregnancy.* Deutsches Ärzteblatt International, 2017. **114**(4): p. 45.
378. Pass, R.F., et al., *Vaccine prevention of maternal cytomegalovirus infection.* New England Journal of Medicine, 2009. **360**(12): p. 1191-1199.

379. Heineman, T.C., et al., *A phase 1 study of 4 live, recombinant human cytomegalovirus Towne/Toledo chimeric vaccines.* Journal of Infectious Diseases, 2006. **193**(10): p. 1350-1360.
380. Taylor-Wiedeman, J., et al., *Monocytes are a major site of persistence of human cytomegalovirus in peripheral blood mononuclear cells.* Journal of General Virology, 1991. **72**(9): p. 2059-2064.
381. Smith, M.S., et al., *Human cytomegalovirus induces monocyte differentiation and migration as a strategy for dissemination and persistence.* Journal of virology, 2004. **78**(9): p. 4444-4453.
382. Gerna, G., et al., *Human cytomegalovirus replicates abortively in polymorphonuclear leukocytes after transfer from infected endothelial cells via transient microfusion events.* Journal of virology, 2000. **74**(12): p. 5629-5638.
383. Kinzler, E.R. and T. Compton, *Characterization of human cytomegalovirus glycoprotein-induced cell-cell fusion.* Journal of virology, 2005. **79**(12): p. 7827-7837.
384. Wirtz, N., et al., *Polyclonal cytomegalovirus-specific antibodies not only prevent virus dissemination from the portal of entry but also inhibit focal virus spread within target tissues.* Medical microbiology and immunology, 2008. **197**(2): p. 151-158.
385. Sattentau, Q., *Avoiding the void: cell-to-cell spread of human viruses.* Nature Reviews Microbiology, 2008. **6**(11): p. 815-826.
386. Ibanez, C.E., et al., *Human cytomegalovirus productively infects primary differentiated macrophages.* Journal of virology, 1991. **65**(12): p. 6581-6588.
387. Lathey, J. and S. Spector, *Unrestricted replication of human cytomegalovirus in hydrocortisone-treated macrophages.* Journal of Virology, 1991. **65**(11): p. 6371-6375.
388. Sinclair, J., et al., *Repression of human cytomegalovirus major immediate early gene expression in a monocytic cell line.* Journal of General Virology, 1992. **73**(2): p. 433-435.
389. Shang, X.Z. and A.C. Issekutz, *Contribution of CD11a/CD18, CD11b/CD18, ICAM‐1 (CD54) and‐2 (CD102) to human monocyte migration through endothelium and connective tissue fibroblast barriers.* European journal of immunology, 1998. **28**(6): p. 1970-1979.
390. Sandig, M., E. Negrou, and K.A. Rogers, *Changes in the distribution of LFA-1, catenins, and F-actin during transendothelial migration of monocytes in culture.* Journal of Cell Science, 1997. **110**(22): p. 2807-2818.
391. Tedder, T.F., L.-J. Zhou, and P. Engel, *The CD19/CD21 signal transduction complex of B lymphocytes.* Immunology today, 1994. **15**(9): p. 437-442.
392. Lee, B.O., et al., *CD40, but not CD154, expression on B cells is necessary for optimal primary B cell responses.* The Journal of Immunology, 2003. **171**(11): p. 5707-5717.
393. Klaus, G.G., M. Holman, and J. Hasbold, *Properties of mouse CD40: the role of homotypic adhesion in the activation of B cells via CD40.* European journal of immunology, 1994. **24**(11): p. 2714-2719.
394. Sola‐Penna, M., *Metabolic regulation by lactate.* IUBMB life, 2008. **60**(9): p. 605-608.
395. Higgins, C., *L-lactate and d-lacate–clinical significance in the difference.* Acute Care Testing. October, 2011.
396. Kawai, T. and S. Akira, *Signaling to NF-κB by Toll-like receptors.* Trends in molecular medicine, 2007. **13**(11): p. 460-469.
397. Heil, F., et al., *Species-specific recognition of single-stranded RNA via toll-like receptor 7 and 8.* Science, 2004. **303**(5663): p. 1526-1529.

398. Aldemir, H., et al., *Cutting edge: lectin-like transcript 1 is a ligand for the CD161 receptor.* The Journal of Immunology, 2005. **175**(12): p. 7791-7795.
399. Rosen, D.B., et al., *Cutting edge: lectin-like transcript-1 is a ligand for the inhibitory human NKR-P1A receptor.* The Journal of Immunology, 2005. **175**(12): p. 7796-7799.
400. Barclay, A.N. and M.H. Brown, *The SIRP family of receptors and immune regulation.* Nature Reviews Immunology, 2006. **6**(6): p. 457.
401. Finocchiaro, G., M. Ito, and K. Tanaka, *Purification and properties of short chain acyl-CoA, medium chain acyl-CoA, and isovaleryl-CoA dehydrogenases from human liver.* Journal of Biological Chemistry, 1987. **262**(17): p. 7982-7989.
402. He, M., et al., *Identification and characterization of new long chain acyl-CoA dehydrogenases.* Molecular genetics and metabolism, 2011. **102**(4): p. 418-429.
403. Jitrapakdee, S., et al., *Structure, mechanism and regulation of pyruvate carboxylase.* Biochemical journal, 2008. **413**(3): p. 369-387.
404. Suzuki, T., A. Nagao, and T. Suzuki, *Human mitochondrial tRNAs: biogenesis, function, structural aspects, and diseases.* Annual review of genetics, 2011. **45**: p. 299-329.

Appendixes

D183

	Geom. MFI	Transcript copies/sample: Allele-*rs1061679-T*	Allele-*rs1061679-C*	Ratio *(rs1061679-C/T)*
RT- (NK-3)	212.1	0.0	0.0	N/A
NK-1	0	0.0	0.0	N/A
NK-2	31.8	0.0	0.0	N/A
NK-3	212.1	2.6	0.0	0.000
NK-4	280.5	2.6	1.3	0.500
NK-5	1223.3	127.5	124.2	0.974
NK-6	6982.3	7.5	7.5	1.000
NK-7	10546.9	6.9	3.6	0.524
NK-8	12653.3	17.0	6.9	0.404

D185

	Geom. MFI	Transcript copies/sample: Allele-*rs1061679-T*	Allele-*rs1061679-C*	Ratio *(rs1061679-C/T)*
RT- (NK-7)	1182.5	0.0	0.0	N/A
NK-1	0	0.0	0.0	N/A
NK-2	77.8	93.3	2.5	0.027
NK-3	85.6	1.3	0.0	0.000
NK-4	475	15.7	0.0	0.000
NK-5	540.7	86.9	0.0	0.000
NK-6	560.7	31.8	0.0	0.000
NK-7	1182.5	5.7	0.0	0.000
NK-8	1472.4	33.9	0.0	0.000
NK-9	1580.4	19.1	12.5	0.656
NK-10	3016	19.1	10.0	0.522
NK-11	5087.1	25.4	6.4	0.250
NK-12	5671.3	237.4	148.4	0.625

D500

	Geom. MFI	Transcript copies/sample: Allele-*rs1061679-T*	Allele-*rs1061679-C*	Ratio *(rs1061679-C/T)*
RT- (NK-7)	1073.0	0.0	0.0	N/A
NK-1	11.6	1.6	0.0	0.000
NK-2	72.9	5.0	0.0	0.000
NK-3	118.7	22.6	0.0	0.000
NK-4	174.4	9.4	1.4	0.149
NK-5	241.1	24.8	2.8	0.113
NK-6	640.0	94.0	52.0	0.553
NK-7	1073.0	70.0	46.0	0.657
NK-8	1322.2	118.0	64.0	0.542
NK-9	1429.7	104.0	76.0	0.731
NK-10	1794.8	306.0	212.0	0.693
NK-11	1820.5	206.0	130.0	0.631

APPENDIX A1 Geom.MFI value with background subtracted, copy number per sample of the two alleles and the ratio between the allele-C and allele-T are listed for each NK clone derived from the three donors shown in Figure 3.1.

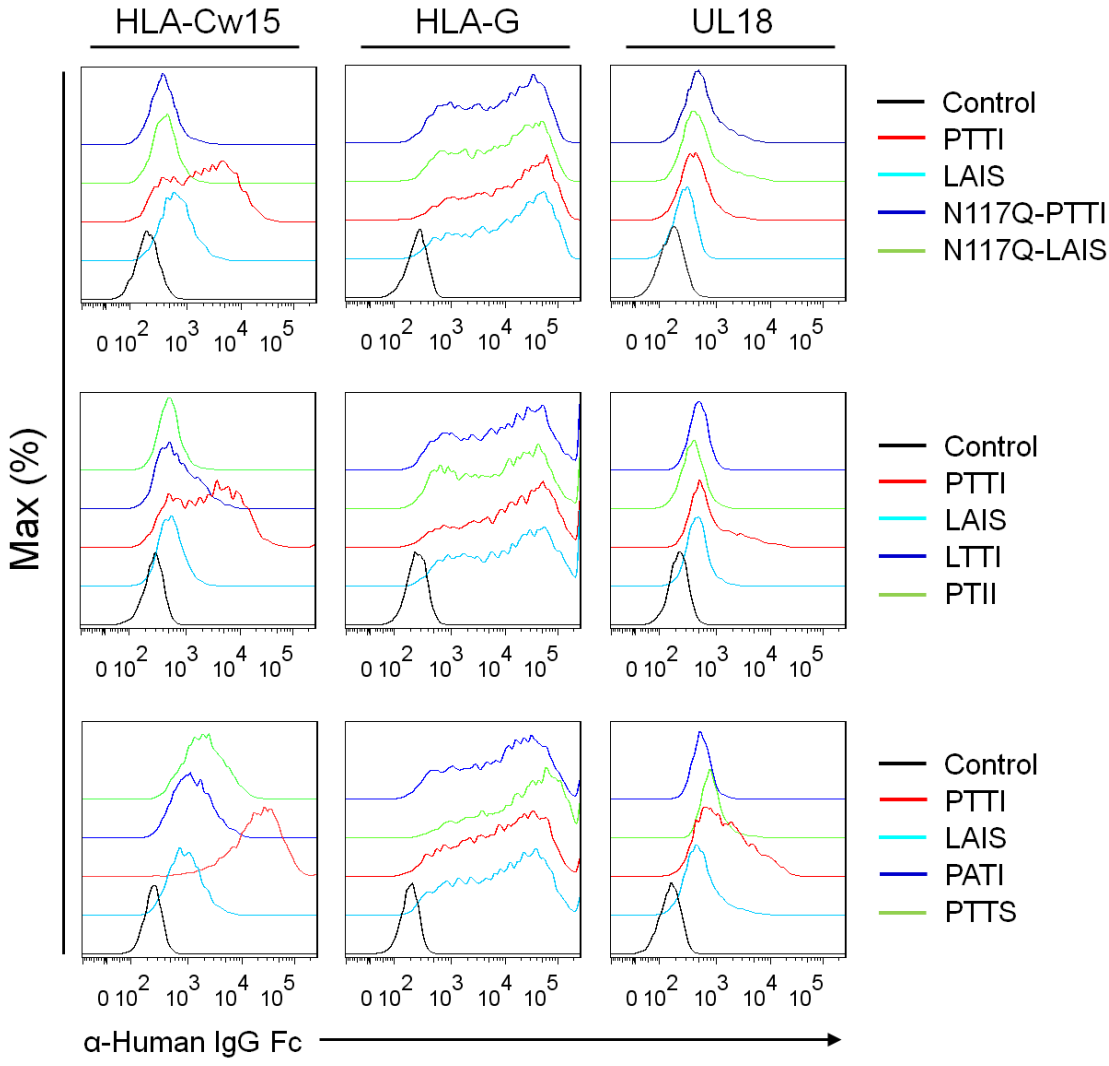

APPENDIX A2 Flow cytometry staining of the LILRB1 mutants binding with HLA-Cw15, HLA-G and UL18.

FACs data shown is the representative data of LILRB1 mutants at one same concentration. The binding with HLA-Cw15, HLA-G was using LILRB1 mutants at 50 μg/ml, and the binding with UL18 was using LILRB1 mutants at 100 μg/ml.

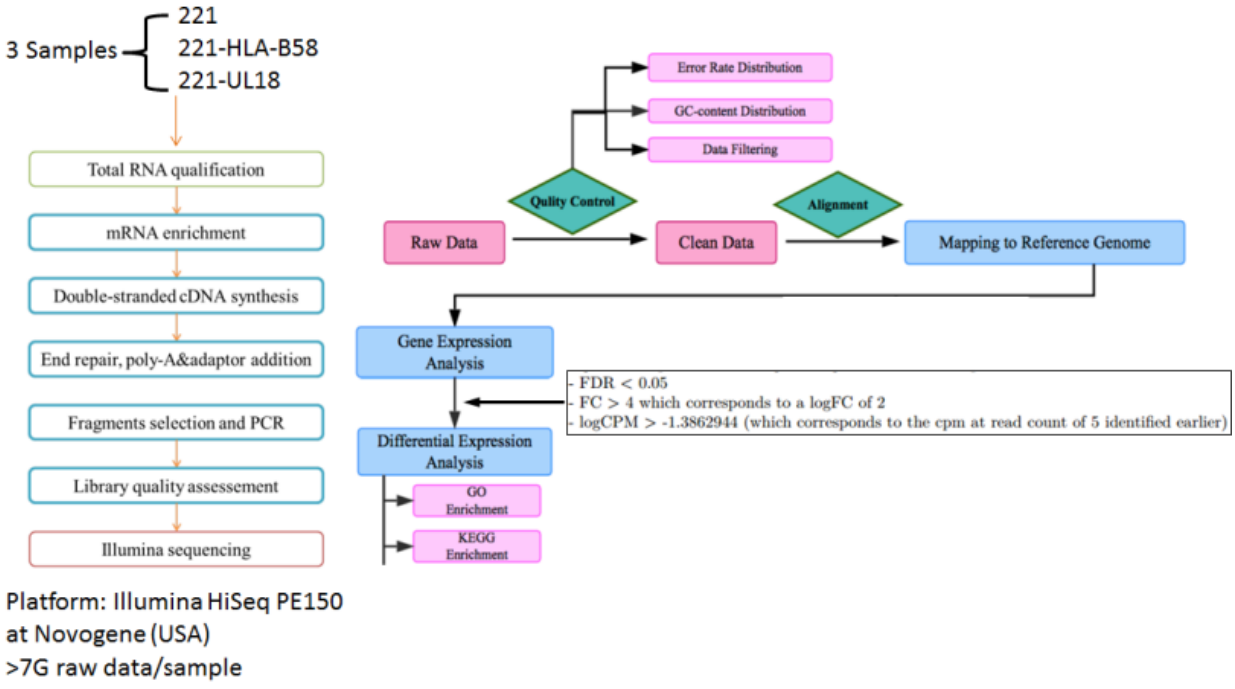

APPENDIX A3 Workflow of the experiment from sample preparation to sequencing and bioinformatics analysis.

The flow chart was adapted and modified from Novogene Bioinformatics Technology Co.,Ltd.

A

UL18 vs 221

gene_biotype	Nr.up	Nr.down
protein_coding	224	223
antisense_RNA	3	43
lincRNA	12	43
processed_pseudogene	4	11
transcribed_unprocessed_pseudogene	5	11
Mt_tRNA	NA	11
processed_transcript	3	8
unprocessed_pseudogene	1	8
TEC	NA	5
IG_C_gene	NA	3
sense_intronic	2	2
sense_overlapping	1	2
transcribed_processed_pseudogene	3	2
miRNA	NA	2
snRNA	NA	2
bidirectional_promoter_lncRNA	NA	1
IG_C_pseudogene	NA	1
TR_J_gene	NA	1
transcribed_unitary_pseudogene	NA	1
misc_RNA	1	NA
polymorphic_pseudogene	1	NA

HLA-B58 vs 221

gene_biotype	Nr.up	Nr.down
protein_coding	276	285
lincRNA	26	38
antisense_RNA	16	19
transcribed_unprocessed_pseudogene	9	8
processed_pseudogene	6	7
processed_transcript	3	6
TEC	2	5
unprocessed_pseudogene	3	5
sense_intronic	1	2
miRNA	1	1
transcribed_processed_pseudogene	3	1
transcribed_unitary_pseudogene	2	1
sense_overlapping	NA	1
TR_J_gene	NA	1
IG_C_gene	2	NA
IG_C_pseudogene	1	NA
IG_V_gene	5	NA
IG_V_pseudogene	1	NA

B

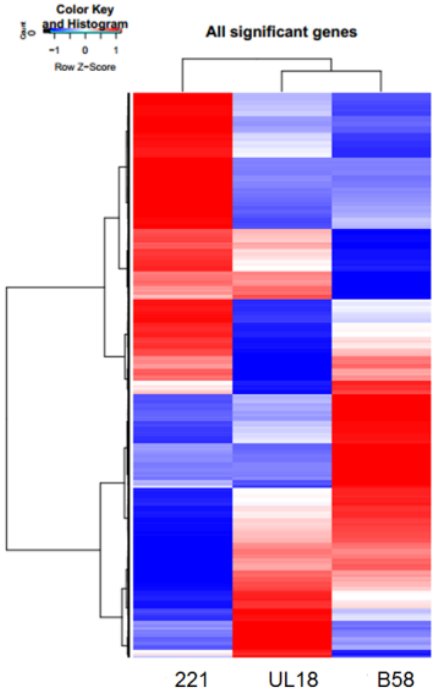

C

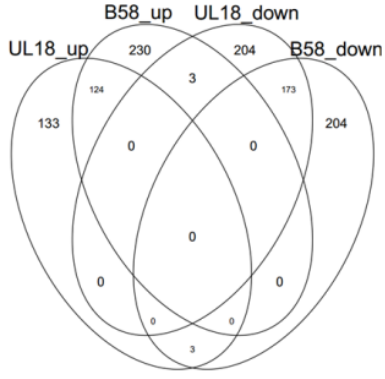

APPENDIX A4 Results of differential expression (DE) analysis of the RNA-Sequencing. (A) List of significant DE genes numbers per 'gene_biotype' category from the analysis comparing 721.221 vs 221-UL18 and 721.221 vs 221-B58, respectively based on the criteria defined in the Materials and Methods. (B) Heat map depicting the expression (in log2CPM scale) differences among the 3 samples for the union of all significant DE genes identified in both comparisons from panel B. (C) Venn diagram depicting the significant up- and down- regulated gene numbers found in the 2 comparisons from panel B.

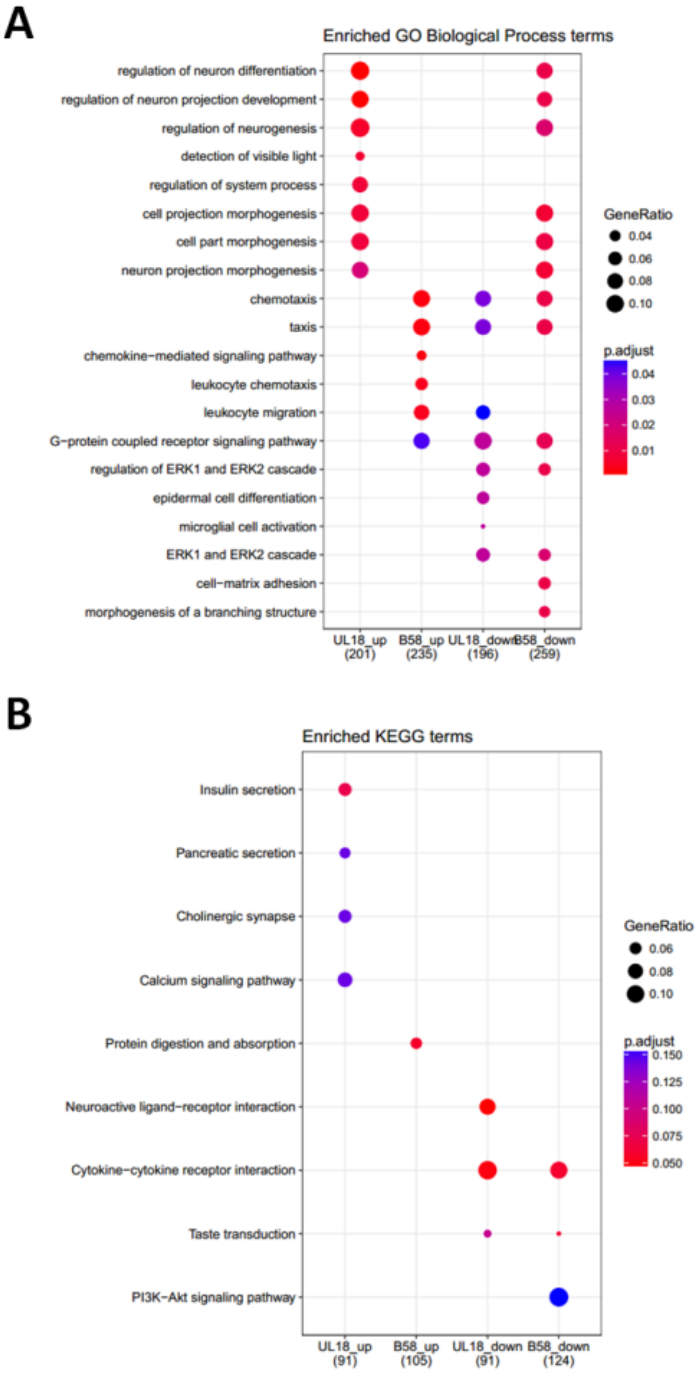

APPENDIX A5 Gene Ontology (GO) (A) and KEGG pathway (B) term enrichment analyses regarding the comparison of 221-UL18 vs 721.221 and 221-B58 vs 721.221. GeneRatio represents the number of genes in the test set annotated to the particular term ID out of the total number of genes in the test set with known GO/KEGG annotations; p.adjust indicates Benjamini-Hochberg multiple testing corrected p-value. Numbers shown under each test group are the counts of genes annotated to the shown term ID.

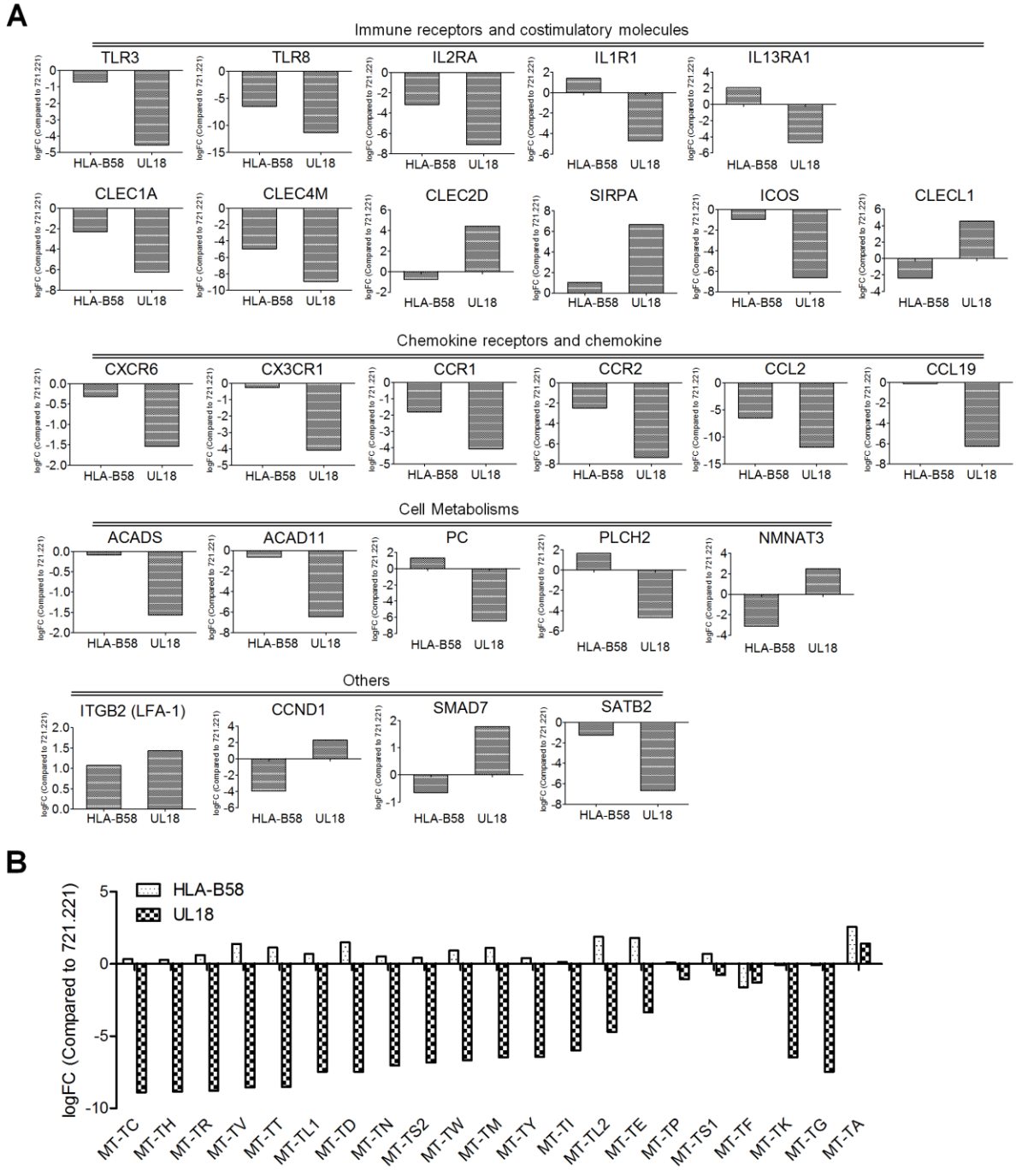

APPENDIX A6 Selected genes comparing the logFC analyzed from the comparison of 221-UL18 vs 721.221 and 221-B58 vs 721.221.

(A) Selected protein-coding genes that have at least a difference of log1.5 are classified based on different biological functions indicated above each group. (B) Mt-tRNA genes identified in the two comparisons.